# Differential Expression of Molecules that Contribute to the Pathogenesis of Bladder Pain Syndrome (BPS)

**Anastasia Kaltsa**

**MSc by Research (MScR)**

**University of York**

**Biology**

**January 2026**

# *Abstract*

Bladder Pain Syndrome (BPS) is a chronic, clinically heterogeneous condition characterised by pelvic pain and urinary urgency, yet it lacks reliable biomarkers and consistently effective treatments. Traditional classification systems—primarily based on cystoscopic findings such as Hunner lesions—do not adequately capture the underlying biological diversity. This thesis investigated whether transcriptomic profiling of bladder tissue could reveal molecular signatures associated with distinct BPS subtypes, thereby informing more targeted diagnostic and therapeutic approaches.

A systematic review of 20 molecular studies was first conducted to identify candidate genes and proteins implicated in BPS pathophysiology. These targets informed analysis of an in-house transcriptomic dataset derived from bladder biopsies of 13 clinically well-characterised female patients, encompassing both BPS and non-BPS cases. Expression data were interpreted in conjunction with cystoscopic findings, histology, trans-epithelial resistance, and O'Leary-Sant symptom scores.

Although differential gene expression between diagnostic groups was limited, individual-level analyses revealed transcriptional variability suggestive of biologically meaningful subtypes. Two samples (Y2336, Y2338) exhibited prominent immune activation—including elevated *IL6*, *TNF*, *CCL2*, and *STAT1/3*—despite differing cystoscopic phenotypes. A third case (Y2610) displayed high *CNR1* expression with minimal inflammatory signalling, consistent with a neuroplasticity-associated profile. Most remaining samples showed muted or heterogeneous expression patterns, potentially reflecting biologically quiescent states, unprofiled mechanisms, or sampling limitations.

These findings provide preliminary support for a stratified model of BPS, including immune-enriched, neurogenic, and oxidative stress–linked subtypes. The heterogeneity observed cautions against population-averaged interpretations and highlights the potential of personalised transcriptomic analysis. This thesis contributes novel data toward molecular characterisation of BPS and sets the stage for future multi-omics studies in larger cohorts. Refining such subtype frameworks could ultimately improve biomarker development and guide personalised management in chronic bladder pain.

## *Author's Declaration*

I declare that this thesis is a presentation of original work, and I am the sole author. This work has not previously been presented for a degree or other qualification at this University or elsewhere. All sources are acknowledged as references.

# *Table of Contents*

## Chapter 2: Literature Review of Candidate Biomarkers for Bladder Pain Syndrome

### 2.1 Introduction

### 2.2 Methods

### 2.3 Results of Systematic Review on Candidate Biomarkers for Bladder Pain Syndrome

### 2.4 Synthesis of Findings

### 2.5 Discussion of Systematic Review Findings

## Chapter 3: Evaluation of Literature-Derived Biomarkers in In-House Bladder Pain Syndrome Data

### 3.1 Introduction to the In-House Dataset

### 3.2 Experimental Methods

### 3.3 Data Analysis Methods

### 3.4 Data analysis

### 3.5 Transcriptomic Insights into BPS Pathophysiology: A Synthesis of In-House Findings

## Chapter 4: Discussion

### 4.1 Strengths of Approach

### 4.2 Limitations of the Study

### 4.3 Future Directions and Clinical Applications

## References

## Appendices

## List of abbreviations

# Chapter 1: Introduction

## 1.1 Lower Urinary Tract Symptoms (LUTS)

The lower urinary tract (LUT) consists of the bladder and urethra, which coordinate urine storage and voiding. In males, the prostate surrounds the urethra and may influence urinary outflow—particularly in pathological conditions such as benign prostatic hyperplasia (BPH)—although it does not directly contribute to the physiological processes of storage or release. The ureters transport urine from the kidneys to the bladder but are not directly implicated in the generation of lower urinary tract symptoms (LUTS).

Histologically, the bladder comprises several layers: the urothelium, which provides barrier and sensory functions; the lamina propria, containing connective tissue, vasculature, and immune cells; the muscularis propria (detrusor muscle), responsible for bladder contraction; and an outer adventitia or serosa. A review by Birder and Andersson (2013) highlights how disruption within any of these compartments can impair bladder function and contribute to LUTS.

LUTS are broadly categorised into:

- Storage symptoms: urgency, frequency, nocturia
- Voiding symptoms: weak stream, hesitancy, straining
- Post-micturition symptoms: dribbling, sensation of incomplete emptying

(*See Table A1 for full classification*)

These symptoms arise from diverse, often overlapping, pathophysiological mechanisms. For instance, interstitial cystitis/bladder pain syndrome (IC/BPS) is characterised by substantial heterogeneity in epithelial barrier integrity, sensory signalling, apoptosis, and—in some cases—mast cell activity. These mechanisms are outlined in a review by Cervigni and Natale (2014), with additional support from primary research by Lee, Jiang and Kuo (2013). In contrast, BPH represents a distinct mechanistic pathway where prostate enlargement obstructs the urethra and alters detrusor function, as described in the review by Roehrborn (2005). Infectious processes such as urinary tract infections (UTIs) also contribute to LUTS;

a review by Flores-Mireles et al. (2015) summarises the mechanisms by which uropathogens initiate urothelial inflammation and, in recurrent cases, disrupt deeper bladder layers.

Understanding the anatomical basis and mechanistic diversity underlying LUTS provides essential context for interpreting chronic bladder symptoms and highlights why conditions such as BPS pose ongoing diagnostic challenges.

### 1.1.1 Acute LUTS: Causes and Mechanisms

Acute LUTS typically present with sudden onset and are most commonly associated with transient inflammatory or infectious processes. These symptoms usually resolve once the underlying cause is addressed.

The most frequent cause of acute LUTS is urinary tract infection (UTI), especially among women. Epidemiological evidence from a review by Foxman (2010) indicates that more than 50% of women experience a UTI during their lifetime. Acute cystitis produces dysuria, urgency, and frequency, most often due to uropathogenic *Escherichia coli* (*E. coli*). Primary research by Mulvey et al. (1998), supported by the review by Flores-Mireles et al. (2015), demonstrates how *E. coli* adheres to the urothelium and triggers local inflammation.

Some individuals develop recurrent UTIs (rUTIs), defined by multiple symptomatic infections within a short timeframe. Primary studies by Hooton et al. (1996), supported by Flores-Mireles et al. (2015), indicate that rUTIs reflect persistent mucosal inflammation or bacterial reservoirs, often influenced by predisposing factors such as incomplete bladder emptying or anatomical abnormalities. Other bacteria-related conditions—such as catheter-associated UTI (CAUTI) or asymptomatic bacteriuria—show distinct clinical and mechanistic features, with CAUTIs frequently involving polymicrobial biofilms on indwelling devices and asymptomatic bacteriuria characterised by colonisation without inflammatory response.

In men, acute LUTS may also arise from acute bacterial prostatitis, typically caused by gram-negative organisms including *E. coli*. A clinical review by Beland, Martin and Han (2022) describes how this condition presents with pelvic pain, dysuria, and systemic features, and notes that persistent inflammation may evolve into chronic pelvic pain.

In summary, acute LUTS most commonly reflect short-term inflammatory or infectious stimuli and generally resolve with treatment. These mechanisms differ substantially from the persistent, multifactorial disruptions seen in chronic bladder syndromes such as BPS/IC, where symptoms persist despite the absence of overt infection. This distinction highlights the need to differentiate transient causes of LUTS from chronic bladder-centric conditions such as BPS.

### 1.1.2 Chronic LUTS: Long-term Conditions and Contributing Factors

Chronic LUTS refer to persistent urinary symptoms lasting several weeks or longer and may arise gradually or abruptly but persist due to ongoing structural, neurological, or functional disturbances. Symptoms include urgency, frequency, nocturia, incomplete emptying, and in some syndromes, bladder pain.

When an identifiable aetiology is present, chronic LUTS may result from direct tissue injury, inflammation, or obstruction. Ketamine-induced cystitis is one example, characterised by severe frequency, urgency, pain, and reduced bladder capacity. The pathophysiology and clinical features of this condition are detailed in the review by Jhang, Birder and Kuo (2023). In men, BPH is another common cause, where progressive prostate enlargement obstructs urinary outflow and alters detrusor function. This is discussed in the clinical review by Beland, Martin and Han (2022).

Neurological disorders—including Parkinson's disease, multiple sclerosis, and spinal cord injury—represent a further category of chronic LUTS. A review by Gajewski and Drake (2018) outlines how disruption of central or peripheral neural pathways can result in varied presentations ranging from detrusor overactivity to urinary retention. Symptom variability and burden across neurological groups are further highlighted in primary research by Torelli et al. (2015).

Finally, chronic symptom-based syndromes such as overactive bladder (OAB) and bladder pain syndrome (BPS) present with LUTS in the absence of clear structural or infectious causes. These conditions share overlapping symptoms—including urgency and frequency—with BPS additionally characterised by bladder-centric pain often exacerbated by filling. The

impact of these syndromes on quality of life is described in a review by Haylen et al. (2010), which also emphasises the need for more refined diagnostic tools.

Taken together, chronic LUTS encompass a wide spectrum of mechanistic pathways, from structural obstruction and neurological dysfunction to complex idiopathic syndromes. These examples illustrate how chronic LUTS arise from diverse and multifactorial mechanisms, underscoring the difficulty of diagnosing bladder-specific syndromes such as BPS based on symptoms alone.

### 1.1.3 Clinical Relevance of Chronic LUTS and BPS

Understanding the clinical significance of chronic lower urinary tract symptoms (LUTS) is vital due to their high prevalence, complex presentation, and substantial impact on patient quality of life and healthcare systems. In the UK alone, bladder dysfunction affects an estimated 14 million people, with chronic conditions such as overactive bladder, bladder pain syndrome (BPS), and urinary incontinence contributing significantly to healthcare utilisation and patient morbidity (NHS England, 2018; Buckley and Lapitan, 2009).
Bladder Pain Syndrome (BPS) is a chronic LUTS manifestation marked primarily by persistent or recurrent bladder-associated pain, urinary urgency, and frequency, in the absence of identifiable infection or overt pathology. Unlike acute conditions such as urinary tract infections (UTIs), where microbial causes are typically identifiable and reversible, BPS is defined by exclusion and characterised by diagnostic ambiguity and symptom overlap with other urological syndromes. A key distinction lies in the chronicity of pain symptoms, their exacerbation with bladder filling, and the absence of response to antimicrobial therapy. Despite decades of research, the true prevalence of BPS remains uncertain due to heterogeneity in diagnostic criteria and study design. Population-based studies in Europe report relatively low estimates (e.g., 1.22%; Hakimi et al., 2017), while higher rates have been observed in clinical cohorts (e.g., 16.4% in Spanish women; Morales-Solchaga et al., 2019). In the United States, the RAND Interstitial Cystitis Epidemiology (RICE) study found that approximately 6.5% of adult women met symptom-based criteria for BPS (Clemens et al., 2005). This wide variability underscores the absence of a unified diagnostic standard and highlights the challenges of estimating disease burden and ensuring consistent clinical identification.

Reflecting these diagnostic uncertainties, the 2023 European Association of Urology (EAU) Guidelines reaffirm that BPS remains a clinical diagnosis, made only after the exclusion of other identifiable urological conditions (European Association of Urology, n.d.). The lack of objective diagnostic tools often leads to delays in recognition and treatment, contributing to patient frustration and decreased quality of life.

While symptom-based frameworks remain important for initial clinical assessment, the field is increasingly shifting toward objective, molecular-level stratification. The current study responds to this unmet need—not by developing symptom-based criteria—but by applying unbiased transcriptomic profiling to identify molecular signatures associated with BPS and its phenotypic subtypes. By comparing gene expression patterns in well-characterised urothelial samples, this research aims to uncover disease-specific biomarkers involved in pathogenic mechanisms and ultimately facilitate a more precise classification system for BPS within the broader spectrum of chronic LUTS. This approach may support the development of future diagnostic and therapeutic tools tailored to specific molecular phenotypes of the syndrome.

## 1.2 Chronic Pelvic Pain and Its Relationship to Bladder Pain Syndrome

Chronic pelvic pain (CPP) is a complex and often debilitating symptom that frequently co-occurs with lower urinary tract symptoms (LUTS), particularly in conditions such as Bladder Pain Syndrome (BPS). Defined as pain perceived in pelvic structures lasting for at least three months (or six months if cyclical), CPP can affect individuals of any sex and poses considerable diagnostic and therapeutic challenges due to its heterogeneous aetiologies and overlapping symptomatology (European Association of Urology, n.d.– *clinical guideline*).

According to the European Association of Urology, CPP is categorised into two principal forms:

- Chronic Secondary Pelvic Pain, in which the pain can be attributed to a specific underlying pathology such as infection, malignancy, or drug-induced bladder damage (e.g. ketamine-associated cystitis); and
- Chronic Primary Pelvic Pain, where no identifiable pathology is present despite evident functional disturbances and biological dysregulation, such as neuroinflammation or altered sensory signalling.

The latter group encompasses Chronic Primary Pelvic Pain Syndromes (CPPPS), which are considered multifactorial and involve nociceptive, neuropathic, and often central sensitisation

mechanisms. These conditions frequently span across organ systems, affecting not only the urinary tract but also gastrointestinal and reproductive domains. Psychological and behavioural comorbidities—including anxiety, catastrophising, and maladaptive coping strategies—are commonly implicated in both the severity and chronicity of symptoms.

The clinical heterogeneity of CPPPS complicates both diagnosis and management, often requiring a multidisciplinary and individualised approach. Importantly, Bladder Pain Syndrome represents a key urological manifestation within the CPPPS spectrum. It exemplifies the diagnostic ambiguity and symptom overlap characteristic of primary pelvic pain disorders, highlighting the need for improved mechanistic understanding and the development of objective molecular markers.

This conceptual framework provides the rationale for the current investigation, which seeks to understand further BPS through transcriptomic profiling of bladder tissues. By placing BPS within the broader context of CPP, this section establishes the clinical relevance and research necessity for subclassifying such syndromes based on molecular features.

Taken together, the mechanisms underlying chronic LUTS, and chronic pelvic pain illustrate a spectrum of overlapping but biologically diverse conditions in which symptoms alone rarely indicate the precise underlying cause. Within this spectrum, Bladder Pain Syndrome (BPS) emerges as one of the most challenging entities to diagnose and classify, due to its symptom overlap with other pelvic pain disorders and the absence of objective biomarkers or consistently identifiable pathology. This complexity reinforces the need for a framework that integrates clinical presentation with underlying biological mechanisms. The following section therefore builds on the CPPPS context outlined above and examines how BPS has been conceptualised, defined, and classified within chronic primary pelvic pain syndromes, highlighting the ongoing challenges that motivate molecular-level investigations such as those undertaken in this thesis.

## 1.3 Bladder Pain Syndrome in the Context of Chronic Primary Pelvic Pain Syndromes

As outlined in Sections 1.1.3 and 1.2, Bladder Pain Syndrome (BPS) is recognised as a urological subtype within the Chronic Primary Pelvic Pain Syndromes (CPPPS). It is defined

by pain perceived in the bladder region, accompanied by urinary symptoms such as urgency, frequency and discomfort during bladder filling, in the absence of infection or overt pathology (European Association of Urology, n.d. – clinical guideline). Because diagnosis relies on symptom profiles and the exclusion of other causes, BPS remains a clinically ambiguous condition with variable definitions across regions and guidelines.

Historically, several overlapping terms—including interstitial cystitis (IC) and painful bladder syndrome (PBS)—were used to describe similar presentations. To address this inconsistency, a report by Abrams, Cardozo and Fall (2002) from the International Continence Society recommended the unified term "bladder pain syndrome". This represented an early effort to standardise terminology across clinical and research settings.

Further classification was proposed in an expert consensus by van de Merwe et al. (2008) on behalf of the European Society for the Study of Interstitial Cystitis (ESSIC). This system stratified patients based on cystoscopic appearance and histological abnormalities, distinguishing those with mucosal changes or inflammatory findings from those without visible pathology. Although influential in research contexts, this approach has not been universally adopted in clinical practice.

A key point of divergence internationally concerns Hunner lesions—distinct inflammatory bladder lesions historically associated with classical interstitial cystitis. Expert consensus in East Asia, such as that described by Homma et al. (2020), distinguishes Hunner-type and non-Hunner-type IC as separate clinical entities. By contrast, other bodies, including the European Association of Urology (*n.d.* – clinical guideline), consider Hunner lesions as defining a specific inflammatory phenotype within the broader BPS spectrum rather than representing a separate diagnosis. This reflects ongoing disagreement regarding whether BPS is best understood as a single syndrome with multiple subtypes or a collection of related but distinct conditions.

Efforts to harmonise definitions have been documented in a review by Hanno and Dmochowski (2009), which summarised discussions from an international consensus workshop. Their report highlighted persistent inconsistencies in diagnostic thresholds—including symptom duration, the role of cystoscopy, and the necessity for biopsy—which continue to hinder cross-study comparison, epidemiological accuracy and biomarker validation.

Together, these evolving frameworks reveal ongoing uncertainty regarding the optimal classification of BPS. The absence of standardised diagnostic criteria contributes to highly variable prevalence estimates and inconsistent reporting of clinical subtypes. Consequently, BPS is increasingly recognised not simply as a clinically defined condition but as a biologically heterogeneous syndrome. This perspective underscores the need for molecular approaches capable of identifying underlying biological subgroups—particularly distinctions such as Hunner versus non-Hunner phenotypes—to support more targeted diagnostic and therapeutic strategies.

### 1.3.1 Epidemiology of Bladder Pain Syndrome

As outlined in Section 1.1.3, prevalence estimates for bladder pain syndrome (BPS) vary widely across studies and regions, largely due to inconsistent diagnostic definitions and differing research methodologies. This lack of standardisation complicates attempts to determine the true global burden of the condition.

Early epidemiological characterisation stemmed from work by the National Institute of Diabetes and Digestive and Kidney Diseases (NIDDK) in the late 1980s. A primary research study by Gillenwater and Wein (1988) defined interstitial cystitis (IC) using stringent cystoscopic and histopathological criteria, including glomerulations and Hunner lesions. However, a clinical review by Parsons (2002) later demonstrated that these criteria applied to fewer than 10% of symptomatic patients, excluding many individuals with bladder-associated chronic pelvic pain and revealing that the NIDDK definition captured only a narrow subset of the broader clinical spectrum.

A key shift occurred when the International Continence Society (ICS) introduced the term “bladder pain syndrome” and proposed a more inclusive symptom-based definition: suprapubic pain related to bladder filling, accompanied by frequency and urgency, not attributable to other pathology. This redefinition, presented in the review by Abrams, Cardozo and Fall (2002), expanded the diagnostic window but increased variability in prevalence estimates due to broader case inclusion.

Recent epidemiological studies illustrate this variability. A cross-sectional community-based study by Hakimi et al. (2017) across five European countries reported a prevalence of

approximately 1.2%. In contrast, Morales-Solchaga et al. (2019) identified a prevalence of 16.4% among women attending functional urology units in Spain. In the United States, primary research by Clemens et al. (2005) using symptom-based RAND Interstitial Cystitis Epidemiology (RICE) criteria estimated a prevalence of 6.5% in adult women. These differences reflect the impact of varying diagnostic frameworks, population types, and study methodologies.

Further complexity arises from gender disparities. A review by Meijlink (2014) highlighted that women are disproportionately diagnosed with BPS, partly due to historically female-focused diagnostic constructs and under-recognition of male presentations. Such inconsistencies complicate accurate prevalence estimation and may affect access to timely diagnosis and treatment.

Together, these findings underscore the need for harmonised diagnostic standards that enable reliable epidemiological assessment and facilitate comparable research across regions and healthcare systems. To support clarity, Table 1.3.1 summarises key prevalence estimates from major epidemiological studies, highlighting the influence of differing diagnostic criteria and population sampling.

**Table 1.3.1.** Key epidemiological and diagnostic studies contributing to variability in reported prevalence of Bladder Pain Syndrome (BPS).
Studies marked as "Not reported" are included because their diagnostic definitions or methodological frameworks substantially influenced subsequent prevalence estimates.

| **Study / Region** | **Diagnostic Criteria Used** | **Population Type** | **Prevalence Estimate** | **Notes** |
|---|---|---|---|---|
| **Gillenwater and Wein (1988)** | NIDDK cystoscopic + histopathological criteria | Clinical | **<10% of symptomatic patients** | Very strict criteria; excluded majority of clinically suspected BPS cases |

| | | | | |
|---|---|---|---|---|
| **Parsons (2002)** | Review of NIDDK criteria | Clinical | **Not reported (diagnostic criteria review)** | Demonstrated NIDDK criteria apply to <10% of patients |
| **Abrams, Cardozo and Fall (2002)** | ICS symptom-based definition | Mixed | **Not reported (definition paper)** | Broadened diagnostic definition of BPS |
| **Hakimi et al. (2017)** | Symptom-based questionnaire | General population (5 EU countries) | **~1.2%** | Community-based prevalence estimate |
| **Morales-Solchaga et al. (2019)** | Clinical diagnosis | Functional urology units (Spain) | **16.4%** | Higher estimate due to specialist clinical cohort |
| **Clemens et al. (2005)** | RICE symptom-based criteria | US adult women | **6.5%** | Large-scale population screening |
| **Meijlink (2014)** | Review | Mixed | **Not reported (review)** | Highlights gender disparities in diagnosis |

### 1.3.2 Diagnosis of Bladder Pain Syndrome

Diagnosing Bladder Pain Syndrome (BPS) remains challenging because it is fundamentally a diagnosis of exclusion. There is no single definitive test or biomarker; instead, BPS is identified after ruling out alternative causes of bladder-related pain and urinary symptoms, such as urinary tract infection, bladder cancer, overactive bladder, endometriosis, or radiation-induced cystitis, as outlined in the clinical guidelines of the European Association

of Urology (n.d.). This exclusion-based approach reflects both the syndrome's heterogeneity and the persistent lack of universally accepted diagnostic criteria.

Cystoscopy—with or without hydrodistension—is frequently used to inspect the bladder mucosa for abnormalities. Two findings are commonly described: glomerulations (petechial haemorrhages) and Hunner lesions, the latter representing a distinct inflammatory lesion associated with a well-defined subtype of the condition. Although Hunner lesions are relatively specific, they occur in only about 10–20% of patients (Clemens et al., 2022), and their absence does not exclude a BPS diagnosis. Glomerulations, by contrast, lack specificity and also appear in other conditions such as radiation cystitis, limiting their diagnostic utility. Primary research by Cox et al. (2016) suggests that Hunner lesions can be identified during baseline cystoscopy without the need for hydrodistension, raising questions about the necessity of this procedure in routine practice.

Bladder biopsy may be undertaken when malignancy or alternative diagnoses must be excluded. Histological findings in BPS—including urothelial denudation, mast cell infiltration, inflammation, and submucosal fibrosis—are variably present and not specific to the condition, further limiting their diagnostic value.

Given these limitations, research has increasingly focused on urinary biomarkers to improve diagnostic precision and support phenotypic stratification. Studies have examined molecules such as cytokines, chemokines, and nerve growth factor as potential non-invasive indicators of underlying pathology. For example, Jiang, Jhang and Hsu (2022) reported biomarker–symptom correlations and associations with lesion subtype, suggesting that urinary assays may assist in distinguishing biologically meaningful subgroups.

Overall, the diagnostic landscape of BPS remains complex, but emerging evidence from biomarker research highlights the potential for more objective and stratified approaches that move beyond reliance on exclusion and variable cystoscopic findings.

### 1.3.3 Management of Bladder Pain Syndrome

The management of Bladder Pain Syndrome (BPS) requires a personalised and multimodal approach that reflects its heterogeneous presentations and variable treatment responses.

Clinical guidelines developed through systematic review and expert consensus (Clemens et al., 2022), alongside those published by the European Association of Urology (n.d. – clinical guideline), recommend a tiered treatment strategy that progresses from conservative measures to more invasive interventions according to symptom severity and patient phenotype.

First-line management focuses on conservative, non-pharmacological interventions such as dietary modification, stress reduction, behavioural therapies, and pelvic floor physical therapy. These strategies aim to reduce modifiable triggers and improve pelvic function, particularly in patients without visible cystoscopic lesions. The American Urological Association (AUA) guidelines emphasise these approaches as the initial standard of care (Clemens et al., 2022).

If conservative management fails, second-line treatments include oral pharmacotherapies such as pentosan polysulfate sodium (PPS), proposed to restore the glycosaminoglycan (GAG) layer of the urothelium, and antihistamines such as hydroxyzine, which may target mast cell-mediated inflammation. However, a meta-analysis by Chermansky and Guirguis (2022), together with findings summarised in the review by Clemens et al. (2022), shows considerable variability in clinical response, underscoring the need for improved patient stratification and biomarker-guided therapy.

Intravesical therapies—including dimethyl sulfoxide (DMSO) and heparin—deliver anti-inflammatory agents directly to the bladder and can benefit selected patients, particularly those with presumed epithelial barrier dysfunction. These options remain symptomatic rather than disease-modifying and often require repeated administration (Clemens et al., 2022). More refined phenotyping may help identify patients most likely to benefit from these treatments.

For individuals unresponsive to standard pharmacological therapy, neuromodulation techniques such as sacral nerve stimulation (SNS), posterior tibial nerve stimulation (PTNS), and pudendal nerve stimulation may alleviate pain and urinary symptoms by modulating afferent pathways. A narrative synthesis by Padilla-Fernández, Hernández-Hernández and Castro-Díaz (2022) highlights their therapeutic potential, although these interventions are limited by cost, resource availability, and variable patient accessibility.

Among emerging treatments, intravesical botulinum toxin A (BoNT-A) has shown moderate efficacy in non-Hunner BPS cohorts. A review by Jhang (2019) describes its mechanisms—primarily inhibition of neurotransmitter release and modulation of inflammation—while primary research by Jiang, Jhang and Hsu (2022) demonstrates symptom improvement in selected patients, albeit with risks such as urinary retention and infection.

Investigational therapies continue to expand. A review by Dayem et al. (2022) discusses the potential of extracellular vesicles derived from stem cells to support urothelial repair and immune regulation. Additional novel approaches include immune-modulating vaccine candidates (Augé et al., 2021) and the development of small molecules such as brimapitide, assessed in early-stage evaluation by Taubert, van der Aa and Heesakkers (2024).

Ultimately, optimising BPS management depends on accurate identification of underlying phenotypes. Distinguishing Hunner-type from non-Hunner BPS is essential, as lesion-directed interventions such as fulguration or intralesional corticosteroids benefit only the former. As biomarker and molecular profiling research advances, increasingly individualised treatment strategies aligned with underlying pathophysiology may improve outcomes for this complex syndrome.

### 1.3.4 Classification and Phenotyping of Bladder Pain Syndrome (BPS)

Efforts to classify Bladder Pain Syndrome (BPS) aim not only to distinguish it from other causes of chronic pelvic pain but also to delineate clinically meaningful subgroups that may reflect differing underlying mechanisms and therapeutic responses. Accurate subclassification is therefore essential—not to identify a single unifying biomarker, but to capture the syndrome's phenotypic and biological heterogeneity. However, despite sustained interest, current frameworks lack consensus and uniform clinical application, leading to variability in diagnosis and research interpretation, as outlined in the comprehensive review by van de Merwe et al. (2008) and reiterated in the recent guideline review by Clemens et al. (2022).

A pivotal contribution came from the European Society for the Study of Interstitial Cystitis (ESSIC), which proposed a classification system based on cystoscopic and histopathological findings. This system distinguishes Hunner-type BPS—characterised by visible inflammatory

lesions—from non-Hunner BPS, where mucosal lesions are absent despite bladder-centric symptoms (van de Merwe et al., 2008). Although widely used in research, subsequent evidence has refined this model. A review by Akiyama and Hanno (2019) and clinical studies by Jiang, Jhang and Hsu (2022) highlight that Hunner-type BPS represents a distinct pathological entity, marked by pronounced inflammation and favourable response to lesion-directed therapies such as fulguration or intralesional corticosteroids.

Histologically, Hunner-type BPS is associated with epithelial denudation, mast cell infiltration, and deep lamina propria inflammation, often corresponding with more severe symptom burden. In contrast, non-Hunner BPS shows no characteristic cystoscopic pathology and is primarily diagnosed on clinical grounds. Its mechanisms are less well defined and likely involve a combination of urothelial dysfunction, neuroimmune activation, and central sensitisation (Jiang, Jhang and Hsu, 2022).

Reliance on cystoscopy with hydrodistension introduces additional practical limitations: the procedure is invasive, may exacerbate symptoms, and yields non-specific findings such as glomerulations, which also occur in conditions including radiation cystitis and bacterial cystitis (Cox et al., 2016). This reduces its value as a universal classification tool and underscores the need for more objective biological measures.

Further reviews, such as Homma et al. (2020), have emphasised that BPS encompasses a wide symptom spectrum—from focal bladder pain to broader pelvic discomfort, urgency, and psychosocial distress—reinforcing the inadequacy of classification systems based solely on visual or histological criteria. As a result, emerging biomarker-based approaches are gaining importance. A 2024 study by Akshay et al. applied machine learning to urinary transcriptomic profiles, enabling molecular stratification of non-ulcerative BPS patients, (Akshay et al., 2024), while Jiang, Jhang and Hsu (2022) demonstrated that urinary cytokine and chemokine signatures may help differentiate biologically distinct subgroups. Together, these findings indicate that integrating clinical, endoscopic, and molecular tools can support a more precise, phenotype-driven classification system.

Ultimately, advancing BPS classification will require an integrated multimodal framework that accounts for symptom heterogeneity, cystoscopic findings, histopathology, and molecular signatures. Such an approach offers the potential for more accurate diagnosis and targeted, mechanism-informed therapy.

Although several transcriptomic studies have examined bladder tissue in BPS, most have relied on small sample sizes, broad diagnostic categories, or targeted analyses of predefined pathways. Few have integrated transcriptomic data with detailed clinical metadata—such as cystoscopic phenotype, trans-epithelial resistance, histology, and validated symptom scores—within the same individuals. This thesis addresses these gaps by (i) re-evaluating literature-derived candidate biomarkers in a clinically well-characterised patient cohort, (ii) applying unbiased whole-transcriptome analysis to identify individual-level molecular heterogeneity, and (iii) examining whether molecular profiles align with clinical phenotypes such as Hunner-type and non-Hunner disease. This combined approach moves beyond population-level averages toward a more personalised understanding of BPS biology.

## 1.4 Project Aims and Objectives

Building on the conceptual and methodological gaps identified in the preceding sections, this project formulates the following research question and objectives to advance the molecular characterisation of BPS.

### 1.4.1 Research Question

In clinical and experimental studies of Bladder Pain Syndrome (BPS) can differentially expressed molecules (gene/transcript/protein) provide unbiased markers for diagnosis, prognosis, and therapeutic targeting of disease subsets?

### 1.4.2 Aims

The limitations of current classification frameworks and the heterogeneity of clinical presentations in BPS demonstrate the need for more refined molecular approaches to characterise the condition. This project aims to contribute to these efforts by examining differential gene, transcript, and protein expression patterns associated with BPS in both human and experimental contexts. The goal is to uncover molecular signatures that could

improve disease stratification and aid in the development of objective, non-invasive diagnostic tools.

By mapping these expression differences, the study seeks to enhance our understanding of the distinct biological pathways involved in BPS and to identify candidate biomarkers that may serve future clinical applications.

More specifically, this study aims to:

- **Identify differentially expressed molecules** (genes, transcripts, and proteins) associated with BPS through a systematic review and molecular profiling of human bladder tissue samples.
- **Characterise the differential expression patterns** of these molecular markers in relation to known clinical variability in BPS, including bladder-centric (e.g., lesion-present) and non-lesion phenotypes, without presuming fixed subtypes.
- **Explore the diagnostic, prognostic, and therapeutic relevance** of identified molecular features to inform future precision medicine approaches in BPS management.

### 1.4.3 Objectives

To address the study aims outlined in Section 1.4.2, this project is guided by the following objectives, each of which aligns with specific sections of the thesis:

1. **To conduct a systematic review** of transcriptomic and proteomic studies investigating bladder pain syndrome (BPS), with the goal of identifying candidate biomarkers and molecular pathways implicated in disease pathophysiology.
   → *This objective is addressed in* Chapter 2: Literature Review of Candidate Biomarkers for Bladder Pain Syndrome (*Sections 2.2–2.5*).
2. **To evaluate the expression of selected literature-derived candidate genes** in primary human bladder tissue using in-house transcriptomic data, comparing BPS and non-BPS samples to detect expression patterns associated with BPS.

→ *This objective is addressed in* Chapter 3: Evaluation of Literature-Derived Biomarkers in In-House BPS Data (*Sections 3.1–3.5*).

3. **To synthesise transcriptomic findings** across multiple biological pathways (e.g., immune, neurogenic, apoptotic, barrier-related) in order to identify candidate molecular subtypes within BPS.

   → *This objective is addressed in* Section 3.5: Transcriptomic Insights into BPS Pathophysiology: A Synthesis of In-House Findings.

4. **To integrate gene expression data with available clinical metadata** (e.g., symptom scores, histology, cystoscopy findings) to explore associations between molecular profiles and clinical phenotypes, and to assess the potential of a stratified, subtype-based framework for diagnosis and treatment.

   → *This objective is addressed in* Chapter 4: Discussion

# Chapter 2: Literature Review of Candidate Biomarkers for Bladder Pain Syndrome

## 2.1 Introduction

Given the clinical and biological complexity of Bladder Pain Syndrome (BPS), there is a pressing need to better understand the molecular pathways contributing to its onset, progression, and phenotypic variability. This chapter presents a systematic review of the current literature focusing on differentially expressed genes, transcripts, and proteins reported in BPS research. The aim is to identify molecular markers relevant to BPS pathophysiology and highlight candidates with potential diagnostic or therapeutic utility.

To achieve this, the review applied clearly defined eligibility criteria, a structured search strategy, and systematic data extraction procedures. While the methodological approach ensures transparency and reproducibility, it also reflects practical constraints common to single-reviewer systematic reviews, which are discussed further below. By collating and critically analysing the available primary research, this chapter establishes the molecular landscape from which candidate biomarkers were selected for further exploration in Chapter 3 using patient-derived datasets.

## 2.2 Methods

### Eligibility criteria

The inclusion and exclusion criteria were designed to capture a comprehensive yet focused body of primary research investigating molecular insights into benign uropathies, with specific attention to BPS. Studies were included irrespective of publication date if they employed experimental (in vivo or in vitro) or clinical designs (cohort, case–control, cross-sectional, comparative, or observational) and addressed molecular characterisation of BPS. Eligible studies reported differential expression of molecules, explored molecular pathways involved in BPS pathogenesis, or assessed biomarkers relevant to diagnosis, prognosis, or therapy.

Exclusion criteria removed studies focused exclusively on malignant uropathies, unrelated benign conditions, non-molecular investigations, non-primary research (reviews, editorials, commentaries), and non-English publications. Studies were grouped according to the BPS-related pathophysiological mechanisms they investigated, providing a structured basis for synthesising molecular findings.

**Search strategy**

Database searches were conducted in PubMed and the Cochrane Library to identify studies investigating molecular mechanisms and biomarkers associated with BPS and related chronic lower urinary tract disorders.

PubMed search terms:
*(bladder pain syndrome OR painful bladder syndrome OR interstitial cystitis OR overactive bladder OR bladder overactivity)*
AND *(sensory OR immunological OR inflammatory OR immune response OR cytokines OR chemokines OR receptors OR ion channels OR neuropeptides)*
AND *(pathophysiology OR pathogenesis OR molecular mechanisms OR cellular processes OR signalling pathways OR inflammation)*.
Filters restricted results to English-language publications and relevant study types (clinical trials, observational studies, comparative studies, randomised controlled trials).

Cochrane Library:
Search terms were adapted to database syntax but retained the same conceptual framework and Boolean structure. Searches were restricted to English-language entries and clinical trials.

The final search update for all databases was completed on 24 November 2024.

Although PubMed and Cochrane capture the majority of clinically focused literature, limiting the search to these two databases introduces the risk of missing mechanistic or omics-focused studies commonly indexed in platforms such as EMBASE, Scopus, Web of Science, or grey literature repositories. This limitation is acknowledged and revisited in the Discussion.

**Screening and Study Selection**

All retrieved records underwent title and abstract screening to determine preliminary eligibility. Studies meeting initial criteria proceeded to full-text review. Screening decisions

were guided by predefined inclusion parameters based on the SPIDER framework (see Table A2), incorporating study design, population characteristics, molecular outcomes, and relevance to the research question. Only studies employing molecular, transcriptomic, or proteomic techniques to explore BPS-related mechanisms were included.

Screening and eligibility assessments were performed manually by a single reviewer. While common in student-led systematic reviews, this approach carries a risk of selection bias. To mitigate this, strict and consistent application of inclusion/exclusion criteria, detailed documentation of decision-making, and use of standardised evaluation procedures were maintained throughout. No automation tools or machine-assisted screening methods were used. The implications of single-reviewer screening are further considered in the Discussion.

**Data Extraction and Preparation for Review**

Summary statistics were extracted manually from study tables and figures where available. When necessary, values were converted or normalised to allow meaningful comparison across studies with differing measurement units or reporting formats. All molecules were mapped to their corresponding human genes using HGNC-approved nomenclature, (HUGO Gene Nomenclature Committee, HGNC, n.d), ensuring consistency with the in-house transcriptomic analyses presented in later chapters.

Metrics that could not be directly compared across studies were excluded from quantitative summaries but were retained within the narrative synthesis to preserve contextual depth.

**Tabulation and Visualisation of Results**

Key findings—including reported molecular markers, pathways, and candidate biomarkers—were tabulated to facilitate comparison across studies. Visualisations such as bar charts were generated using Microsoft Excel to summarise differential expression patterns and pathway involvement. Gene-level annotations were incorporated using the Human Protein Atlas to enhance interpretability and ensure alignment with subsequent analyses.

**Synthesis of Results and Rationale**

Given the heterogeneity of molecular targets, study designs, and experimental approaches, a narrative synthesis was adopted. A meta-analysis was not feasible due to substantial variability in molecular endpoints, methodological approaches, and tissue sources. The

narrative method enabled integration of diverse findings and supported identification of convergent molecular themes relevant to BPS pathophysiology.

### Exploration of Heterogeneity

To explore potential sources of heterogeneity, qualitative subgroup comparisons considered factors such as population demographics, experimental model (in vivo vs. in vitro), sample size, and BPS phenotype (e.g., presence or absence of Hunner lesions). Meta-regression was considered but deemed inappropriate given the limited number of studies and diversity of molecular targets. Instead, descriptive comparison enabled identification of technical and biological factors influencing variability in molecular findings.

## 2.3 Results of Systematic Review on Candidate Biomarkers for Bladder Pain Syndrome

### Study selection

A total of 316 records were identified through database searches (PubMed and the Cochrane Library). After removal of 8 duplicates, 308 titles and abstracts were screened for relevance. Of these, 255 were excluded for not meeting the inclusion criteria. Full texts were sought for 53 articles, but 14 could not be accessed due to institutional limitations at the time of review. Thirty-nine full-text articles were assessed for eligibility, and 19 were excluded—8 due to a non-molecular focus and 11 for insufficient relevance to the research question. Ultimately, 20 studies met the predefined criteria and were included in the review. The selection process is summarised in the PRISMA flow diagram (Figure A1). The inaccessibility of some full texts and the modest number of eligible studies should be borne in mind when interpreting the overall strength and generalisability of the evidence.

### Overview of Included Studies

The 20 included studies comprised a mixture of human and animal models and used diverse methodologies, including transcriptomics, proteomics, immunohistochemistry, in vivo experimental cystitis models, and functional assays. Collectively, they interrogated immune and inflammatory signalling, epithelial barrier integrity, neurogenic mechanisms, and

epigenetic regulation. This diversity provides a broad view of potential molecular contributors to BPS but also introduces substantial methodological heterogeneity, which limits the feasibility of quantitative synthesis and complicates direct comparison between studies.

Below, the key molecular contributions of each study are summarised, followed by a comparative appraisal of methodological strengths and limitations.

Zhao et al. (2022) used immunohistochemistry, flow cytometry, and qRT-PCR in experimental autoimmune cystitis and human BPS tissue to show that activation of the *CXCL13*/*CXCR5* axis is associated with heightened bladder inflammation and increased pro-inflammatory cytokine expression, supporting a role for adaptive immune cell recruitment.
Zhang et al. (2023) combined transcriptomic analysis with in vitro assays to demonstrate that *IL17RA* overexpression impairs urothelial proliferation and activates the *TLR4–NLRP3–IL1B* pathway, suggesting a link between Th17-related signalling, immunogenic cell death, and urothelial dysfunction.
Ward et al. (2020) performed proteomic profiling of bladder biopsies from patients with and without Hunner lesions. They identified distinct expression patterns of inflammatory, structural, and endoplasmic reticulum stress–related proteins, indicating divergent molecular mechanisms in Hunner-type versus non-Hunner BPS.

Christmas and Bottazzo (1992) used immunohistochemistry to show increased urothelial HLA-DR expression in interstitial cystitis (IC) patients compared with controls, implying an interferon-γ–driven autoimmune component.

Liu, Jiang and Kuo (2015) examined bladder tissues from BPS, recurrent urinary tract infection, and ketamine cystitis patients using immunofluorescence and TUNEL assays. They reported reduced expression of the junctional protein E-cadherin (encoded by *CDH1*) and increased urothelial apoptosis in IC/BPS and ketamine cystitis, suggesting that epithelial compromise and cell death are shared features of these conditions.
Green et al. (2004) used immunohistochemistry to show increased ICAM1 and VCAM1 expression (encoded by *ICAM1* and *VCAM1*) in IC bladder tissue, correlating with mast cell activity and vascular alterations and supporting a pro-inflammatory microenvironment.
Yang et al. (2012) integrated proteomic and transcriptomic data to investigate the effects of antiproliferative factor (APF) in IC/BPS. They identified multiple APF-regulated molecules

involved in cell adhesion, immune signalling, and cell cycle regulation, positioning APF as a central modulator of urothelial dysfunction.

Shie, Liu and Kuo (2012) focused on inflammation-associated apoptosis and showed that elevated TNF and phosphorylated p38 MAPK (encoded by *TNF* and *MAPK14*) correlate with increased urothelial cell death, linking chronic inflammation to barrier breakdown.

Liu et al. (2012) evaluated mast cell infiltration and expression of *CDH1* and *TJP1* in IC/BPS and overactive bladder. They observed downregulation of E-cadherin and ZO-1 alongside increased inflammation, emphasising the interplay between barrier dysfunction and immune activation.

Lee, Jiang and Kuo (2013) compared bladder biopsies from ketamine cystitis and BPS and found pronounced reductions in *CDH1* expression, increased mast cell activation, and higher levels of apoptosis in both groups, with greater severity in ketamine cystitis, supporting a shared but amplified pathological pathway.

Mukerji et al. (2010) reported increased suburothelial *CNR1*-immunoreactive nerve fibres in BPS and idiopathic detrusor overactivity, suggesting that cannabinoid receptor 1–mediated modulation of sensory signalling may contribute to pain and urgency.

Saban et al. (2000) demonstrated in an antigen-induced cystitis model that TACR1 (neurokinin-1, encoded by *TACR1*) receptor activation enhances bladder inflammation, vascular permeability, and mast cell activation, highlighting substance P–mediated neuroinflammation.

Girard et al. (2012) examined PACAP/VIP signalling in cyclophosphamide-induced cystitis in mice overexpressing nerve growth factor and found altered expression of *ADCYAP1*, *VIP*, *VIPR1*, *VIPR2*, *ADCYAP1R1*, and *NGF* associated with changes in bladder function and inflammation, implicating neuropeptide pathways in neurogenic inflammation.

Chopra et al. (2005) used rat models to show that bradykinin B1 and B2 receptor expression (encoded by *BDKRB1* and *BDKRB2*) increases in inflamed bladder tissue and correlates with elevated inflammatory cytokines such as those encoded by *PTGS2*, *TNF*, *IL6* and *IL1B*, and

with heightened sensory nerve activity, linking bradykinin signalling to pain and bladder hyperactivity.

Peskar et al. (2023) applied RNA sequencing and histology in male and female mouse models of IC/BPS and identified sex-dependent differences in inflammatory gene expression, including *IL6*, *TNF* and chemokine-related genes, along with histological differences, suggesting sex as an important biological modifier.

Kumar et al. (2021) investigated microRNA-mediated regulation in experimental autoimmune cystitis and reported upregulation of microRNAs *miR-146a*, *miR-181*, *miR-1931* and *miR-5112*. These were associated with altered expression of target genes such as *IRAK1*, *TRAF6*, *STAT1*, *STAT3*, *TNF* and *IL2*, together with increased cytokine production and immune cell infiltration, indicating that epigenetic mechanisms contribute to inflammatory amplification.

Kiran, Rakib and Singh (2022) examined *NLRP3* inflammasome activation in cyclophosphamide-induced cystitis and showed that dapansutrile treatment reduced *NLRP3* activity and downstream mediators *IL1B* and *IL18*, alongside reduced pain behaviours, providing proof-of-concept for targeting inflammasome signalling.

Braas et al. (2006) studied PACAP-mediated neuroplasticity in rat cystitis models and demonstrated that increased *ADCYAP1* and *ADCYAP1R1* expression exacerbates bladder dysfunction and alters micturition reflex circuits, linking neuropeptide signalling to sensory plasticity.

Liu and Kuo (2007) evaluated *NGF* expression in BPS patients and showed that intravesical botulinum toxin A and hydrodistension reduced *NGF* levels and were associated with symptomatic improvement, supporting *NGF* as both a biomarker and therapeutic target.

Ostardo et al. (2018) investigated combination treatment with adelmidrol and sodium hyaluronate in cyclophosphamide-induced cystitis. They reported reductions in *NGF* and inflammatory mediators encoded by *TNF*, *IL1B*, *NOS2*, *CCL2* and genes within the *NFKB1* pathway, improved urothelial integrity (including changes in ZO-1 encoded by *TJP1*), and inhibition of NF-κB signalling, reinforcing the centrality of inflammatory and barrier-restorative mechanisms.

To summarise these molecular insights, Table 2.3.1 provides an at-a-glance overview of each included study, indicating (i) the candidate genes examined in this project (mapped via the Human Protein Atlas), (ii) the original molecules or biomarkers highlighted in each study, (iii) the main findings, and (iv) the corresponding reference. This structured summary bridges the literature findings with the experimental focus of the present work and underpins candidate selection for subsequent analyses.

**Table 2.3.1**: Summary of Key Studies Identifying Molecular Biomarkers in Bladder Pain

| **Study** | **Candidate Genes Studied** (Human Protein Atlas) | **Molecule/Biomarker suggested by Study** | **Result suggested by Study** | **Study Reference** |
|---|---|---|---|---|
| **1** | ***CXCL13, CXCR5*** | *CXCL13, CXCR5* | Activation of the *CXCL13/CXCR5* axis correlated positively with elevated levels of pro-inflammatory cytokines | Zhao et al., 2022 |
| **2** | ***TNF, IL17RA, NLRP3, IL1B, IL10*** | *IL17RA* | *IL6* expression increased with *IL17RA* overexpression<br><br>*IL17RA* overexpression upregulated the TLR4-NLRP3-IL1B pathway | Zhang et al., 2023 |
| **3** | ***UBE2L3, UBE2I, HUWE1***<br><br>***EPX, PTPRC, RNASE3, PRG2, HLA-B, PSMD7, HLA-DPB1,*** | *UBE2L3, UBE2I, HUWE1*<br><br>*EPX, PTPRC, RNASE3, PRG2, HLA-B, PSMD7, HLA-DPB1, TXNDC5, MRC1, PRG3* | Decreased in diseased areas of HIC patients compared to NDA areas in HIC patients<br><br>Increased in diseased HIC tissue compared to diseased NHIC tissue (involved in immune response and inflammatory diseases) | Ward et al., 2020 |

| | | | | |
|---|---|---|---|---|
| | ***TXNDC5, MRC1, PRG3*** | | | |
| | ***STT3B, SSR3, RRBP1, DNAJB11, STT3A, LMAN1, TXDNC5, LMAN2, SSR4*** | *STT3B, SSR3, RRBP1, DNAJB11, STT3A, LMAN1, TXDNC5, LMAN2, SSR4* | Increased in diseased HIC tissue compared to diseased NHIC tissue (associated with protein processing in the endoplasmic reticulum) | |
| | ***COL4A6, CTNNA1, CTNND1, COL3A1, COL12A1*** | *COL4A6, CTNNA1, CTNND1, COL3A1, COL12A1* | Decreased in diseased HIC tissue compared to diseased NHIC tissue (involved in collagen formation and cellular adhesion) | |
| | ***HLA-B, CYBB, CTSZ*** | *HLA-B, CYBB, CTSZ* | Altered in NDA HIC tissue compared to NDA NHIC tissue (involved in immune response) | |

| | | | | |
|---|---|---|---|---|
| | ***ALDH4A1, PYGL, HIBADH, BLVRA, PLCD1, ALDH6A1, FAHD1, MAOA, MTHFD1*** | *ALDH4A1, PYGL, HIBADH, BLVRA, PLCD1, ALDH6A1, FAHD1, MAOA, MTHFD1* | Altered in NDA HIC tissue compared to NDA NHIC tissue (involved in protein metabolism) | |
| | ***RALA, PFN2, GNAI1, CTNNB1*** | *RALA, PFN2, GNAI1, CTNNB1* | Altered in NDA HIC tissue compared to NDA NHIC tissue (linked to the Rap1 signalling pathway, which regulates cell proliferation and adhesion) | |
| **4** | ***HLA-DRA, HLA-DRB1, HLA-DPA1, HLA-DPB1, IFNG, STAT1, IRF1, CIITA*** | HLA-DR | Increased HLA-DR expression in the urothelium that could be influenced by IFN-gamma | Christmas and Bottazzo, 1992 |
| **5** | ***CDH1, MAPK14, TNF, CASP3, BAX*** | E-cadherin | Decreased E-cadherin expression/ Increased urothelial apoptosis in IC/BPS associates | Liu, Jiang and Kuo, 2015 |

| | | | | |
|---|---|---|---|---|
| | | | with inflammatory markers, including p38 mitogen-activated protein kinase and TNF-α | |
| **6** | ***ICAM1, VCAM1, TPSAB1, TPSB2, VEGFA*** | ICAM-1 | Increased Expression of ICAM-1 and VCAM-1 that correlates with increased mast cell activity and vascular changes in the bladder wall | Green et al., 2004 |
| **7** | ***TJP1, CLDN4, DSG2, CDKN1A, MKI67, TP53, IL6, MAPK14, HSPA1A*** | APF | Identified 10 potential molecules regulated by APF, including MAPKSP1 and GSPT1, which are downregulated APF evokes an inflammatory response by up-regulating PTGS2/COX-2 | Yang et al., 2012 |
| **8** | ***MAPK14, TNF, IL6, IL1B, CASP3, BAX, CASP8*** | TNF-a | Increased apoptosis in the urothelium correlated with elevated levels of p38 MAPK and TNF-α | Shie, Liu and Kuo, 2012 |

| | | | | |
|---|---|---|---|---|
| **9** | ***CDH1,*** ***TJP1*** | Mast cell infiltration, E-cadherin, Zonula Occludens-1 (ZO-1) | The downregulation of E-cadherin and ZO-1 in IC/BPS is associated with impaired urothelial barrier function and heightened inflammation | Liu et al., 2012 |
| **10** | ***CDH1, TJP1, CASP3, CASP8, BAX, TNF, VEGFA*** | Mast cell infiltration, E-cadherin | E-cadherin expression was significantly reduced in both KC and IC/BPS.<br><br>Increased mast cell activation was observed in both KC and IC/BPS.<br><br>Apoptotic cell numbers were significantly higher in both KC and IC/BPS | Lee, Jiang and Kuo, 2013 |
| **11** | ***CNR1, CNR2, FAAH, TRPV1*** | Cannabinoid receptor 1 (CB1) | Sub urothelial CB1 nerve fibre density was significantly increased in both PBS and IDO patients indicating that cannabinoid receptors may modulate bladder function via nerve activity | Mukerji et al., 2010 |

| | | | | |
|---|---|---|---|---|
| **12** | ***TACR1, TAC1, TNF, IL6*** | NK-1 receptor | NK-1 receptor activation correlated with increased substance P and inflammatory cytokine levels | Saban et al., 2000 |
| **13** | ***ADCYAP1, VIP, VIPR1, VIPR2, ADCYAP1R1, NGF*** | PACAP/VIP and their receptors | PACAP/VIP overexpression correlated with NGF upregulation and bladder dysfunction | Girard et al., 2012 |
| **14** | ***BDKRB1, BDKRB2, PTGS2, TNF, IL6, IL1B*** | Bradykinin B1 and B2 receptors | Increased bradykinin receptor expression correlated with elevated inflammatory cytokines and enhanced sensory nerve activity | Chopra et al., 2005 |
| **15** | ***IL6, TNF, CCL2, CXCL1*** | IL-6, TNF-α, and chemokine-related pathways | Differential gene expression analysis identified key inflammatory markers and sex-based variations in bladder pathology | Peskar et al., 2023 |
| **16** | **miR-146a Targets: *IRAK1, TRAF6,*** | Micro- RNA panel (miR-146a, -181, -1931, -5112) | Dysregulated microRNA expression correlated with altered cytokine levels and immune cell | Kumar et al., 2021 |

| | | | | |
|---|---|---|---|---|
| | ***STAT1, IL6, TNF***<br><br>**miR-181a/b Targets:**<br><br>***PTPN22, STAT3, TNF, IL2*** | | | |
| **17** | ***NLRP3, PYCARD, CASP1, IL1B, IL18, TNF, IL6*** | NLRP3 inflammasome, IL-1β, IL-18 | NLRP3 inhibition correlated with decreased IL-1β and IL-18 levels in bladder tissue reducing inflammation and pain | Kiran, Rakib and Singh, 2022 |
| **18** | ***ADCYAP1, ADCYAP1R1, VIP, VIPR1, VIPR2, NGF*** | PACAP, PACAP receptor | PACAP receptor activation correlated with altered bladder function and neuroplasticity in response to inflammation | Braas et al., 2006 |
| **19** | ***NGF, NTRK1, BDNF, GFRA1*** | NGF (Nerve Growth Factor) | NGF reduction correlated with improvement in pain and bladder function | Liu and Kuo, 2007 |
| **20** | ***NGF, TJP1, TNF, IL1B, NOS2, CCL2, NFKB1*** | NGF, nitrotyrosine, ZO-1, iNOS, IL-1β, MCP-1, NF-κB and IKB-α | Treatment with adelmidrol + sodium hyaluronate significantly reduced NGF, improved | Ostardo et al., 2018 |

| | | | | |
|---|---|---|---|---|
| | | | urothelial integrity (increased nitrotyrosine, reduced ZO-1 expression) and inhibited the NFκB pathway and decreased levels of TNF-α, IL-1β, iNOS and MCP-1 with improvement in symptoms and tissue recovery | |

**Comparative appraisal of included studies**

Across the 20 studies, several patterns and methodological issues emerge. Immune and inflammatory pathways are the most consistently implicated, with convergent evidence from human biopsy studies (e.g. Christmas and Bottazzo, 1992; Green et al., 2004; Ward et al., 2020) and multiple animal models (e.g. Zhao et al., 2022; Kiran, Rakib and Singh, 2022; Ostardo et al., 2018). However, the strength of evidence varies: human studies often rely on small, single-centre cohorts and semi-quantitative histological assessments, whereas animal experiments provide mechanistic depth but may not fully recapitulate chronic human disease.

Findings on epithelial barrier dysfunction and apoptosis are broadly consistent across studies examining *CDH1* and *TJP1* expression and TUNEL staining (Liu et al., 2012; Liu, Jiang and Kuo, 2015; Lee, Jiang and Kuo, 2013), strengthening confidence that barrier compromise is a core feature of BPS and related cystitides. By contrast, neurogenic and epigenetic mechanisms are supported by fewer studies and often by pre-clinical models only (e.g. Mukerji et al., 2010; Braas et al., 2006; Kumar et al., 2021), indicating promising but less mature evidence streams.

Methodological heterogeneity is substantial: tissue sources range from human bladder biopsies to whole-bladder animal preparations; outcome measures vary from protein expression to behavioural pain endpoints; and phenotypic definitions of BPS/IC differ across studies. These differences limit direct comparability and occasionally make it difficult to determine whether reported discrepancies reflect biological variation (e.g. ketamine cystitis versus non-ulcerative BPS) or technical differences in sampling and analysis. Nonetheless, when interpreted collectively, the studies point toward a multi-component model of BPS involving inflammatory, barrier, neurogenic, and regulatory pathways—an integrated view that informs the thematic synthesis presented in Section 2.4 and the candidate selection strategy in Chapter 3.

## 2.4 Synthesis of Findings

### Overview of Molecular Pathways Implicated in BPS

The systematic review revealed that Bladder Pain Syndrome (BPS) is driven by multiple intersecting biological mechanisms, including immune dysregulation, epithelial barrier dysfunction, neurogenic inflammation and broader inflammatory signalling. Across studies, however, the strength of evidence varied considerably, with findings shaped by differences in sample type (human vs. animal), analytic techniques and clinical phenotyping. The following thematic synthesis integrates these mechanisms while critically comparing methodological contributions and limitations.

Immune Dysregulation and Autoimmunity

Several studies support a role for dysregulated or excessive immune activation in BPS, but the depth of evidence differs across decades. Early work by Christmas and Bottazzo (1992)—although limited by small sample sizes and older immunohistochemical methods—identified abnormal expression of HLA-DR, suggesting aberrant antigen presentation in IC/BPS. More recent studies provide stronger mechanistic data, such as Zhang et al. (2023), who showed that overexpression of *IL17RA* activates the TLR4–NLRP3–IL1B pathway, and Zhao et al. (2022), who demonstrated *CXCL13/CXCR5*–mediated immune recruitment.

Comparatively, studies with human tissue (e.g., Ward et al., 2020) offer greater clinical relevance, especially in their demonstration that Hunner-type BPS shows elevated inflammatory protein expression. However, mechanistic insights are limited by cross-sectional design and susceptibility to sampling bias. In contrast, murine autoimmune cystitis models (Zhao et al., 2022, Kumar et al., 2021) provide mechanistic resolution but may overrepresent autoimmune pathways compared with human disease.

Overall, convergent evidence supports immune dysregulation, but the relative contribution of adaptive vs. innate pathways remains unclear due to the heterogeneity of study designs.

Inflammatory Signalling and Cytokine Pathways

Inflammatory signalling was one of the most consistently reported findings, yet studies varied widely in analytic rigour. Multiple groups—including Liu, Jiang and Kuo (2015) and Green et al. (2004)—demonstrated alterations in epithelial–immune interface molecules such as *E*-

*cadherin*, *ICAM1* and *VCAM1*. These human biopsy-based studies provide robust pathological correlation but often lack matched controls or quantification across phenotypes.

Transcriptomic and in vivo studies (e.g., Yang et al., 2012; Shie, Liu and Kuo, 2012) identified upregulation of *TNF*, *MAPK14*, *IL6* and *PTGS2*, confirming activation of canonical inflammatory cascades. Later work by Peskar et al. (2023) expanded this by identifying sex-specific inflammatory signatures—an area previously underexplored.

Comparatively, interventional models such as Kiran, Rakib and Singh (2022) offer compelling evidence that inflammasome inhibition (targeting *NLRP3*, *IL1B*, *IL18*) can reverse symptoms, although cyclophosphamide-induced cystitis may not fully recapitulate human BPS. Similarly, Ostardo et al. (2018) demonstrated that anti-inflammatory treatment restores *ZO-1* and reduces *TNF* and *IL1B*, providing therapeutic validation.

Across studies, inflammatory pathways appear consistently implicated, yet differences in tissue sources, disease models and analytic endpoints create variability in pathway emphasis.

Epithelial Barrier Dysfunction and Apoptosis

Epithelial barrier compromise is one of the most consistently reported findings across human BPS studies. Multiple groups demonstrated reduced expression of key junctional proteins such as *CDH1* (E-cadherin) and *TJP1* (ZO-1), alongside increased apoptosis markers including *CASP3* and *BAX*. For example, Liu et al. (2012) and Liu, Jiang and Kuo (2015) reported concurrent loss of E-cadherin and elevated urothelial apoptosis in patient biopsies, supporting the hypothesis that epithelial weakening facilitates inflammatory infiltration. Lee, Jiang and Kuo (2013) observed even more severe epithelial disruption in ketamine-associated cystitis compared with IC/BPS, including marked downregulation of *CDH1* and extensive urothelial cell death, suggesting an amplified form of barrier failure.

The interaction between inflammation and apoptosis was underscored by Shie, Liu and Kuo (2012), who identified activation of *TNF* and *MAPK14* (p38 MAPK) as a key driver of urothelial apoptosis. These data support an inflammatory–apoptotic feedback loop in which chronic cytokine signalling accelerates epithelial breakdown.

Overall, studies in this thematic group benefit from direct human tissue sampling, which strengthens external validity; however, most rely on semi-quantitative histology or protein

staining, with limited transcriptomic profiling. This constrains molecular resolution and limits definitive conclusions about mechanistic causality. Importantly, epithelial barrier dysfunction appears in both Hunner-type and non-Hunner BPS, but whether it is a primary disease driver, or a secondary consequence of persistent inflammation remains unresolved.

## Neurogenic Inflammation and Sensory Plasticity

Neurogenic contributors to BPS were supported across several experimental and clinical studies. In human bladder biopsies, Mukerji et al. (2010) reported increased *CNR1* (CB1 receptor)-positive nerve fibres in BPS, which corresponded with enhanced nociceptive signalling. Experimental models provided further mechanistic insight: Girard et al. (2012) and Braas et al. (2006) demonstrated that dysregulation of the PACAP/VIP signalling pathway (involving *ADCYAP1*, *VIPR1*, *VIPR2*) induced neuroplastic changes in bladder reflex pathways, contributing to heightened sensory responsiveness. Similarly, Saban et al. (2000) implicated *TACR1* (NK-1 receptor) activation in neurogenic inflammation, while Chopra et al. (2005) showed that inflammatory upregulation of bradykinin receptors (*BDKRB1*, *BDKRB2*) enhances sensory nerve activity and bladder hyperreactivity.

These findings align with clinical symptoms such as pain, urgency and hypersensitivity; however, much of the mechanistic evidence arises from chemically induced cystitis models, which may not fully replicate chronic human BPS. Human studies remain relatively limited in size and scope, underscoring the need for multimodal approaches that integrate neural, immune and epithelial data. Nevertheless, the accumulated evidence strongly suggests that neurogenic signalling contributes to both symptom severity and chronicity in BPS.

## Epigenetic and Regulatory Mechanisms

Epigenetic regulation emerged as an important but underexplored dimension of BPS pathophysiology. The study by Kumar et al. (2021) provided the clearest evidence to date, demonstrating upregulation of several microRNAs—*miR-146a*, *miR-181*, *miR-1931* and *miR-5112*—in an autoimmune cystitis model. These microRNAs targeted inflammatory regulators including *IRAK1*, *TRAF6*, *STAT1* and *TNF*, indicating that post-transcriptional control may

amplify or sustain chronic inflammatory signalling. Their dysregulation was associated with increased cytokine expression and heightened immune cell infiltration, suggesting that epigenetic shifts may help explain interindividual variation in disease severity and treatment response.

Although only one included study directly examined epigenetic pathways, its findings highlight a potentially crucial upstream regulatory layer not captured by protein-level or histological studies. This paucity of epigenetic research represents a notable gap in the current BPS literature and identifies a promising direction for future biomarker discovery and precision medicine approaches.

**Differential Expression of Molecules across BPS Phenotypes**

The heterogeneity of Bladder Pain Syndrome (BPS) is increasingly recognised, with mounting evidence that distinct molecular signatures underpin its various clinical subtypes. Through this systematic review, several key phenotypic distinctions have emerged, particularly among patients with Hunner's lesions (HIC), non-Hunner's BPS, ketamine-associated cystitis, and sex-related differences. These findings contribute to the growing rationale for stratifying BPS based on molecular and histopathological criteria.

Hunner's Lesion vs. Non-Hunner's BPS

Evidence from Ward et al. (2020) indicates that BPS encompasses at least two biologically distinct molecular endotypes. In patients with Hunner's lesions, there was marked upregulation of inflammatory mediators and proteins associated with endoplasmic reticulum (ER) stress, consistent with a more immune-driven and tissue-destructive disease process. In contrast, non-Hunner BPS samples demonstrated comparatively higher expression of adhesion- and structure-related proteins, suggesting relative preservation of epithelial integrity. Together, these findings support the hypothesis that Hunner's lesion disease may represent a distinct inflammatory subtype within the broader BPS spectrum. However, validation in larger, transcriptome-level datasets is needed to confirm the stability and clinical relevance of these molecular distinctions.

### Ketamine-Associated Cystitis

Studies examining ketamine-associated cystitis (KC) provide further evidence of phenotypic divergence within BPS-like bladder conditions. Lee, Jiang and Kuo (2013) reported that KC exhibits a more severe pattern of pathology than non-ulcerative IC/BPS, characterised by pronounced downregulation of *CDH1*, extensive urothelial apoptosis and high levels of mast cell infiltration. These findings indicate that KC shares key pathogenic pathways with IC/BPS—particularly epithelial barrier breakdown and neurogenic inflammation—while also demonstrating exaggerated molecular and histopathological changes that may reflect a distinct aetiology.

### Sex-Related Molecular Differences

Sex-based molecular differences were highlighted by Peskar et al. (2023), who identified divergent inflammatory gene expression profiles between male and female mice with induced IC/BPS. Differential expression of cytokine-related genes such as *IL6* and *TNF*, alongside sex-specific variations in immune cell infiltration and urothelial morphology, suggests that biological sex may modify both the inflammatory response and tissue-level manifestations of disease. Although limited in number, these findings underscore the importance of incorporating sex as a biological variable in future BPS research, particularly given the known sex disparity in clinical prevalence.

## 2.5 Discussion of Systematic Review Findings

### Key Insights

This systematic review demonstrates that Bladder Pain Syndrome (BPS) encompasses multiple intersecting biological processes rather than a single unifying mechanism. Evidence across molecular studies indicates contributions from immune dysregulation, chronic inflammatory signalling, epithelial barrier breakdown, neurogenic inflammation, and upstream regulatory influences such as microRNA-mediated control. The identification of distinct molecular patterns across clinical phenotypes—including Hunner-type BPS, non-Hunner disease, ketamine-associated cystitis, and sex-related differences—supports the concept of biologically meaningful subgroups within the wider BPS population. These findings provide a rationale for stratified diagnostic and therapeutic approaches that better reflect the heterogeneous nature of the condition.

### Limitations of Existing Research

Despite strong thematic convergence across studies, several limitations constrain the strength of current evidence:

- Heterogeneity in study designs and methodologies:
  Variability in tissue sources, experimental platforms, analytical methods, and clinical definitions of BPS reduces comparability across studies and limits the feasibility of quantitative synthesis.

- Limited availability of high-quality human data:
  A substantial proportion of the molecular literature relies on animal or chemically induced cystitis models. Although these provide mechanistic insight, the extent to which they recapitulate chronic human BPS remains uncertain.

- Small sample sizes and underpowered analyses:
  Many human studies involve small cohorts, particularly those using invasive biopsy-based methods, constraining the ability to detect robust, generalisable molecular signals.

- Reliance on cross-sectional designs:
  Most studies provide single time-point data, restricting understanding of temporal dynamics, causal relationships, or treatment-related changes.

- Gaps in certain biological domains:
  Epigenetic regulation, sex-specific mechanisms, and multi-omics integration remain underexplored relative to inflammation and immune signalling.

Collectively, these limitations highlight the need for larger, clinically well-phenotyped, multi-modal studies—particularly those incorporating transcriptomic datasets directly linked to patient-level metadata.

**Implications for Current Study**

The findings of this systematic review provide a clear rationale for the design and objectives of the present thesis. First, the literature identifies numerous differentially expressed molecules across immune, epithelial, neurogenic, and regulatory pathways, many of which have not been examined within the same individuals or in relation to clinical phenotype. Second, distinct molecular patterns reported in Hunner-type versus non-Hunner BPS, as well as sex-related differences, underscore the need to move beyond population-averaged comparisons toward a more nuanced assessment of individual-level variation.

Accordingly, the current study builds upon these insights by analysing transcriptomic profiles from primary human bladder tissue, comparing BPS and non-BPS samples and integrating findings with available clinical metadata. This approach provides an opportunity to:

- validate or challenge molecular signatures reported in the literature;

- explore the extent to which transcriptomic patterns align with established clinical phenotypes; and

- identify potential molecular subgroups within BPS that may inform future diagnostic and therapeutic stratification.

By addressing gaps identified in previous research—particularly the need for clinically anchored, unbiased whole-transcriptome analysis—the study aims to advance understanding

of the biological heterogeneity underlying BPS and contribute evidence toward a more personalised framework for its diagnosis and management.

# Chapter 3: Evaluation of Literature-Derived Biomarkers in In-House Bladder Pain Syndrome Data

## 3.1 Introduction to the In-House Dataset

The transcriptomic dataset analysed in this study was generated from urothelial biopsy samples collected during routine diagnostic cystoscopy from patients with bladder pain syndrome (BPS) and a range of benign urological conditions. All samples were obtained under appropriate ethical approval and informed consent. Processing steps—including RNA extraction, transcriptomic profiling, and in vitro urothelial re-differentiation assays—were completed prior to the present project; consequently, the current analyses focus exclusively on the interpretation of existing molecular data without involvement in sample acquisition or laboratory preparation.

The dataset comprises 48 patient-derived samples, including 27 from individuals diagnosed with BPS and 21 from patients with non-BPS conditions (Table 3.1.1). The non-BPS group spans several benign uropathies such as overactive bladder (OAB), stress urinary incontinence (SUI), microscopic haematuria, cystitis cystica, and recurrent urinary tract infections (rUTIs), as well as cases of pelvic organ prolapse (POP). The cohort is predominantly female, with only two male participants, and spans a broad age range (16–78 years), reflecting the typical demographic distribution of BPS while also introducing clinical diversity relevant to comparative analyses.

Clinical phenotyping was performed using multiple sources of metadata, including patient-reported symptoms, cystoscopic documentation, and histopathological assessment of biopsy tissue. Symptom burden was assessed using the O'Leary–Sant Interstitial Cystitis Symptom Index (ICSI) and Problem Index (ICPI), which quantify pain, urgency, and urinary frequency. These indices are widely used to characterise BPS severity and track treatment response, and in the present study they provide an essential framework for linking transcriptional profiles to clinical presentation (Yoshimura et al., 2022). Where available, cystoscopic phenotypes—such as the presence or absence of Hunner lesions—and histology findings were incorporated to contextualise gene expression differences within established biological and pathological features of the disease.

Together, the breadth of accompanying clinical metadata enhances the translational value of this dataset and enables the exploration of molecular–clinical relationships, even though the sample size and heterogeneity necessitate an emphasis on effect sizes and biologically coherent patterns rather than strictly powered statistical comparisons. This chapter therefore evaluates literature-derived candidate biomarkers across these clinically defined groups, with particular attention to individual-level variation and alignment with phenotypic data.

**Table 3.1.1: Summary of the patient samples included in the in-house dataset.**

The dataset consists of 48 samples, with 27 from BPS patients and 21 from individuals diagnosed with other benign uropathies. The breakdown of specific benign uropathies is provided where available.

| **Condition** | **Number of Samples (n)** |
|---|---|
| **Bladder Pain Syndrome (BPS)** | **27** |
| **Other Conditions (Non-BPS)** | **21** |
| • Overactive Bladder (OAB) | 10 |
| • Stress Urinary Incontinence (SUI) | 4 |
| • Microscopic Haematuria | 1 |
| • Cystitis Cystica | 1 |
| • Recurrent UTIs (rUTIs) | 1 |
| • Pelvic Organ Prolapse (POP) | 3 |
| **Total** | **48** |

## 3.2 Experimental Methods

### Sample processing and cell culture

The Jack Birch Unit (JBU), Department of Biology, University of York, has established a well-validated protocol for isolating intact urothelium from the basement membrane of surgical bladder specimens (Southgate, Masters and Trejdosiewicz, 2002). All urothelial samples used in the present study were previously isolated by the JBU team and were available in three biological states: the native *in situ* urothelium, an undifferentiated *in vitro* state, and a differentiated *in vitro* state.

The *in situ* samples—obtained directly from patient biopsies—provide the most physiologically relevant representation of the urothelial environment, capturing in vivo cell–cell interactions, exposure to inflammatory stimuli, and potential disease-related alterations. Because the aims of this project centre on identifying clinically meaningful transcriptional changes associated with BPS, only *in situ* samples were included in all analyses. Restricting the dataset in this way avoids confounding effects introduced by culture conditions and ensures that gene expression reflects the native pathological context rather than *in vitro* adaptation.

For reference, the undifferentiated *in vitro* state models a proliferative basal-like phenotype ($CK14^{+}$) maintained under serum-free conditions lacking nuclear receptor ligands. This phenotype arises through an amphiregulin-driven EGFR autocrine loop, facilitating extensive expansion for mechanistic studies (Varley et al., 2005). Differentiation is induced by culturing finite NHU cell lines in adult bovine serum (ABS) with elevated calcium concentrations (2 mM $Ca^{2+}$), producing a biomimetic urothelium characterised by robust barrier formation, evidenced by transepithelial electrical resistance (TER) values exceeding 3500 $\Omega \cdot cm^2$ (Cross et al., 2005).

These states collectively support research into urothelial plasticity and environmental responsiveness; however, exclusively analysing *in situ* samples provides a consistent, clinically anchored baseline appropriate for evaluating biomarker expression across patient phenotypes.

**Bioinformatics Analysis**

To evaluate literature-derived biomarkers of BPS (Table A), transcript abundance values for each candidate gene were examined across BPS and non-BPS samples. These data were generated using polyA-enriched RNA sequencing of the *in situ* patient biopsies described above. Raw sequencing reads underwent quality assessment using FastQC v0.12.1 (Andrews, 2010), followed by pseudoalignment to the GENCODE v44 human transcriptome using kallisto v0.48 (Bray et al., 2016). Gene-level transcripts per million (TPM) values were derived via Tximport v1.24.0 within R v4.2.1, which provides a robust framework for collapsing transcript-level estimates into gene-level quantification (Soneson, Love and Robinson, 2015; R Core Team, 2022).

TPM values were selected for analysis because they enable comparison of relative expression levels across samples while accounting for sequencing depth and gene length. However, the cohort characteristics—specifically, clinical heterogeneity within the BPS group, variability among control conditions, and unequal sample sizes—substantially limit statistical power for detecting differential expression at the group level. Previous analyses conducted on this dataset did not yield statistically significant differences after multiple-testing correction, consistent with the small cohort and broad phenotypic variation.

Accordingly, the present study adopts a targeted, exploratory approach focused on individual-level expression patterns. Each candidate gene was examined to determine whether any BPS sample exhibited expression consistent with molecular signatures reported in the literature. This analytic strategy prioritises pattern recognition, biological coherence, and alignment with available clinical metadata (e.g., cystoscopic findings, histopathology, symptom indices), rather than formal differential expression testing. While inherently qualitative, this approach is appropriate for hypothesis generation and for characterising potential molecular heterogeneity within a clinically diverse cohort, directly addressing the study aims and reflecting methodological transparency.

## 3.3 Data Analysis Methods

### Transcript Visualisation and Quantification

Transcriptomic data from Bladder Pain Syndrome (BPS) and non-BPS samples were explored using a bespoke visualisation tool developed within the Jack Birch Unit (JBU). This platform enabled interactive inspection of gene-level expression patterns across the cohort and provided graphical summaries to support qualitative comparison of candidate biomarker expression. Processed TPM values generated from the RNA-seq pipeline (Section 3.2) were imported directly into the tool, allowing efficient examination of inter-individual variation and alignment of expression trends with clinical metadata.

### Data Management and Visualisation

Initial data handling and descriptive visualisation were performed using Microsoft Excel. Bar charts, scatter plots, and distributional summaries were generated to characterise variability within and between clinical groups. Excel's statistical functions were used to calculate measures such as mean, median, and standard deviation, providing a preliminary understanding of cohort-level dispersion before undertaking more formal statistical exploration. These visual summaries also served to highlight heterogeneity within the BPS group, informing subsequent emphasis on individual-level interpretation.

### Statistical Analysis

Statistical analyses were carried out using the online StatsKingdom platform (StatsKingdom, n.d.). Given the modest sample size, unequal group numbers and non-normal distribution of several variables, non-parametric methods were applied throughout, and all tests were treated as exploratory.

The Mann–Whitney U test was used to compare gene expression levels between two independent groups (e.g. BPS vs. non-BPS). In addition, multiple linear regression was employed to examine whether expression of a putative upstream regulator (for example *IL17RA*) could predict expression levels of downstream genes of interest. This approach

allowed preliminary assessment of potential regulatory relationships within the candidate pathways identified in Chapter 2.

To investigate links between molecular profiles and clinical phenotype, Spearman's rank correlation coefficient was used to assess associations between gene expression and symptom severity scores derived from the O'Leary–Sant Interstitial Cystitis Symptom Index (ICSI) and Problem Index (ICPI) (Figure A2). This method is appropriate for detecting monotonic relationships in non-normally distributed data and enabled integration of transcriptomic and clinical information at the individual-patient level.

For exploratory purposes, statistical significance was provisionally defined as $p < 0.05$, and where relevant, effect sizes, correlation coefficients and regression coefficients are reported to aid interpretation. Because the primary aim of this chapter was hypothesis-generating rather than confirmatory, *p*-values were not adjusted for multiple testing; results are therefore interpreted cautiously as exploratory signals rather than definitive evidence of differential expression. More sophisticated differential expression frameworks (e.g. DESeq2 or edgeR with false discovery rate correction) would be appropriate for larger cohorts and are highlighted in Chapter 4 as potential improvements for future work.

## 3.4 Data analysis

### Study 1

Zhao et al. (2022) proposed that activation of the CXCL13/*CXCR5* chemokine axis contributes to bladder inflammation in BPS. To examine this in our cohort, TPM values for *CXCL13* and *CXCR5* were compared between BPS and non-BPS primary (P0) urothelial samples. No statistically significant group-level differences were observed (*CXCL13* $p = 0.58$; *CXCR5* $p = 0.54$; Figure 3.4.1), likely reflecting limited power and the clinical heterogeneity characteristic of BPS.

Individual-level inspection, however, revealed a distinct outlier. Sample Y2336 showed pronounced overexpression of both *CXCL13* and *CXCR5* (Figure 3.4.2), a pattern absent in all other BPS and non-BPS samples. Clinical metadata align closely with this molecular profile: Y2336 reported bladder and suprapubic pain, intermittent frequency, and post-coital

discomfort, and cystoscopy demonstrated glomerulations with reduced cystometric capacity (350 ml). Symptom scores were moderately elevated (ICSI = 8; ICPI = 7), consistent with an inflammatory phenotype.

Most other BPS samples showed minimal or undetectable *CXCL13* expression, emphasising biological heterogeneity within the cohort. Spearman correlations revealed no coordinated regulation of the chemokine pair (BPS: $\rho = -0.11$, $p = 0.70$; non-BPS: $\rho = 0.19$, $p = 0.65$), indicating that axis activation, where present, is restricted to select individuals rather than representing a cohort-wide signature.

Overall, although group-level comparisons did not support universal activation of the CXCL13/*CXCR5* axis, integration of transcriptomic and clinical data identifies Y2336 as a plausible immune-enriched BPS subtype. These findings introduce the central theme of this chapter: the importance of patient-level transcriptional profiling for uncovering mechanistically distinct BPS endotypes.

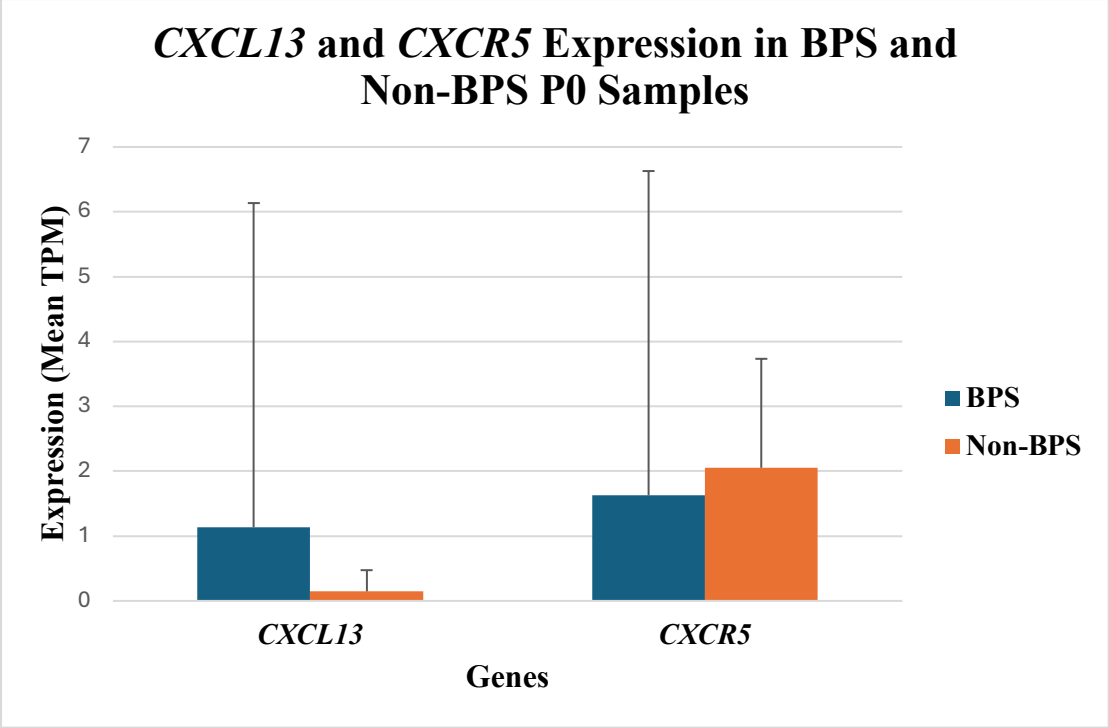


**Figure 3.4.1: *CXCL13* and *CXCR5* Expression in P0 BPS and Non-BPS Samples.** Bar chart comparing mean transcript expression levels (TPM) of *CXCL13* and *CXCR5* in primary (P0) bladder tissue from BPS (blue) and non-BPS (orange) patients. Error bars represent standard deviation and are displayed only in the positive direction, with the y-axis set to a minimum of zero to reflect the non-negative nature of TPM values. This figure highlights the lack of significant differential expression between the two groups.

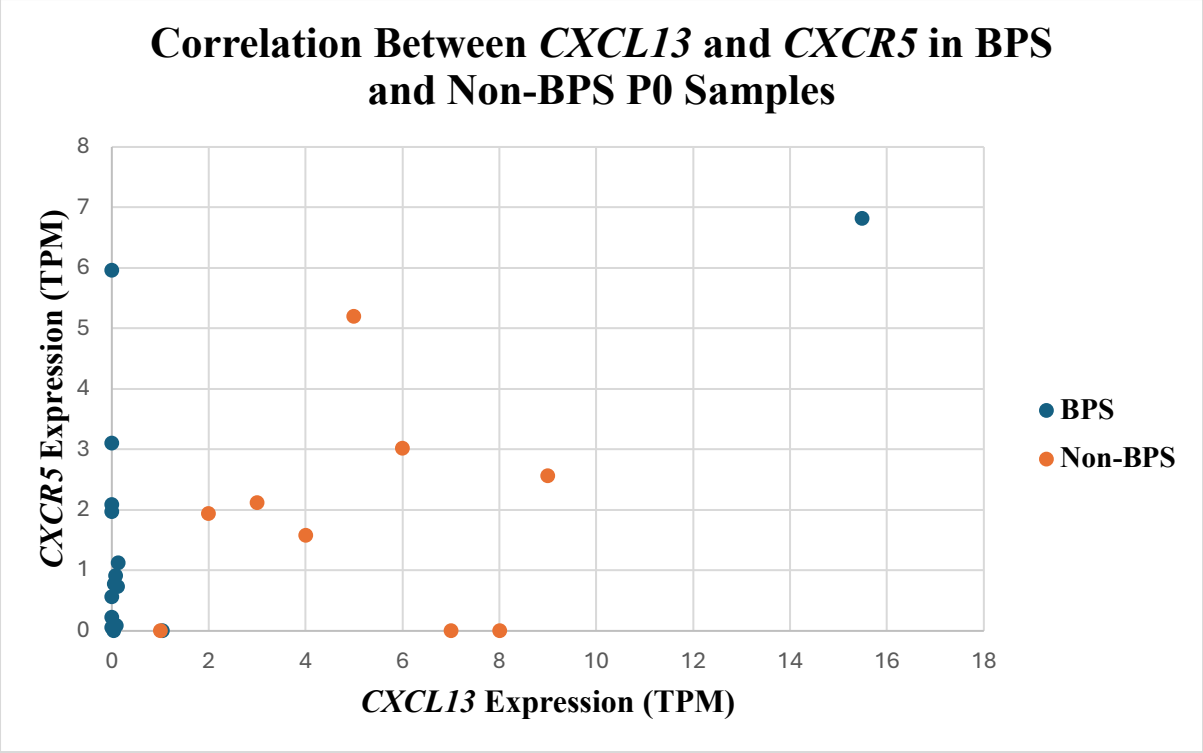


**Figure 3.4.2: Correlation Between *CXCL13* and *CXCR5* in BPS and Non-BPS Samples.**
Scatter plot illustrating the relationship between *CXCL13* and *CXCR5* expression (TPM) in primary bladder tissue from BPS (blue) and non-BPS (orange) samples.
Spearman correlation analysis revealed no strong association in either group:
BPS samples: $\rho = -0.11$, $p = 0.70$
Non-BPS samples: $\rho = 0.19$, $p = 0.65$
No trendlines or regression models are shown, as Spearman's method evaluates non-linear monotonic relationships.

**Table 3.4.1: Summary of Candidate Gene Expression in BPS and Non-BPS P0 Samples.**
The table presents the mean expression values (TPM) and standard deviations (SD) for *CXCL13* and *CXCR5* in both BPS and non-BPS conditions.
These values summarise the dataset instead of showing individual sample plots, emphasising the lack of differences between the groups.

| Gene | Condition | Mean Expression TPM | Standard Deviation (SD) |
|---|---|---|---|
| ***CXCL13*** | BPS | 1.13 | 3.98 |
| ***CXCL13*** | Non-BPS | 0.15 | 0.33 |
| ***CXCR5*** | BPS | 1.63 | 2.06 |
| ***CXCR5*** | Non-BPS | 2.05 | 1.68 |

**Study 2**

Zhang et al. (2023) proposed that *IL17RA* contributes to BPS by engaging the TLR4–NLRP3–IL1B inflammatory axis. To evaluate this in our cohort, transcript levels of *IL17RA*, *TLR4*, *NLRP3* and *IL1B* were examined in primary (P0) urothelial samples. None showed statistically significant group-level differences, and *IL17RA* was not upregulated in BPS ($p = 0.55$; Figure 3.4.3), reflecting the cohort's modest size and clinical variability.

Correlation analyses offered limited evidence for coordinated activation of this pathway. The association between *IL17RA* and *TNF* in BPS approached a large effect size ($\rho = 0.51$, $p = 0.06$), whereas relationships with *IL1B* were negligible in both diagnostic groups (Figure 3.4.4–3.4.5). Regression modelling in BPS samples yielded a significant overall model ($R^2 = 0.74$, $p = 0.01$), with *IL10* emerging as the only significant predictor ($\beta = 0.33$, $p = 0.02$), suggesting that *IL17RA* may, in some patients, align more closely with immunoregulatory rather than pro-inflammatory signalling.

Individual profiles further highlighted heterogeneity. Y2336—previously identified as immune-active—showed elevated *IL17RA*, *TNF*, *NLRP3* and *IL10*, accompanied clinically by suprapubic pain, frequency, post-coital discomfort, glomerulations and reduced bladder capacity (350 ml), consistent with an inflamed phenotype. Y2338 demonstrated a similar but milder transcriptional pattern alongside pain, frequency and dyspareunia, though cystoscopy lacked overt abnormalities. Y2590 showed prominent *NLRP3* and *IL1B* expression with moderate *IL10*, aligning with their chronic symptom profile and limited bladder capacity (600 ml).

In contrast, no regression models were significant in non-BPS samples, and *IL17RA* did not predict downstream mediators, apart from a non-supported trend with *NLRP3* ($\beta = 0.63$, $p = 0.06$).

Overall, the findings do not support *IL17RA* as a universal upstream driver of TLR4–NLRP3–IL1B signalling in BPS. Instead, they reinforce biological heterogeneity, with a subset of patients—most notably Y2336, Y2338 and Y2590—exhibiting transcriptional features consistent with inflammatory or mixed inflammatory–regulatory phenotypes. When combined with clinical metadata, these patterns refine Zhang et al. (2023)'s model by indicating that *IL17RA*-linked inflammation may be relevant only in selected BPS subgroups rather than across the condition as a whole.

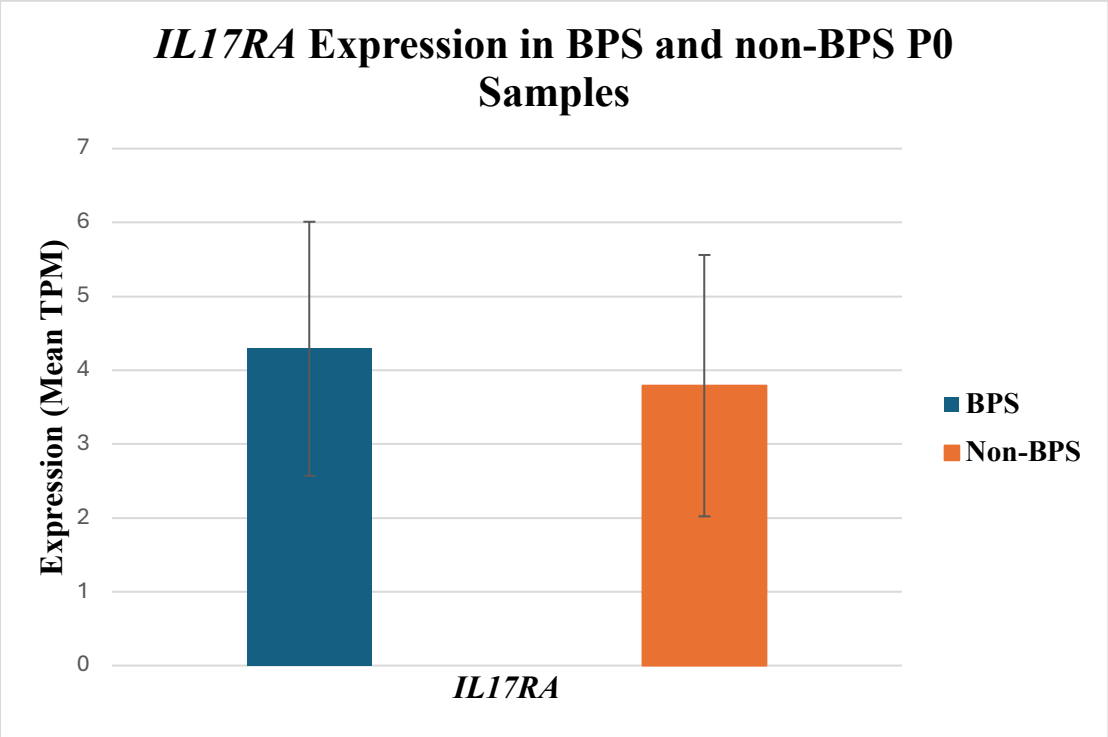


**Figure 3.4.3: *IL17RA* Expression in P0 BPS and Non-BPS Samples.**
Bar chart showing the mean expression (TPM) of *IL17RA* in BPS (blue) and non-BPS (orange) P0 samples. Error bars represent the standard deviation of expression levels within each group. No statistically significant difference in *IL17RA* expression was observed between BPS and non-BPS samples ($p = 0.55$), suggesting no strong differential regulation at the transcript level.

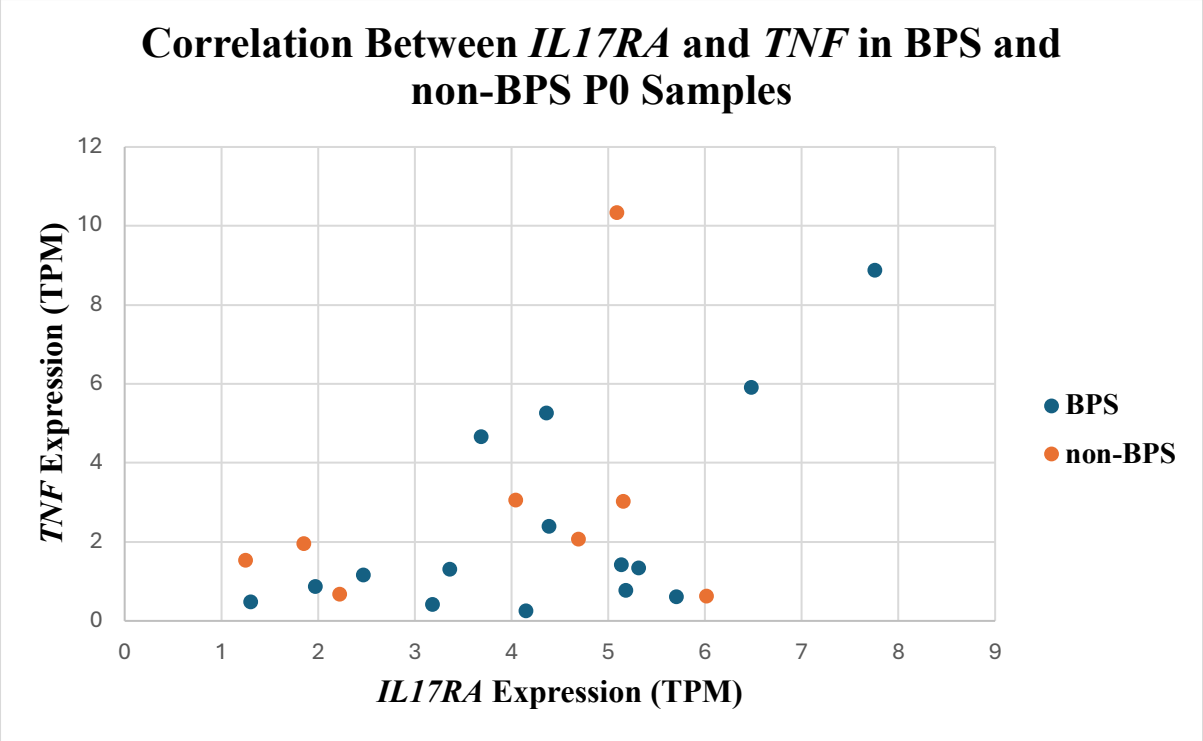


**Figure 3.4.4: Correlation of *IL17RA* and *TNF* expression in P0 BPS and non-BPS samples.** Scatter plot showing the relationship between *IL17RA* and *TNF* expression (TPM) in primary (P0) bladder tissue samples from BPS (blue) and non-BPS (orange) patients. Each point represents an individual sample. In BPS samples, a non-significant large positive correlation was observed between *IL17RA* and *TNF* (Spearman's $\rho = 0.51$, $p = 0.06$), while non-BPS samples showed a weak, non-significant correlation ($\rho = 0.14$, $p = 0.92$). Although not statistically significant, the stronger correlation in BPS samples may suggest a potential condition-specific association between *IL17RA* and *TNF* expression in the context of bladder inflammation.

**Table 3.4.2: Summary of Spearman Rank Correlations between *IL17RA* and Candidate Genes in P0 Samples.**

Spearman correlation coefficients (ρ) and corresponding p-values are presented for the relationship between ***IL17RA*** expression and selected inflammatory genes (***TNF, TLR4, NLRP3, IL1B***, and ***IL10***) in BPS and non-BPS P0 bladder tissue samples. While a non-significant large positive correlation was observed between *IL17RA* and *TNF* in BPS samples (ρ = 0.51, p = 0.06), other correlations across both groups were weak and non-significant. These findings suggest that ***IL17RA* expression does not consistently correlate with these inflammatory markers**, highlighting the complexity of its regulatory role in bladder inflammation.

| Gene | Condition | ρ | p-value | Relationship Type |
|---|---|---|---|---|
| ***TNF*** | BPS | 0.51 | 0.06 | Large Positive (ns) |
| ***TNF*** | Non-BPS | 0.14 | 0.92 | Small Positive (ns) |
| ***TLR4*** | BPS | 0.26 | 0.34 | Small Positive (ns) |
| ***TLR4*** | Non-BPS | 0.50 | 0.23 | Large Positive (ns) |
| ***NLRP3*** | BPS | 0.33 | 0.24 | Medium Positive (ns) |
| ***NLRP3*** | Non-BPS | 0.55 | 0.18 | Large Positive (ns) |
| ***IL1B*** | BPS | 0.01 | 0.97 | Very Weak Positive (ns) |
| ***IL1B*** | Non-BPS | 0.24 | 0.64 | Small Positive (ns) |
| ***IL10*** | BPS | 0.33 | 0.24 | Medium Positive (ns) |
| ***IL10*** | Non-BPS | -0.62 | 0.12 | Large Negative (ns) |

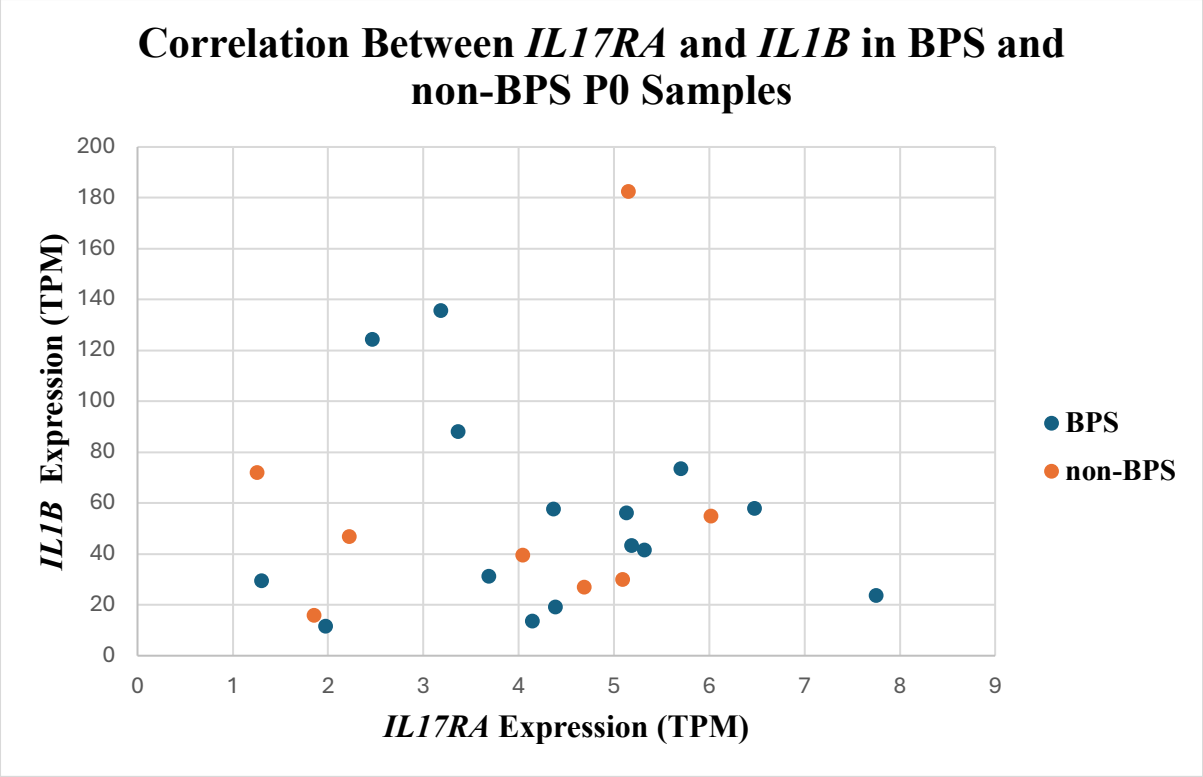


**Figure 3.4.5: Correlation between *IL17RA* and *IL1B* Expression in P0 BPS and Non-BPS Samples.**

Scatter plot showing the relationship between *IL17RA* and *IL1B* transcript levels (TPM) in primary (P0) bladder tissue samples from BPS (blue dots) and non-BPS (orange dots) patients. Each point represents an individual sample. In BPS samples, a very small and non-significant positive correlation was observed (Spearman's $\rho = 0.01$, $p = 0.95$), while non-BPS samples showed a small, non-significant positive correlation ($\rho = 0.24$, $p = 0.64$). Axes are labelled with TPM values for *IL17RA* (x-axis) and *IL1B* (y-axis). These findings suggest that *IL17RA* expression is not predictively or functionally linked to *IL1B* transcript levels in either group.

**Table 3.4.3: Summary of Multiple Regression Analyses: *IL17RA* Predicting Inflammatory Markers in BPS and Non-BPS P0 Samples.**

Summary of multiple linear regression analyses investigating *IL17RA* (TPM) as a predictor of key inflammatory genes—***TLR4, NLRP3, IL1B,*** and ***IL10***—in primary bladder tissue samples from BPS and non-BPS patients. The table reports regression coefficients (β), and associated p-values for each model, alongside $R^2$ and adjusted $R^2$ values indicating model fit. In BPS samples, the model for *IL10* was statistically significant ($R^2 = 0.33$, $p = 0.02$), with *IL17RA* significantly predicting *IL10* expression ($p = 0.02$). All other models, including those in non-BPS samples, showed non-significant relationships. These findings suggest a **potential condition-specific regulatory role for *IL17RA* in *IL10* expression**, with limited predictive influence on *TLR4*, *NLRP3*, or *IL1B* across groups.

| Group | Dependent Variable | $R^2$ | Adj. $R^2$ | Coefficient (β) (IL17RA) | p-value | Interpretation |
|---|---|---|---|---|---|---|
| **BPS** | ***TLR4*** | 0.03 | -0.05 | 0.35 | 0.56 | Not significant |
| | ***NLRP3*** | 0.09 | 0.02 | 0.55 | 0.28 | Not significant |
| | ***IL1B*** | 0.03 | -0.05 | -3.64 | 0.56 | Not significant |
| | ***IL10*** | 0.33 | 0.28 | 0.33 | 0.02 | **Significant** |
| **Non-BPS** | ***TLR4*** | 0.14 | -0.01 | 0.70 | 0.37 | Not significant |
| | ***NLRP3*** | 0.46 | 0.37 | 0.63 | 0.06 | *Borderline* significance |
| | ***IL1B*** | 0.06 | -0.10 | 7.15 | 0.57 | Not significant |
| | ***IL10*** | 0.18 | 0.05 | -0.09 | 0.29 | Not significant |

**Study 3**

Ward et al. (2020) reported distinct protein expression signatures in bladder tissue from patients with Hunner-type interstitial cystitis (HIC), identifying alterations in proteostasis, immune activation, extracellular matrix (ECM) remodelling, antigen processing, and intracellular signalling. Their findings suggest that molecular profiling can help differentiate clinically relevant subtypes within the IC/BPS spectrum. To explore whether comparable transcriptional patterns were present in the current cohort, expression levels of 40 genes spanning eight functional categories corresponding to those described by Ward et al. (2020) were examined.

Primary urothelial (P0) samples were used to maintain the native transcriptional context, thereby increasing the sensitivity for detecting disease-associated variation. For each functional group, Mann–Whitney U tests were performed, and results summarised using TPM values, expression distributions, and directionality of change. As statistical power was constrained by sample size and clinical heterogeneity, the analysis focused on identifying coherent biological patterns and individual-level deviations rather than establishing definitive differential expression. Integrating these transcriptomic findings with available clinical metadata (symptom indices, cystoscopic features, and duration of symptoms) enabled a more nuanced interpretation, particularly in recognising potential molecular subgroups that may correspond to divergent clinical presentations within BPS.

**Proteostasis-Related Genes**

(*UBE2L3*, *UBE2I*, *HUWE1*)
*UBE2L3*, *UBE2I*, and *HUWE1* encode enzymes involved in ubiquitination and SUMOylation, processes central to maintaining cellular proteostasis. None of the genes showed statistically significant differential expression between BPS and non-BPS samples (all $p > 0.05$); however, *UBE2I* demonstrated a modest trend toward lower expression in BPS ($p = 0.12$) (Table 3.4.4; Figure 3.4.6). This directional shift parallels proteostasis disturbances described in HIC by Ward et al. (2020), although the present data do not provide definitive evidence for altered proteostatic regulation in BPS at the cohort level.

Individual expression profiles revealed notable variability within the BPS group. *UBE2L3* expression was highest in sample Y2306, a patient reporting long-standing bladder and suprapubic pain with relatively high symptom indices (ICSI 3–5–6–4; total = 18). *UBE2I* expression exceeded 100 TPM in samples Y2338, Y2339, Y2371, and Y2610. These individuals shared clinical features suggestive of more pronounced bladder dysfunction, including reduced cystometric capacities (e.g., Y2339: 500 ml; Y2610: 300 ml) and moderate-to-severe symptom scores. In contrast, sample Y2383—showing very low *HUWE1* expression—was one of the few BPS cases with documented Hunners lesions, glomerulations, and haematuria, features consistent with a more overt inflammatory phenotype.

Although these transcriptional differences do not reach statistical significance, the combined molecular and clinical patterns suggest that proteostasis-related disturbances may be relevant to a subset of BPS patients, particularly those with greater cystoscopic abnormalities or higher symptom burden. Larger cohorts integrating transcriptomic and proteomic assessments will be required to establish whether proteostasis dysregulation represents a consistent mechanistic feature within specific BPS subgroups.

**Table 3.4.4 Expression Differences of Proteostasis-Related Genes Between BPS and Non-BPS P0 Samples.**

Summary of transcriptomic expression differences in proteostasis-related genes between BPS and non-BPS P0 bladder samples. Mean TPM values are reported for each group. Statistical comparisons were performed using the non-parametric Mann–Whitney U test. While none of the comparisons reached statistical significance ($p > 0.05$), a trend toward reduced expression of *UBE2I* and *HUWE1* was observed in BPS samples, consistent with previous findings in Hunner's Interstitial Cystitis (Ward et al., 2020).

| Gene | Function | Mean TPM (BPS) | Mean TPM (non-BPS) | Test Used | p-value | Direction of Change |
|---|---|---|---|---|---|---|
| ***UBE2L3*** | Ubiquitin conjugation | 25.58 | 23.99 | Mann–Whitney U | 0.73 | No significant difference |
| ***UBE2I*** | SUMO-conjugation enzyme | 93.96 | 118.57 | Mann–Whitney U | 0.12 | No significant difference |
| ***HUWE1*** | E3 ubiquitin ligase | 47.89 | 51.67 | Mann–Whitney U | 0.92 | No significant difference |

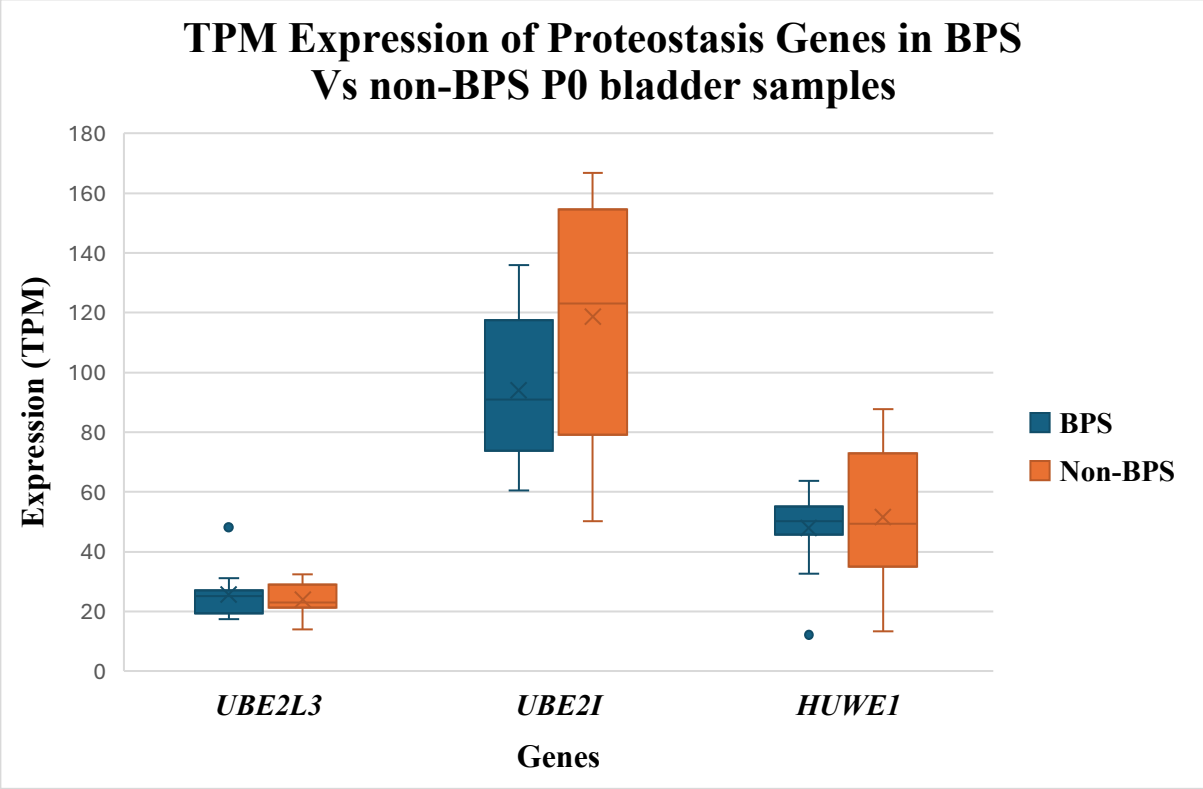


**Figure 3.4.6. Box-and-whisker plot showing transcript per million (TPM) expression of proteostasis-related genes—*UBE2L3*, *UBE2I*, and *HUWE1*—in BPS (blue) and non-BPS (orange) P0 bladder tissue samples.**

Each gene is represented on the x-axis with adjacent boxplots for BPS and non-BPS groups. Boxes indicate the interquartile range (IQR), the horizontal line marks the median, and whiskers extend to 1.5× IQR. Outliers are plotted individually. No statistically significant differences were detected between conditions for any gene (Mann–Whitney U test, $p > 0.05$), though *UBE2I* and *HUWE1* showed a trend toward reduced expression in BPS samples, aligning with proteomic observations in Hunner-type IC (Ward et al., 2020).

**Immune and Inflammation-Associated Genes**

(*EPX, PTPRC, RNASE3, PRG2, HLA-B, PSMD7, HLA-DPB1, TXNDC5, MRC1, PRG3*)

Immune-associated transcripts previously highlighted by Ward et al. (2020) as characteristic of inflammatory Hunner-type IC were examined to determine whether similar signatures were detectable within this BPS cohort. Although none of the genes demonstrated statistically significant differences between BPS and non-BPS groups (all $p > 0.05$), the distribution of expression values revealed substantial inter-individual variation, with several BPS samples displaying marked transcriptional immune activation (Table 3.4.5; Figures 3.4.7–3.4.8).

Among the most striking patterns was the elevated expression of *PTPRC* (CD45), a pan-leukocyte marker indicative of mucosal immune infiltration. Expression peaks occurred in Y2336 (68.5 TPM), Y2337, Y2338 and Y2590 — four individuals who also displayed clinical evidence of inflammation or high symptom burden. For example, Y2336 exhibited cystoscopic glomerulations, reduced bladder capacity (350 ml), and moderate pain scores (ICSI = 8), while Y2590 presented with persistent symptoms (ICSI = 14) despite a similarly reduced bladder capacity (600 ml). The convergence of immune gene activation and clinical features of inflammation in these individuals supports the interpretation that transcriptional immune activation corresponds, at least in some cases, with symptomatic or cystoscopic evidence of disease severity.

A similar pattern emerged for *HLA-B* and *HLA-DPB1*, key mediators of antigen presentation. Y2336 and Y2338 again stood out, with *HLA-B* expression exceeding 1.6 TPM and "HLA-DPB1" reaching 314.6 and 148.5 TPM respectively. Both individuals exhibited cystoscopic abnormalities consistent with immune involvement: Y2338 showed trabeculations and glomerulations, while Y2336 presented with glomerulations and haematuria. These transcriptional–clinical correspondences suggest that in a subset of patients, antigen-presentation pathways may be actively engaged, echoing molecular features described in Hunner-type IC, even in the absence of frank Hunner lesions.

Markers associated with regulatory, or resolution-phase immune responses also showed selective elevation. *MRC1*, which encodes the M2 macrophage receptor CD206, was most highly expressed in Y2336 (2.92 TPM) and Y2590 (1.42 TPM). Both individuals reported long-standing symptoms (Y2590 for 4.2 years; Y2336 with an intermittently symptomatic course) and belonged to the subgroup also showing increased *HLA* and *PTPRC* expression.

This suggests that the macrophage compartment may be activated in tandem with lymphocyte-associated pathways, potentially representing a compensatory or tissue-repair response in more inflamed bladders.

Other immune-related genes, including *TXNDC5* and *PSMD7*, displayed more modest variability but nonetheless identified additional individuals with potential immune involvement. Y2590 and Y2589 showed elevated *TXNDC5*, while Y2610 and Y2589 showed higher *PSMD7*. These individuals also had reduced bladder capacities (300 ml in Y2610; 300 ml in Y2589) and moderate-to-severe symptom scores, suggesting that even subtle molecular deviations may track with clinical severity.

In contrast, eosinophil-associated transcripts (*EPX*, *RNASE3*, *PRG2*, *PRG3*) were virtually absent across all participants, including those with high leukocyte or antigen-presentation signatures. This indicates that eosinophilic inflammation is unlikely to contribute meaningfully to the pathology of the present BPS cohort — a finding consistent with the lack of cystoscopic eosinophilic lesions in clinical records.

Taken together, the immune-related transcriptional landscape observed here is not uniformly elevated across all BPS cases but instead concentrated within a distinct subset of individuals, most notably Y2336, Y2338, and Y2590. The fact that these same individuals exhibit clinical features suggestive of heightened inflammatory activity — reduced bladder capacity, glomerulations, haematuria or elevated symptom indices — reinforces the interpretation that immune-enriched molecular phenotypes may correspond to clinically meaningful subgroups. This pattern mirrors the stratification proposed by Ward et al. (2020) and supports the broader view that BPS is a heterogeneous condition with divergent inflammatory endotypes.

**Table 3.4.5: Expression Differences of Inflammatory and Immune-Associated Genes Between BPS and Non-BPS P0 Samples.**

Summary of transcriptomic expression differences in immune- and inflammation-related genes between BPS and non-BPS P0 bladder samples. Mean TPM values are reported for each group. Statistical comparisons were performed using the non-parametric Mann–Whitney U test. While none of the comparisons reached statistical significance ($p > 0.05$), the observed trends—particularly in genes such as ***PTPRC***, ***HLA-B***, ***HLA-DPB1***, and ***MRC1***—support prior reports of increased immune activation in BPS tissue. These results align with findings from Ward et al. (2020), which identified elevated expression of immune-related genes in diseased HIC tissue compared to NHIC.

| Gene | Function | Mean TPM (BPS) | Mean TPM (non-BPS) | Test Used | p-value | Direction of Change |
|---|---|---|---|---|---|---|
| ***EPX*** | Eosinophil peroxidase | 0.02 | 0.02 | Mann–Whitney U | 0.81 | No significant difference |
| ***PTPRC*** | Immune cell marker (CD45) | 13.16 | 7.70 | Mann–Whitney U | 0.92 | No significant difference |
| ***RNASE3*** | Eosinophil cationic protein | 0.06 | 0.01 | Mann–Whitney U | 0.91 | No significant difference |
| ***PRG2*** | Eosinophil major basic protein 2 | 0.00 | 0.02 | Mann–Whitney U | 0.06 | Non-significant trend ↓ in BPS |

| | | | | | | |
|---|---|---|---|---|---|---|
| ***HLA-B*** | MHC class I molecule | 610.72 | 484.82 | Mann–Whitney U | 0.87 | No significant difference |
| ***PSMD7*** | Proteasome subunit | 50.41 | 50.40 | Mann–Whitney U | 0.97 | No significant difference |
| ***HLA-DPB1*** | MHC class II molecule | 76.48 | 48.12 | Mann–Whitney U | 0.64 | No significant difference |
| ***TXNDC5*** | Protein disulfide isomerase family | 30.50 | 29.40 | Mann–Whitney U | 0.68 | No significant difference |
| ***MRC1*** | Mannose receptor (macrophage marker) | 0.47 | 0.23 | Mann–Whitney U | 0.55 | No significant difference |
| ***PRG3*** | Proteoglycan 3 (eosinophil granule protein) | 0.003 | 0.00 | Mann–Whitney U | 0.52 | No significant difference |

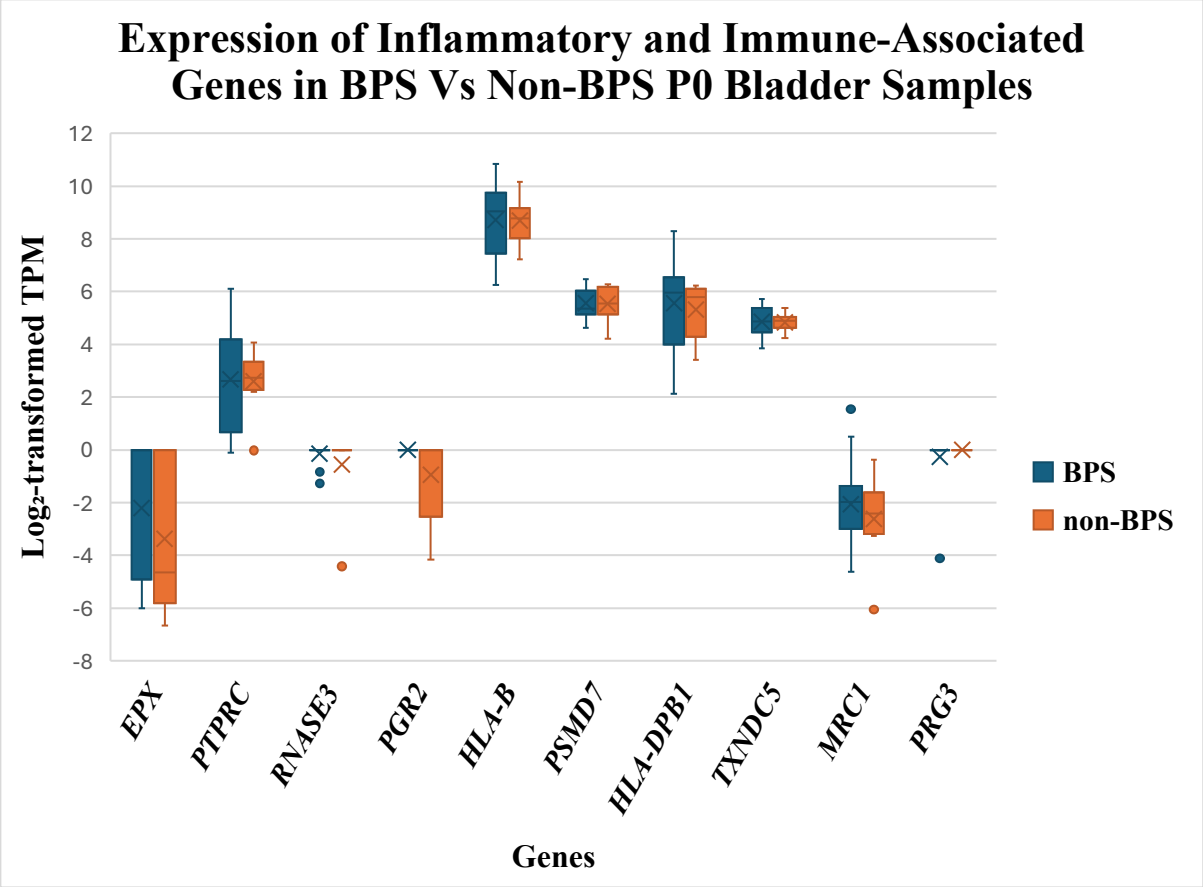


**Figure 3.4.7: Paired Box-and-Whisker Plots of Inflammatory and Immune-Associated Gene Expression (Excluding *HLA-B*) in BPS and Non-BPS P0 Samples.**

Box-and-whisker plots showing $\log_2$-transformed transcript per million (TPM) expression levels for nine inflammatory and immune-related genes across BPS and non-BPS P0 bladder samples. Each gene appears on the x-axis with paired boxplots: BPS (blue) and non-BPS (orange). Boxes represent the interquartile range (IQR) with a horizontal line marking the median; whiskers extend to 1.5× the IQR, and outliers are plotted individually. No statistically significant differences were observed between BPS and non-BPS for any gene (all $p > 0.05$). However, trends in genes such as *PTPRC*, *HLA-DPB1*, and *MRC1* suggest enhanced immune activation in BPS tissue. These findings are consistent with those of Ward et al. (2020), who reported increased immune gene expression in Hunner's lesion IC (HIC) relative to NHIC tissue.

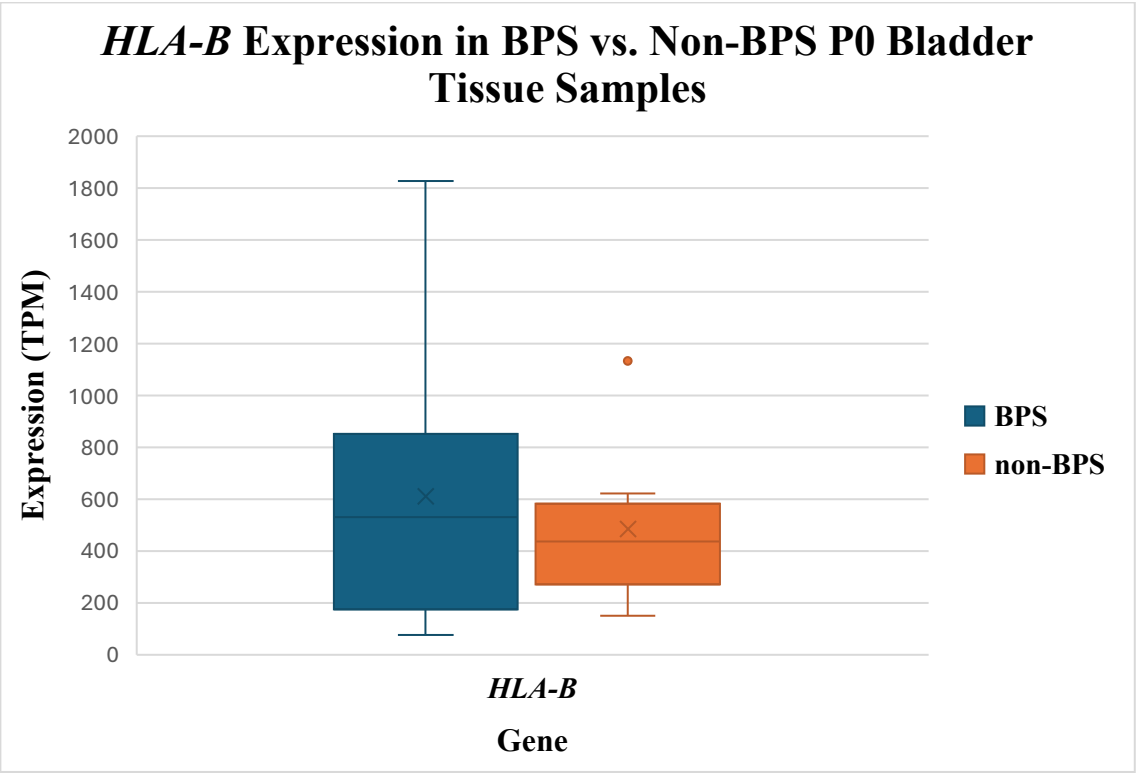


**Figure 3.4.8: Box-and-Whisker Plot of *HLA-B* Expression in BPS and Non-BPS P0 Samples.**

Box-and-whisker plot showing TPM expression levels of *HLA-B* in BPS (blue) and non-BPS (orange) P0 bladder tissue samples. *HLA-B* was plotted separately due to its wider expression range compared to other immune-related genes. Boxes represent the interquartile range (IQR), with a horizontal line indicating the median and an "×" for the mean. Whiskers extend to 1.5× IQR, and outliers are plotted individually. While the difference between groups was not statistically significant ($p > 0.05$), BPS samples showed a trend toward higher *HLA-B* expression. This observation supports findings by Ward et al. (2020), which identified increased immune-related gene expression in HIC bladder tissue.

**ER Protein Processing Genes**

(*STT3B, SSR3, RRBP1, DNAJB11, STT3A, LMAN1, TXNDC5, LMAN2, SSR4*)

We next evaluated transcriptional markers associated with endoplasmic reticulum (ER) protein processing and stress responses, focusing on genes previously reported by Ward et al. (2020) to be upregulated in Hunner-type IC (HIC). These included *STT3B, SSR3, RRBP1, DNAJB11, STT3A, LMAN1, TXNDC5, LMAN2,* and *SSR4*. In contrast to findings in HIC, none of these genes showed statistically significant expression differences between BPS and non-BPS samples in the present cohort (all $p > 0.05$; Table 3.4.6; Figure 3.4.9). Nonetheless, *SSR3* demonstrated a modest trend toward increased expression in BPS ($p = 0.08$), paralleling the direction of HIC-associated ER activation, though not reaching significance here.

Despite the absence of group-level differences, several BPS samples exhibited pronounced elevations in individual ER-related genes. Notably, *SSR4* expression exceeded 200 TPM in Y2383, Y2595, and Y2590. These patients span a range of clinical presentations: Y2383 had long-standing IC with cystoscopic glomerulations, Y2595 reported moderate-to-severe symptoms (ICSI = 14), and Y2590 had both glomerulations and reduced bladder capacity (600 ml), together suggesting that ER-processing gene upregulation may track with more symptomatic or cystoscopically inflamed cases.

Similarly, *DNAJB11*, a molecular chaperone involved in ER-associated degradation (ERAD), was highest in Y2590 and Y2589. Both cases had relatively low maximum cystometric capacities (600 ml and 300 ml, respectively), suggestive of reduced bladder compliance or chronic irritation. Elevated *RRBP1* expression was also observed in Y2610 (>80 TPM), a patient with the highest symptom burden in the cohort (ICSI = 20) and multiple cystoscopic inflammatory features (Hunner-like ulceration and glomerulations). This convergence between heightened ER-stress gene expression and more severe clinical profiles supports the possibility that ER stress may be biologically relevant in a subset of clinically severe BPS cases.

Expression of *LMAN2* was similarly enriched in Y2589, Y2595, and Y2610—each case previously identified as demonstrating elevated immune or proteostatic gene expression—further suggesting an intersection between ER stress, immune activation, and symptom

severity. Although non-significant at the cohort level, these patterns reinforce that ER-associated transcription is not randomly distributed but clustered within clinically and molecularly distinct BPS profiles.

Taken together, these findings suggest that while ER protein-processing pathways are not universally altered in BPS, a subgroup of patients—particularly Y2590, Y2595, Y2589, and Y2610—exhibit concurrent ER-stress signatures and clinically meaningful indicators such as high symptom scores, reduced bladder capacity, or cystoscopic evidence of inflammation. The overlap between ER-associated and immune-associated transcriptional changes echoes mechanisms described in HIC, where unresolved ER stress contributes to dysregulated cytokine production, antigen presentation, and epithelial dysfunction. Although exploratory, these observations support the emerging view that BPS contains identifiable molecular subtypes in which ER stress may act as a co-driver of inflammation and urothelial pathology.

**Table 3.4.6: Expression Differences of ER Protein-Processing Genes Between BPS and Non-BPS P0 Samples.**

Summary of transcriptomic expression differences in genes associated with protein processing in the endoplasmic reticulum (ER) between BPS and non-BPS P0 bladder samples. Mean TPM values are reported for each group. Statistical comparisons were performed using the non-parametric Mann–Whitney U test. While none of the differences reached statistical significance ($p > 0.05$), several genes—including *SSR3* and *LMAN2*—exhibited upward trends in BPS samples. These findings are consistent with observations by Ward et al. (2020), who reported increased expression of ER-associated processing genes in diseased HIC tissue compared to NHIC.

| Gene | Function | Mean TPM (BPS) | Mean TPM (non-BPS) | Test Used | p-value | Direction of Change |
|---|---|---|---|---|---|---|
| ***STT3B*** | Catalytic subunit of oligosaccharyltransferase | 13.47 | 14.43 | Mann–Whitney U | 0.64 | No significant difference |
| ***SSR3*** | Signal sequence receptor subunit | 63.56 | 53.59 | Mann–Whitney U | 0.08 | Non-significant trend ↑ in BPS |
| ***RRBP1*** | Ribosome binding protein, ER localization | 50.52 | 48.31 | Mann–Whitney U | 0.83 | No significant difference |
| ***DNAJB11*** | ER-resident co-chaperone of HSP70 | 39.21 | 37.38 | Mann–Whitney U | 0.87 | No significant difference |

| | | | | | | |
|---|---|---|---|---|---|---|
| ***STT3A*** | Catalytic subunit of oligosaccharyltransferase | 47.97 | 48.25 | Mann–Whitney U | 0.93 | No significant difference |
| ***LMAN1*** | Lectin, mannose-binding 1 | 24.75 | 24.54 | Mann–Whitney U | 0.92 | No significant difference |
| ***TXDNC5*** | Protein disulfide isomerase family | 30.50 | 29.40 | Mann–Whitney U | 0.68 | No significant difference |
| ***LMAN2*** | Lectin, mannose-binding 2 | 98.08 | 95.18 | Mann–Whitney U | 0.87 | No significant difference |
| ***SSR4*** | Signal sequence receptor subunit | 169.07 | 164.97 | Mann–Whitney U | 0.39 | No significant difference |

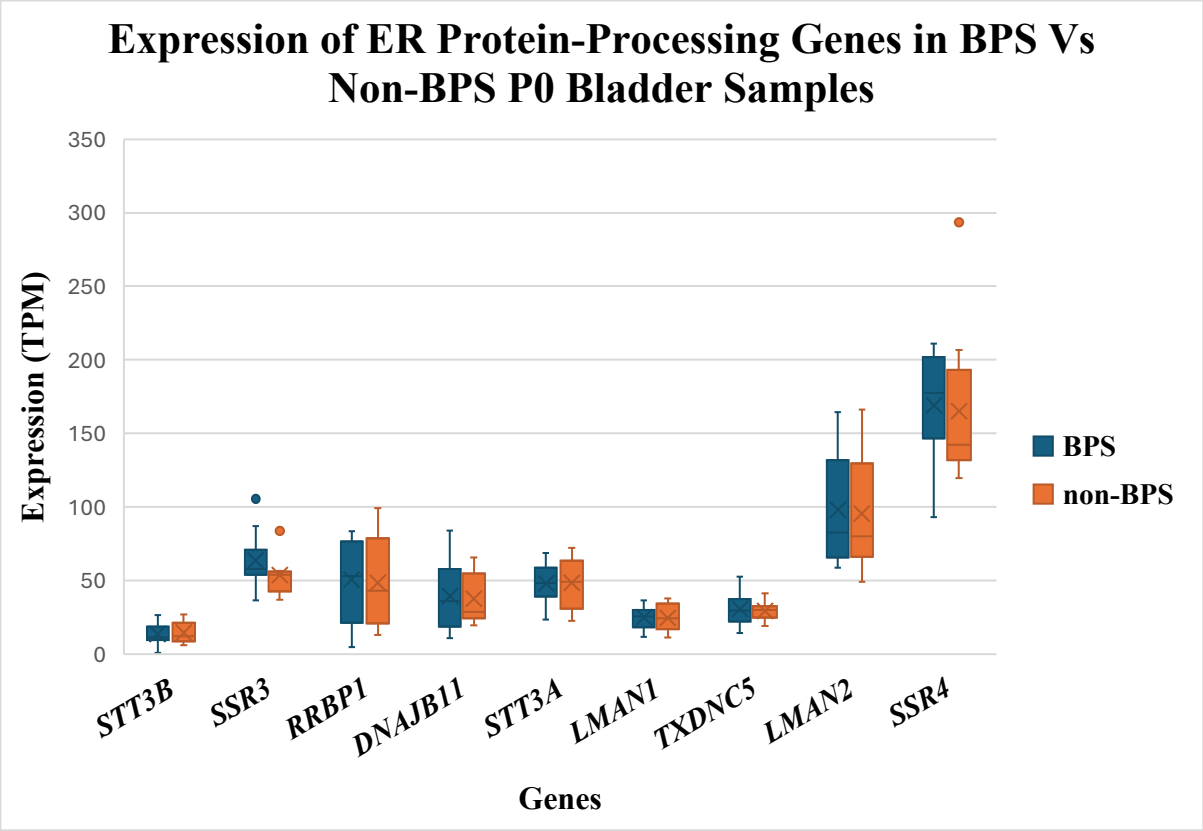


**Figure 3.4.9: Expression of ER Protein-Processing Genes in BPS and Non-BPS P0 Bladder Samples.**

Box-and-whisker plots comparing transcript expression levels (TPM) of endoplasmic reticulum (ER) protein-processing genes between BPS (blue) and non-BPS (orange) P0 bladder samples. Each gene is displayed along the x-axis with two adjacent boxplots representing each condition. Boxes represent the interquartile range (IQR), with the median marked by a horizontal line and the mean shown as "×". Whiskers extend to 1.5× the IQR; outliers are plotted individually. While no statistically significant differences were observed between groups (all $p > 0.05$), trends toward increased expression in BPS were noted for genes such as *SSR3* and *LMAN2*. These findings align with proteomic data reported by Ward et al. (2020), suggesting enhanced ER stress and protein-processing activity in inflamed bladder tissue.

**Collagen and Adhesion Genes**

(*COL4A6, CTNNA1, CTNND1, COL3A1, COL12A1*)

Genes involved in extracellular matrix (ECM) structure and epithelial adhesion were examined to determine whether transcriptional patterns in this BPS cohort aligned with the reductions previously reported in Hunner-type IC (HIC) by Ward et al. (2020). In contrast to those proteomic findings, none of the ECM- or adhesion-related genes demonstrated statistically significant differences between BPS and non-BPS samples (all $p > 0.05$; Table 3.4.7; Figure 3.4.10). Nevertheless, several BPS samples showed notable increases in ECM gene expression, suggesting that while downregulation is not characteristic of this cohort, individual-level variation may still reflect biologically meaningful tissue remodelling processes.

COL4A6 expression was elevated in Y2320, Y2338, Y2590 and Y2595 (>20 TPM), each of which presented with moderate to high symptom burden based on ICSI/ICPI scores (e.g., Y2590: ICSI = 14; ICPI = 11). COL3A1 was highly expressed in Y2336—an individual already identified as an immune-activated outlier in earlier analyses—who also exhibited cystoscopic glomerulations and the lowest maximum cystometric capacity in the BPS subgroup (350 ml), features compatible with urothelial compromise or remodelling. CTNNA1 expression was highest in Y2306 and Y2590, both symptomatic individuals reporting severe frequency and suprapubic pain; Y2306 also demonstrated glomerulations and a high overall symptom index (ICSI = 18). These associations suggest that ECM-related transcriptional increases may coincide with clinically evident bladder dysfunction.

CTNND1 expression was greatest in Y2538, Y2590 and Y2595. Notably, Y2538 presented with a long duration of symptoms (22 years) and high ICSI scores (16), whereas Y2595 exhibited glomerulations and elevated symptom indices (ICSI = 14; ICPI = 11), raising the possibility that chronic tissue injury or longstanding epithelial stress may drive compensatory adhesion-related gene expression.

The overlap between samples demonstrating increased ECM transcription and those identified as outliers in immune and ER-stress signatures (particularly Y2336, Y2338 and Y2590) is especially noteworthy. Individuals such as Y2590—a persistent outlier across immune activation, ER stress, and ECM categories—display a constellation of features including reduced bladder capacity, glomerulations, and high symptom burden. This

convergence suggests that ECM remodelling may not occur in isolation but rather in the context of heightened inflammatory or proteostatic challenge, supporting the concept of coordinated molecular responses within specific BPS endotypes.

Taken together, although group-level comparisons show no statistically significant differences, individual transcriptional patterns point to heterogeneity in ECM and adhesion gene expression across BPS patients. In some individuals, increased ECM transcription appears to align with clinical indicators of chronicity, reduced bladder compliance, or epithelial stress. These findings reinforce the emerging model of BPS as a collection of molecularly distinct phenotypes rather than a uniform entity, and they highlight the importance of integrating transcriptomic signals with cystoscopic and symptom-based metadata to resolve clinically meaningful subgroups.

**Table 3.4.7 Expression Differences of ECM- and Adhesion-Related Genes Between BPS and Non-BPS P0 Samples.**

Summary of transcriptomic expression differences in genes related to extracellular matrix (ECM) structure and cell adhesion between BPS and non-BPS P0 bladder samples. Mean TPM values are reported for each group. Statistical comparisons were performed using the non-parametric Mann–Whitney U test. While no genes reached statistical significance ($p > 0.05$), observed trends—such as elevated expression of *COL3A1* and *CTNNA1* in BPS—are consistent with potential alterations in ECM remodelling and epithelial integrity in BPS tissue.

| Gene | Function | Mean TPM (BPS) | Mean TPM (non-BPS) | Test Used | p-value | Direction of Change |
|---|---|---|---|---|---|---|
| ***COL4A6*** | Type IV collagen, basement membrane component | 15.09 | 19.21 | Mann–Whitney U | 0.27 | No significant difference |
| ***CTNNA1*** | Alpha-catenin, cell-cell adhesion | 186.59 | 177.88 | Mann–Whitney U | 0.87 | No significant difference |
| ***CTNND1*** | Delta-catenin, cell adhesion and signalling | 117.06 | 118.13 | Mann–Whitney U | 0.64 | No significant difference |
| ***COL3A1*** | Type III collagen, ECM component | 1.89 | 0.92 | Mann–Whitney U | 0.83 | No significant difference (low values) |
| ***COL12A1*** | Type XII collagen, ECM organization | 1.50 | 2.42 | Mann–Whitney U | 0.39 | No significant difference (low values) |

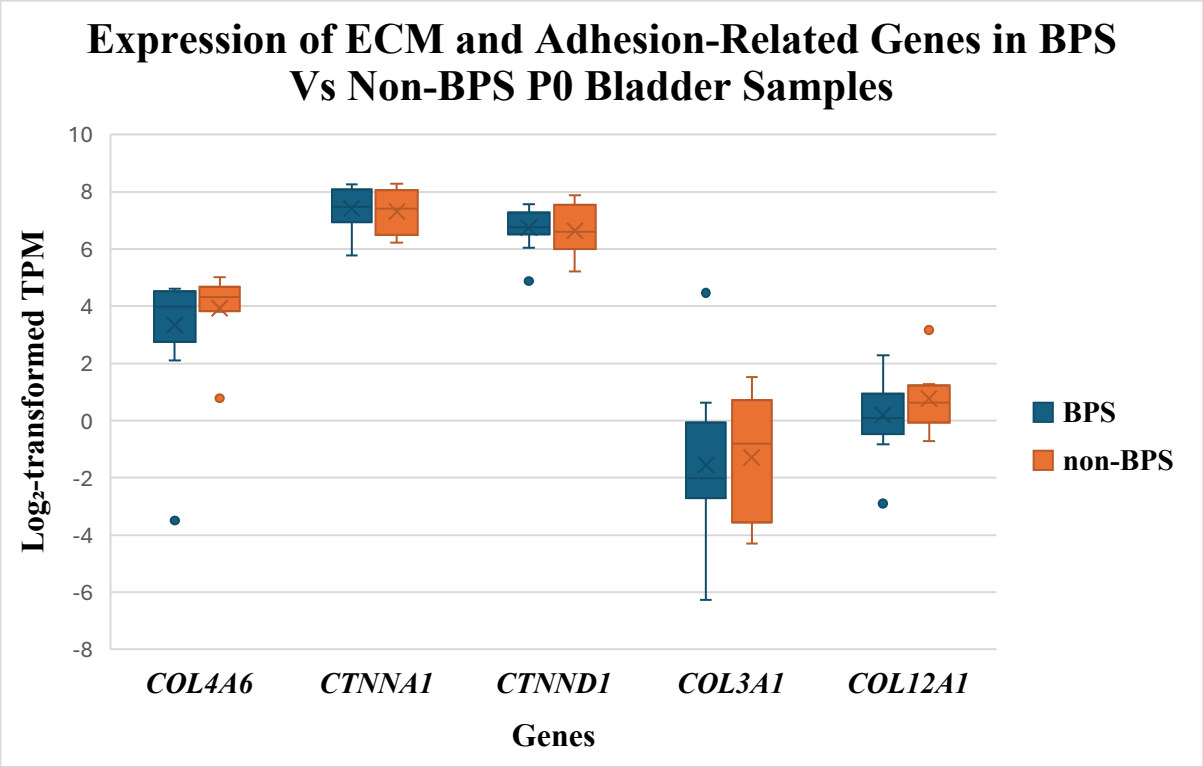


**Figure 3.4.10: Expression of ECM and Adhesion-Related Genes in BPS and Non-BPS P0 Bladder Samples ($log_2$-transformed TPM).**

Box-and-whisker plots showing $log_2$-transformed transcript expression (TPM) for *COL4A6*, *CTNNA1*, *CTNND1*, *COL3A1*, and *COL12A1* in P0 bladder tissue. Each gene is represented with side-by-side plots for BPS (blue) and non-BPS (orange) samples. Each gene is displayed along the x-axis with adjacent boxplots for the two groups. Boxes indicate the interquartile range (IQR), the central line denotes the median, and an "×" marks the mean. Whiskers extend to 1.5× the IQR, with outliers plotted individually. While none of the comparisons reached statistical significance ($p > 0.05$), *COL4A6*, *COL3A1*, and *CTNNA1* showed higher mean expression in BPS, contrasting with the downregulation reported in HIC tissue by Ward et al. (2020), suggesting possible subtype-specific differences in ECM remodelling.

**Antigen Processing and Lysosomal Genes**

(*HLA-B, CYBB, CTSZ*)

To investigate whether antigen presentation or lysosomal activation contributed to the transcriptional landscape of BPS in this cohort, expression levels of *HLA-B*, *CYBB*, and *CTSZ* were examined. These genes form part of immune pathways previously shown to be elevated in Hunner-type IC (HIC) (Ward et al., 2020). Consistent with other gene categories, Mann–Whitney U testing revealed no statistically significant differences between BPS and non-BPS groups (all $p > 0.05$; Table 3.4.8; Figure 3.4.11). Nonetheless, individual-level expression patterns again indicated a subset of BPS cases with marked transcriptional activation of these pathways.

*HLA-B*, a key MHC class I gene involved in antigen presentation, showed particularly high expression in Y2336 (1.63 TPM) and Y2338 (1.83 TPM). Both samples also demonstrated elevated expression of *PTPRC* and *HLA-DPB1*, suggesting coordinated recruitment of antigen-presenting and adaptive immune pathways. These transcriptional signatures correspond with clinical observations: Y2336 exhibited glomerulations, haematuria and low cystometric capacity (350 ml), along with moderate symptom severity (ICSI = 8, ICPI = 7). Y2338 similarly presented with increased cystoscopic inflammation (glomerulations present) and notable symptom burden (ICSI = 10, ICPI = 10). Together, these features strengthen the interpretation that elevated *HLA-B* expression in these individuals reflects genuine immune activation rather than stochastic variation.

*CYBB*, which encodes a catalytic subunit of the NADPH oxidase complex responsible for phagocyte oxidative burst, showed the highest expression in Y2336 (16.1 TPM) and Y2338 (6.3 TPM). This pattern further supports enhanced phagocyte or macrophage activity within these samples. In both individuals, symptom histories included long-standing bladder pain and frequency, and each exhibited trabeculations or glomerulations at cystoscopy—features consistent with chronic inflammation.

Expression of *CTSZ*, a lysosomal protease involved in antigen processing, was similarly elevated in Y2590, Y2595, and Y2336 (>90 TPM). Samples Y2590 and Y2595 represent clinically distinct phenotypes: Y2590 exhibited reduced bladder capacity (600 ml), long symptom duration (4 years), glomerulations, and consistently moderate symptom severity (ICSI = 14, ICPI = 11), while Y2595 displayed high detrusor overactivity and substantial

symptom burden (ICSI = 14, ICPI = 11). In both cases, *CTSZ* upregulation may reflect increased proteolytic turnover and lysosomal engagement within immune cell populations infiltrating the bladder wall. The recurrence of these samples across multiple gene categories—including immune markers and ER stress pathways—supports the possibility that they represent an immune-enriched BPS subgroup with heightened inflammatory and lysosomal signalling.

Although these transcriptional elevations were not observed at the group level, the convergence of increased antigen-processing and lysosomal gene expression within particular individuals aligns with the interpretation that BPS is molecularly heterogeneous. Importantly, the overlap between molecular outliers and clinical indicators of inflammation (e.g., glomerulations, low bladder capacity, long symptom duration) suggests that these transcriptomic signatures may correspond to clinically meaningful phenotypes rather than random noise. Such patterns parallel elements of the immune-activated profile described in HIC (Ward et al., 2020), albeit without the widespread epithelial ulceration characteristic of that condition.

Overall, these findings underscore the importance of considering individual-level transcriptional variation alongside clinical metadata. Elevated expression of *HLA-B*, *CYBB*, and *CTSZ* in specific BPS cases suggests that antigen presentation, oxidative activity, and lysosomal processing contribute to disease mechanisms in a subset of patients. These results highlight the potential value of molecular stratification within BPS and warrant future integration of transcriptomic, histopathological, and symptom-based data to clarify whether these immune-activated profiles predict distinct clinical trajectories or therapeutic responses.

**Table 3.4.8: Expression Differences of Immune-Related Genes Between BPS and Non-BPS P0 Samples.**

Summary of transcriptomic expression differences in selected immune-related genes between BPS and non-BPS P0 bladder samples. Mean TPM values are reported for each group. Statistical comparisons were performed using the non-parametric Mann–Whitney U test. While none of the differences reached statistical significance ($p > 0.05$), all three genes—*HLA-B, CYBB*, and *CTSZ*—showed a trend toward increased expression in BPS tissue. These findings are consistent with those reported by Ward et al. (2020), which identified elevated immune gene expression in diseased HIC tissue compared to NHIC.

| Gene | Function | Mean TPM (BPS) | Mean TPM (non-BPS) | Test Used | p-value | Direction of Change |
|---|---|---|---|---|---|---|
| ***HLA-B*** | MHC class I molecule | 610.72 | 484.82 | Mann–Whitney U | 0.87 | No significant difference |
| ***CYBB*** | NADPH oxidase component (oxidative burst) | 3.19 | 1.72 | Mann–Whitney U | 0.55 | No significant difference (low values) |
| ***CTSZ*** | Lysosomal cysteine protease | 69.74 | 66.40 | Mann–Whitney U | 0.68 | No significant difference |

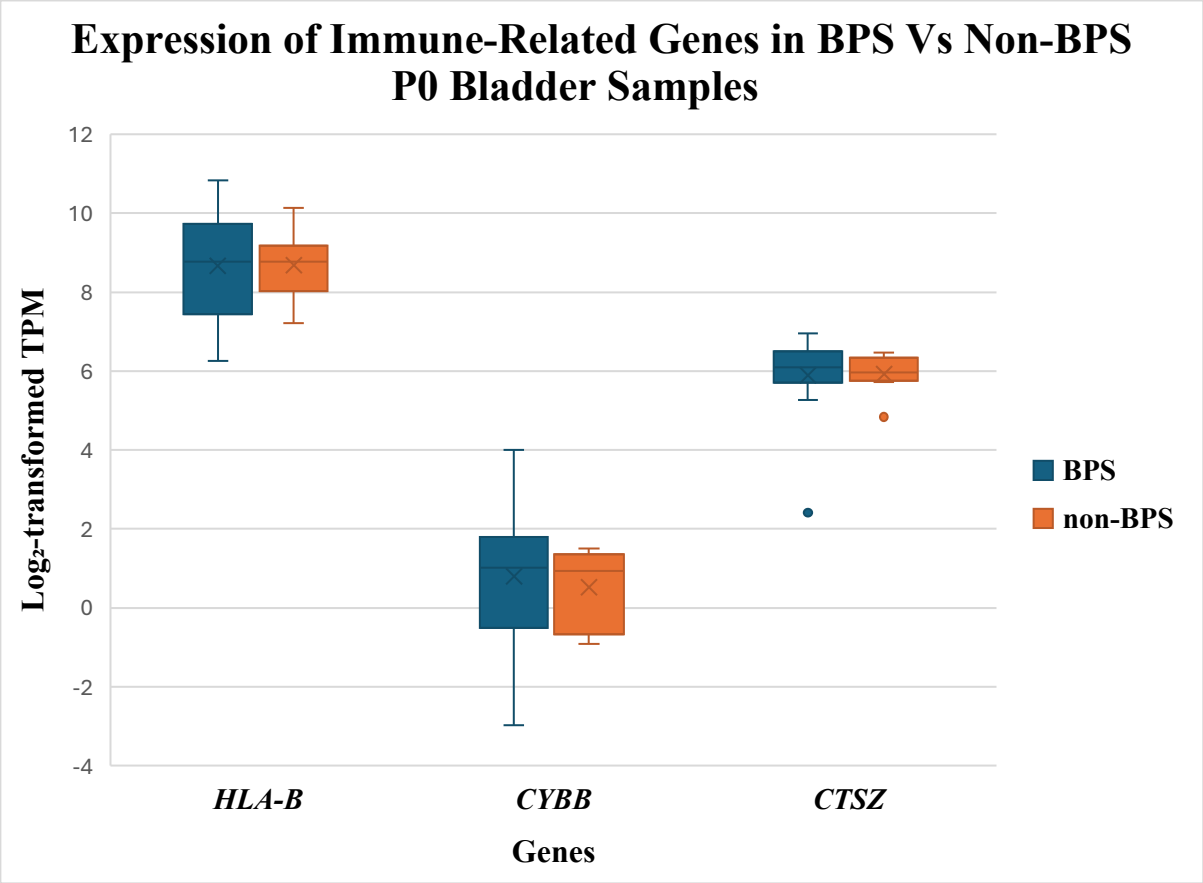


**Figure 3.4.11: Expression of Immune-Related Genes in BPS and Non-BPS P0 Bladder Samples.**

Box-and-whisker plots show transcript expression ($log_2$ TPM) of *HLA-B*, *CYBB*, and *CTSZ* in BPS (blue) and non-BPS (orange) P0 bladder samples. Each gene is displayed with side-by-side plots to allow direct comparison. Boxes represent the interquartile range (IQR), with medians marked by horizontal lines and means by "×". Whiskers extend to 1.5× IQR, with outliers shown as individual points. While differences did not reach statistical significance (all $p > 0.05$), all three genes showed a trend toward increased expression in BPS samples, consistent with elevated immune activity previously reported in HIC tissue (Ward et al., 2020).

**Protein Metabolism Genes**

(*ALDH4A1, PYGL, HIBADH, BLVRA, PLCD1, ALDH6A1, FAHD1, MAOA, MTHFD1*)

To investigate whether metabolic pathway alterations contribute to transcriptional heterogeneity in BPS, we examined genes involved in amino acid catabolism, mitochondrial processing, and protein turnover. Consistent with patterns seen in previous gene groups, no statistically significant differences were detected between BPS and non-BPS samples for any of the metabolic genes analysed (all $p > 0.05$; Table 3.4.9; Figure 3.4.12). Nonetheless, individual-level expression patterns again revealed notable divergence within the BPS cohort, with several samples displaying marked upregulation of *PYGL*, *FAHD1*, and *MAOA*.

Two BPS samples—Y2590 and Y2595—stood out with consistently elevated expression across multiple metabolic genes. Y2590, a patient with a four-year history of symptoms, reduced bladder capacity (600 ml), and moderate-to-high symptom scores (ICSI = 14; ICPI = 11), exhibited increased expression of *PYGL*, *FAHD1*, and *MAOA*. Y2595, who reported two years of symptoms and demonstrated reduced functional bladder capacity (500 ml), showed a similar transcriptional pattern. These metabolic elevations occurred alongside previously observed immune and ER-stress signatures in both samples, suggesting a broader shift in cellular physiology that may reflect heightened energetic demands or metabolic adaptation in conjunction with inflammatory activity.

Such convergence across pathways is particularly evident for Y2590, which displayed upregulation in antigen-processing (*CTSZ*), immune activation (*HLA-B*, *PTPRC*), and ER stress-associated genes (*DNAJB11*, *RRBP1*). Clinically, this individual showed glomerulations on cystoscopy and elevated pain and urgency scores, features consistent with an active inflammatory microenvironment. The coordinated metabolic, inflammatory, and ER-stress transcriptional profile in Y2590 raises the possibility that metabolic reprogramming may accompany or exacerbate specific immune-dominant BPS phenotypes.

In contrast, most BPS samples exhibited relatively low and uniform expression of metabolic genes, suggesting that metabolic reprogramming is not a universal feature of BPS, at least at the transcript level. This diverges from findings in Hunner-type IC, where Ward et al. (2020) reported more widespread alterations in protein and amino acid metabolism. The present results therefore emphasise that metabolic changes in BPS may be highly individualised rather than cohort-wide.

From a clinical standpoint, the presence of metabolic upregulation in transcriptional outliers—particularly those with higher symptom burden or evidence of inflammatory features—highlights a possible mechanistic link between local tissue stress, immune activation, and altered cellular energetics. Although the current sample size limits firm interpretation, these observations strengthen the developing view that BPS comprises multiple molecular subtypes, including individuals in whom metabolic reconfiguration may contribute to symptom persistence or tissue dysfunction. Further work integrating metabolomic profiling with transcriptomic and histopathological data would help clarify whether these metabolic signatures hold diagnostic or prognostic relevance within the broader BPS population.

**Table 3.4.9: Expression Differences of Metabolic and Enzymatic Activity-Related Genes Between BPS and Non-BPS P0 Samples.**
Summary of transcriptomic expression differences in metabolic and enzyme-related genes between BPS and non-BPS P0 bladder samples. Mean TPM values are reported for each group. Statistical comparisons were performed using the non-parametric Mann–Whitney U test. While no statistically significant differences were observed (all $p > 0.05$), trends such as decreased expression of *ALDH4A1, PYGL,* and *BLVRA* in BPS samples suggest subtle metabolic alterations. These findings are in line with prior suggestions of disrupted cellular metabolism in bladder pain syndrome (Ward et al., 2020).

| Gene | Function | Mean TPM (BPS) | Mean TPM (non-BPS) | Test Used | p-value | Direction of Change |
|---|---|---|---|---|---|---|
| ***ALDH4A1*** | Proline catabolism enzyme | 65.53 | 69.28 | Mann–Whitney U | 0.47 | No significant difference |

| | | | | | | |
|---|---|---|---|---|---|---|
| ***PYGL*** | Glycogen phosphorylase (liver form) | 110.69 | 123.23 | Mann–Whitney U | 0.47 | No significant difference |
| ***HIBADH*** | 3-Hydroxyisobutyrate dehydrogenase | 19.27 | 17.94 | Mann–Whitney U | 0.63 | No significant difference |
| ***BLVRA*** | Biliverdin reductase A | 25.12 | 27.47 | Mann–Whitney U | 0.97 | No significant difference |
| ***PLCD1*** | Phospholipase C delta 1 | 32.73 | 29.69 | Mann–Whitney U | 0.68 | No significant difference |
| ***ALDH6A1*** | Methylmalonate-semialdehyde dehydrogenase | 6.33 | 5.53 | Mann–Whitney U | 0.55 | No significant difference |
| ***FAHD1*** | Fumarylacetoacetate hydrolase domain protein | 17.97 | 16.75 | Mann–Whitney U | 0.83 | No significant difference |
| ***MAOA*** | Monoamine oxidase A | 74.97 | 67.49 | Mann–Whitney U | 0.43 | No significant difference |
| ***MTHFD1*** | Methylenetetrahydrofolate dehydrogenase | 18.92 | 20.24 | Mann–Whitney U | 0.64 | No significant difference |

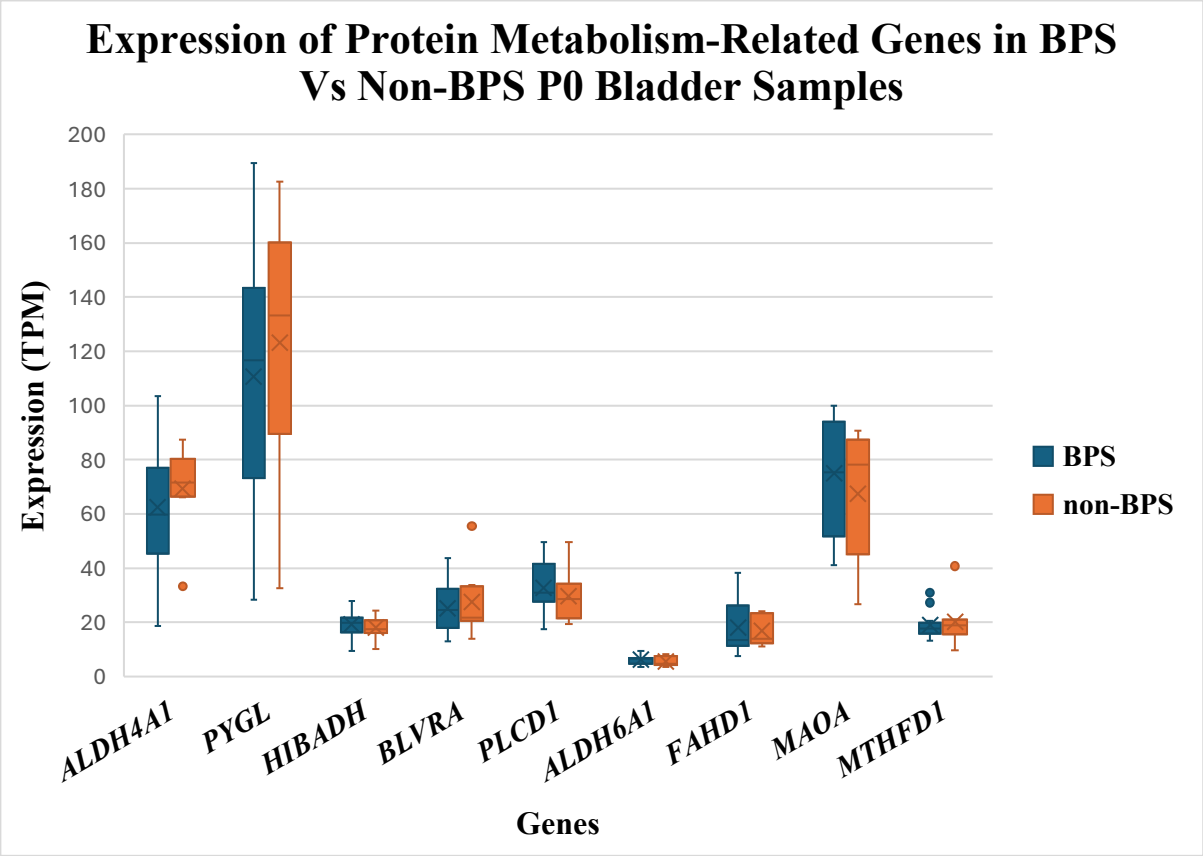


**Figure 3.4.12: Expression of Protein Metabolism-Related Genes in BPS and Non-BPS P0 Bladder Samples.**

Box-and-whisker plots show TPM expression levels of *ALDH4A1, PYGL, HIBADH, BLVRA, PLCD1, ALDH6A1, FAHD1, MAOA*, and *MTHFD1* in BPS (blue) and non-BPS (orange) P0 bladder samples. Each gene is shown with paired plots to facilitate direct condition-wise comparison. Boxes represent the interquartile range (IQR), with medians indicated by horizontal lines and means by "×". Whiskers extend to 1.5× IQR, and outliers are shown as individual points. Although differences were not statistically significant (all $p > 0.05$), subtle expression shifts suggest altered metabolic activity in BPS samples. These patterns are in line with observations from Ward et al. (2020), in HIC tissue.

**Rap1 Signalling Genes**

(*RALA, PFN2, GNAI1, CTNNB1*)

To investigate whether alterations in adhesion- and trafficking-related pathways contribute to transcriptional variability in BPS, we assessed expression of *RALA*, *PFN2*, *GNAI1*, and *CTNNB1*, key components of the Rap1 signalling pathway. In contrast to the pronounced pathway shifts reported in Hunner-type IC by Ward et al. (2020), none of the Rap1-associated genes showed statistically significant differences between BPS and non-BPS samples in the present dataset (all $p > 0.05$; Table 3.4.10; Figure 3.4.13). Nonetheless, several individual-level patterns emerged that may hold biological relevance when considered alongside clinical metadata and other pathway deviations identified in this cohort.

Expression of *CTNNB1* was notably increased in samples Y2590 and Y2610. Both individuals exhibited comparatively high symptom scores (ICSI totals of 14 and 20, respectively) and reduced cystometric capacities (600 ml and 300 ml), which may indicate bladder dysfunction severe enough to elicit compensatory changes in adhesion or Wnt-associated signalling. Elevated *CTNNB1* in these samples also coincided with upregulation of ER stress-related and immune-related transcripts identified in earlier analyses, suggesting that adhesion signalling changes may form part of a broader molecular response in certain BPS subsets.

In contrast, *GNAI1* expression was modestly reduced across a large proportion of BPS samples. Although not statistically significant, this downward trend mirrors findings reported in Hunner-type IC, where cytoskeletal and adhesion dynamics appear disrupted. The subtle nature of this shift suggests that Rap1 pathway involvement in BPS—if present—is likely restricted to a small subset of individuals and may function as a downstream consequence of other transcriptional perturbations such as inflammation or proteostatic stress.

Taken together, these findings indicate that alterations in Rap1 signalling are not uniformly present in BPS but may occur in conjunction with other pathway deviations in a select group of patients. In samples such as Y2590 and Y2610, convergence of elevated *CTNNB1* expression with clinical indicators of symptom severity and reduced bladder capacity supports the possibility that cytoskeletal or adhesion-related dysregulation contributes to disease phenotype in specific molecular subtypes. While exploratory, these data reinforce the

overarching theme of heterogeneity within BPS and highlight the value of integrating transcriptomic and clinical information to uncover potential mechanistic endotypes.

**Table 3.4.10: Expression Differences of Rap1 Signalling Pathway–Associated Genes Between BPS and Non-BPS P0 Samples.**
Summary of transcriptomic expression differences in genes linked to the Rap1 signalling pathway—implicated in cell proliferation and adhesion—between BPS and non-BPS P0 bladder samples. Mean TPM values are reported for each group. Statistical comparisons were performed using the non-parametric Mann–Whitney U test. While no comparisons reached statistical significance ($p > 0.05$), observed trends, particularly in *RALA* and *PFN2*, may reflect subtle dysregulation of Rap1-mediated pathways in BPS tissue. Most of these observations align with prior findings in NDA HIC versus NDA NHIC tissue (Ward et al., 2020).

| Gene | Function | Mean TPM (BPS) | Mean TPM (non-BPS) | Test Used | p-value | Direction of Change |
|---|---|---|---|---|---|---|
| ***RALA*** | Small GTPase involved in vesicle trafficking | 15.46 | 13.15 | Mann–Whitney U | 0.43 | No significant difference |
| ***PFN2*** | Actin-binding protein involved in cytoskeleton dynamics | 66.13 | 58.96 | Mann–Whitney U | 0.30 | No significant difference |
| ***GNAI1*** | G-protein subunit alpha-i1, involved in signalling | 15.67 | 16.40 | Mann–Whitney U | 0.64 | No significant difference |

| | | | | | | |
|---|---|---|---|---|---|---|
| ***CTNNB1*** | Beta-catenin, involved in Wnt signalling and adhesion | 140.60 | 124.81 | Mann–Whitney U | 0.55 | No significant difference |

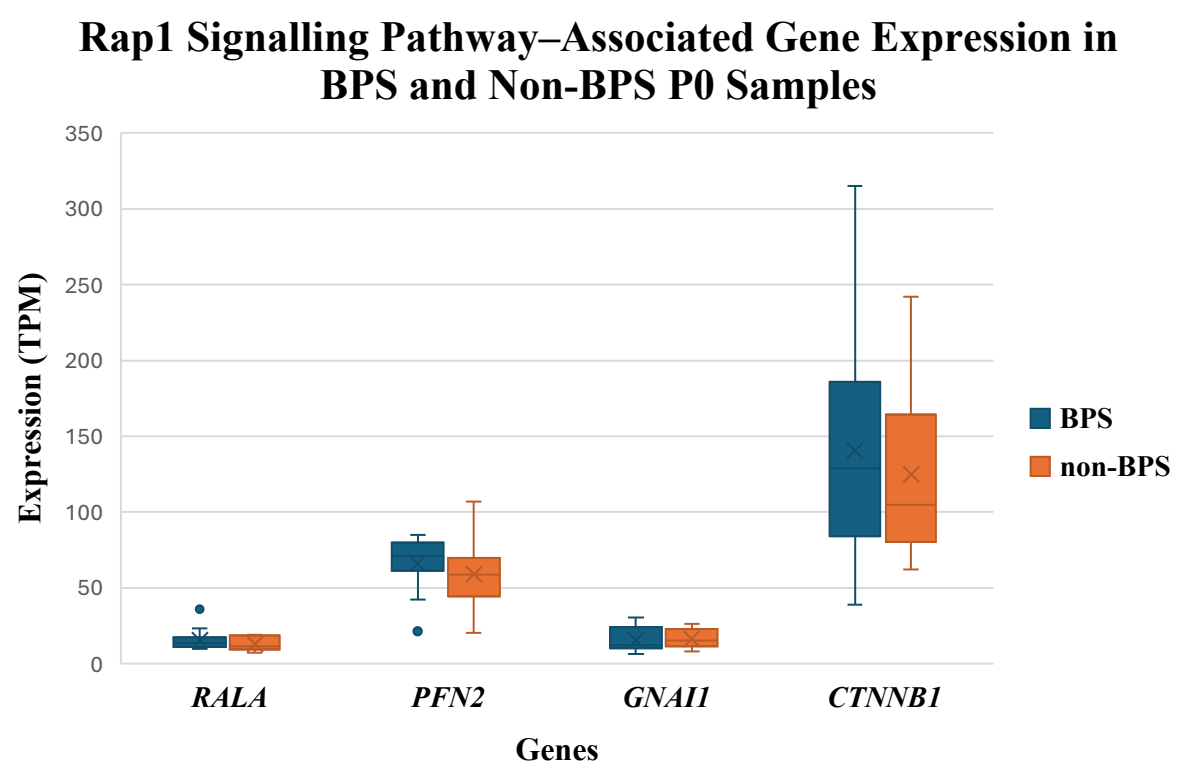


**Figure 3.4.13: Paired Box-and-Whisker Plots of Rap1 Signalling Pathway–Associated Gene Expression in BPS and Non-BPS P0 Samples.**

Box-and-whisker plots showing transcript per million (TPM) expression levels of Rap1 signalling–associated genes in BPS and non-BPS P0 bladder tissue samples. Each gene appears on the x-axis with paired boxplots for BPS (blue) and non-BPS (orange) groups. Boxes represent the interquartile range (IQR), with the central line indicating the median and an "×" marking the mean. Whiskers extend to 1.5× the IQR, and outliers are shown as individual points. No statistically significant differences were observed between BPS and non-BPS for any gene (all $p > 0.05$). These genes were previously reported as differentially expressed in non–disease-associated (NDA) HIC compared to NDA NHIC tissue by Ward et al. (2020).

Across all functional categories examined—including proteostasis; immune and inflammatory signalling (e.g. *PTPRC*, *HLA-DPB1*, *MRC1*); ER stress responses; extracellular matrix (ECM) and adhesion pathways; metabolic genes; and Rap1-associated signalling—no individual transcripts showed statistically significant differences between BPS and non-BPS groups. This absence of cohort-wide shifts aligns with the modest sample size and the clinical heterogeneity of BPS and suggests that molecular changes are unlikely to operate uniformly across all patients.

Even so, a consistent pattern of sample-specific transcriptional elevation was evident. Several individuals—most notably Y2336, Y2338, and Y2590, with contributions from Y2595 and Y2610—demonstrated recurrent upregulation across multiple mechanistic domains. These included antigen-presentation markers (e.g. *HLA-B*, *HLA-DPB1*), lysosomal or oxidative genes (*CTSZ*, *CYBB*), ER stress-associated transcripts (*SSR4*, *DNAJB11*, *RRBP1*), and selected ECM or adhesion-related genes (e.g. *COL4A6*, *CTNNA1*). The coherence of these multi-pathway elevations suggests the presence of biologically meaningful molecular subtypes within the broader BPS population.

These outlier profiles show conceptual parallels with the immune-activated and remodelling signatures described in Hunner-type IC (Ward et al., 2020), but their restricted distribution underscores a key difference: unlike HIC, where inflammation is relatively uniform, BPS appears to encompass distinct molecular endotypes, ranging from immune- and stress-responsive phenotypes to comparatively quiescent states.

Taken together, these findings—summarised in Figures 3.4.6–3.4.13 and Tables 3.4.4–3.4.10—establish the rationale for the integrative clinical–molecular analyses presented in Chapter 4.

**Study 4**

Christmas and Bottazzo (1992) suggested that IFN-γ–driven upregulation of MHC class II molecules—particularly *HLA-DR*—may contribute to autoimmune processes in BPS/IC. To evaluate this mechanism at the transcriptomic level, we analysed expression of key class II genes (*HLA-DRA*, *HLA-DRB1*, *HLA-DPA1*, *HLA-DPB1*) and upstream regulators (*IFNG*, *STAT1*, *IRF1*, *CIITA*) in P0 bladder tissue from BPS and non-BPS patients.

As with earlier studies, group-level comparisons showed no statistically significant differences (all $p > 0.05$; Table 3.4.11), though mean *HLA-DRA*, *HLA-DPA1* and *HLA-DPB1* levels were modestly higher in BPS. Importantly, several individual BPS cases showed pronounced class II elevation, indicating that antigen-presentation pathways may be active in select patients rather than uniformly across the cohort.

Two samples—Y2336 and Y2338—formed a consistent immune-enriched cluster. Y2336 exhibited the highest *HLA-DRA* and *HLA-DRB1* expression, mirroring its immune-dominant profile noted in earlier analyses (e.g., elevated *CXCL13*, *CXCR5*, *HLA-B*, *PTPRC*). Clinically, this patient reported suprapubic pain, intermittent frequency, and post-coital discomfort; cystoscopy revealed glomerulations and trabeculations, with moderate symptom (8/20) and problem (7/16) scores. These features align with a non-Hunner inflammatory phenotype.

Y2338 displayed similarly strong class II activation, with high *HLA-DPB1*, *IFNG* and *IRF1*. This individual reported suprapubic pain, urinary frequency and dyspareunia, and cystoscopy again showed glomerulations without ulceration. Symptom scores (10/20; problem index 10/16) were higher than Y2336, consistent with its more pronounced inflammatory transcriptional signature.

Other BPS samples (e.g., Y2590, Y2595) showed moderate class II elevation—particularly *HLA-DPB1* and *HLA-DPA1*—alongside isolated inflammatory or lysosomal markers (*NLRP3*, *CTSZ*), but without strong induction of canonical regulators *IFNG* or *CIITA*. These patterns suggest possible interferon-independent mechanisms or local microenvironmental influences on class II gene expression.

Across the cohort, *IFNG* and *CIITA* expression remained low, and *STAT1* and *IRF1* displayed variable but non-discriminatory patterns. Thus, while class II activity is clearly detectable in certain individuals, it does not appear to be uniformly driven by classical IFN-γ signalling.

In summary, although no significant group-level differences were observed, several BPS samples—most notably Y2336 and Y2338—showed coordinated class II upregulation coupled with cystoscopic evidence of mucosal abnormality. These findings support the existence of a non-Hunner, immune-enriched BPS subtype characterised by enhanced antigen-presentation capacity and recurrent immune activation across multiple pathways. They reinforce the need for molecular stratification and for larger studies assessing whether such transcriptional signatures predict clinical severity or therapeutic response.

**Table 3.4.11 Expression Differences in MHC Class II Genes and IFN-γ Regulators Between BPS and Non-BPS Samples.**
Summary of mean TPM values and Mann–Whitney U test results for MHC class II genes and their transcriptional regulators in BPS vs. non-BPS P0 bladder tissue. No statistically significant differences were observed, but expression patterns may reflect modest immune activation in a subset of BPS patients.

| Gene | Function | Mean TPM (BPS) | Mean TPM (non-BPS) | Test Used | p-value | Direction of Change |
|---|---|---|---|---|---|---|
| ***HLA-DRA*** | MHC class II alpha chain | 204.17 | 130.44 | Mann–Whitney U | 0.73 | No significant difference |
| ***HLA-DRB1*** | MHC class II beta chain | 78.25 | 52.03 | Mann–Whitney U | 1.03 | No significant difference |

| | | | | | | |
|---|---|---|---|---|---|---|
| ***HLA-DPA1*** | MHC class II alpha chain | 101.57 | 56.87 | Mann–Whitney U | 1.03 | No significant difference |
| ***HLA-DPB1*** | MHC class II beta chain | 76.48 | 48.12 | Mann–Whitney U | 0.64 | No significant difference |
| ***IFNG*** | Cytokine inducing MHC class II expression | 11.58 | 12.02 | Mann–Whitney U | 0.73 | No significant difference |
| ***STAT1*** | IFN-γ signalling transcription factor | 34.60 | 35.07 | Mann–Whitney U | 0.47 | No significant difference |
| ***IRF1*** | Regulator of interferon response genes | 90.50 | 140.75 | Mann–Whitney U | 0.10 | No significant difference |
| ***CIITA*** | Master regulator of MHC class II transcription | 4.92 | 3.33 | Mann–Whitney U | 0.78 | No significant difference |

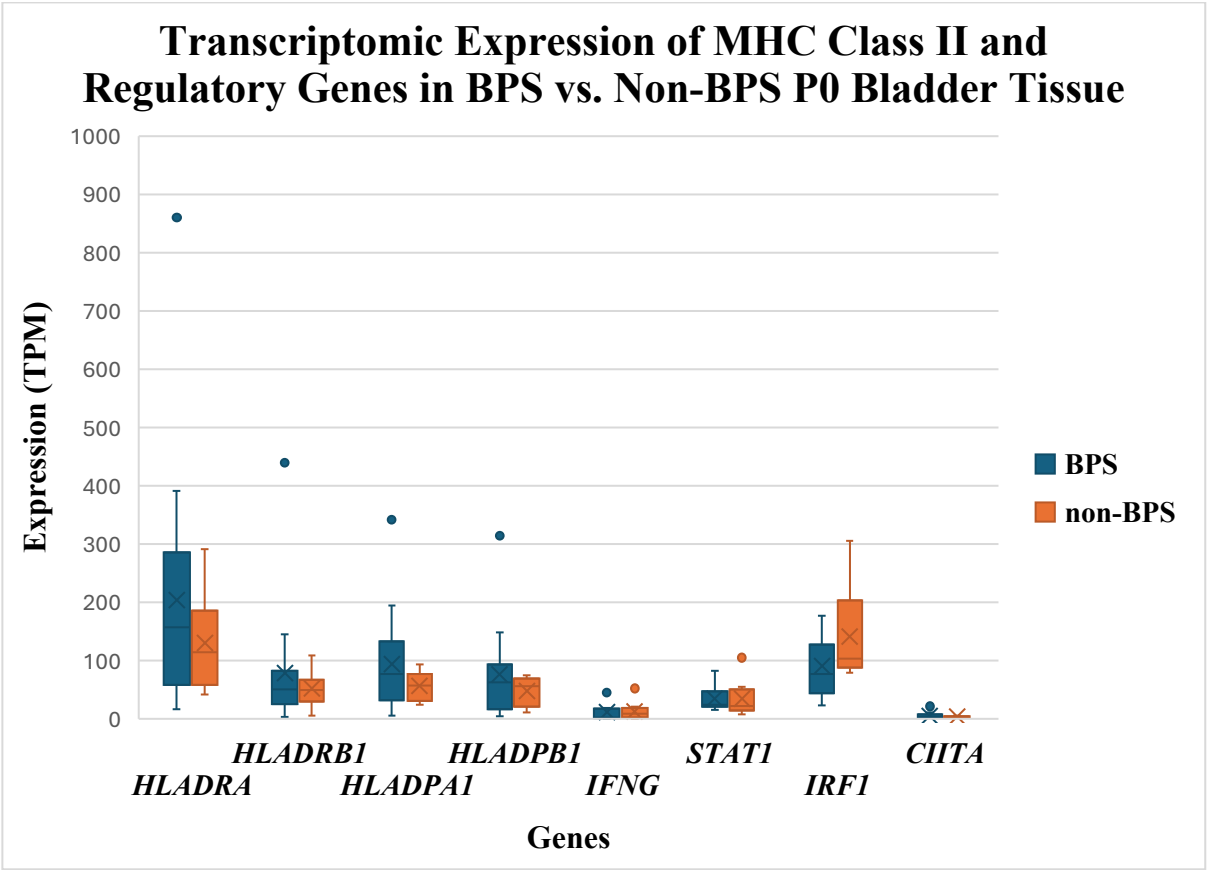


**Figure 3.4.14: Paired Box-and-Whisker Plot of MHC Class II and Regulatory Gene Expression in BPS and Non-BPS Samples.**

Box-and-whisker plots showing transcript per million (TPM) expression levels for MHC class II–related genes (*HLA-DRA, HLA-DRB1, HLA-DPA1, HLA-DPB1*) and transcriptional regulators (*IFNG, STAT1, IRF1, CIITA*) in BPS (blue) and non-BPS (orange) P0 bladder samples. Each gene is plotted on the x-axis with paired boxplots by condition. Boxes represent the interquartile range (IQR), with the median shown as a horizontal line and the mean marked with "×". Whiskers extend to 1.5× the IQR, and outliers are shown as individual points. Although no comparisons reached statistical significance (all $p > 0.05$), a trend toward higher MHC class II gene expression in BPS is noted.

**Study 5**

Liu, Jiang and Kuo (2015) proposed that urothelial barrier dysfunction in BPS reflects reduced *CDH1* (E-cadherin) expression together with inflammatory and apoptotic activation via *TNF*, *MAPK14*, and downstream mediators such as *CASP3* and *BAX*. To evaluate whether similar mechanisms were evident in this cohort, TPM values for these genes were examined in primary (P0) bladder urothelial tissue from BPS and non-BPS patients.

No group-level differences reached statistical significance (all $p > 0.05$; Table 3.4.12; Figure 3.4.15). Mean *CDH1*, *MAPK14*, *CASP3*, and *BAX* expression was slightly higher in BPS, whereas *TNF* was marginally reduced—contrasting with the reduced *CDH1* protein expression reported by Liu et al. (2015). These findings suggest that barrier impairment in BPS may arise from post-transcriptional mechanisms or altered protein turnover rather than consistent transcriptional suppression. Similarly, although apoptotic genes were numerically higher in BPS, their patterns did not indicate a cohort-wide apoptotic programme.

At the individual level, however, several BPS samples showed coordinated activation of inflammatory and apoptotic transcripts. Y2336 exhibited elevated *TNF*, *STAT1*, *CDH1*, and *CASP3*. Clinically, this patient reported suprapubic pain, intermittent frequency, and post-intercourse discomfort, with cystoscopy showing glomerulations and trabeculations. Moderate symptom (8/20) and problem (7/16) scores, combined with pronounced immune–apoptotic transcriptional activity, point to an actively inflamed phenotype, consistent with this sample's previously noted upregulation of *CXCL13*, *CXCR5*, *HLA-B*, and *IFNG*.

Y2338 displayed a similar transcriptional pattern, with increased *TNF*, *CDH1*, *CASP3*, and *BAX*. This patient presented with suprapubic pain, urinary frequency, and dyspareunia; cystoscopy confirmed glomerulations without Hunner lesions. Symptom burden was higher (10/20; 10/16), matching its strong interferon-associated profile (*IFNG*, *IRF1*, MHC class II genes) observed across multiple studies.

Y2538, while not strongly immune-activated, showed high *CDH1* together with elevated *CASP3* and *BAX*, suggesting epithelial stress or compensatory repair. Clinically, this patient reported long-standing symptoms (22 years) and exhibited glomerulations, consistent with chronic epithelial turnover in the absence of a marked inflammatory signature.

Although the overall cohort did not demonstrate a unified *CDH1–MAPK14–TNF–*apoptosis axis, the convergence of transcriptomic and clinical features in Y2336 and Y2338 highlights a biologically distinct subgroup characterised by inflammation-linked epithelial stress and apoptotic activation. These findings reinforce the broader chapter theme of molecular heterogeneity within BPS and underscore the value of integrating clinical metadata with transcriptomic profiling to identify mechanistically meaningful patient endotypes.

**Table 3.4.12: Transcriptomic Expression of Barrier, Inflammation, and Apoptosis-Related Genes in BPS and Non-BPS P0 Samples.**
Summary of TPM expression for selected genes involved in urothelial barrier function (*CDH1*), inflammatory signalling (*MAPK14, TNF*), and apoptosis (*CASP3, BAX*) in BPS and non-BPS primary (P0) bladder tissue samples. Statistical comparisons were conducted using the Mann–Whitney U test. Although no gene reached statistical significance (all $p > 0.05$), slight increases were observed in *CDH1, MAPK14, CASP3*, and *BAX* in BPS samples, while *TNF* was marginally decreased.

| Gene | Function | Mean TPM (BPS) | Mean TPM (non-BPS) | Test Used | p-value | Direction of Change |
|---|---|---|---|---|---|---|
| ***CDH1*** | E-cadherin, epithelial adhesion | 145.96 | 138.89 | Mann–Whitney U | 0.83 | No significant difference |
| ***MAPK14*** | p38 MAPK, inflammatory signalling | 15.66 | 14.40 | Mann–Whitney U | 0.78 | No significant difference |

| | | | | | | |
|---|---|---|---|---|---|---|
| ***TNF*** | Tumour necrosis factor, pro-inflammatory cytokine | 2.38 | 2.91 | Mann–Whitney U | 0.36 | No significant difference |
| ***CASP3*** | Caspase-3, executioner of apoptosis | 21.49 | 18.48 | Mann–Whitney U | 0.73 | No significant difference |
| ***BAX*** | Pro-apoptotic Bcl-2 family protein | 55.03 | 51.81 | Mann–Whitney U | 0.43 | No significant difference |

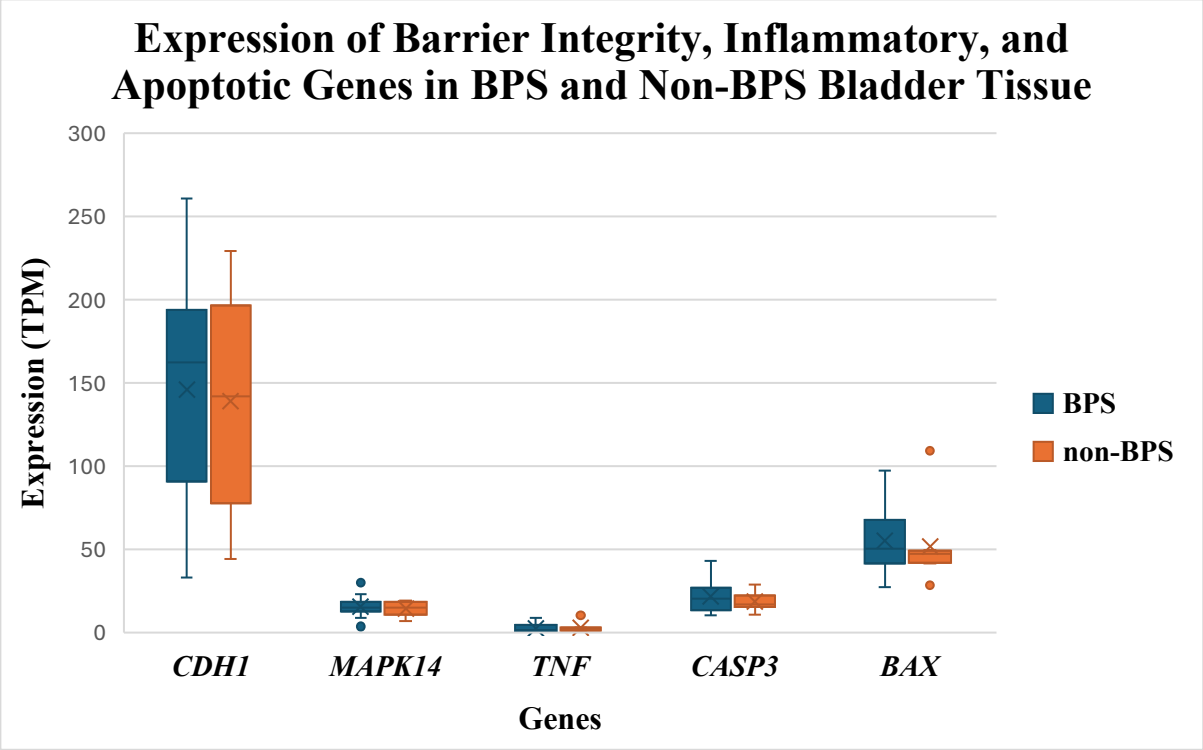


**Figure 3.4.15: Paired Box-and-Whisker Plot of Barrier, Inflammatory, and Apoptosis-Related Gene Expression in BPS and Non-BPS P0 Samples.**

Box-and-whisker plots show TPM expression of *CDH1, MAPK14, TNF, CASP3*, and *BAX* across P0 bladder tissue from BPS (blue) and non-BPS (orange) groups. Each gene is represented by a pair of boxplots. Boxes indicate the interquartile range (IQR), the horizontal line marks the median, and "×" denotes the mean. Whiskers extend to 1.5× IQR, and outliers are shown individually. No statistically significant differences were observed, though modest expression differences suggest gene-specific trends.

**Study 6**

Green et al. (2004) reported increased expression of the adhesion molecules *ICAM1* and *VCAM1* in IC bladder tissue, proposing roles in leukocyte recruitment, mast-cell activity, and vascular signalling. To examine whether similar mechanisms were detectable in the present BPS cohort, TPM expression of *ICAM1*, *VCAM1*, *TPSAB1*, *TPSB2*, and *VEGFA* was assessed in P0 urothelial samples.

No statistically significant differences were observed between BPS and non-BPS groups (all $p > 0.05$; Table 3.4.13; Figure 3.4.16). Nonetheless, several BPS samples showed transcriptional patterns consistent with immune–vascular activation. Y2338 again emerged as a marked outlier, with elevated *ICAM1* (57.43 TPM), *VCAM1* (12.05 TPM), *VEGFA* (413.36 TPM), and detectable mast-cell tryptase transcripts (*TPSAB1*, *TPSB2*). Clinically, this patient presented with suprapubic pain, urinary frequency, dyspareunia, and glomerulations, together with moderate symptom and problem scores (10/20 and 10/16), features aligning with a transcriptionally immune-enriched phenotype identified in earlier studies.

Y2336, previously noted for broad immune activation, showed the highest *ICAM1* expression in the cohort (74.32 TPM) and moderately raised *VCAM1*. This sample also demonstrated cystoscopic abnormalities (trabeculations and glomerulations) and a moderate symptom burden (8/20), further supporting its classification within an immune-dominant subgroup. Y2590 displayed milder but coherent increases in *ICAM1*, *VCAM1*, and *VEGFA*, again consistent with the multi-pathway deviations observed in other analyses.

Spearman correlations indicated a significant positive relationship between *ICAM1* and *TNF* expression in BPS samples ($\rho = 0.66$, $p = 0.01$; Figure 3.4.17), suggesting shared cytokine-driven regulation. Correlations involving mast-cell markers were weaker and inconsistent across groups, and *VCAM1* did not correlate meaningfully with *VEGFA*, indicating a lack of coordinated angiogenic–adhesion transcript regulation at the cohort level.

Overall, while group-level expression did not mirror the broad adhesion molecule upregulation described by Green et al. (2004), several BPS individuals—particularly Y2338 and Y2336—demonstrated concurrent elevation of adhesion, vascular, and immune-related transcripts. When integrated with symptom profiles and cystoscopic findings, these data reinforce the presence of an immune-activated BPS subtype characterised by coordinated inflammatory–epithelial signalling rather than a uniform disease-wide shift.

**Table 3.4.13: Expression Differences of Adhesion and Vascular-Associated Genes Between BPS and Non-BPS P0 Samples.**

Summary of transcriptomic expression levels of intercellular adhesion and vascular signalling–associated genes in BPS and non-BPS P0 bladder tissue samples. Mean TPM values are shown for each group. Statistical differences were assessed using the Mann–Whitney U test. Although no comparisons reached statistical significance (all $p > 0.05$), small effect sizes and directional shifts in *ICAM1* and *VCAM1* expression may suggest low-grade immune activation in some BPS cases, particularly sample Y2338. These findings are evaluated in the context of previously reported protein-level changes in IC patient tissue Green et al. (2004).

| Gene | Function | Mean TPM (BPS) | Mean TPM (non-BPS) | Test Used | p-value | Direction of Change |
|---|---|---|---|---|---|---|
| ***ICAM1*** | Leukocyte adhesion molecule | 29.48 | 40.63 | Mann–Whitney U | 0.39 | No significant difference |
| ***VCAM1*** | Endothelial adhesion molecule | 2.30 | 0.67 | Mann–Whitney U | 0.98 | No significant difference |
| ***TPSAB1*** | Mast cell tryptase marker | 1.17 | 1.99 | Mann–Whitney U | 0.16 | No significant difference |
| ***TPSB2*** | Mast cell tryptase (isoform B) | 0.94 | 2.13 | Mann–Whitney U | 0.73 | No significant difference |
| ***VEGFA*** | Angiogenesis and vascular signalling | 258.31 | 333.90 | Mann–Whitney U | 0.78 | No significant difference |

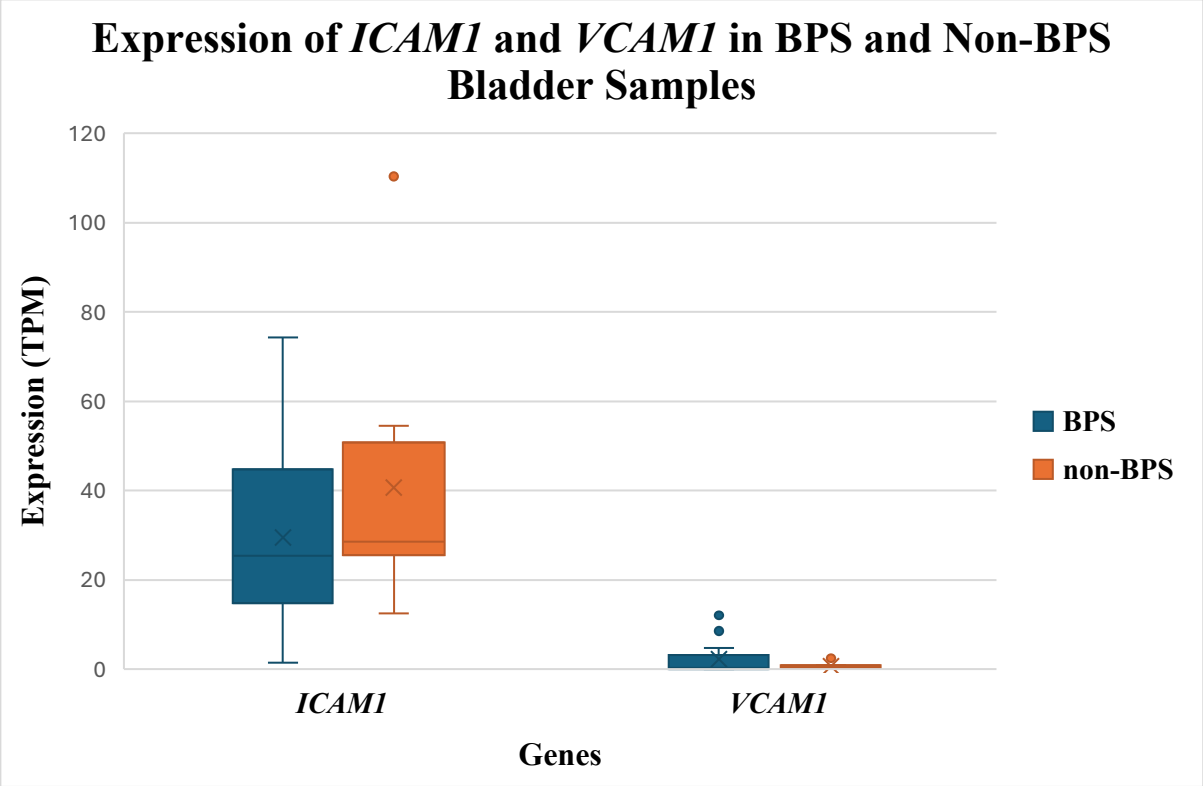


**Figure 3.4.16: Paired Box-and-Whisker Plot of ICAM1 and VCAM1 Expression in BPS and Non-BPS P0 Samples.**

Box-and-whisker plots showing transcript per million (TPM) expression levels of the intercellular adhesion molecules *ICAM1* (blue) and *VCAM1* (orange) in primary (P0) bladder tissue samples from BPS and non-BPS patients. Each gene is displayed with paired boxplots for the BPS and non-BPS groups. Boxes represent the interquartile range (IQR), with the horizontal line marking the median and the "×" symbol indicating the mean. Whiskers extend to 1.5× the IQR, and outliers are shown individually.

While *VCAM1* showed slightly elevated expression in BPS (mean TPM = 2.30 vs. 0.67), *ICAM1* was moderately lower in BPS than non-BPS (mean TPM = 29.48 vs. 40.63); neither difference reached statistical significance ($p > 0.05$). These genes were selected based on findings by Green et al. (2004), who reported increased expression of *ICAM-1* and *VCAM-1* in IC tissue, implicating them in leukocyte adhesion, inflammation, and vascular activation.

Together, these results highlight variable expression patterns in adhesion molecules across samples and may point toward differential vascular-immune activity within BPS subsets.

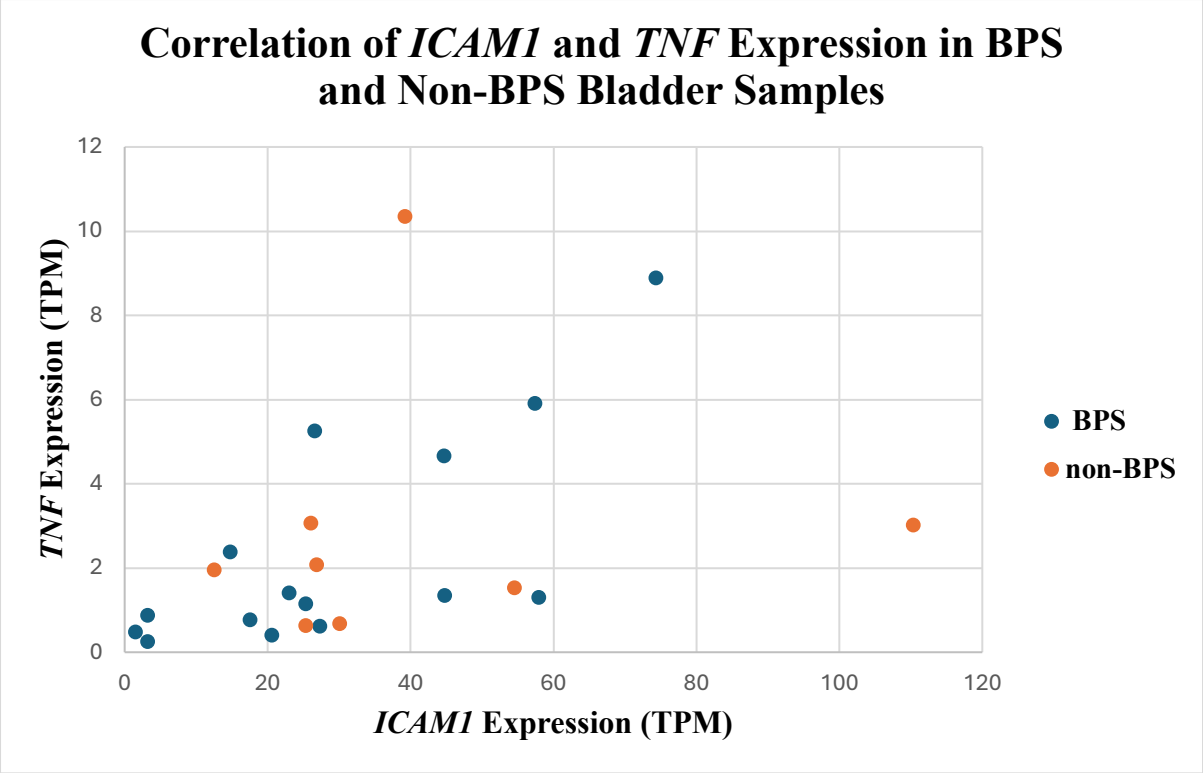


**Figure 3.4.17: Correlation Between *ICAM1* and *TNF* Expression in BPS and Non-BPS P0 Bladder Samples.**

Scatter plot showing transcript per million (TPM) expression values for *ICAM1* and *TNF* in primary (P0) bladder tissue samples from BPS (blue) and non-BPS (orange) patients. A significant large positive correlation was observed in BPS samples (Spearman's $\rho = 0.66$, $p = 0.01$), indicating coordinated upregulation of these inflammatory genes. In contrast, non-BPS samples showed a small, non-significant correlation ($\rho = 0.29$, $p = 0.55$). These results support a pro-inflammatory transcriptional profile in a subset of BPS patients and are consistent with previous reports linking intercellular adhesion molecules to cytokine-driven immune activation in bladder pain syndromes Green et al. (2004). This subset-specific co-expression further contributes to the emerging molecular heterogeneity within the BPS group.

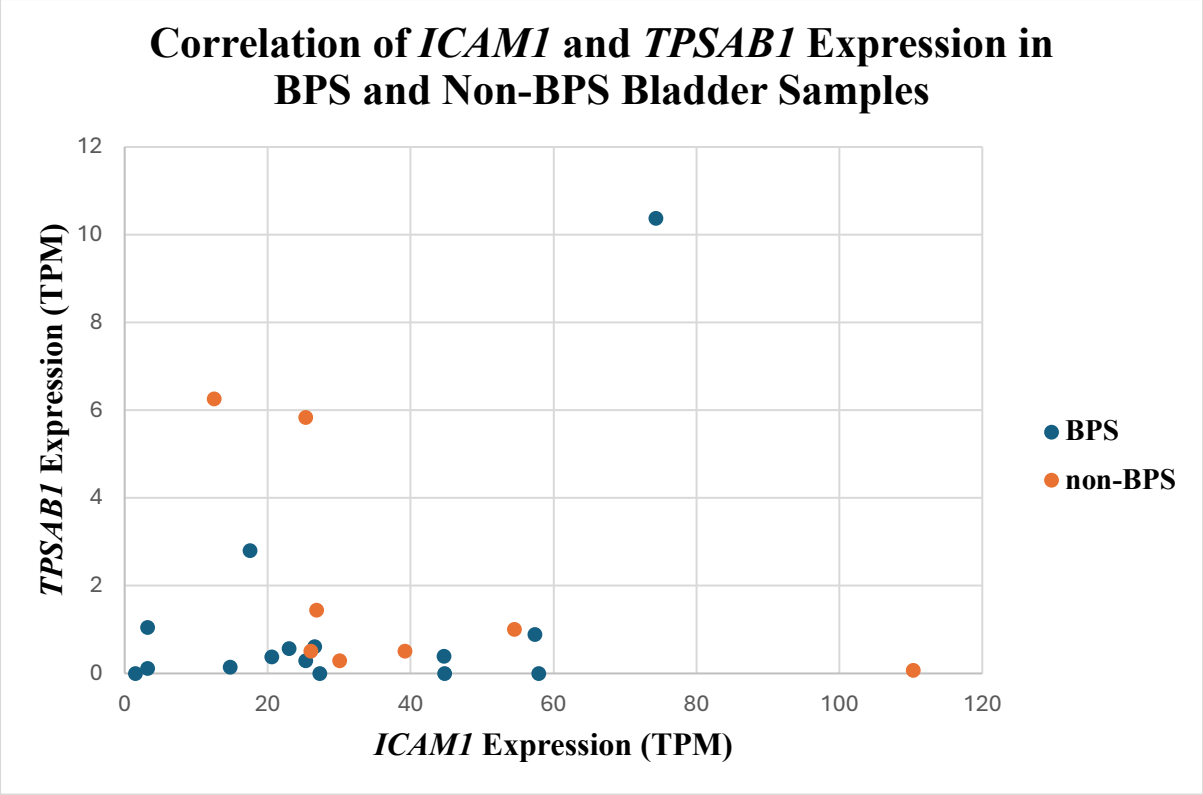


**Figure 3.4.18: Correlation of *ICAM1* and *TPSAB1* Expression in BPS and Non-BPS Bladder Samples.**

This scatter plot illustrates the relationship between *ICAM1* and *TPSAB1* transcript expression (TPM) in BPS (blue) and non-BPS (orange) P0 bladder tissue samples. *ICAM1* encodes a key adhesion molecule involved in leukocyte recruitment and endothelial interaction, while *TPSAB1* is a marker of mast cell activity—both implicated in the chronic inflammatory landscape of bladder pain conditions. Spearman rank correlation analysis revealed a **non-significant, very weak positive association in BPS samples** ($r_s = 0.07$, $p = 0.79$), suggesting minimal co-regulation between immune cell adhesion and mast cell activation in this group. In contrast, **a significant strong negative correlation was observed in non-BPS samples** ($r_s = –0.79$, $p = 0.03$), potentially indicating distinct immune cell dynamics or spatial segregation of inflammatory activity in non-BPS tissues.

These divergent patterns further support the hypothesis that BPS is a heterogeneous condition, encompassing multiple transcriptional subtypes. The lack of coordinated *ICAM1–TPSAB1* expression in BPS contrasts with findings from IC-focused studies like Green et al. (2004), suggesting that not all BPS patients exhibit the same inflammatory cell recruitment profiles. Such observations reinforce the utility of exploring transcriptional variability as a route toward better BPS stratification.

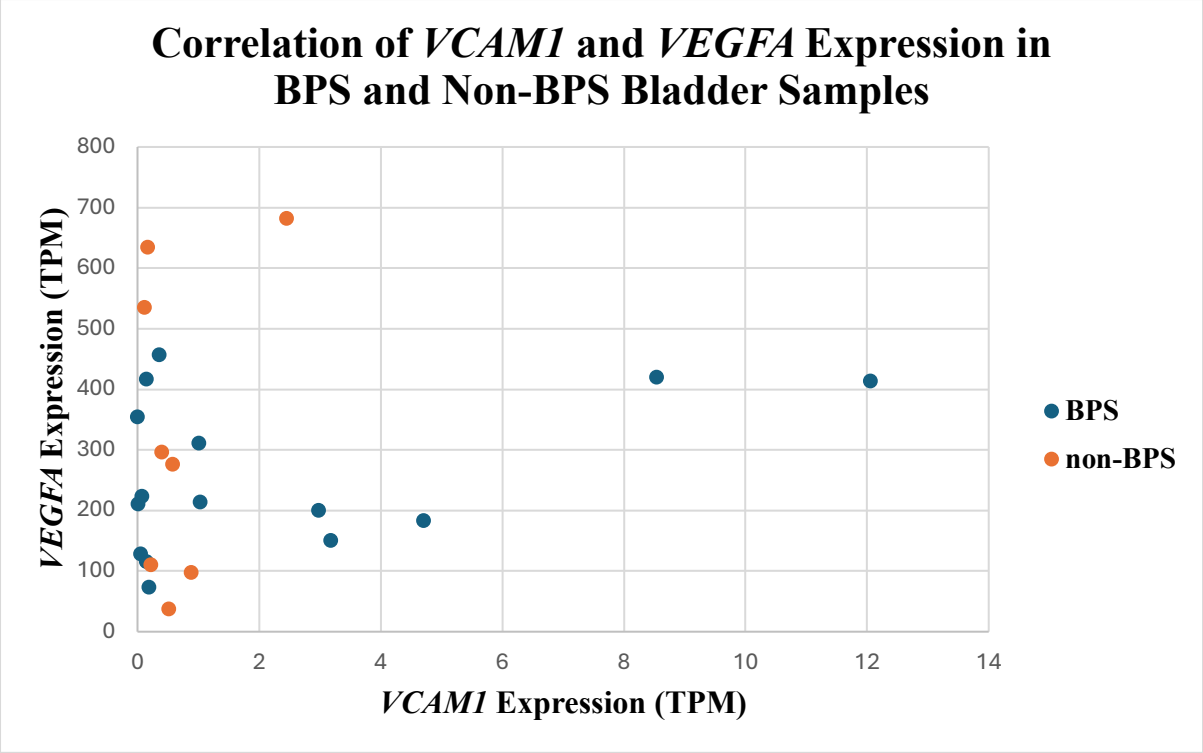


**Figure 3.4.19 Correlation of *VCAM1* and *VEGFA* Expression in BPS and Non-BPS Bladder Samples.**

Scatter plot displaying the relationship between *VCAM1* and *VEGFA* transcript expression (TPM) in BPS (blue) and non-BPS (orange) P0 bladder tissue samples. *VCAM1* encodes a vascular adhesion molecule involved in leukocyte recruitment and endothelial activation, while *VEGFA* plays a central role in angiogenesis and vascular permeability—processes previously implicated in IC/BPS pathophysiology in Green et al. (2004).

Spearman rank correlation analysis showed a non-significant small positive correlation in BPS samples ($r_s = 0.14$, $p = 0.70$), and a non-significant small negative correlation in non-BPS samples ($r_s = –0.14$, $p = 0.92$). These weak associations suggest limited transcriptional coordination between vascular adhesion and angiogenic signalling pathways in either group.

The absence of a consistent *VCAM1–VEGFA* relationship across groups may reflect inter-patient variability in vascular remodelling and immune-endothelial interactions—further supporting the hypothesis that BPS encompasses molecularly distinct subtypes. Each point on the plot represents one patient sample.

**Study 7**

Yang et al. (2012) reported that antiproliferative factor (APF) modulates epithelial proliferation, tight-junction integrity, and inflammatory signalling in IC/BPS. To evaluate whether similar transcriptional features were detectable in our cohort, we assessed expression of APF-associated genes involved in epithelial junctional structure (*TJP1*, *CLDN4*, *DSG2*), cell-cycle regulation (*CDKN1A*, *MKI67*, *TP53*), and inflammatory or stress-related responses (*IL6*, *MAPK14*, *HSPA1A*).

As with previous analyses, none of the genes showed statistically significant differences between BPS and non-BPS samples (all $p > 0.05$; Table 3.4.14; Figure 3.4.20). However, several individual BPS samples displayed pronounced deviations from the cohort average, indicating potential APF-linked pathway activity at the patient level.

Sample Y2338, which consistently emerged as an immune-activated outlier in Studies 1–6, again demonstrated substantial upregulation across multiple APF-related genes. Elevated *TJP1*, *CLDN4*, and *DSG2* expression suggests enhanced tight-junction signalling, while markedly increased *CDKN1A* and reduced *MKI67* imply a shift toward anti-proliferative regulation. This was accompanied by strong induction of *IL6* and *HSPA1A*, consistent with inflammatory and cellular stress activity. Clinically, Y2338 presented with suprapubic pain, urinary frequency, and dyspareunia; cystoscopy revealed glomerulations without ulceration, and symptom scores were relatively high (IC Symptom Index 10; Problem Index 10), features compatible with an inflamed but non-ulcerative BPS phenotype.

Sample Y2336 similarly demonstrated elevated *IL6*, *MAPK14*, and modestly raised *TP53*. Together with high *TNF*, *ICAM1*, *CXCL13*, and MHC class II expression reported in previous studies, this pattern suggests activation of inflammatory and stress-response pathways. Clinically, Y2336 exhibited pain with intermittent frequency, post-intercourse discomfort, and cystoscopic evidence of both glomerulations and trabeculations, with moderate symptom severity (IC Symptom Index 8; Problem Index 7).

Other BPS samples exhibited more selective APF-related transcriptional features. For example, Y2538 and Y2595 displayed particularly high *CLDN4* and *CDKN1A* expression with low *MKI67*, suggestive of a tight-junction–preserved but anti-proliferative urothelial state. Both individuals had longstanding symptoms (22 years in Y2538; 2 years in Y2595),

and each demonstrated glomerulations at cystoscopy, which may reflect chronic epithelial stress or adaptation.

Correlation analyses (e.g., *TP53* vs. *CDKN1A*, *TP53* vs. *MKI67*) were non-significant in both BPS and non-BPS groups, indicating that coordinated suppression of proliferation—one hallmark of APF activity—was not apparent at the cohort level.

In summary, although APF-related pathways were not broadly dysregulated across the entire BPS group, several samples—most prominently Y2338 and Y2336—exhibited transcriptional patterns compatible with APF-responsive signalling, including tight-junction modulation, inflammation, cellular stress responses, and reduced proliferative potential. When interpreted alongside their clinical metadata and the multi-pathway immune activation documented in earlier studies, these findings reinforce the presence of a transcriptionally distinct BPS subset. Such cases underscore ongoing disease heterogeneity and highlight the potential value of integrating APF-related transcriptional markers into future stratification frameworks.

**Table 3.4.14: Summary of transcriptomic expression analyses of APF-related candidate genes in bladder pain syndrome (BPS) and non-BPS samples.**

This table summarises the expression levels of selected genes associated with antiproliferative factor (APF) pathways in primary (P0) bladder tissue samples from BPS and non-BPS patients. Genes were chosen based on the study by Yang et al. (2012), which identified APF-mediated changes in pathways related to cell adhesion, proliferation, and inflammation. Mean transcripts per million (TPM) values are shown for each group, alongside the results of Mann–Whitney U tests comparing gene expression between BPS and non-BPS samples. Direction of change indicates the trend in expression in BPS relative to non-BPS. No statistically significant differences were detected (all $p > 0.05$), indicating that transcriptional regulation of these pathways may not be a universal feature in BPS or may require additional clinical context to be informative.

| Gene | Function | Mean TPM (BPS) | Mean TPM (non-BPS) | Test Used | p-value | Direction of Change |
|---|---|---|---|---|---|---|
| ***TJP1*** | Tight junction integrity | 51.65 | 50.90 | Mann–Whitney U | 0.93 | No significant difference |
| ***CLDN4*** | Tight junction protein | 2644.81 | 3113.07 | Mann–Whitney U | 0.68 | No significant difference |
| ***DSG2*** | Cell adhesion protein | 71.07 | 79.68 | Mann–Whitney U | 0.68 | No significant difference |
| ***CDKN1A*** | Cell cycle arrest | 557.81 | 568.22 | Mann–Whitney U | 0.93 | No significant difference |

| | | | | | | |
|---|---|---|---|---|---|---|
| ***MKI67*** | Proliferation marker | 0.73 | 0.75 | Mann–Whitney U | 0.78 | No significant difference |
| ***TP53*** | Tumour suppressor gene | 21.04 | 19.61 | Mann–Whitney U | 0.33 | No significant difference |
| ***IL6*** | Inflammatory cytokine | 1.64 | 0.74 | Mann–Whitney U | 0.56 | No significant difference |
| ***MAPK14*** | Stress-response kinase | 15.66 | 14.40 | Mann–Whitney U | 0.78 | No significant difference |
| ***HSPA1A*** | Heat shock protein, cellular stress | 3062.24 | 1032.51 | Mann–Whitney U | 0.47 | No significant difference |

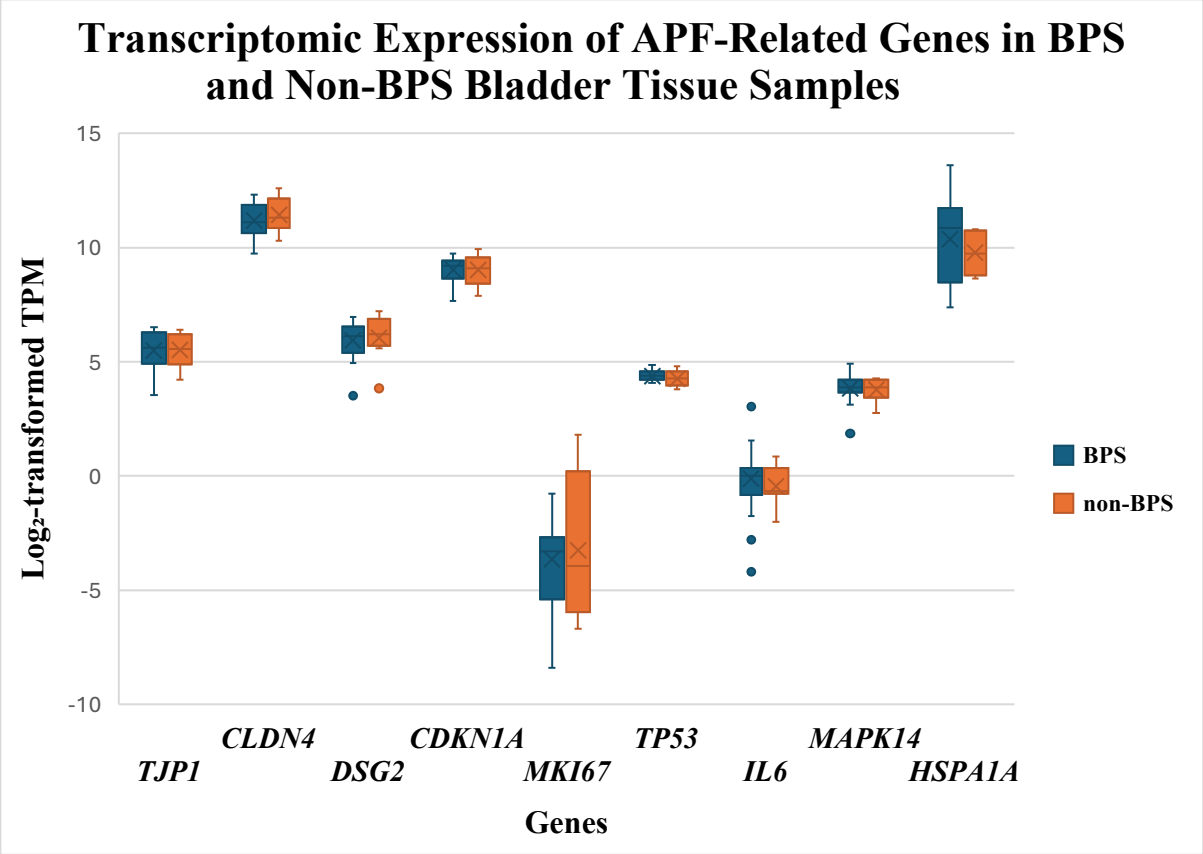


**Figure 3.4.20: Box-and-whisker plots comparing $log_2$-transformed transcriptomic expression of APF-related candidate genes in BPS and non-BPS samples.**

This figure displays the $log_2$-transformed transcriptomic expression levels (TPM) of selected genes associated with antiproliferative factor (APF) pathways—including those involved in cell adhesion, proliferation, and inflammation—in bladder tissue samples from BPS (blue) and non-BPS (orange) patients. Genes shown include *DKK1*, *CDH1*, *EGR1*, *IL6*, and *TGFB1*. Each plot shows individual sample points, median values, and interquartile ranges, providing a visual comparison of gene expression distributions across groups. No statistically significant differences were observed between BPS and non-BPS samples for any gene (all $p > 0.05$; see Table 3.4.14). This suggests that transcriptional dysregulation of APF-related pathways is not a consistent feature of BPS in this cohort.

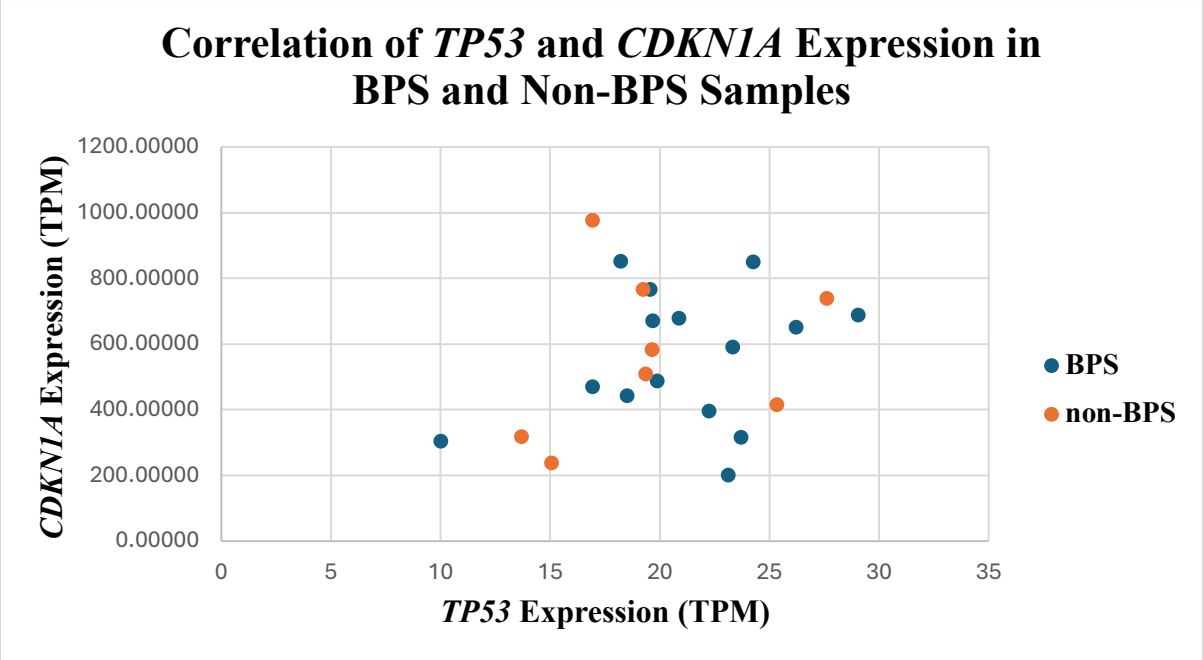


**Figure 3.4.21: Spearman correlation analysis between *TP53* and *CDKN1A* expression in BPS and non-BPS samples.**

Spearman rank correlation analysis between *TP53* and *CDKN1A* transcript expression in bladder pain syndrome (BPS) and non-BPS primary (P0) bladder tissue samples revealed a non-significant small positive correlation in BPS ($r_s = 0.14$, $p = 0.70$), indicating minimal evidence of coordinated transcriptional regulation between these key cell cycle regulators in BPS. In contrast, non-BPS samples exhibited a non-significant medium positive correlation ($r_s = 0.31$, $p = 0.50$). Data points represent individual sample TPM values, and the dashed line indicates the line of best fit. These results suggest that *TP53* and *CDKN1A* are not significantly co-regulated at the transcriptomic level in BPS, highlighting the complex transcriptional landscape of cell cycle control in bladder pain syndrome.

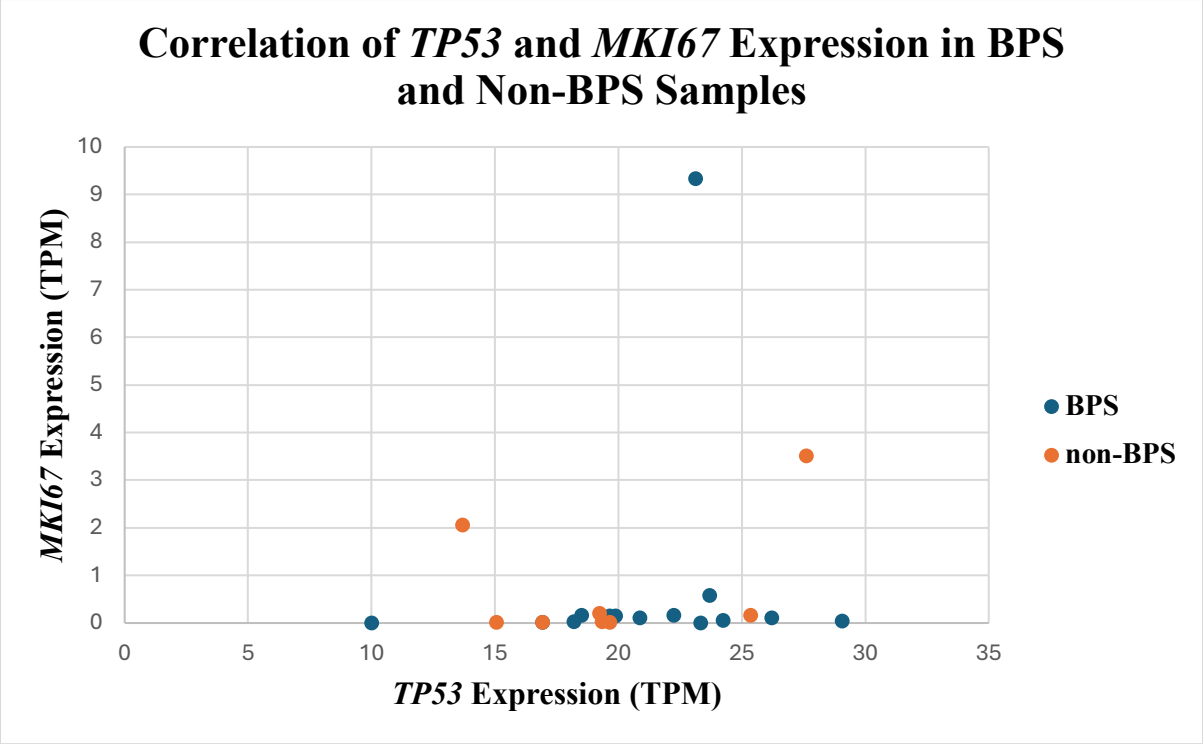


**Figure 3.4.22: Correlation of *TP53* and *MKI67* Expression in BPS and Non-BPS Samples.** Spearman rank correlation analysis assessed the relationship between *TP53* and *MKI67* gene expression levels in BPS and non-BPS primary bladder tissue samples. In BPS samples, a non-significant small positive correlation was observed ($r_s = 0.21$, $p = 0.46$), while non-BPS samples also exhibited a non-significant small positive correlation ($r_s = 0.21$, $p = 0.70$). These findings suggest a limited association between cell cycle regulatory genes *TP53* and *MKI67* in the pathophysiology of BPS.

**Study 8**

Shie, Liu and Kuo (2012) proposed that urothelial apoptosis in IC/BPS is driven by inflammation—particularly activation of the *TNF–MAPK14* axis—with downstream engagement of apoptotic mediators such as *CASP3*, *CASP8*, and *BAX*. To evaluate whether similar transcriptional features were present in this cohort, TPM expression levels of *MAPK14*, *TNF*, *IL6*, *IL1B*, *CASP3*, *CASP8*, and *BAX* were examined in P0 bladder tissue from BPS and non-BPS patients.

Group-level analyses showed no statistically significant differences for any transcript (all $p > 0.05$; Table 3.4.15; Figure 3.4.23), and average expression changes were modest. Mean values for *MAPK14*, *CASP3*, *CASP8*, *BAX*, and *IL6* trended slightly higher in BPS, whereas *TNF* and *IL1B* were marginally lower—patterns that diverge from the histological findings of Shie, Liu and Kuo (2012). These discrepancies may reflect post-transcriptional regulation, cellular composition differences, or cohort heterogeneity. Nevertheless, individual-level expression patterns revealed several biologically meaningful deviations.

Sample Y2336 again exhibited a highly distinctive transcriptional profile, characterised by concurrent elevation of *MAPK14*, *TNF*, *IL6*, *IL1B*, and *CASP8*. Clinically, this individual presented with bladder/suprapubic pain, intermittent frequency, glomerulations, and moderate symptom scores, a profile compatible with an active inflammatory environment capable of engaging apoptotic pathways. Y2338 showed a similar pattern, with strong expression of *TNF*, *IL6*, *IL1B*, *CASP3*, and *BAX*, and likewise presented with suprapubic pain, frequency, dyspareunia, and glomerulations. Together, these samples illustrate a recurring transcriptional phenotype characterised by inflammatory activation coupled with apoptotic signalling, consistent with Shie et al.'s mechanistic model.

Correlational analyses provided further support for pathway-level interactions. *MAPK14* and *CASP3* were strongly positively correlated in BPS samples ($\rho = 0.85$, $p < .001$; Figure 3.4.24), suggesting coordinated regulation of apoptosis via p38 MAPK signalling. By contrast, associations between *MAPK14* and *TNF*, and between *TNF* and *CASP3*, were weak and non-significant, implying that apoptosis in some BPS cases may proceed through *TNF*-independent mechanisms.

In summary, although cohort-level comparisons did not indicate widespread activation of the *TNF–MAPK14* apoptotic axis, individual-level analysis identified a subset of BPS patients—

most prominently Y2336 and Y2338—with transcriptional features consistent with inflammation-linked apoptosis. These same individuals repeatedly emerged as immune-activated transcriptomic outliers in Studies 1–7, reinforcing the broader conclusion that BPS comprises molecularly heterogeneous endotypes. Study 8 adds further evidence for an immune–apoptotic subtype within BPS, highlighting the importance of integrating transcriptional data with clinical metadata to resolve clinically relevant patterns of disease biology.

**Table 3.4.15: Expression of Apoptosis and Inflammatory Genes in BPS and Non-BPS Samples.**

Summary of transcriptomic expression data for genes associated with inflammation (*MAPK14, TNF, IL6, IL1B*) and apoptosis (*CASP3, BAX, CASP8*) in primary bladder tissue samples from BPS and non-BPS patients. Mean TPM values are presented alongside Mann–Whitney U test results. Although no gene reached statistical significance, several showed mild expression differences between groups. These genes were selected based on their reported involvement in the p38 MAPK-mediated inflammatory apoptosis pathway described by Shie et al., (2012) aiming to explore whether a similar transcriptional profile was present in the BPS cohort.

| Gene | Function | Mean TPM (BPS) | Mean TPM (non-BPS) | Test Used | p-value | Direction of Change |
|---|---|---|---|---|---|---|
| ***MAPK14*** | p38 MAPK, inflammation signalling | 15.66 | 14.40 | Mann–Whitney U | 0.78 | No significant difference |
| ***TNF*** | Pro-inflammatory cytokine | 2.38 | 2.91 | Mann–Whitney U | 0.36 | No significant difference |

| | | | | | | |
|---|---|---|---|---|---|---|
| ***IL6*** | Inflammatory cytokine | 1.64 | 0.74 | Mann–Whitney U | 0.56 | No significant difference |
| ***IL1B*** | Inflammatory cytokine | 53.80 | 58.55 | Mann–Whitney U | 0.98 | No significant difference |
| ***CASP3*** | Executioner caspase in apoptosis | 21.49 | 18.48 | Mann–Whitney U | 0.73 | No significant difference |
| ***BAX*** | Pro-apoptotic regulator | 55.03 | 51.81 | Mann–Whitney U | 0.43 | No significant difference |
| ***CASP8*** | Initiator caspase in extrinsic apoptosis | 14.51 | 12.81 | Mann–Whitney U | 0.55 | No significant difference |

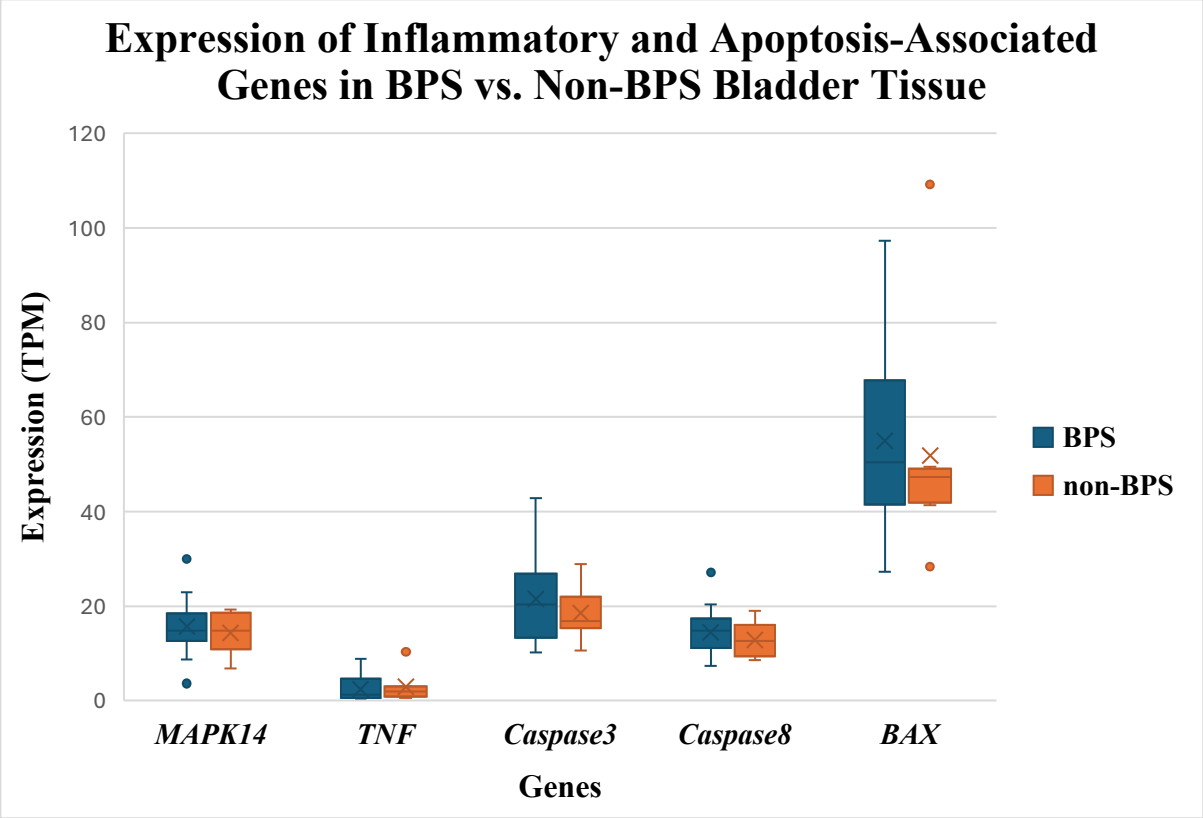


**Figure 3.4.23: Paired Box-and-Whisker Plot of Inflammatory and Apoptosis-Related Gene Expression in BPS and Non-BPS P0 Samples.**

Box-and-whisker plots showing transcript expression levels (TPM) of five genes—*MAPK14, TNF, CASP3, CASP8*, and *BAX*—associated with inflammatory and apoptotic pathways in primary (P0) bladder tissue samples from BPS and non-BPS patients. Each gene is represented by two adjacent box plots: BPS (blue) and non-BPS (orange). Boxes indicate the interquartile range (IQR), with the median marked by a central line and the mean denoted by "×". Whiskers extend to 1.5× IQR, and individual points represent outliers. No genes showed statistically significant differences between BPS and non-BPS groups (all $p > 0.05$), though subtle upward trends in *BAX, CASP3*, and *MAPK14* were observed in BPS samples. These genes were selected to assess evidence for the p38 MAPK-driven inflammatory apoptosis pathway proposed by Shie et al., (2012).

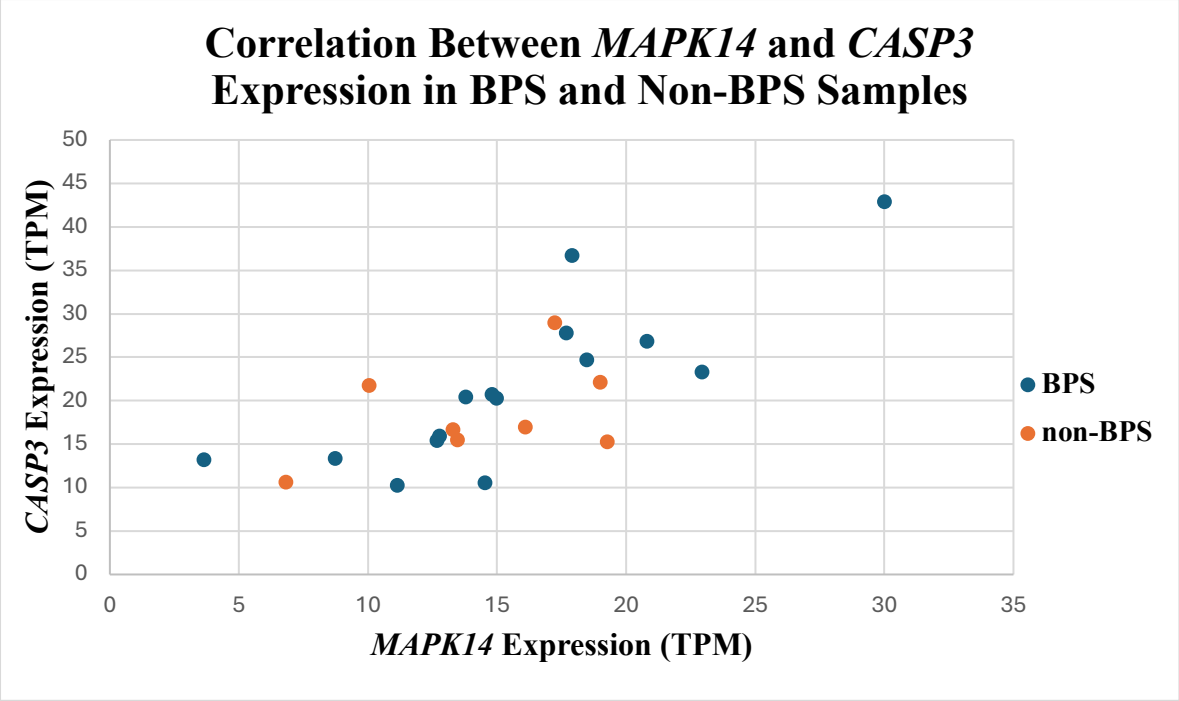


**Figure 3.4.24: Correlation Between *MAPK14* and *CASP3* Expression in BPS and Non-BPS Samples.**

Scatter plot showing the relationship between *MAPK14* and *CASP3* expression (TPM) in primary (P0) bladder tissue samples from BPS (blue) and non-BPS (orange) patients. In BPS samples, a significant large positive correlation was observed between *MAPK14* and *CASP3* expression (*Spearman's* $\rho = 0.85$, $p < 0.001$), suggesting a strong potential link between p38 MAPK signalling and apoptosis in this subgroup. In contrast, a non-significant medium positive correlation was found in non-BPS samples ($\rho = 0.31$, $p = 0.50$). Each point represents an individual sample. These findings support inflammation-mediated apoptosis as a possible mechanism active in a subset of BPS patients.

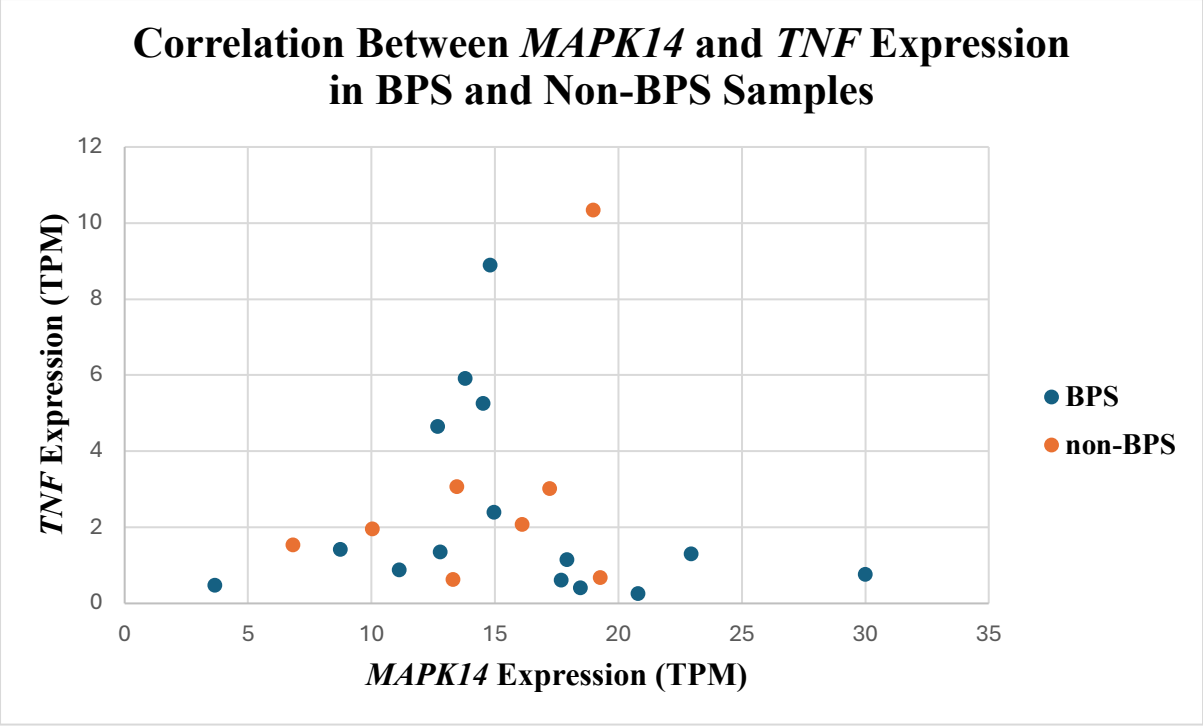


**Figure 3.4.25: Correlation Between *MAPK14* and *TNF* Expression in BPS and Non-BPS Samples.**

Scatter plot showing the relationship between *MAPK14* and *TNF* expression (TPM) in primary (P0) bladder tissue samples from BPS (blue) and non-BPS (orange) groups. In BPS samples, a non-significant medium negative correlation was observed (*Spearman's* $\rho = 0.33$, $p = 0.24$), while non-BPS samples demonstrated a non-significant medium positive correlation ($\rho = 0.31$, $p = 0.50$). Each dot represents an individual patient sample. These findings suggest that while *MAPK14* and *TNF* may both be elevated in inflammation-related contexts, they are not tightly co-regulated at the transcriptomic level in either group, further supporting mechanistic divergence within BPS subtypes.

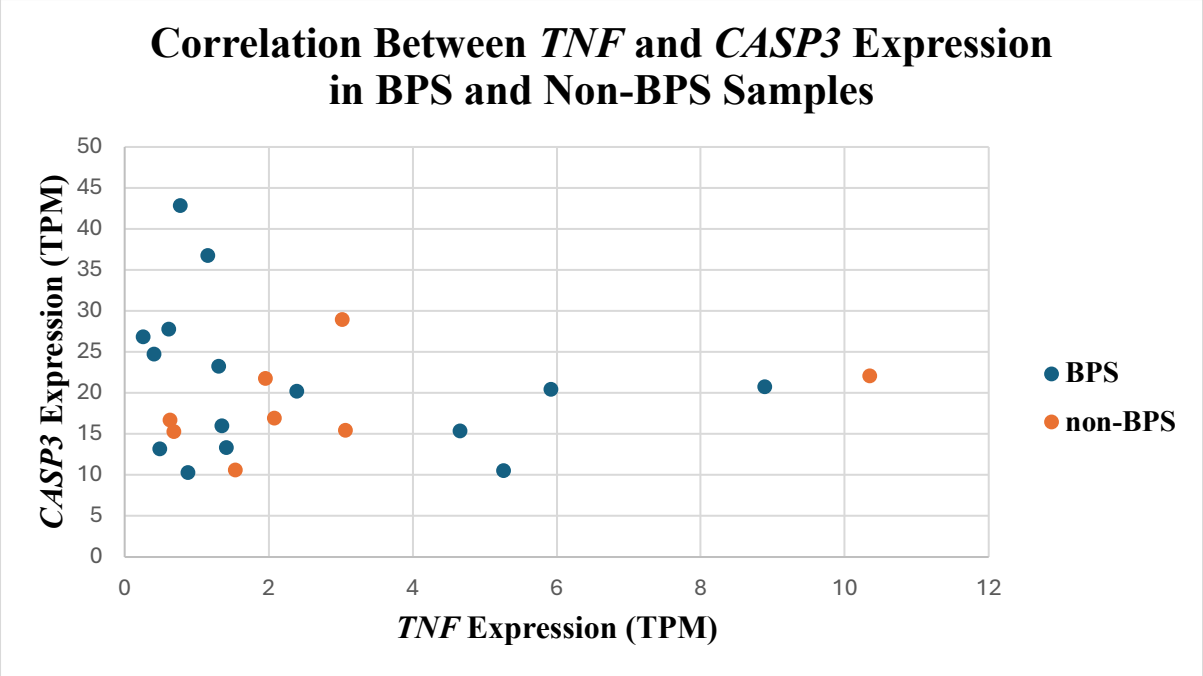


**Figure 3.4.26: Correlation Between *TNF* and *CASP3* Expression in BPS and Non-BPS Samples.**

Scatter plot illustrating the relationship between *TNF* and *CASP3* transcript expression (TPM) in BPS (blue) and non-BPS (orange) P0 bladder tissue samples. In BPS samples, a non-significant medium negative correlation was observed (*Spearman's* $\rho = -0.36$, $p = 0.19$), while non-BPS samples showed a non-significant large positive correlation ($\rho = 0.55$, $p = 0.18$). Each point represents an individual sample. Although not statistically significant, these opposing trends may reflect subgroup-specific apoptotic or inflammatory responses, contributing to the transcriptional heterogeneity observed in BPS.

**Study 9**

Liu et al. (2012) reported reduced protein expression of E-cadherin and ZO-1—encoded by *CDH1* and *TJP1*—in patients with IC/BPS, associating these deficits with impaired epithelial barrier function and increased mast cell infiltration. To determine whether similar changes were detectable at the transcriptomic level in the present cohort, *CDH1* and *TJP1* expression was examined in P0 bladder tissue from BPS and non-BPS patients.

Neither gene demonstrated statistically significant differential expression between groups (all $p > 0.05$). Mean *CDH1* expression was slightly higher in BPS (145.96 vs. 138.89 TPM), and *TJP1* showed a similarly small increase (51.65 vs. 50.90 TPM), with both differences being negligible (Table 3.4.16; Figure 3.4.27). These findings indicate that transcription of major junctional components is broadly preserved in BPS, in contrast to the reductions in E-cadherin and ZO-1 protein levels previously described by Liu et al. (2012).

Inspection of individual samples revealed no notable outliers among BPS patients—including immune-activated cases such as Y2336 and Y2338, which consistently showed deviations in inflammatory and antigen-presentation pathways across Studies 1–8. The absence of marked transcriptional suppression in these individuals further suggests that junctional deficits, where present, may arise from post-transcriptional mechanisms such as altered protein turnover, trafficking, or localisation. Such mechanisms would not be captured by bulk RNA profiling and may instead align with structural or functional disruptions observed cystoscopically in some patients.

This pattern parallels findings from Studies 5 and 8, where apoptosis-related and inflammatory genes showed no consistent group-level dysregulation despite biological plausibility. Across the dataset, epithelial barrier dysfunction therefore does not appear to be driven by reduced transcription of *CDH1* or *TJP1*. Nonetheless, this does not preclude barrier involvement in specific molecular subtypes, nor does it rule out the contribution of post-transcriptional or spatially restricted changes not detectable in homogenised tissue.

Overall, Study 9 supports the broader conclusion emerging across Studies 1–8: transcriptional heterogeneity characterises BPS, but widespread suppression of urothelial adhesion or tight-junction genes is not evident at the RNA level. Future analyses integrating proteomic, spatial, or single-cell approaches may be required to determine whether junctional compromise plays a role in defined patient subsets.

**Table 3.4.16: Expression of junctional complex genes in BPS vs non-BPS samples.**

Transcriptomic analysis of primary urothelial (P0) bladder tissue samples from BPS and non-BPS patients revealed no statistically significant differences in the expression of ***CDH1*** and ***TJP1***, as shown in the table. This analysis was conducted to assess the hypothesis put forward by Liu et al. (2012), who reported that **reduced E-cadherin (*CDH1*)** and **ZO-1 (*TJP1*)** expression contributes to **urothelial barrier dysfunction and inflammation** in IC/BPS. Although both genes showed a slight increase in expression in the BPS group, these differences were not statistically significant ($p = 0.83$ for *CDH1* and $p = 0.93$ for *TJP1*), suggesting that the transcriptional levels of these junctional proteins may not be substantially altered in this cohort. These findings do not support the original hypothesis, at least at the transcript level, in this dataset.

| Gene | Function | Mean TPM (BPS) | Mean TPM (non-BPS) | Test Used | p-value | Direction of Change |
|---|---|---|---|---|---|---|
| ***CDH1*** | Encodes E-cadherin, a transmembrane adhesion protein critical for maintaining epithelial integrity and cell–cell junctions | 145.96 | 138.89 | Mann–Whitney U | 0.83 | No significant difference |
| ***TJP1*** | Encodes ZO-1 (Zonula Occludens-1), a scaffolding protein essential for tight junction formation and barrier maintenance | 51.65 | 50.90 | Mann–Whitney U | 0.93 | No significant difference |

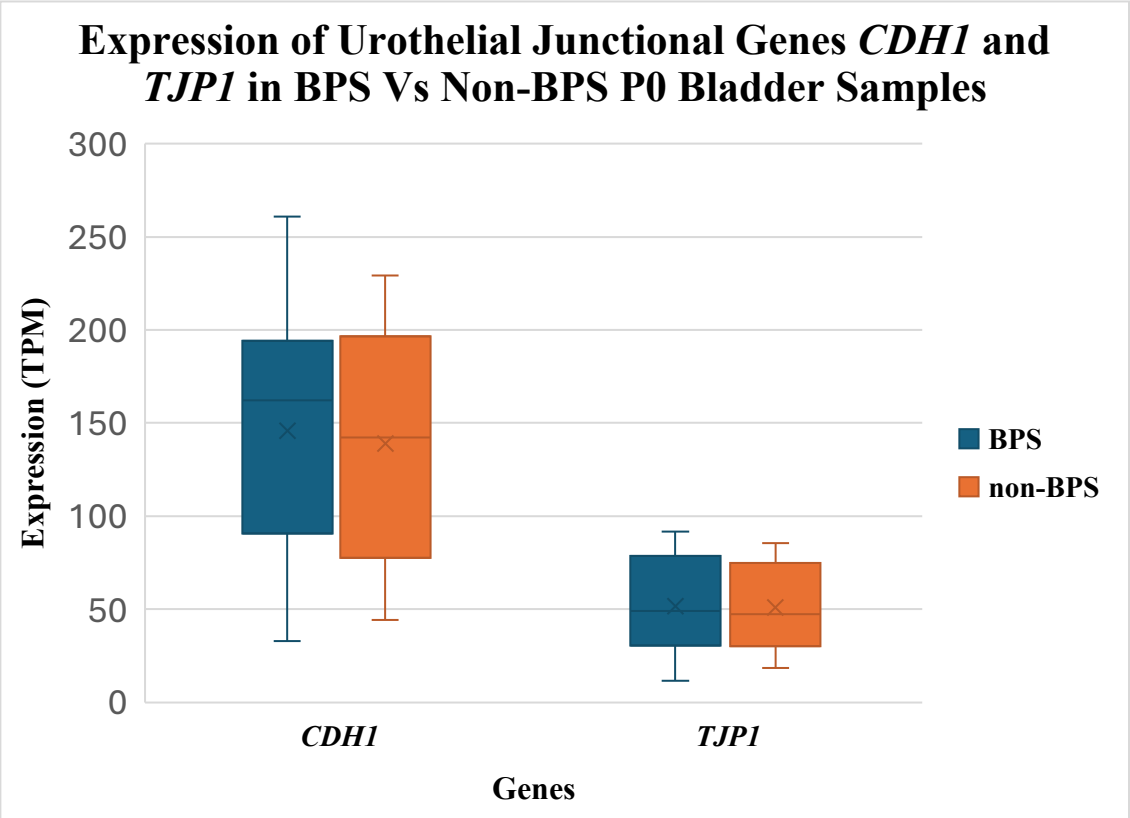


**Figure 3.4.27: Box-and-Whisker Plot of Urothelial Junctional Gene Expression in BPS and Non-BPS P0 Samples.**

Box-and-whisker plot showing transcript per million (TPM) expression levels for the junctional genes *CDH1* and *TJP1* across primary (P0) bladder tissue from BPS and non-BPS patients. Each gene is displayed on the x-axis with paired boxplots: BPS (blue) and non-BPS (orange). Boxes represent the interquartile range (IQR), with the median as a horizontal line and the mean marked with an "×". Whiskers extend to 1.5× the IQR, and outliers are shown as individual points. No statistically significant differences in gene expression were observed between BPS and non-BPS groups ($p > 0.05$). These genes were assessed based on previous findings by Liu et al. (2012), which reported reduced E-cadherin and ZO-1 protein expression in IC/BPS urothelium, associated with impaired barrier integrity and mast cell infiltration.

**Study 10**

Lee, Jiang and Kuo (2013) reported reduced protein expression of E-cadherin and associated tight-junction components in both ketamine cystitis and IC/BPS, accompanied by heightened apoptosis and mast cell infiltration. These findings suggested a shared pathogenic mechanism featuring urothelial barrier disruption, inflammatory activation and epithelial injury. Their conclusions built directly on earlier work by Liu et al. (2012), who likewise associated impaired junctional protein expression with increased permeability and mast cell recruitment.

In the present dataset, however, transcriptional patterns did not reproduce these protein-level reductions. *CDH1* expression was slightly higher in BPS than in non-BPS samples (145.96 vs. 138.89 TPM; $p = 0.83$), and *TJP1* showed no meaningful difference between groups (51.65 vs. 50.90 TPM; $p = 0.93$) (Figure 3.4.27; Table 3.4.16). These findings, consistent with Studies 5, 7, and 9, suggest that the loss of junctional integrity observed histologically in prior work may not arise from transcriptional suppression, but instead from post-transcriptional mechanisms, altered protein localisation or turnover, or disease-stage differences not captured in early-passage P0 tissue.

To explore the proposed inflammatory–apoptotic axis, we additionally examined *CASP3*, *CASP8*, *BAX*, *TNF*, *TPSAB1*, and *VEGFA*. None showed statistically significant group-wise differences, although modestly higher mean expression of *CASP3*, *CASP8* and *BAX* in BPS samples was directionally consistent with the apoptotic involvement described by Lee, Jiang and Kuo (2013). These trends parallel findings in Studies 5 and 8, where apoptotic mediators exhibited mild upregulation without reaching significance.

Correlation analysis provided stronger mechanistic support for an apoptosis-linked pathway. A large, statistically significant positive association was observed between *MAPK14* and *CASP3* in BPS samples ($\rho = 0.85$, $p < 0.001$; Figure 3.4.24), consistent with p38-MAPK–dependent apoptotic signalling. By contrast, *MAPK14* showed no significant association with *TNF*, and *TNF* correlated negatively with *CASP3*, suggesting that TNF-driven apoptosis is not uniformly active and may operate only in selected cases or be overshadowed by TNF-independent pathways.

At the individual-sample level, Y2338 again exhibited transcriptional features concordant with an immune–apoptotic phenotype, including elevated *TNF* (5.91 TPM), *MAPK14* (13.80 TPM), and modest increases in apoptotic markers. This pattern aligns with findings from

Studies 4, 6, and 8, where Y2338 consistently showed heightened immune activation, adhesion molecule upregulation and stress-responsive transcription. Other samples, such as Y2336 and Y2538, showed elevated gene expression within specific pathways but did not demonstrate the broader co-expression observed in Y2338, suggesting heterogeneity in the extent and combination of pathway activation.

Overall, Study 10 supports the overarching conclusion that BPS does not exhibit uniform transcriptional suppression of epithelial junctional genes, nor consistent activation of inflammatory–apoptotic cascades at the cohort level. Instead, individual-level patterns—particularly in samples such as Y2338—indicate that distinct molecular subtypes may underlie the clinical heterogeneity observed in BPS. These findings reinforce the rationale for subtype-focused analyses integrating transcriptomic, clinical and cystoscopic features.

**Study 11**

Mukerji et al. (2010) reported increased protein expression of cannabinoid receptor 1 (CB1) in bladder tissue from BPS patients and suggested a link between CB1 activation, symptom severity, and pain modulation. To assess whether similar patterns were evident at the transcript level, expression of *CNR1*, *CNR2*, *FAAH*, and *TRPV1* was examined in primary (P0) bladder tissue from BPS and non-BPS patients.

No statistically significant differences were observed between groups for any of the cannabinoid-related genes (all $p > 0.05$; Table 3.4.17; Figure 3.4.28). Mean *CNR1* expression was only marginally higher in BPS than non-BPS samples (1.06 vs. 0.95 TPM; $p = 0.98$), and transcript levels of *CNR2*, *FAAH*, and *TRPV1* were similarly comparable. Correlation analysis also revealed no significant association between *CNR1* expression and O'Leary–Sant Symptom Index scores within the BPS group ($\rho = –0.18$, $p = 0.51$; Figure 3.4.29), providing little evidence that symptom severity is reflected in cannabinoid receptor transcript abundance at the cohort level.

Despite the absence of group-level differences, individual sample patterns suggested a possible link between cannabinoid signalling and pain perception in selected patients.

Notably, Y2610 exhibited the highest *CNR1* expression (3.04 TPM) and also the highest symptom burden (total score 20/20), alongside severe cystoscopic findings including glomerulations and low bladder capacity (300 ml). Unlike the immune-activated samples observed in earlier studies (e.g., Y2336 and Y2338), Y2610 showed relatively low *TNF* expression (0.77 TPM) and only moderate *TRPV1* expression (1.50 TPM), suggesting that heightened *CNR1* transcription in this individual may reflect a neuro-sensory rather than inflammatory mechanism.

This contrasts with samples such as Y2338, which demonstrated strong immune and adhesion signatures but did not show elevated cannabinoid pathway expression, reinforcing the distinction between immune-driven and sensory-driven symptom profiles within BPS. The dissociation between pain severity and inflammatory markers observed here is consistent with findings from Studies 8 and 10, where apoptosis- and inflammation-related genes did not consistently align with symptom intensity.

Taken together, these results do not indicate widespread upregulation of cannabinoid receptor or sensory transduction genes in BPS at the transcript level. However, individual-level variation—particularly in samples such as Y2610—suggests that cannabinoid-mediated sensory pathways may contribute to symptom severity in specific BPS subtypes. This interpretation further emphasises the heterogeneous molecular landscape of BPS and underscores the importance of integrating sensory, immune, and epithelial signalling pathways when interpreting patient-specific disease mechanisms.

**Table 3.4.17: Differential expression of cannabinoid and related pain signalling genes in BPS and non-BPS samples.**

Mean transcript per million (TPM) values and Mann–Whitney U test results for *CNR1*, *CNR2*, *FAAH*, and *TRPV1* expression in primary (P0) bladder tissue from patients with BPS (n = x) and non-BPS controls (n = y). Direction of change indicates higher expression in BPS (↑), lower expression in BPS (↓), or no difference compared to non-BPS. No statistically significant differences were observed for any genes (all $p > 0.05$).

| Gene | Function | Mean TPM (BPS) | Mean TPM (non-BPS) | Test Used | p-value | Direction of Change |
|---|---|---|---|---|---|---|
| ***CNR1*** | Encodes cannabinoid receptor 1 (CB1) | 1.06 | 0.95 | Mann–Whitney U | 0.98 | No significant difference |
| ***CNR2*** | Encodes cannabinoid receptor 2 (CB2) | 0.15 | 0.15 | Mann–Whitney U | 0.27 | No significant difference |
| ***FAAH*** | Fatty acid amide hydrolase, endocannabinoid breakdown | 44.46 | 42.68 | Mann–Whitney U | 0.64 | No significant difference |
| ***TRPV1*** | Pain signalling receptor, sensory neuron expression | 1.93 | 2.44 | Mann–Whitney U | 0.27 | No significant difference |

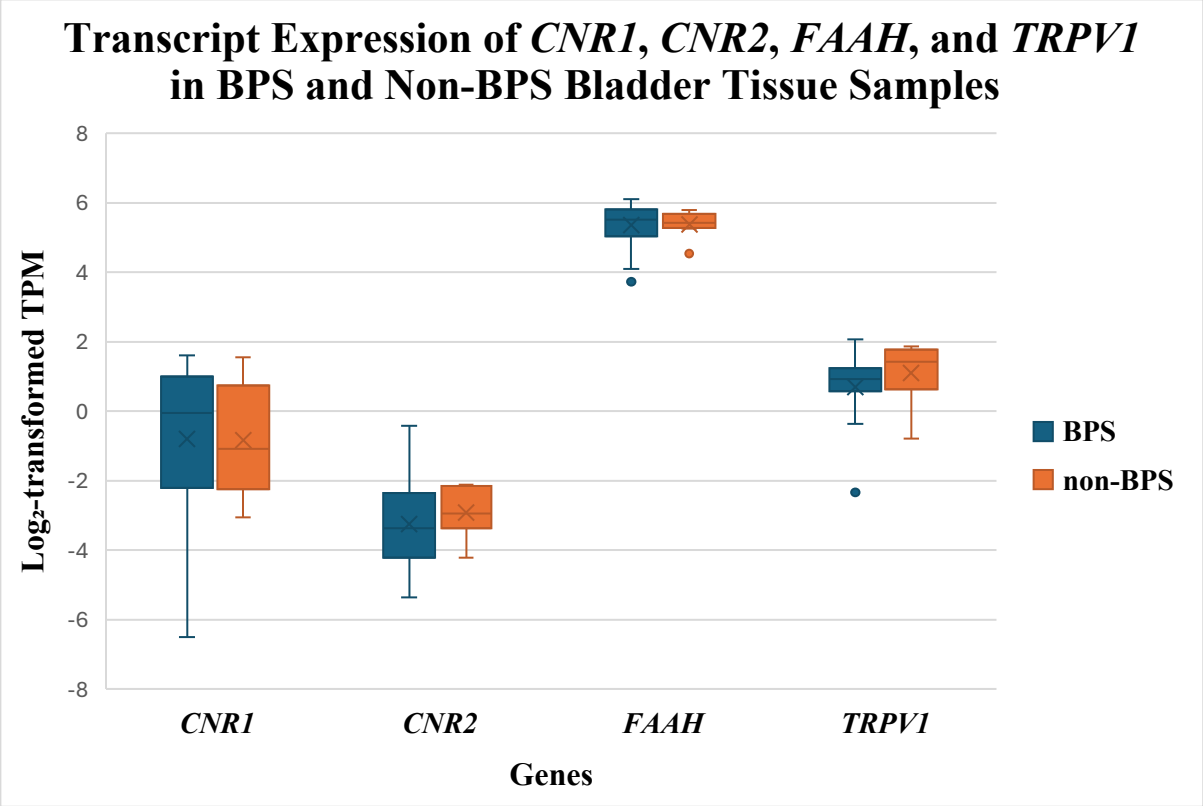


**Figure 3.4.28: Box-and-whisker plots showing transcript expression levels ($log_2$-transformed transcripts per million, TPM) of *CNR1*, *CNR2*, *FAAH*, and *TRPV1* in bladder tissue samples from BPS (blue) and non-BPS (orange) patients.**

Boxes represent the interquartile range (IQR), with horizontal lines indicating the median; whiskers extend to the 1.5× IQR or the range of the data. Individual data points are displayed to illustrate variability across samples.

No significant differences in expression were observed between groups (all $p > 0.05$), indicating limited transcriptional evidence for differential endocannabinoid system activation between BPS and non-BPS groups.

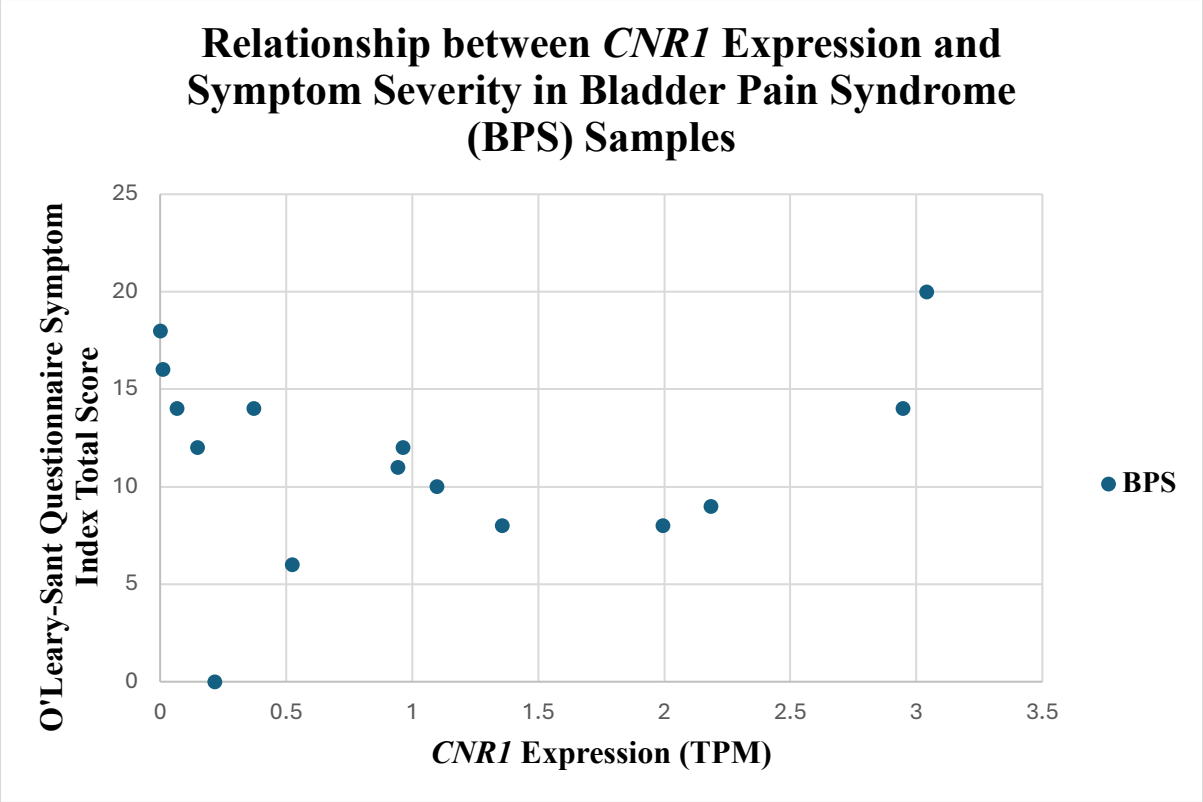


**Figure 3.4.29: Correlation between *CNR1* Expression and Symptom Severity (O'Leary-Sant Symptom Index Total Score) in BPS Samples.**

This scatterplot illustrates the relationship between *CNR1* transcript expression levels (TPM) and the O'Leary-Sant Symptom Index Total Score in bladder pain syndrome (BPS) samples. Spearman's rank correlation coefficient was calculated to assess the strength and direction of the association. A non-significant small negative relationship was observed ($r_s = –0.18$, $p = 0.51$), indicating that transcriptomic *CNR1* expression is not closely associated with symptom burden in this cohort.

**Study 12**

Saban et al. (2000) demonstrated that activation of the neurokinin-1 receptor (NK-1R), encoded by *TACR1*, amplifies bladder inflammation through mast cell activation and downstream cytokine release. To explore whether similar transcriptional patterns were present in the current cohort, expression of *TACR1*, its ligand *TAC1*, and downstream mediators *TNF* and *IL6* was evaluated in primary (P0) bladder tissue from BPS and non-BPS patients.

Group-level comparisons revealed no statistically significant differences for any transcripts examined (*TACR1* p = 0.77, *TAC1* p = 0.36, *TNF* p = 0.36, *IL6* p = 0.56; Table 3.4.18; Figure 3.4.30). However, several BPS samples demonstrated expression patterns suggestive of enhanced NK-1R–associated inflammatory signalling. Notably, Y2336 and Y2338 showed elevated *TACR1* expression (1.09 and 0.48 TPM), accompanied by increased *TNF* (8.89 and 5.92 TPM) and *IL6* (8.20 and 9.18 TPM). These two samples have recurrently appeared as immune-enriched outliers in earlier analyses—exhibiting heightened antigen presentation (*HLA-DRA*, *HLA-DPB1*), adhesion molecule expression (*ICAM1*, *VCAM1*), and apoptotic markers (e.g., *CASP3*, *BAX*). The co-occurrence of these signals with elevated *TACR1* further strengthens the interpretation that these individuals represent a transcriptionally distinct, inflammation-dominant BPS subtype.

Correlation analyses provided additional evidence for transcript-level coordination. In the non-BPS group, *TACR1* and *TNF* were positively associated ($\rho = 0.71$, $p = 0.05$; Figure 3.4.31), whereas in BPS samples, *TACR1* correlated strongly with *IL6* ($\rho = 0.63$, $p = 0.01$; Figure 3.4.32). This divergence may reflect differing regulatory environments in inflamed versus non-inflamed tissue. A significant negative association between *TACR1* and *TAC1* in BPS ($\rho = -0.58$, $p = 0.02$; Figure 3.4.33) suggests possible ligand–receptor feedback regulation or cell-type-specific expression patterns within the bladder mucosa.

Taken together, these findings do not support a cohort-wide increase in NK-1R signalling but do reveal a subset of BPS patients—particularly Y2336 and Y2338—with transcriptional profiles indicative of heightened neurogenic inflammation. When viewed alongside their elevated immune, apoptotic, and adhesion-related gene expression in prior studies (4, 6, and 8), these data reinforce the emerging pattern of an immune-activated BPS endotype. This supports the broader thesis interpretation that BPS is molecularly heterogeneous and that

neuroimmune pathways such as NK-1R signalling may contribute to symptom generation in specific patient subsets.

**Table 3.4.18: Summary of gene expression analysis for *TACR1*, *TAC1*, *TNF*, and *IL6* in bladder pain syndrome (BPS) and non-BPS primary (P0) bladder tissue samples**.

Mean transcript-per-million (TPM) values, Mann–Whitney U test p-values, and the direction of change (↑ or ↓ in BPS) are provided. No statistically significant differences were found for any gene between groups.

| Gene | Function | Mean TPM (BPS) | Mean TPM (non-BPS) | Test Used | p-value | Direction of Change |
|---|---|---|---|---|---|---|
| ***TACR1*** | Neurokinin-1 receptor | 0.12 | 0.04 | Mann–Whitney U | 0.77 | No significant difference |
| ***TAC1*** | Substance P precursor | 18.10 | 10.36 | Mann–Whitney U | 0.36 | No significant difference |
| ***TNF*** | Pro-inflammatory cytokine | 2.38 | 2.91 | Mann–Whitney U | 0.36 | No significant difference |
| ***IL6*** | Pro-inflammatory cytokine | 1.64 | 0.74 | Mann–Whitney U | 0.56 | No significant difference |

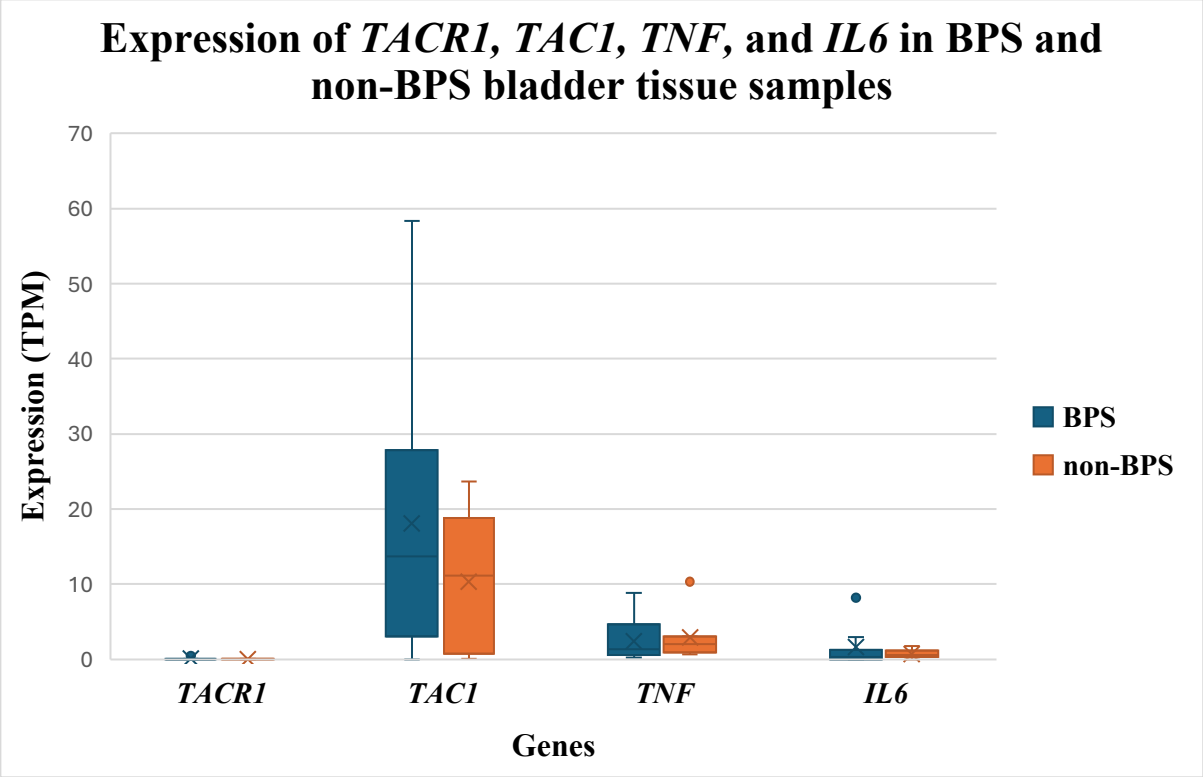


**Figure 3.4.30: Expression levels of *TACR1, TAC1, TNF,* and *IL6* in BPS and non-BPS bladder tissue samples.**

Box-and-whisker plots illustrating the expression levels (TPM) of *TACR1*, *TAC1*, *TNF*, and *IL6* in primary bladder tissue samples from patients with bladder pain syndrome (BPS) and non-BPS controls. Individual sample points are overlaid on the plots to highlight data distribution. BPS samples are shown in blue, and non-BPS samples in orange. No statistically significant differences were observed between groups (all $p > 0.05$, see Table 3.4.18).

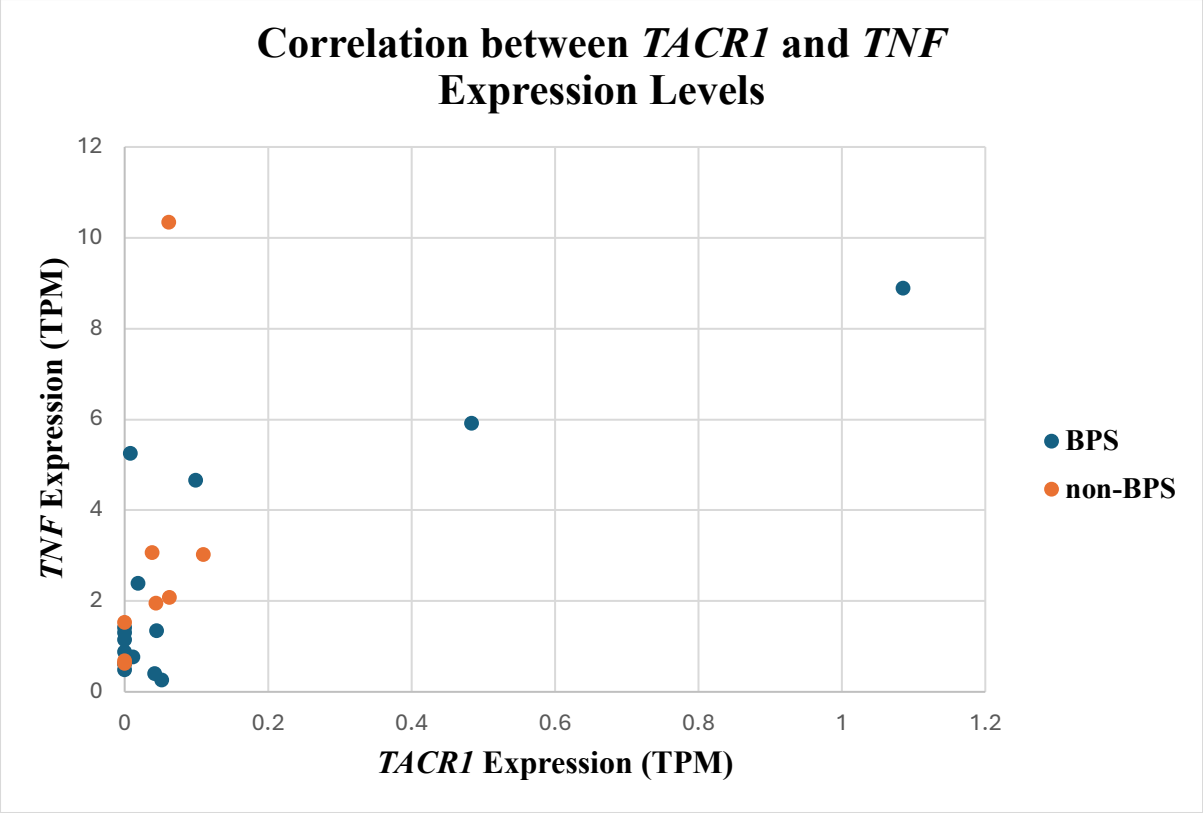


**Figure 3.4.31: Correlation between *TACR1* and *TNF* Expression Levels.**

Spearman rank correlation analysis revealed a non-significant medium positive relationship between *TACR1* and *TNF* in BPS samples ($r_s = 0.41$, $p = 0.13$), and a significant large positive relationship in non-BPS samples ($r_s = 0.71$, $p = 0.05$). These findings suggest a potential differential co-expression pattern between these genes across clinical groups.

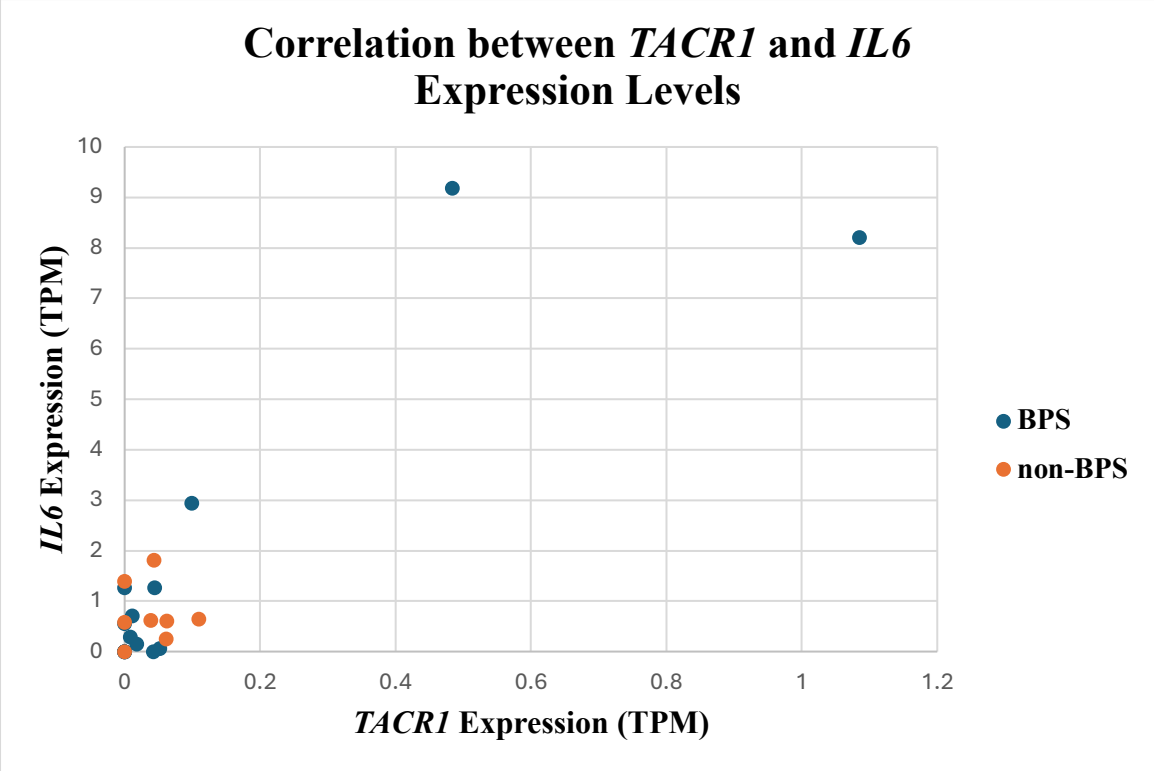


**Figure 3.4.32: Correlation between *TACR1* and *IL6* Expression Levels**.

Spearman rank correlation analysis indicated a significant large positive relationship between *TACR1* and *IL6* in BPS samples ($r_s = 0.63$, $p = 0.01$), but a non-significant small positive relationship in non-BPS samples ($r_s = 0.20$, $p = 0.64$). This result supports a potential link between *TACR1* expression and inflammatory cytokine activity in BPS.

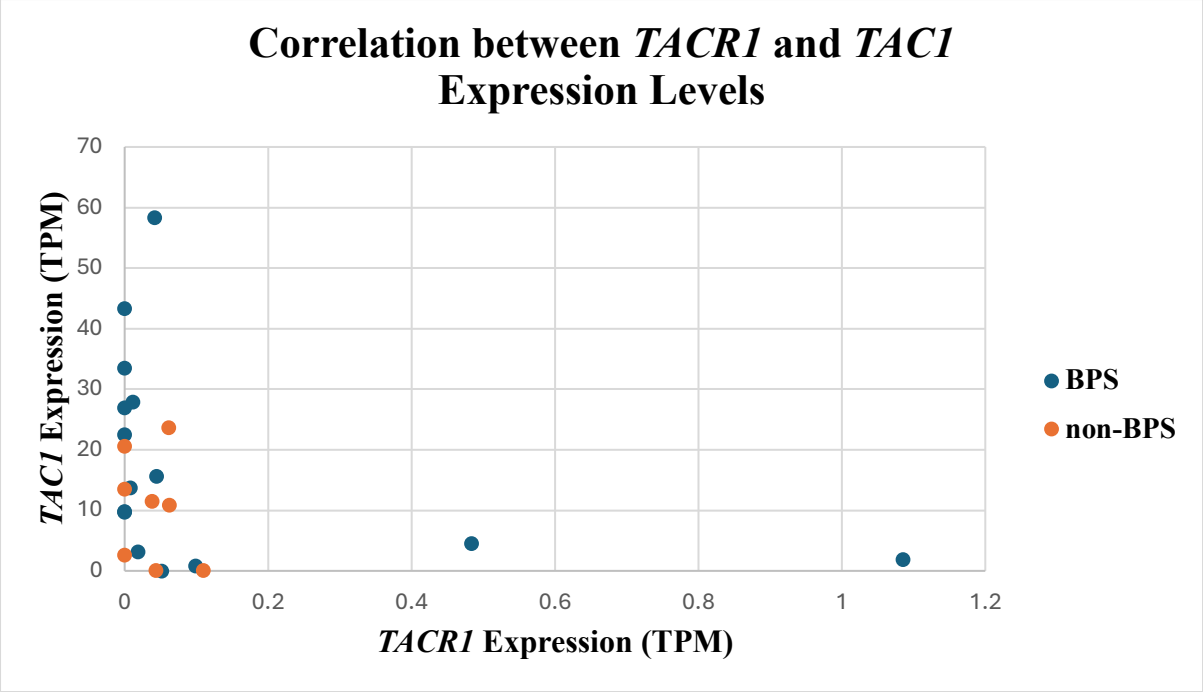


**Figure 3.4.33: Correlation between *TACR1* and *TAC1* Expression Levels**.

Spearman rank correlation analysis demonstrated a significant large negative relationship between *TACR1* and *TAC1* in BPS samples ($r_s = –0.58$, $p = 0.02$), but a non-significant medium negative relationship in non-BPS samples ($r_s = –0.39$, $p = 0.34$). This pattern suggests a potential inverse regulatory interaction between these genes in BPS.

**Study 13**

Girard et al. (2012) showed that bladder inflammation in mice increases expression of the neuropeptides PACAP (encoded by *ADCYAP1*) and VIP, together with their receptors (*VIPR1*, *VIPR2*, *ADCYAP1R1*), contributing to altered sensory processing and micturition reflexes. To examine whether similar neurogenic mechanisms operate in human BPS, we assessed expression of *ADCYAP1*, *VIP*, *VIPR1*, *VIPR2*, *ADCYAP1R1*, and *NGF* in primary (P0) bladder tissue.

Group-level expression of *ADCYAP1*, *VIP*, and *NGF* was extremely low and showed no significant differences between BPS and non-BPS samples (all $p > 0.05$; Table 3.4.19; Figure 3.4.34). Among receptors, *VIPR1* showed the highest transcript abundance across both groups, while *VIPR2* and *ADCYAP1R1* were minimally expressed. Although overall expression was low, individual-level variation was evident. Sample Y2336 displayed the highest *VIP*, *NGF*, and *ADCYAP1* levels within the BPS cohort—values that were small in absolute terms but substantially higher than the near-zero expression in most samples. This pattern complements Y2336's broader immune-activated phenotype identified in Studies 4, 6, and 12, suggesting potential convergence of inflammatory and neurogenic signalling in this individual. Y2338 also showed detectable expression of these neuropeptides, albeit at lower levels.

Correlation analysis indicated a significant positive association between *VIP* and *NGF* in non-BPS samples ($r_s = 0.76$, $p = 0.03$), a relationship not observed in BPS ($r_s = 0.28$, $p = 0.31$), implying possible disruption of coordinated neuropeptide–neurotrophin signalling within the BPS urothelium. The isolated elevations in Y2336, however, suggest that such coordination may persist in selected individuals.

Overall, the cohort-level findings do not mirror the pronounced neuropeptide upregulation described in Girard et al.'s murine model. Nevertheless, individual outliers with elevated *ADCYAP1*, *VIP*, or *NGF* support the existence of a neurogenic-inflammation phenotype in a subset of BPS patients. These observations reinforce the recurring theme of molecular heterogeneity and highlight neuropeptide pathways as potential targets in transcriptionally defined BPS subgroups.

**Table 3.4.19: Mean TPM expression and Mann–Whitney U test results for key genes in PACAP/VIP signalling pathways between BPS and non-BPS groups.**

This table summarises the mean transcript expression levels (TPM) of key genes involved in the PACAP/VIP signalling pathways in BPS versus non-BPS bladder tissue samples. Genes included are *ADCYAP1* (PACAP), *VIP*, and their respective receptors (*VIPR1*, *VIPR2*, and *ADCYAP1R1*), as well as *NGF* (a neurotrophic factor linked to PACAP/VIP expression). Statistical analysis using the Mann–Whitney U test showed no significant differences between groups for any gene (all $p > 0.05$), with small effect sizes noted. This analysis provides a transcriptomic overview of neuropeptide signalling pathways implicated in bladder pain syndrome (BPS) pathophysiology.

| Gene | Function | Mean TPM (BPS) | Mean TPM (non-BPS) | Test Used | p-value | Direction of Change |
|---|---|---|---|---|---|---|
| ***ADCYAP1*** | Encodes PACAP | 0.05 | 0.07 | Mann–Whitney U | 0.18 | No significant difference |
| ***VIP*** | Encodes VIP | 0.02 | 0.01 | Mann–Whitney U | 0.59 | No significant difference |
| ***VIPR1*** | VIP receptor 1 | 29.64 | 33.16 | Mann–Whitney U | 0.33 | No significant difference |
| ***VIPR2*** | VIP receptor 2 | 0.18 | 0.27 | Mann–Whitney U | 0.17 | No significant difference |

| | | | | | | |
|---|---|---|---|---|---|---|
| ***ADCYAP1R1*** | PACAP receptor | 0.01 | 0.03 | Mann–Whitney U | 0.97 | No significant difference |
| ***NGF*** | Nerve Growth Factor | 0.03 | 0.03 | Not calculated | – | No change |

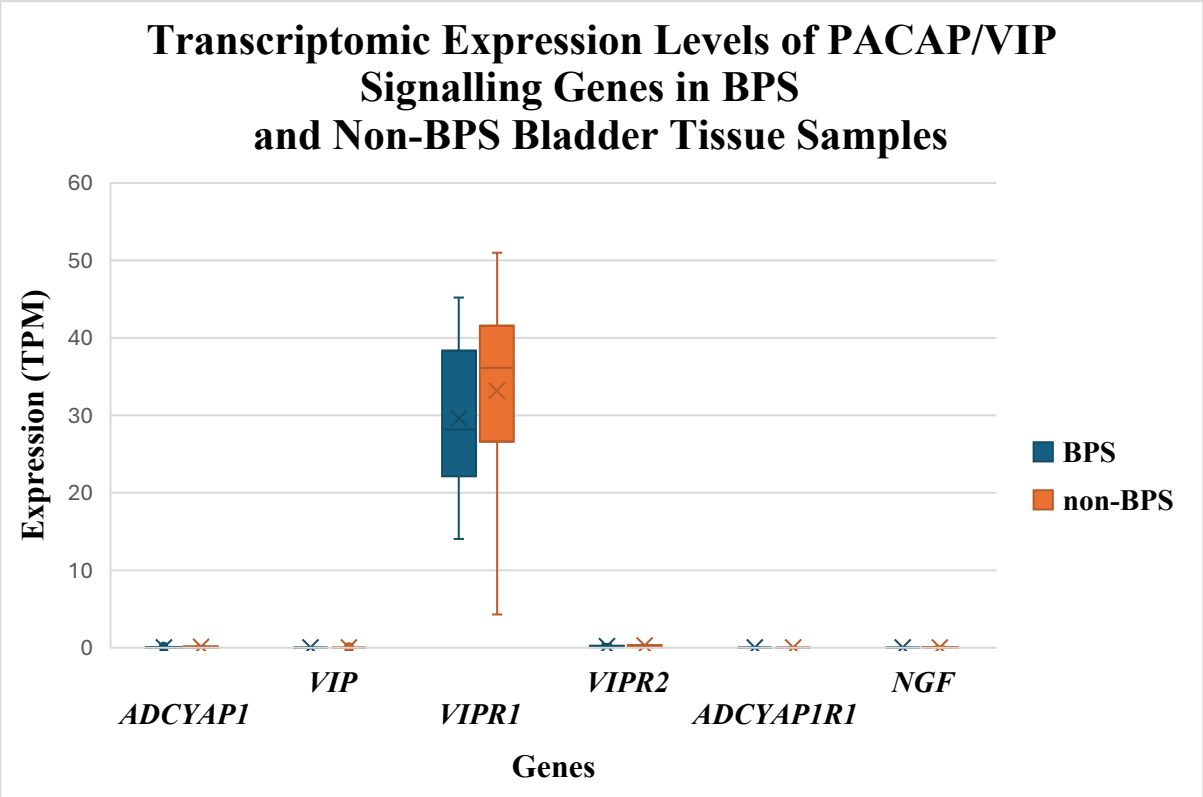


**Figure 3.4.34: Box-and-whisker plots comparing transcript expression levels of key PACAP/VIP signalling genes between BPS and non-BPS samples.**

This figure illustrates the distribution of transcript expression levels (TPM) for *ADCYAP1*, *VIP*, *VIPR1*, *VIPR2*, and *ADCYAP1R1* in BPS (blue) and non-BPS (orange) bladder tissue samples. No statistically significant differences were observed between groups for any gene (all $p > 0.05$, Mann–Whitney U tests; see Table 3.4.19). Boxes represent interquartile ranges (IQR), with the median shown as a horizontal line; whiskers indicate the 1.5 × IQR range, and individual points represent sample values. These data provide insight into the transcriptomic profile of neuropeptide signalling pathways in BPS pathogenesis.

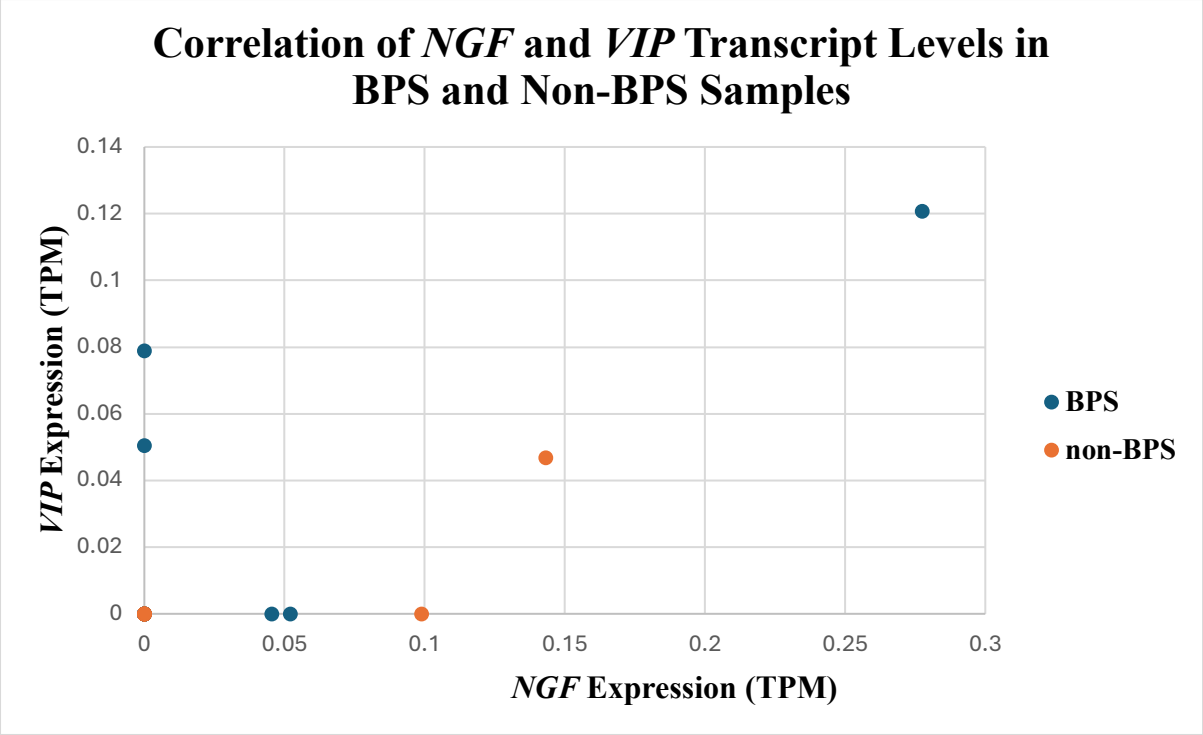


**Figure 3.4.35: Spearman rank correlation between *NGF* and *VIP* transcript levels in BPS and non-BPS bladder samples.**

Spearman rank correlation analysis between *NGF* and *VIP* transcript levels in BPS (blue) and non-BPS (orange) samples. Results showed a non-significant small positive correlation in BPS ($r_s$ = 0.28, p = 0.31) and a significant large positive correlation in non-BPS ($r_s$ = 0.76, p = 0.03). These findings suggest a stronger co-regulation of neurotrophic and neuropeptide pathways in non-BPS samples.

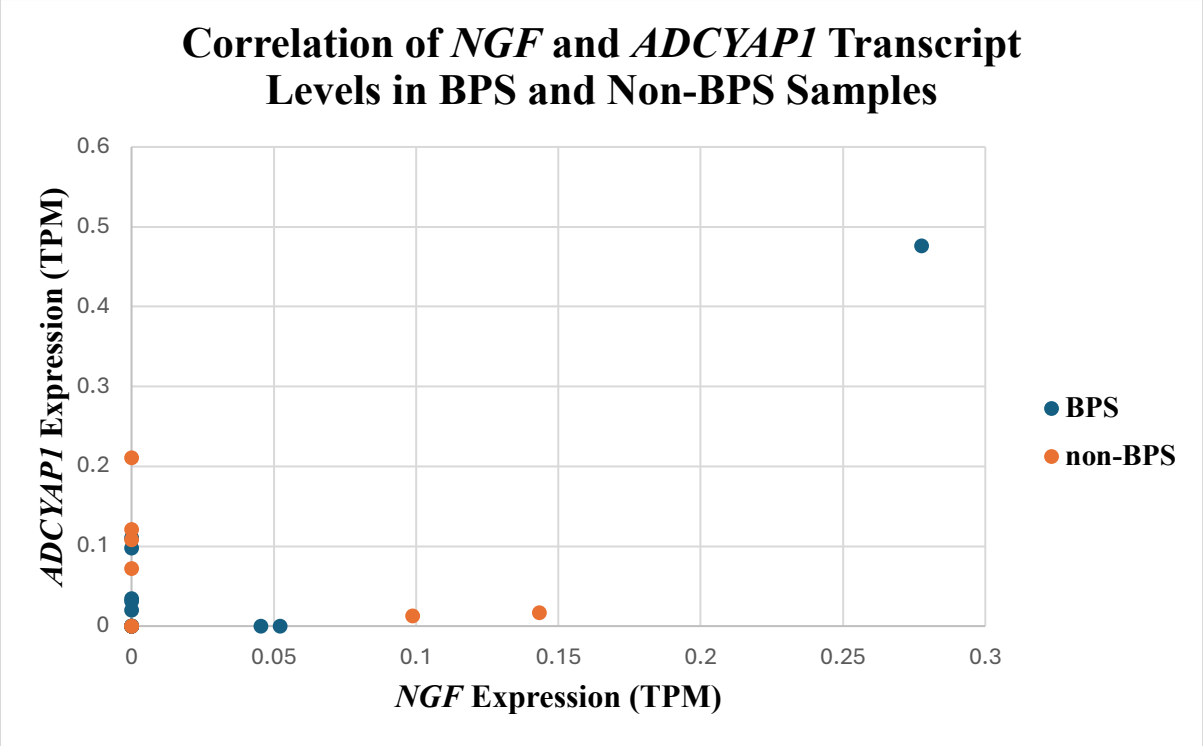


**Figure 3.4.36 Spearman rank correlation between *NGF* and *ADCYAP1* transcript levels in BPS and non-BPS bladder samples.**

Spearman rank correlation analysis between *NGF* and *ADCYAP1* transcript levels in BPS (blue) and non-BPS (orange) samples. Results showed a non-significant small positive correlation in BPS ($r_s = 0.10$, $p = 0.72$) and a non-significant small negative correlation in non-BPS ($r_s = -0.24$, $p = 0.58$). This indicates limited evidence for coordinated expression between *NGF* and *ADCYAP1* in both groups.

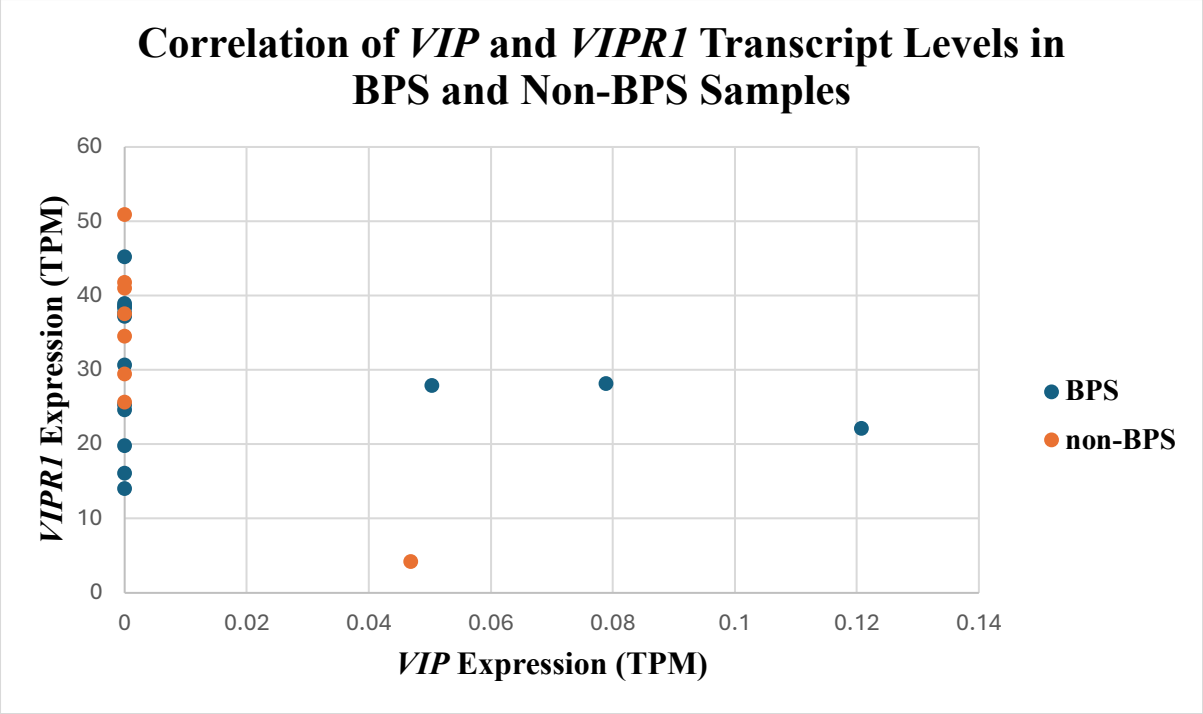


**Figure 3.4.37: Spearman rank correlation between *VIP* and *VIPR1* transcript levels in BPS and non-BPS bladder samples.**

Spearman rank correlation analysis between *VIP* and *VIPR1* transcript levels in BPS (blue) and non-BPS (orange) samples. Results showed a non-significant small negative correlation in BPS ($r_s$ = -0.21, p = 0.46) and a non-significant large negative correlation in non-BPS ($r_s$ = -0.58, p = 0.13). This suggests potential decoupling of ligand-receptor signalling in non-BPS samples.

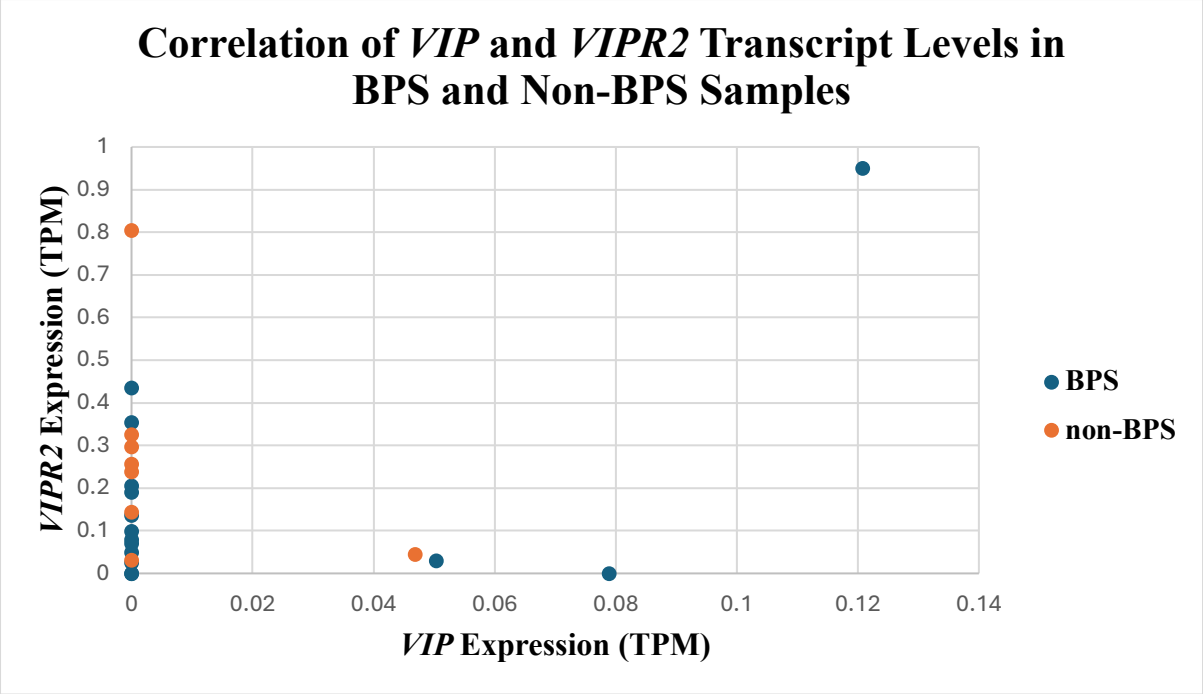


**Figure 3.4.38: Spearman rank correlation between *VIP* and *VIPR2* transcript levels in BPS and non-BPS bladder samples.**

Spearman rank correlation analysis between *VIP* and *VIPR2* transcript levels in BPS (blue) and non-BPS (orange) samples. Results showed a non-significant very small negative correlation in BPS ($r_s$ = -0.03, p = 0.93) and a non-significant medium negative correlation in non-BPS ($r_s$ = -0.41, p = 0.31). No meaningful ligand-receptor co-expression was observed.

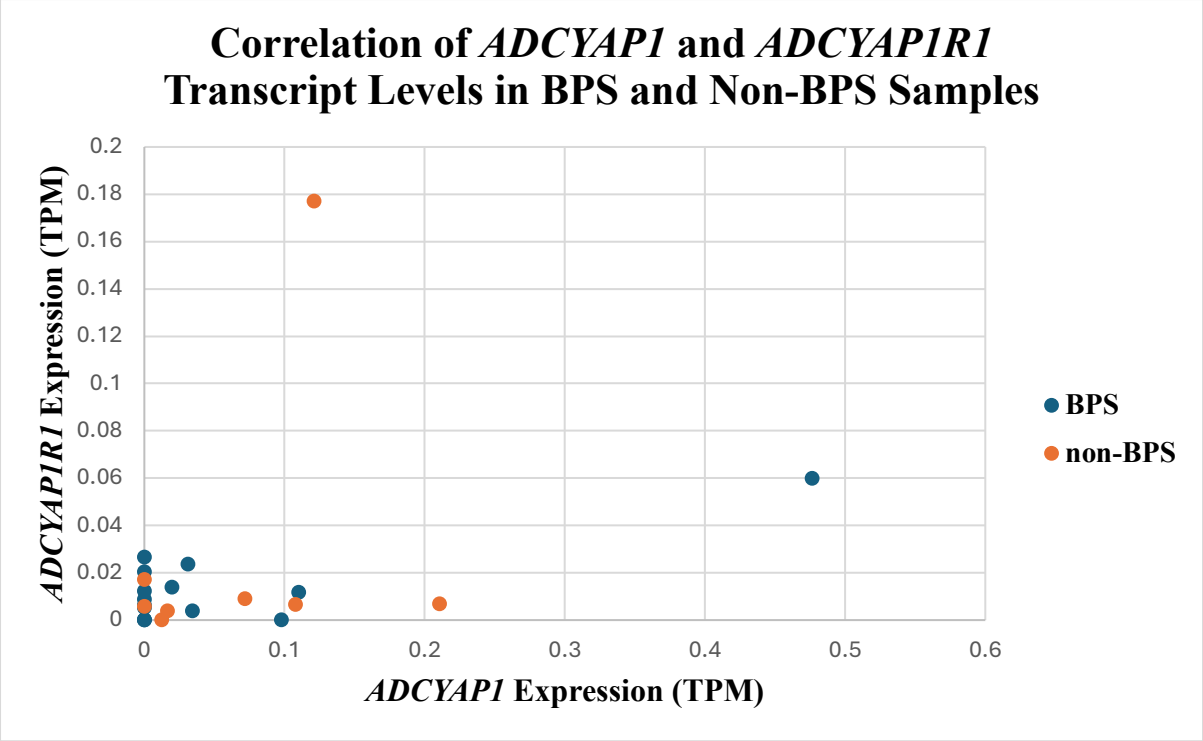


**Figure 3.4.39: Spearman rank correlation between *ADCYAP1* and *ADCYAP1R1* transcript levels in BPS and non-BPS bladder samples.**

Spearman rank correlation analysis between *ADCYAP1* and *ADCYAP1R1* transcript levels in BPS (blue) and non-BPS (orange) samples. Results showed a non-significant small positive correlation in BPS ($r_s = 0.240$, $p = 0.39$) and a non-significant medium positive correlation in non-BPS ($r_s = 0.34$, $p = 0.42$). These results indicate minimal evidence for functional co-expression of PACAP and its receptor.

**Study 14**

Chopra et al. (2005) showed that bladder inflammation and nociception in rodent cystitis are mediated through upregulation of the inducible bradykinin receptor BDKRB1 and the constitutive receptor BDKRB2. To explore whether similar transcriptional changes occur in human BPS, we evaluated *BDKRB1*, *BDKRB2*, and the downstream inflammatory enzyme *PTGS2* (COX-2) in primary (P0) bladder tissue.

Group-level comparisons revealed no statistically significant differences between BPS and non-BPS samples (all $p > 0.05$; Table 3.4.20; Figure 3.4.40). *BDKRB1* showed a modest, non-significant tendency toward higher expression in BPS (mean TPM 1.27 vs. 0.61), consistent with its inducible profile, whereas *BDKRB2* expression was slightly lower in BPS (0.88 vs. 2.74). *PTGS2* expression was high in both groups and showed no meaningful difference, suggesting that COX-2–mediated inflammatory tone is not restricted to BPS.

Correlation analyses provided no evidence of coordinated transcriptional regulation among *BDKRB1*, *BDKRB2*, *PTGS2*, *IL6*, or *TNF* within the BPS group (Figures 3.4.41–3.4.43). These findings imply that if bradykinin signalling contributes to symptom generation, it may do so through cell-type–specific, post-transcriptional, or dynamically regulated mechanisms that are not captured at the bulk RNA level.

Although no sample displayed clear co-activation of both bradykinin receptors, several BPS cases showed inflammatory features relevant to the pathway. In particular, Y2336 exhibited elevated *PTGS2* (48.97 TPM) together with *IL6* and *TNF*, aligning with its broader immune-activated phenotype described in Studies 4, 6, 8, and 12. Clinically, this sample also showed glomerulations and moderate symptom burden, features compatible with an inflammatory endotype. Y2338 demonstrated a similar inflammatory profile, though without notable upregulation of bradykinin receptors. These patterns suggest that the inflammatory context required for ligand-dependent activation of *BDKRB1* and *BDKRB2* may be present in selected individuals even in the absence of receptor overexpression.

In summary, our transcriptional data do not replicate the pronounced bradykinin receptor induction reported in rodent cystitis. Nonetheless, the presence of elevated inflammatory mediators in subgroups of BPS patients maintains the possibility that bradykinin signalling contributes indirectly to pain and hypersensitivity. These findings further support the

overarching conclusion that BPS is molecularly heterogeneous, with specific inflammatory subtypes potentially engaging distinct nociceptive pathways.

**Table 3.4.20: Summary of Differential Gene Expression in BPS versus Non-BPS for Bradykinin Receptor Pathway and Inflammatory Markers.**
This table presents the results of differential expression analysis for key genes involved in bradykinin receptor signalling (*BDKRB1, BDKRB2, PTGS2*) and supporting inflammatory markers (*TNF, IL6, IL1B*) in bladder pain syndrome (BPS) compared to non-BPS controls. The table includes gene name, function, mean transcript per million (TPM) values for BPS and non-BPS samples, the statistical test used (Mann–Whitney U), the corresponding p-value, and the direction of change in BPS relative to non-BPS. Direction of change indicates whether gene expression is higher (↑) or lower (↓) or no significant difference in BPS samples. A p-value < 0.05 would typically indicate a statistically significant difference.

| Gene | Function | Mean TPM (BPS) | Mean TPM (non-BPS) | Test Used | p-value | Direction of Change |
|---|---|---|---|---|---|---|
| ***BDKRB1*** | Inducible bradykinin receptor involved in pain and leukocyte recruitment | 1.27 | 6.10 | Mann–Whitney U | 0.09 | No significant difference |
| ***BDKRB2*** | Constitutive bradykinin receptor involved in inflammation and vascular tone | 0.88 | 2.74 | Mann–Whitney U | 0.33 | No significant difference |
| ***PTGS2*** | Cyclooxygenase-2, involved in prostaglandin synthesis | 161.84 | 199.86 | Mann–Whitney U | 0.88 | No significant difference |

| | | | | | | |
|---|---|---|---|---|---|---|
| ***TNF*** | Pro-inflammatory cytokine | 2.38 | 2.91 | Mann–Whitney U | 0.36 | No significant difference |
| ***IL6*** | Inflammatory cytokine | 1.64 | 0.74 | Mann–Whitney U | 0.56 | No significant difference |
| ***IL1B*** | Inflammatory cytokine | 53.80 | 58.55 | Mann–Whitney U | 0.98 | No significant difference |

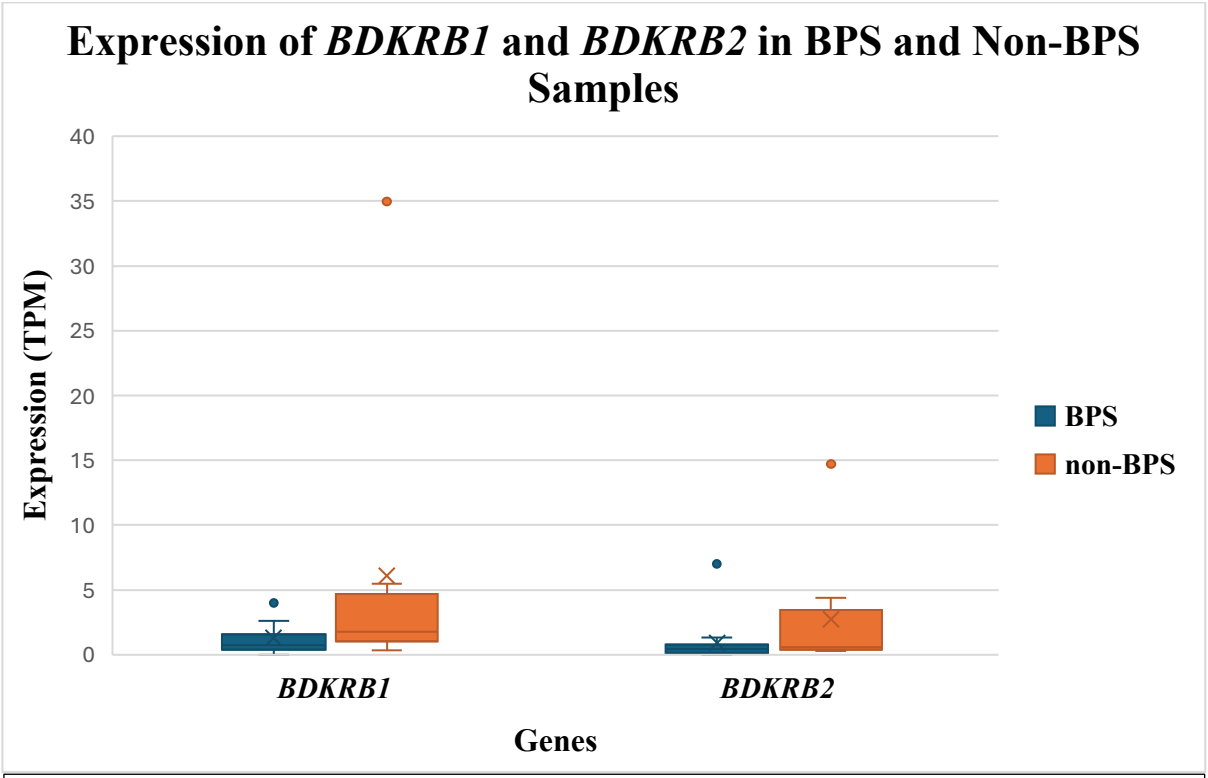


**Figure 3.4.40: Comparative Expression of *BDKRB1* and *BDKRB2* in BPS and Non-BPS Primary Bladder Tissue.**

Paired box-and-whisker plots comparing transcript per million (TPM) expression levels of *BDKRB1* and *BDKRB2* in bladder pain syndrome (BPS; blue) and non-BPS (orange) primary bladder tissue samples. Each box represents the interquartile range (IQR) with the median line shown. Individual data points represent sample-specific expression values. Mann–Whitney U tests were performed to assess differences in gene expression between groups; however, neither *BDKRB1* ($p = 0.09$) nor *BDKRB2* ($p = 0.33$) reached statistical significance. *BDKRB1* showed a trend toward lower expression in BPS compared to non-BPS, while *BDKRB2* expression also tended to be lower but not significantly so. These results align with prior literature suggesting bradykinin receptor involvement in bladder inflammation, though their transcriptional regulation appears variable in this dataset (Table 3.4.20).

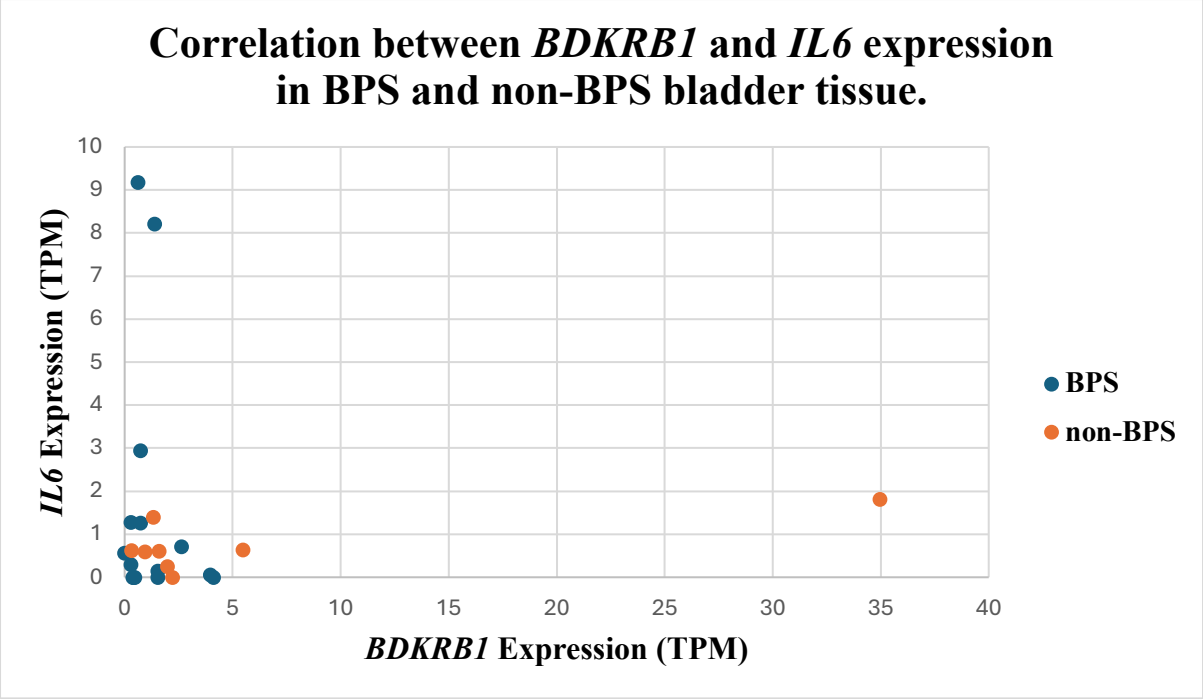


**Figure 3.4.41: Correlation Analysis between *BDKRB1* and *IL6* Expression Levels in BPS and Non-BPS Bladder Tissue Samples.**

Scatterplots depict the relationship between *BDKRB1* and *IL6* transcript levels in BPS (blue) and non-BPS (orange) samples. Spearman rank correlation was used to assess the strength and direction of association. Results indicated a non-significant small negative correlation in BPS ($r_s$ = –0.14, p = 0.62) and a non-significant small positive correlation in non-BPS ($r_s$ = 0.19, p = 0.77). No statistically significant relationships were observed.

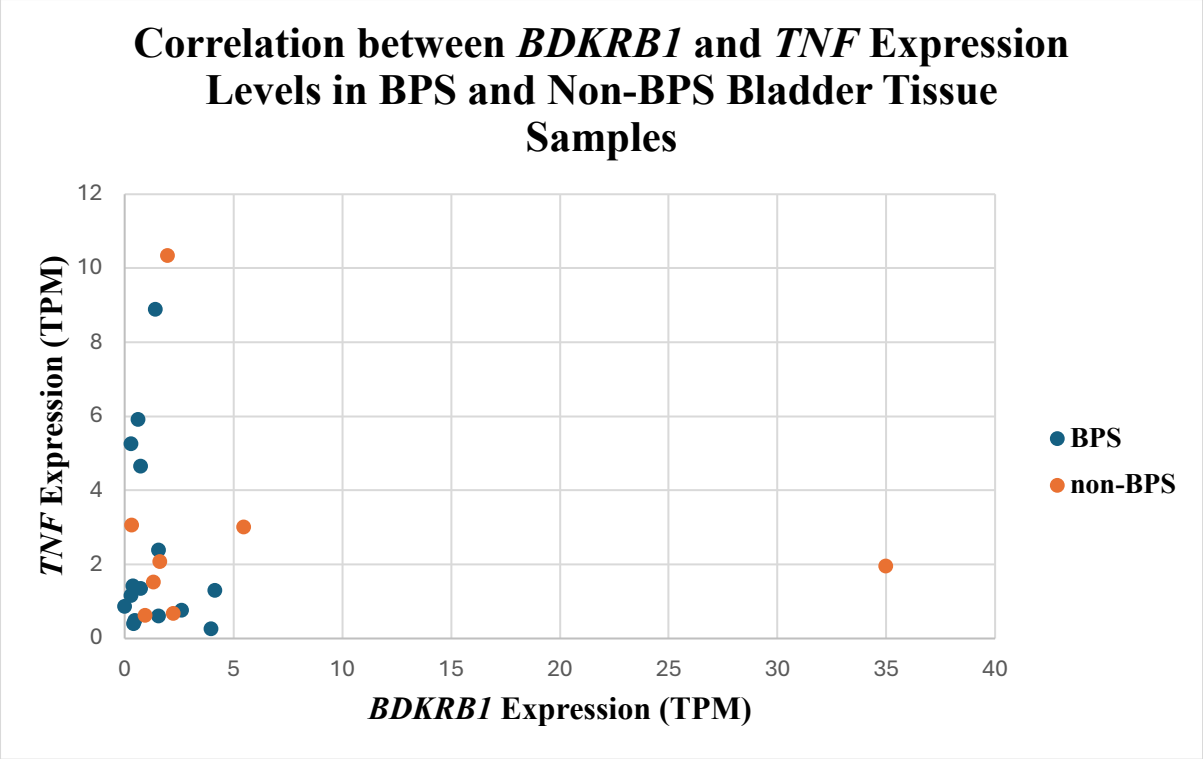


**Figure 3.4.42: Correlation Analysis between *BDKRB1* and *TNF* Expression Levels in BPS and Non-BPS Bladder Tissue Samples.**

Spearman rank correlation analyses were performed to investigate potential co-regulation between *BDKRB1* (bradykinin receptor B1) and *TNF* (tumour necrosis factor) in bladder pain syndrome (BPS) and non-BPS groups. Results indicated a non-significant small negative relationship between *BDKRB1* and *TNF* in BPS samples (rs = -0.14, p = 0.69), suggesting limited evidence of coordinated expression. In non-BPS samples, a very small positive relationship was observed (rs = 0.05, p = 0.48), indicating a weak association between these genes. The low correlation coefficients across groups suggest independent regulation of *BDKRB1* and *TNF* expression in bladder tissue.

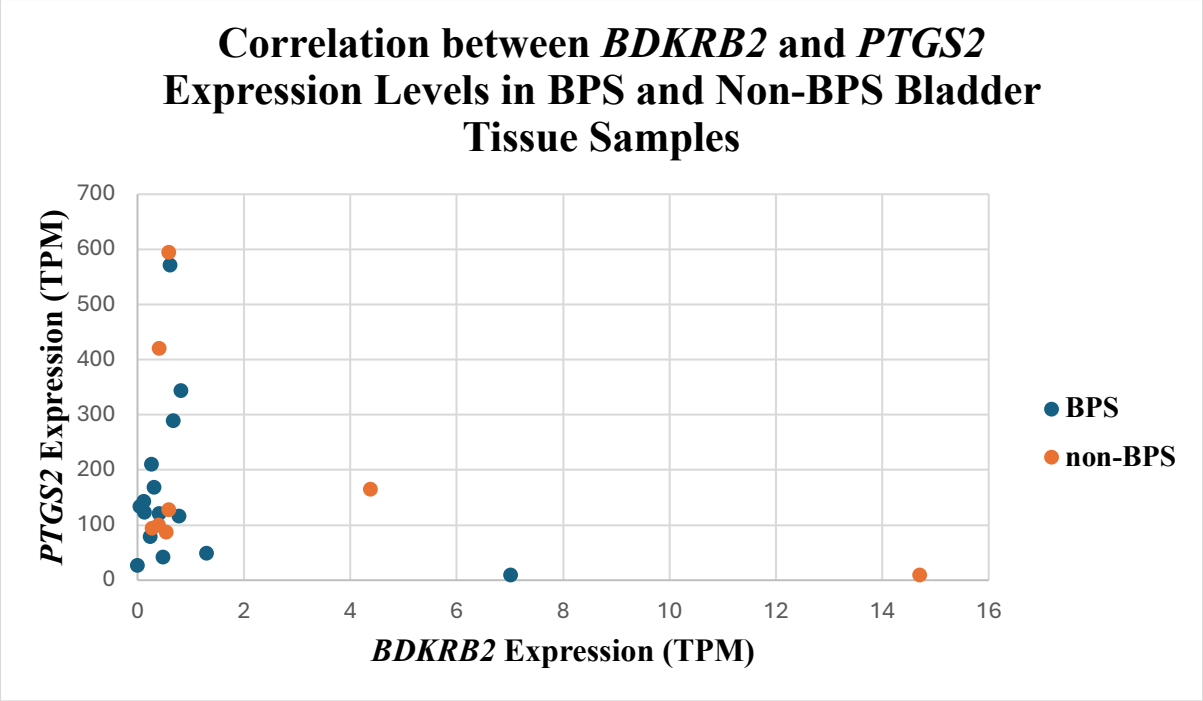


**Figure 3.4.43: Correlation Analysis between *BDKRB2* and *PTGS2* Expression Levels in BPS and Non-BPS Bladder Tissue Samples.**

Spearman rank correlation analyses were performed to explore potential co-expression between *BDKRB2* (bradykinin receptor B2) and *PTGS2* (prostaglandin-endoperoxide synthase 2, also known as COX-2) in bladder pain syndrome (BPS) and non-BPS groups. In BPS samples, a very weak negative relationship was found (rs = -0.01, p = 0.97), indicating no meaningful co-expression. In non-BPS samples, a very small positive relationship was observed (rs = 0.02, p = 0.10), again suggesting no significant correlation. Overall, these results do not support a strong regulatory link between *BDKRB2* and *PTGS2* expression in bladder tissue.

**Study 15**

Peskar et al. (2023), reported sex-specific inflammatory transcriptional responses in a mouse model of IC/BPS, with female animals showing stronger upregulation of *Il6*, *Tnf*, *Ccl2*, and *Cxcl1*. To explore whether comparable mechanisms were evident in our human cohort, we examined expression of *IL6*, *TNF*, *CCL2*, and *CXCL1* in primary (P0) bladder tissue from BPS and non-BPS patients.

Group-level comparisons showed no statistically significant differences (all $p > 0.05$; Table 3.4.21; Figure 3.4.44). Mean *IL6* expression was slightly higher in BPS, whereas *TNF*, *CCL2*, and *CXCL1* were modestly lower, diverging from the direction of change reported in the mouse model. Despite this, *IL6* and *TNF* showed a significant positive association within the BPS group ($\rho = 0.62$, $p = 0.01$; Figure 3.4.45), echoing coordinated inflammatory activity observed in Studies 8 and 12. No meaningful correlations involving *CCL2* or *CXCL1* were detected.

Individual expression patterns again highlighted Y2336 and Y2338 as inflammation-enriched cases. Y2336 showed particularly high *CCL2* and *CXCL1*, consistent with its recurrently elevated inflammatory and immune markers across Studies 6, 8, and 12. Y2338 also exhibited increased *IL6*, *TNF*, and *CCL2*, aligning with its broad immune-activated phenotype identified throughout this chapter. These findings reinforce the presence of a transcriptionally defined inflammatory subset within BPS, even in the absence of cohort-wide differential expression.

As all BPS samples analysed here were from female patients, we were unable to assess sex-specific differences analogous to those described by Peskar et al. (2023). Nevertheless, the sample-specific inflammatory signatures observed in Y2336 and Y2338 further support the overarching theme of molecular heterogeneity and underscore the value of individual-level transcriptomic stratification in understanding BPS pathophysiology.

**Table 3.4.21: Summary of Expression Levels and Statistical Analyses for Key Inflammatory Genes in Study** Peskar et al. (2023)**.**

This table presents the results of transcriptomic analyses of selected inflammatory genes relevant to the study by Peskar et al. (2023) investigating sex-specific inflammatory signatures in bladder pain syndrome (BPS). Mean transcript per million (TPM) values are shown for BPS and non-BPS groups. The Mann–Whitney U test was used to assess group differences in expression levels. The "Direction of Change" column indicates whether the gene's mean expression was higher (↑) or lower (↓) in the BPS group compared to the non-BPS group, highlighting trends even when differences did not reach statistical significance (all $p > 0.05$).

| Gene | Function | Mean TPM (BPS) | Mean TPM (non-BPS) | Test Used | p-value | Direction of Change |
|---|---|---|---|---|---|---|
| ***IL6*** | Pro-inflammatory cytokine | 1.64 | 0.74 | Mann–Whitney U | 0.56 | No significant difference |
| ***TNF*** | Master regulator of inflammation | 2.38 | 2.91 | Mann–Whitney U | 0.36 | No significant difference |
| ***CCL2*** | Monocyte chemoattractant | 4.37 | 15.73 | Mann–Whitney U | 0.23 | No significant difference |
| ***CXCL1*** | Neutrophil chemoattractant | 13.70 | 59.83 | Mann–Whitney U | 0.73 | No significant difference |

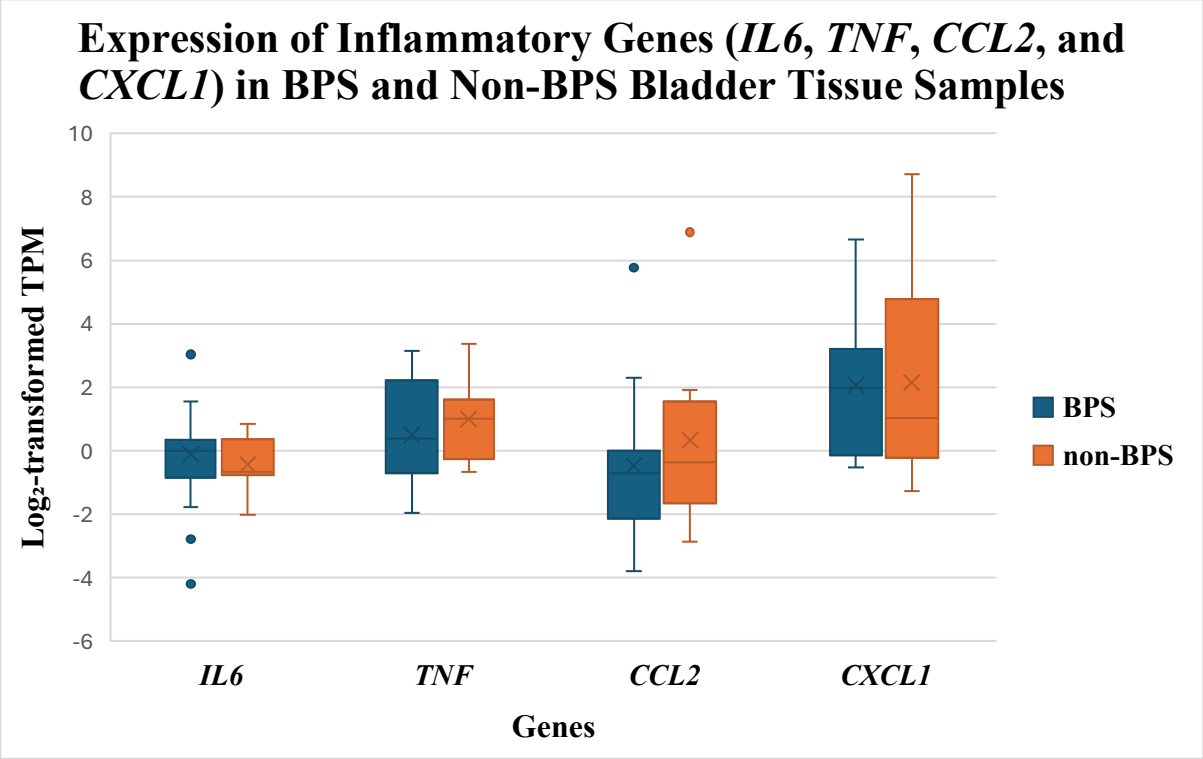


**Figure 3.4.44: Box-and-whisker plots showing $log_2$-transformed expression levels of key inflammatory genes (*IL6*, *TNF*, *CCL2*, *CXCL1*) in BPS and non-BPS bladder tissue samples.** Expression levels are shown as $log_2$(TPM) values for each gene. Blue boxes represent BPS samples and orange boxes represent non-BPS samples. The boxes indicate the interquartile range (IQR) with the horizontal line representing the median; whiskers represent the range excluding outliers. The Mann–Whitney U test was used to assess group differences, with no statistically significant differences observed for any gene (all $p > 0.05$). Mean $log_2$(TPM) values are indicated by "×". Overall, *IL6* exhibited a trend towards higher expression in BPS compared to non-BPS, while *TNF*, *CCL2*, and *CXCL1* showed lower mean expression in BPS samples, though not reaching statistical significance.

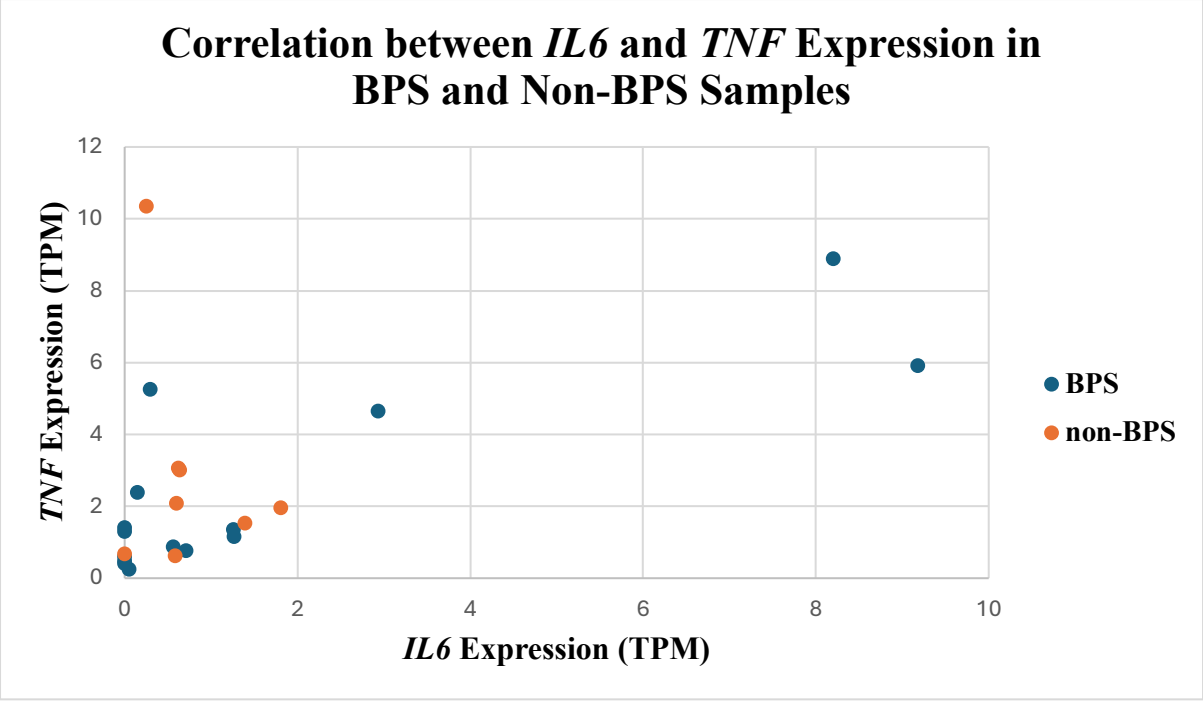


**Figure 3.4.45: Correlation Analysis between *IL6* and *TNF* Expression in BPS and Non-BPS Samples.**

Spearman rank correlation analysis showed a significant large positive relationship between *IL6* and *TNF* in BPS samples ($r_s = 0.62$, $p = 0.01$) and a non-significant very small positive relationship in non-BPS samples ($r_s = 0.07$, $p = 0.70$). This suggests potential co-expression of key inflammatory markers in BPS (Table 3.4.21).

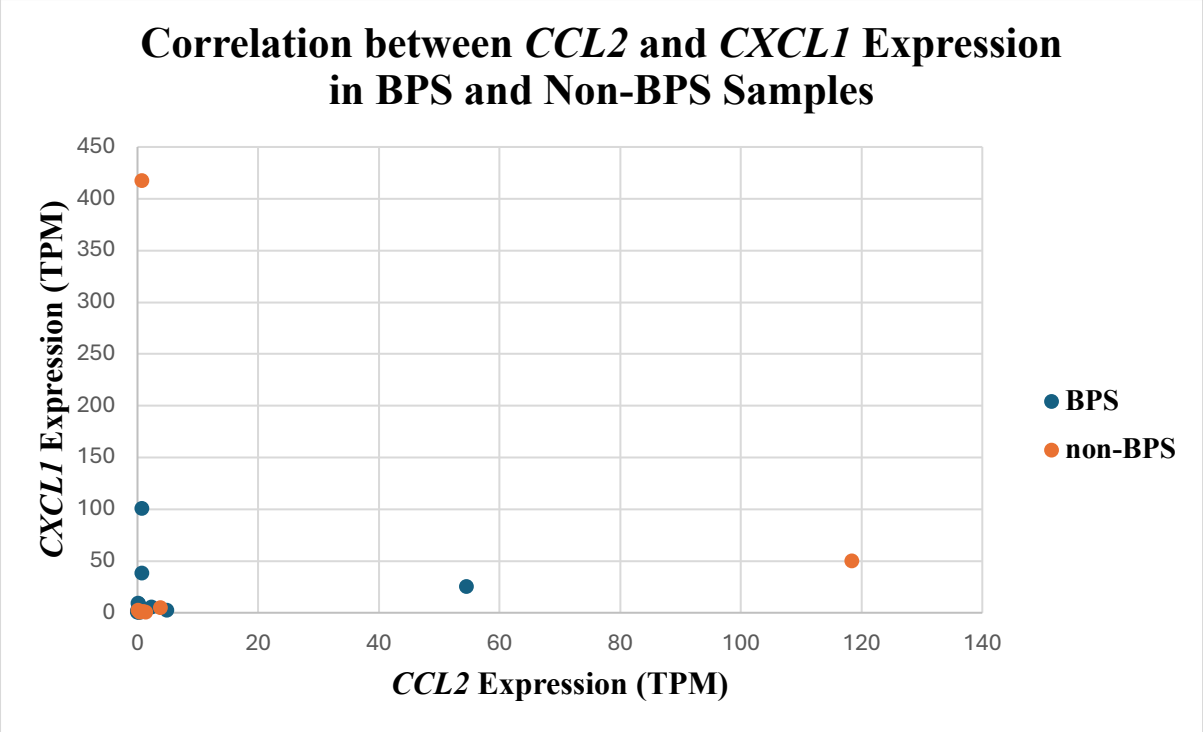


**Figure 3.4.46: Correlation Analysis between *CCL2* and *CXCL1* Expression in BPS and Non-BPS Samples.**

Spearman rank correlation analysis revealed a non-significant medium positive relationship between *CCL2* and *CXCL1* in BPS samples ($r_s = 0.49$, $p = 0.06$) and a non-significant small positive relationship in non-BPS samples ($r_s = 0.26$, $p = 0.59$). This may indicate potential co-activation of chemokine pathways in certain BPS cases (Table 3.4.21).

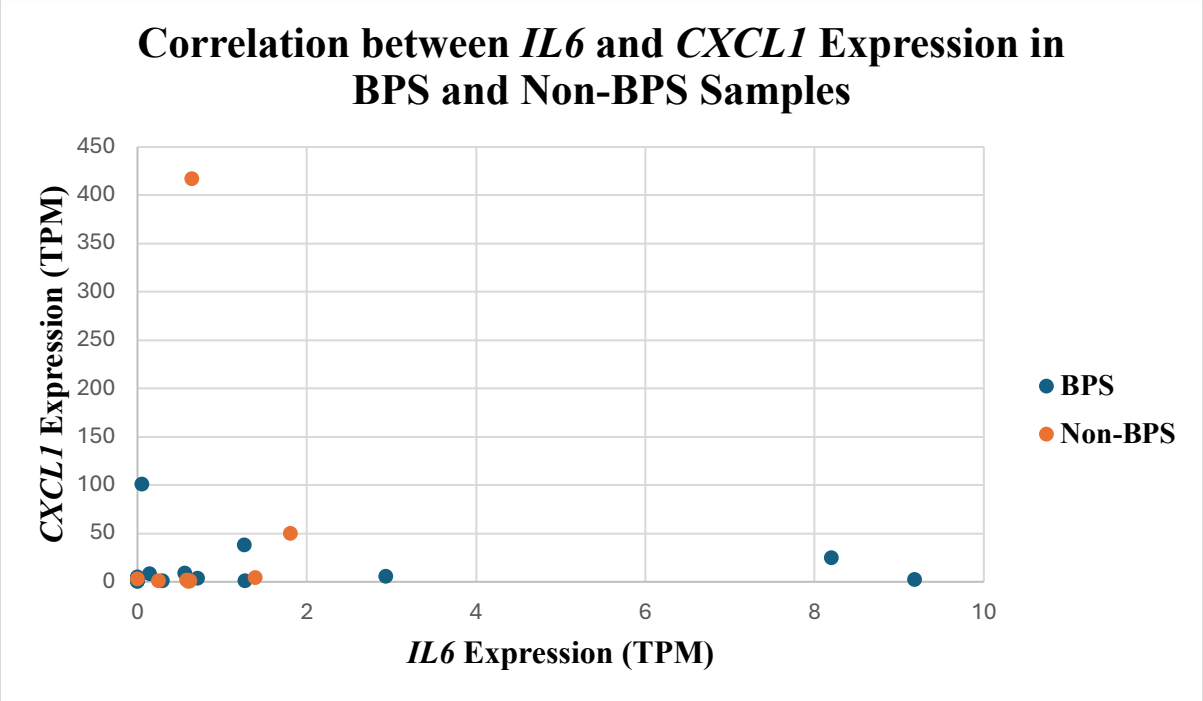


**Figure 3.4.47: Correlation Analysis between *IL6* and *CXCL1* Expression in BPS and Non-BPS Samples**.

Spearman rank correlation analysis demonstrated a non-significant medium positive relationship between *IL6* and *CXCL1* in BPS samples ($r_s = 0.40$, $p = 0.14$) and a non-significant large positive relationship in non-BPS samples ($r_s = 0.50$, $p = 0.23$). These findings suggest possible co-regulation of inflammatory mediators, warranting further investigation (Table 3.4.21).

**Study 16**

Kumar et al. (2021) demonstrated that dysregulation of miR-146a and miR-181a/b amplifies inflammatory signalling in autoimmune cystitis through altered expression of downstream targets such as *IRAK1*, *TRAF6*, *STAT1*, *STAT3*, *PTPN22*, *IL6*, and *TNF*. Although miRNA abundance could not be assessed in the present dataset, we evaluated transcriptional levels of these target genes in P0 bladder tissue to assess whether analogous regulatory patterns may contribute to BPS.

None of the examined transcripts differed significantly between BPS and non-BPS samples (all $p > 0.05$; Table 3.4.22; Figures 3.4.48–3.4.49), and group-level effect sizes were uniformly small. Nevertheless, several BPS samples displayed expression patterns compatible with enhanced inflammatory signalling. Sample Y2336, previously identified as immune-active in Studies 6, 8, 12, and 15, showed elevated *PTPN22* (19.20 TPM), while Y2338 demonstrated high expression of *STAT1* (61.06 TPM) and *STAT3* (102.00 TPM). These values exceed the cohort median and align with the broader inflammatory phenotype described for these individuals, raising the possibility of altered miRNA–target control in a subset of patients.

Correlation analyses did not reveal significant associations among the inferred miRNA targets (Figures 3.4.50–3.4.53). A moderate, near-significant positive correlation between *STAT3* and *IL2* in BPS ($\rho = 0.50$, $p = 0.06$) suggests potential co-regulation in some individuals, though confirmation would require direct miRNA profiling or larger sample sizes.

Overall, while group-level comparisons did not indicate widespread miRNA-target dysregulation, individual-level patterns—particularly in Y2336 and Y2338—suggest that epigenetic modulation of inflammatory pathways may contribute to a transcriptionally distinct BPS subtype. These findings are consistent with recurring immune-enriched signatures highlighted across earlier studies and reinforce the importance of sample-specific analyses in uncovering mechanistic variability within BPS.

**Table 3.4.22: Transcriptomic Expression of miR-146a and miR-181a/b Target Genes in BPS vs Non-BPS Bladder Tissue Samples.**

Summary of transcriptomic expression of known miR-146a and miR-181a/b target genes in BPS vs non-BPS bladder tissue. TPM values represent mean expression across samples. Statistical comparisons were performed using Mann–Whitney U tests. p-values >0.05 indicate no statistically significant difference between groups. Direction of change indicates the trend in expression in BPS compared to non-BPS samples, providing insight into potential transcriptional regulation by miRNAs.

| Gene | Function | Mean TPM (BPS) | Mean TPM (non-BPS) | Test Used | p-value | Direction of Change |
|---|---|---|---|---|---|---|
| **miR-146a Targets** | | | | | | |
| ***IRAK1*** | TLR/IL1 receptor signalling | 27.11 | 28.29 | Mann–Whitney U | 0.93 | No significant difference |
| ***TRAF6*** | Immune signalling adaptor | 6.18 | 5.65 | Mann–Whitney U | 0.88 | No significant difference |
| ***STAT1*** | Interferon signalling transcription factor | 34.60 | 35.07 | Mann–Whitney U | 0.47 | No significant difference |
| ***IL6*** | Pro-inflammatory cytokine | 1.64 | 0.74 | Mann–Whitney U | 0.56 | No significant difference |

| | | | | | | |
|---|---|---|---|---|---|---|
| ***TNF*** | Pro-inflammatory cytokine | 2.38 | 2.91 | Mann–Whitney U | 0.36 | No significant difference |
| **miR-181a/b Targets** | | | | | | |
| ***PTPN22*** | T cell signalling regulator | 3.42 | 1.69 | Mann–Whitney U | 0.83 | No significant difference |
| ***STAT3*** | Cytokine signalling transcription factor | 82.84 | 84.80 | Mann–Whitney U | 1.03 | No significant difference |
| ***TNF*** | Pro-inflammatory cytokine | 2.38 | 2.91 | Mann–Whitney U | 0.36 | No significant difference |
| ***IL2*** | T cell growth factor | 0.64 | 1.12 | Mann–Whitney U | 0.63 | No significant difference |

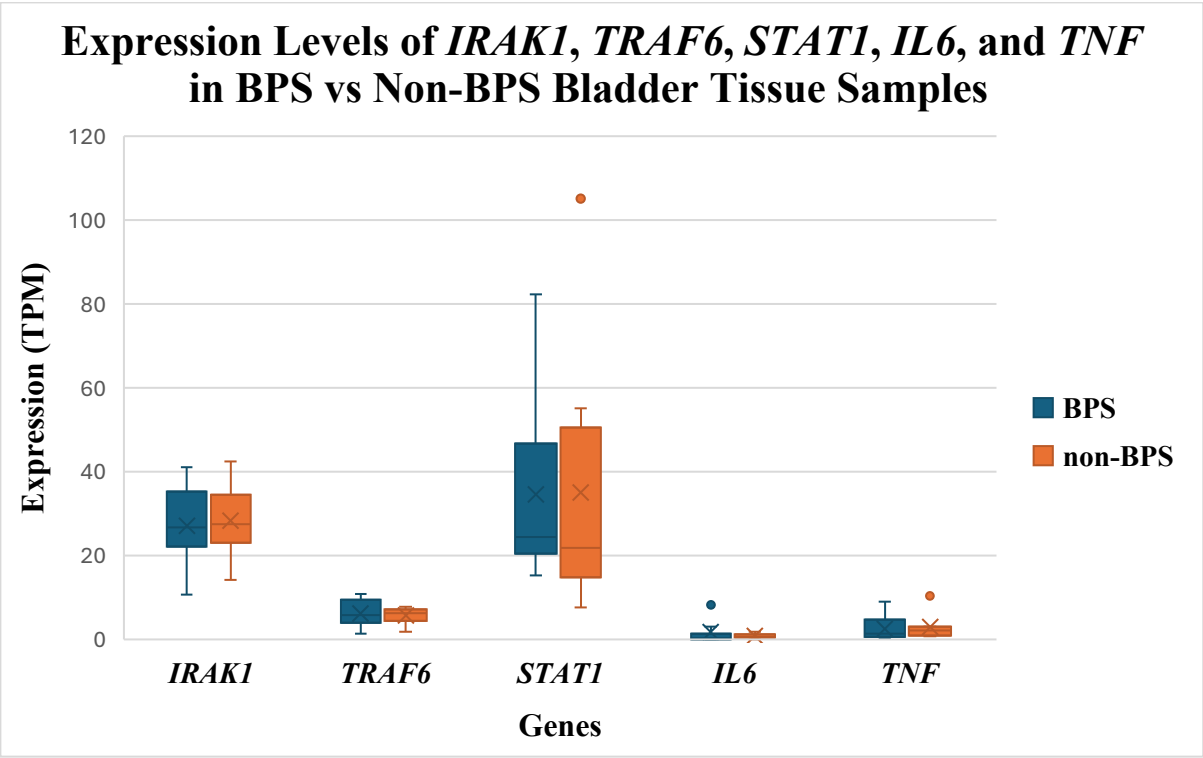


**Figure 3.4.48: Paired box-and-whisker plots comparing transcriptomic expression (TPM) of miR-146a target genes (*IRAK1*, *TRAF6*, *STAT1*, *IL6*, and *TNF*) between BPS (blue) and non-BPS (orange) bladder tissue samples.**

Each box represents the interquartile range with the median indicated by a horizontal line; whiskers show the range. No statistically significant differences were found between groups for any gene (all $p > 0.05$), but trends in direction of change are indicated in Table 3.4.22. Individual data points represent single sample TPM values. This figure supports the investigation of miRNA-mediated regulatory pathways in BPS.

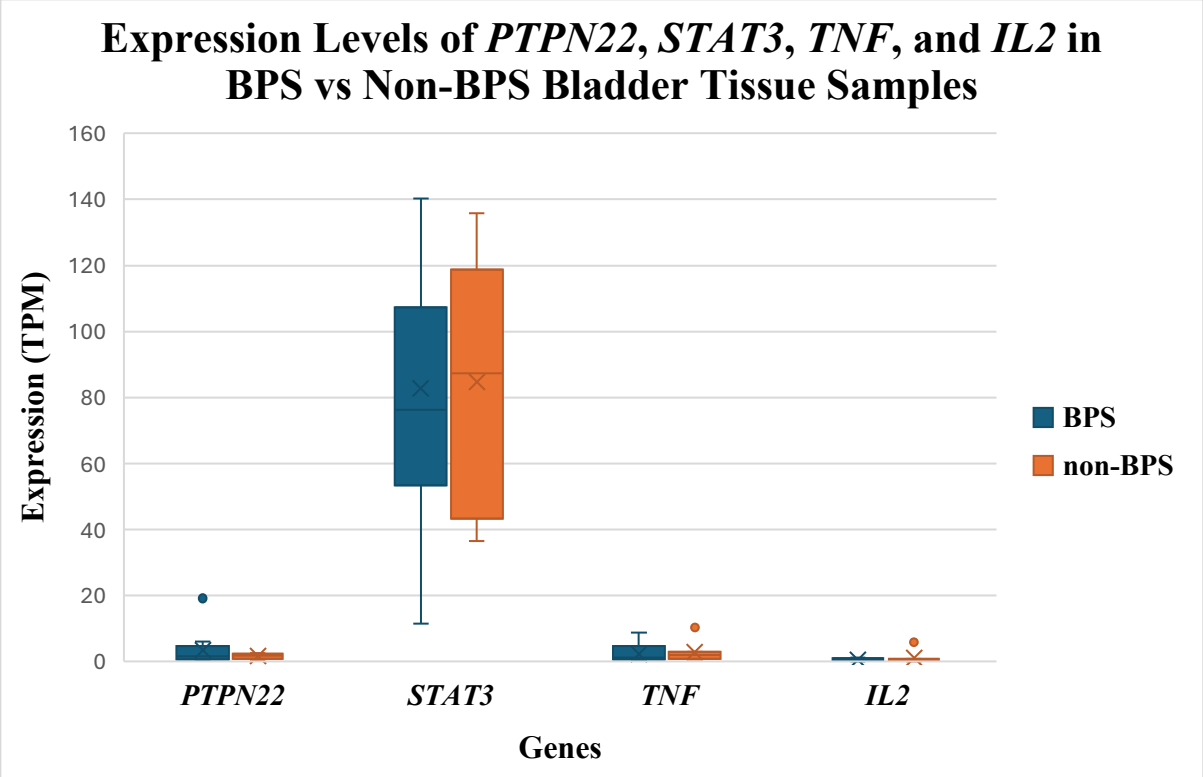


**Figure 3.4.49: Paired box-and-whisker plots comparing transcriptomic expression (TPM) of miR-181a/b target genes (*PTPN22*, *STAT3*, *TNF*, and *IL2*) between BPS (blue) and non-BPS (orange) bladder tissue samples.**

Each box represents the interquartile range with the median indicated by a horizontal line; whiskers show the range. No statistically significant differences were observed between groups for any gene (all $p > 0.05$), but direction of change is indicated in Table 24. Individual data points represent single sample TPM values. This figure contextualises potential epigenetic regulation mechanisms in BPS pathogenesis.

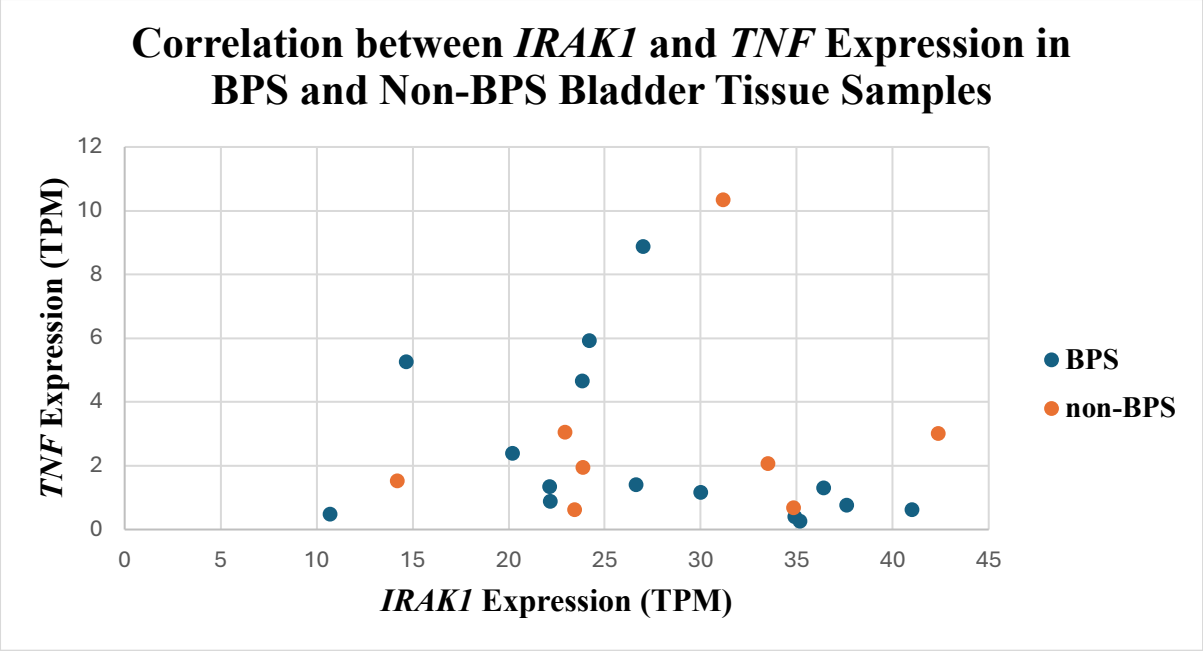


**Figure 3.4.50: Correlation Analysis between *IRAK1* and *TNF* Expression in BPS and Non-BPS Bladder Tissue Samples**.

Scatter plots showing the relationship between *IRAK1* and *TNF* expression (TPM) in bladder tissue samples from BPS (blue) and non-BPS (orange) groups. No significant correlations were observed in either group (BPS: $r_s = -0.39$, $p = 0.16$; non-BPS: $r_s = 0.14$, $p = 0.92$), although BPS samples showed a moderate negative trend. These results suggest limited evidence for coordinated regulation of *IRAK1* and *TNF* in the current dataset.

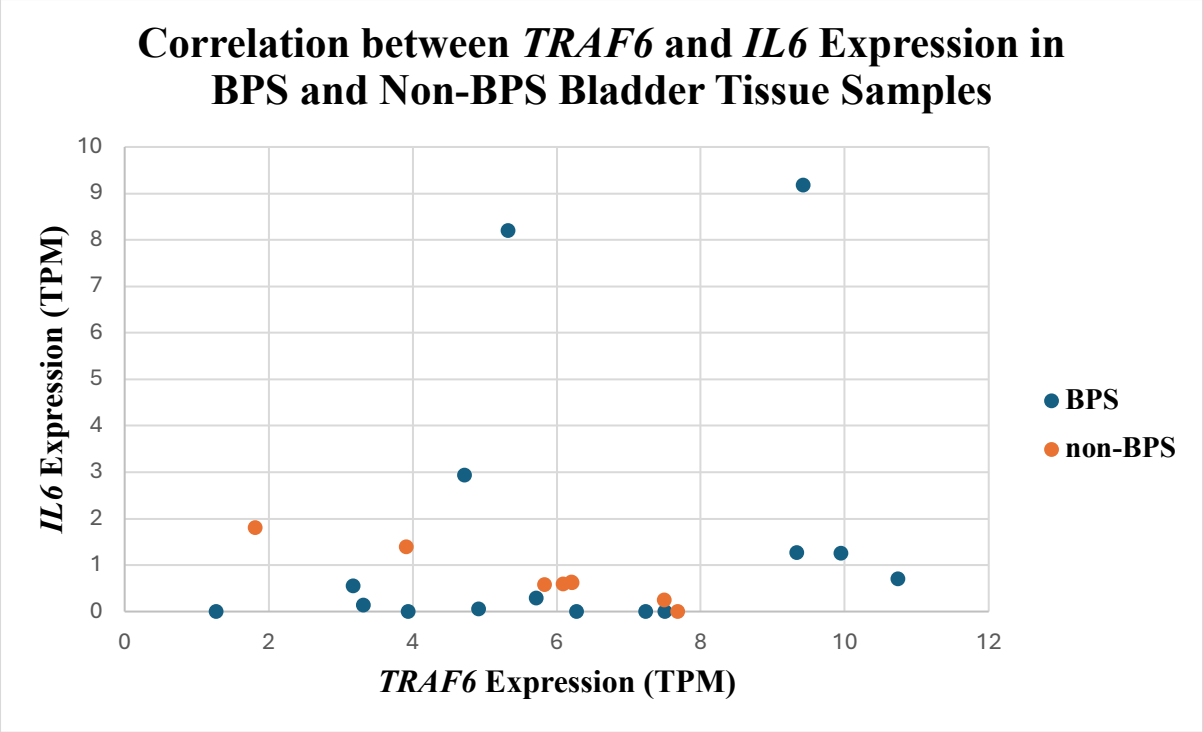


**Figure 3.4.51: Correlation Analysis between *TRAF6* and *IL6* Expression in BPS and Non-BPS Bladder Tissue Samples.**

Scatter plots showing the relationship between *TRAF6* and *IL6* expression (TPM) in BPS (blue) and non-BPS (orange) groups. A non-significant moderate positive relationship was observed in BPS samples ($r_s = 0.33$, $p = 0.23$). Notably, non-BPS samples showed a significant large negative correlation ($r_s = -0.79$, $p = 0.03$). These findings may indicate potential dysregulation of *TRAF6*-related pathways in non-BPS samples.

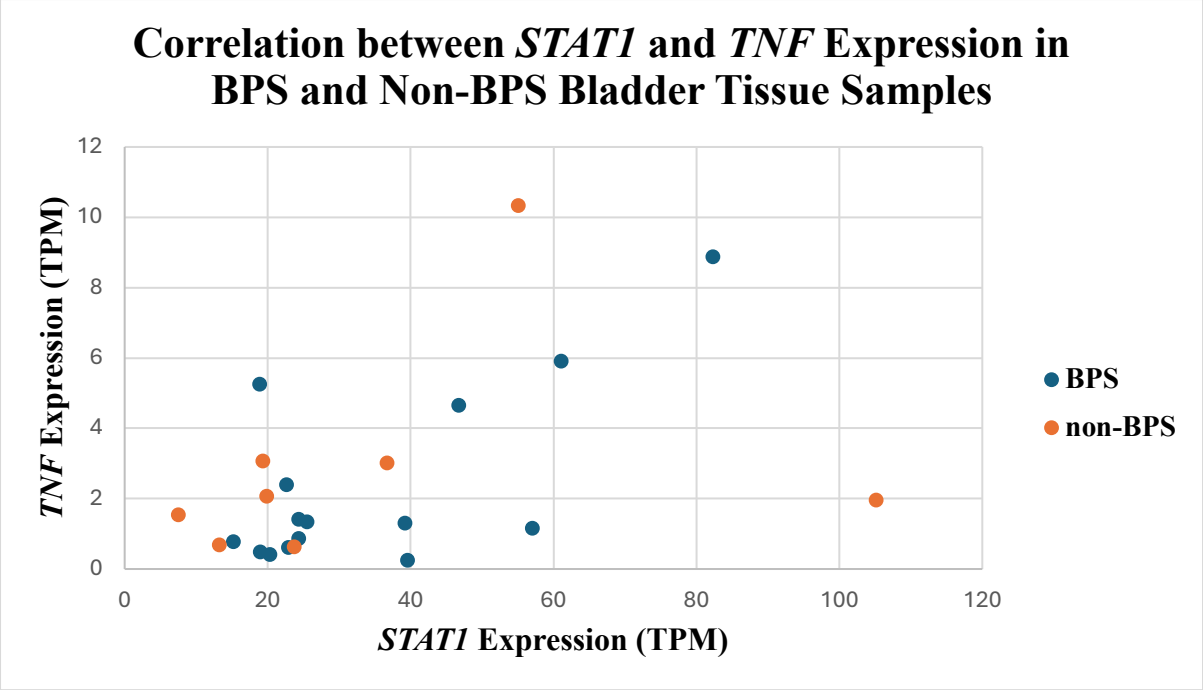


**Figure 3.4.52: Correlation Analysis between *STAT1* and *TNF* Expression in BPS and Non-BPS Bladder Tissue Samples.**

Scatter plots of *STAT1* versus *TNF* expression (TPM) in BPS (blue) and non-BPS (orange) groups. No significant correlations were found (BPS: $r_s = 0.42$, $p = 0.13$; non-BPS: $r_s = 0.36$, $p = 0.42$), although moderate positive trends suggest possible co-regulation of inflammatory pathways. Further analysis could clarify these relationships in specific molecular subgroups.

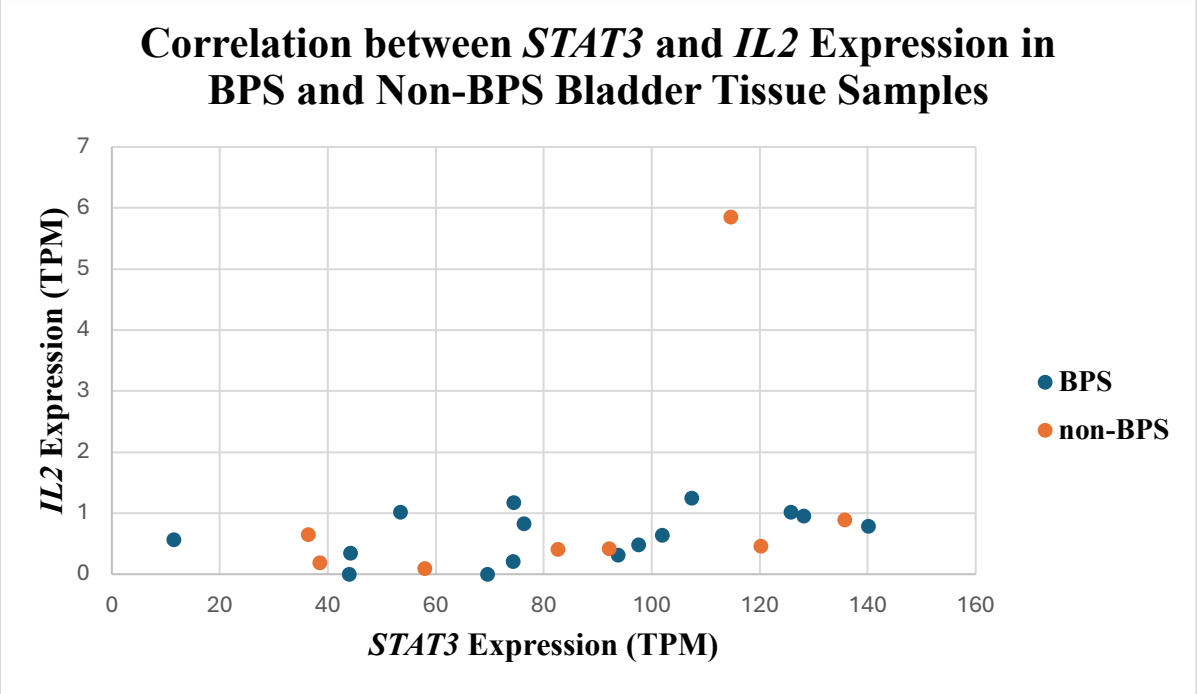


**Figure 3.4.53: Correlation Analysis between *STAT3* and *IL2* Expression in BPS and Non-BPS Bladder Tissue Samples.**

Scatter plots of *STAT3* and *IL2* expression (TPM) in BPS (blue) and non-BPS (orange) samples. In BPS samples, a non-significant medium positive relationship was observed ($r_s = 0.50$, $p = 0.06$), while in non-BPS samples, a non-significant large positive relationship was seen ($r_s = 0.52$, $p = 0.20$). These trends suggest a potential link between *STAT3*-mediated transcription and *IL2* expression, though further validation is required.

**Study 17**

To evaluate whether inflammasome-mediated inflammation contributes to BPS pathophysiology, we examined expression of *NLRP3*, *PYCARD*, *CASP1*, *IL1B*, and *IL18*, based on the inflammasome model proposed by Kiran, Rakib and Singh (2022). No statistically significant group-level differences were detected for any transcript (Table 3.4.23; Figure 3.4.54), although *NLRP3* displayed a modest trend toward higher mean expression in BPS (2.72 TPM) compared with non-BPS samples (1.64 TPM). Expression of *IL18* was similar across groups, echoing the subtle inflammatory shifts observed in Studies 8 and 15 for *IL1B*, *TNF*, and *IL6*.

Individual-level inspection again highlighted sample Y2338, which showed elevated *NLRP3* (6.18 TPM), *IL1B* (57.81 TPM), and *IL18* (60.09 TPM). This pattern suggests activation of the *NLRP3–IL1B–IL18* axis and is consistent with the broader immune-activated phenotype this sample has exhibited throughout preceding analyses, including high *IL6* and *TNF* (Studies 8, 12, and 15) and upregulated *STAT1* and *STAT3* (Study 16). Y2338 therefore continues to represent a potential inflammatory BPS subtype marked by coordinated cytokine and stress-response signalling.

Correlation analyses supported this interpretation: *NLRP3* and *IL1B* were significantly positively correlated in BPS samples ($r_s = 0.62$, $p = 0.02$; Figure 3.4.55), suggesting a degree of transcriptional coordination within the inflammasome pathway. By contrast, *NLRP3* showed no meaningful association with *CASP1* or *PYCARD*, indicating that downstream activation mechanisms may vary between individuals.

In summary, although group-level differences were limited, the combined evidence of elevated inflammasome-related transcripts in Y2338 and the strong *NLRP3–IL1B* correlation points to an inflammasome-linked inflammatory signature in a subset of BPS patients. These findings complement the inflammatory and epigenetic patterns described in Studies 6, 8, 15, and 16, strengthening the emerging view that BPS comprises multiple molecular subtypes with divergent inflammatory mechanisms.

**Table 3.4.23: Summary of Differential Expression Analysis for Inflammasome-Related Genes in BPS vs. Non-BPS.**

This table summarises the differential expression of key inflammasome-related genes (*NLRP3*, *PYCARD*, *CASP1*, *IL1B*, *IL18*) and relevant inflammatory cytokines (*TNF*, *IL6*) between BPS and non-BPS groups. Expression levels are expressed as mean TPM (Transcripts Per Million). The direction of change indicates relative differences between groups; "NS" denotes non-significant findings ($p > 0.05$). All tests used the Mann–Whitney U test. This table supports the investigation of the NLRP3 inflammasome pathway in BPS Kiran, Rakib and Singh (2022) by assessing transcriptional activation of these immune genes in bladder tissue samples.

| Gene | Function | Mean TPM (BPS) | Mean TPM (non-BPS) | Test Used | p-value | Direction of Change |
|---|---|---|---|---|---|---|
| ***NLRP3*** | Inflammasome sensor protein | 2.72 | 1.64 | Mann–Whitney U | 0.78 | No significant difference |
| ***PYCARD*** | Adapter protein in inflammasome complex | 34.15 | 41.99 | Mann–Whitney U | 1.03 | No significant difference |
| ***CASP1*** | Activates *IL1B* and *IL18* | 26.73 | 27.82 | Mann–Whitney U | 0.78 | No significant difference |
| ***IL1B*** | Pro-inflammatory cytokine | 53.80 | 58.55 | Mann–Whitney U | 0.98 | No significant difference |
| ***IL18*** | Inflammasome-processed cytokine | 62.35 | 64.37 | Mann–Whitney U | 0.55 | No significant difference |

| | | | | | | |
|---|---|---|---|---|---|---|
| ***TNF*** | Broad pro-inflammatory cytokine | 2.38 | 2.91 | Mann–Whitney U | 0.36 | No significant difference |
| ***IL6*** | Pro-inflammatory cytokine | 1.64 | 0.74 | Mann–Whitney U | 0.56 | No significant difference |

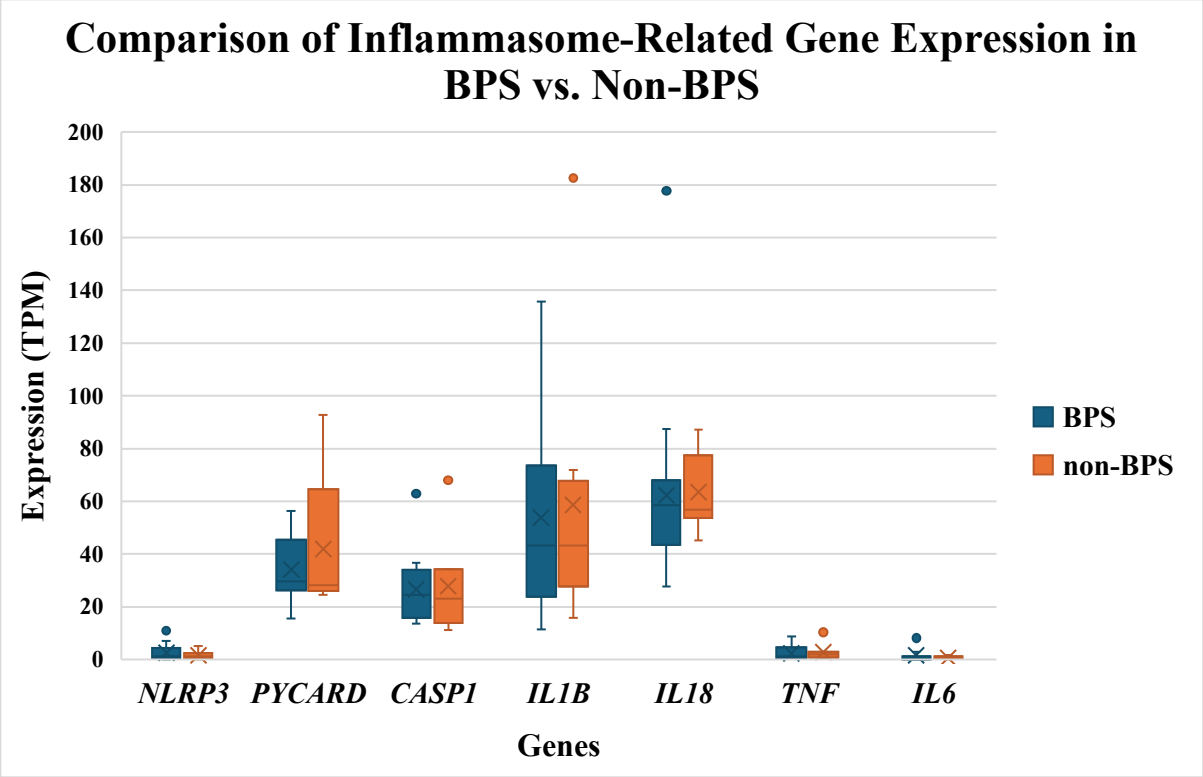


**Figure 3.4.54: Box-and-Whisker Plot of *NLRP3*, *PYCARD*, *CASP1*, *IL1B*, *IL18*, *TNF*, and *IL6* Expression in BPS vs. Non-BPS.**

This figure shows the distribution of transcript levels (TPM) for key inflammasome-related genes and relevant cytokines between BPS and non-BPS groups. Blue boxes represent BPS samples, while orange boxes represent non-BPS samples. No statistically significant differences were found for any gene based on Mann–Whitney U tests (all $p > 0.05$). The figure supports the analysis presented in Table 3.4.23 and highlights the modest expression differences within the NLRP3–IL1B–IL18 axis proposed in Kiran, Rakib and Singh (2022).

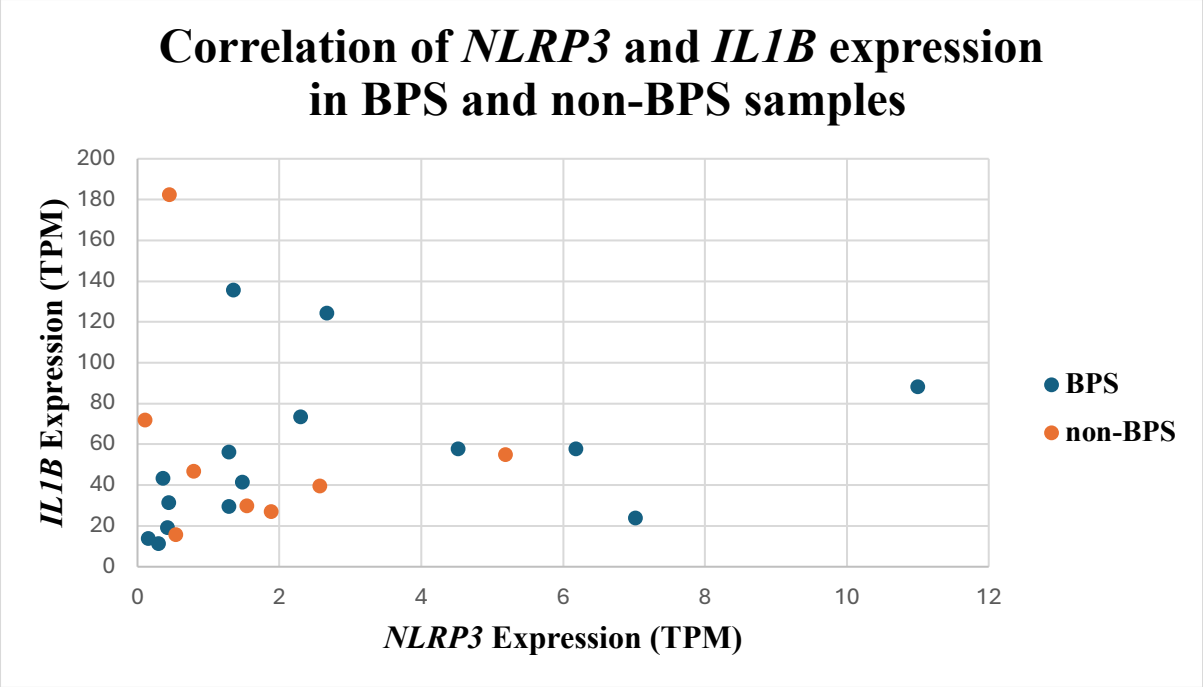


**Figure 3.4.55: Spearman Rank Correlation analysis of *NLRP3* and *IL1B* expression in BPS and non-BPS samples.**

In BPS samples, a significant large positive correlation was observed ($r_s = 0.62$, $p = 0.02$), suggesting coordinated inflammasome-related activity. In contrast, a non-significant medium negative correlation was found in non-BPS samples ($r_s = -0.31$, $p = 0.50$). Points represent individual samples; the trend line indicates the relationship between *NLRP3* and *IL1B* expression levels.

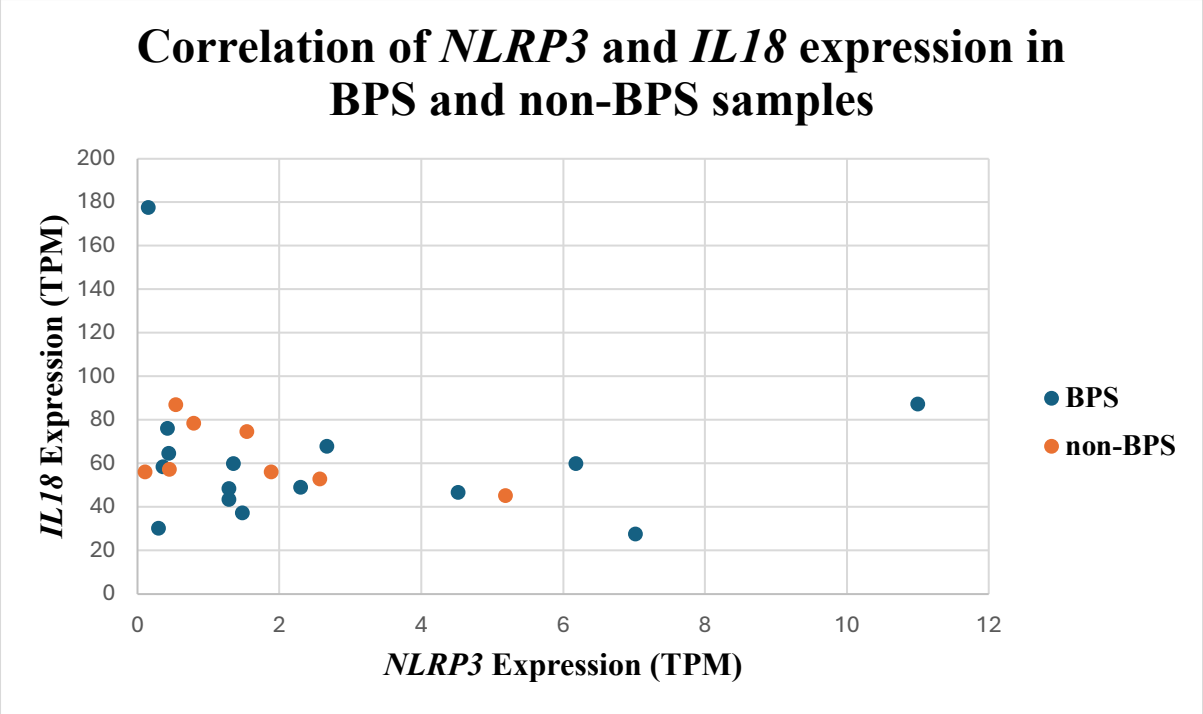


**Figure 3.4.56: Spearman Rank Correlation analysis of *NLRP3* and *IL18* expression in BPS and non-BPS samples.**

A non-significant small negative relationship was observed in BPS ($r_s$ = -0.13, p = 0.76), while a non-significant large negative relationship was noted in non-BPS samples ($r_s$ = -0.50, p = 0.23). These findings indicate limited evidence of inflammasome pathway co-activation between these genes in this cohort.

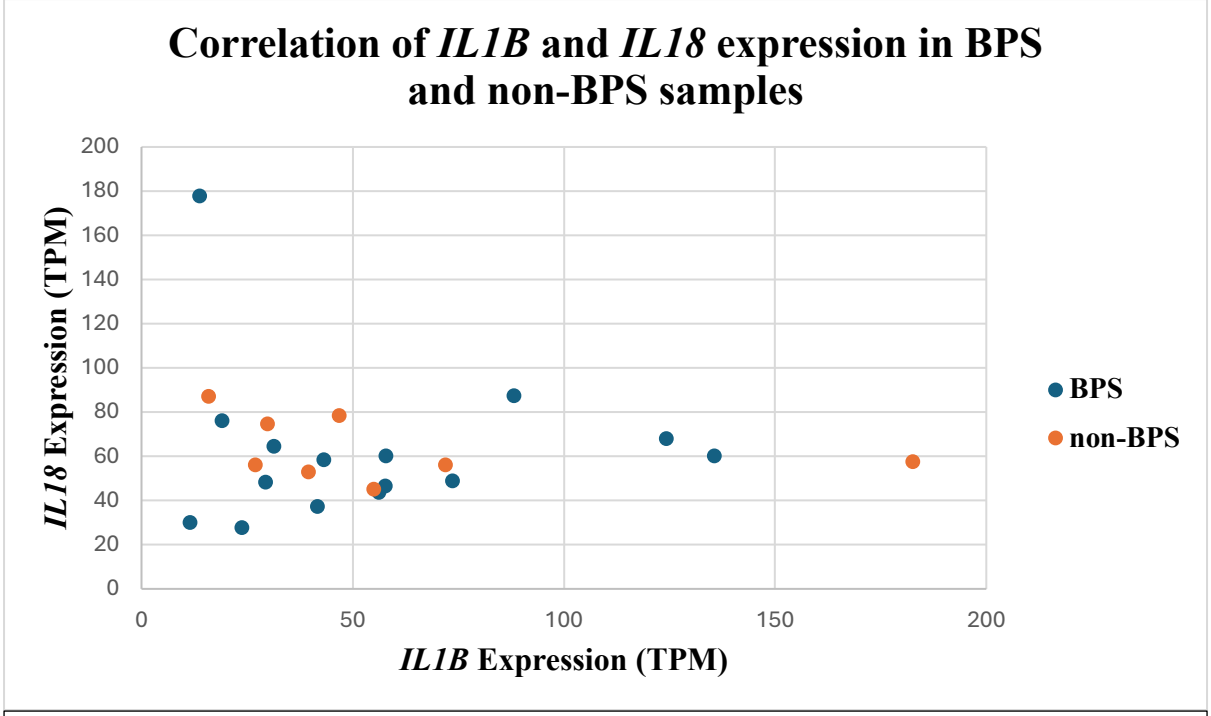


**Figure 3.4.57: Spearman Rank Correlation analysis of *IL1B* and *IL18* expression in BPS and non-BPS samples.**

A non-significant small positive relationship was observed in BPS ($r_s = 0.23$, $p = 0.40$), suggesting weak evidence of co-regulation. Conversely, a non-significant medium negative correlation was noted in non-BPS samples ($r_s = -0.43$, $p = 0.32$). Overall, these results do not support a strong coordinated expression pattern between these inflammasome pathway cytokines in this dataset.

**Study 18**

Braas et al. (2006) demonstrated PACAP upregulation in cystitis models, implicating *ADCYAP1*-driven neuroplasticity and altered bladder reflex pathways. To evaluate whether comparable neuropeptide signalling features are present in human BPS, we re-examined *ADCYAP1* and its receptor *ADCYAP1R1*, together with the related VIP axis (*VIP*, *VIPR1*, *VIPR2*) and *NGF*, drawing on the same dataset analysed in Study 13.

Mean transcript levels of *ADCYAP1*, *VIP*, *NGF*, and their receptors were uniformly low and did not differ significantly between BPS and non-BPS samples (all $p > 0.05$; Table 3.4.19; Figure 3.4.34). *VIPR1* remained the only receptor with appreciable expression across the cohort, yet also showed no group-level shift. The significant positive correlation between *NGF* and *VIP* observed in non-BPS samples ($r_s = 0.76$, $p = 0.03$) was absent in BPS, suggesting disrupted neurotrophin–neuropeptide coordination in the disease state.

Despite low overall abundance, individual-level variation again highlighted sample Y2336, which showed the highest *NGF* and *VIP* expression within the BPS group and one of the highest *ADCYAP1* values. This pattern, consistent with its profile in Studies 13, 15, and 16, points to a neurogenic–inflammatory subtype characterised by modest but coordinated elevation of neurotrophic and neuropeptide markers. Y2338 also demonstrated detectable but lower expression of these genes, reinforcing the presence of sporadic neurogenic signatures within the broader inflammatory heterogeneity of BPS.

Although the cohort did not replicate the neuropeptide upregulation described in experimental cystitis, these sample-specific deviations suggest that neuroplasticity-associated pathways may contribute to symptom mechanisms in a subset of patients. This interpretation aligns with emerging patterns across preceding studies, in which inflammatory, apoptotic, and neurogenic signals cluster within particular individuals rather than defining the condition as a whole.

**Study 19**

Liu and Kuo (2007) demonstrated that intravesical botulinum toxin A reduces bladder *NGF* expression in IC/BPS, suggesting that neurogenic inflammation contributes to symptom generation. To assess whether this mechanism is reflected at the transcriptional level in human bladder tissue, we examined *NGF* and its signalling partners—*NTRK1* (TrkA), *BDNF*, and *GFRA1*—in primary (P0) bladder samples from BPS and non-BPS patients.

Across all genes, group-level comparisons showed no statistically significant differences (all $p > 0.05$; Table 3.4.24; Figure 3.4.58). Mean expression levels were uniformly low in both groups (*NGF*: 0.02 vs. 0.03 TPM; *NTRK1*: 0.45 vs. 0.51 TPM), indicating an absence of broad transcriptional upregulation of neurotrophin pathways in BPS.

Despite this, individual-level analysis again highlighted sample Y2336, which showed the highest *NGF* expression in the cohort (0.278 TPM). This sample has repeatedly emerged across Studies 13, 15, and 18 with elevated *NGF*, *VIP*, *ADCYAP1*, *IL6*, and *TNF*, forming a coherent neuroinflammatory expression profile. The recurrence of this pattern strengthens the interpretation that a subset of BPS patients may exhibit enhanced neurotrophin and neuropeptide signalling, consistent with the neurogenic inflammation model proposed by Liu and Kuo.

Correlation analyses within the BPS cohort showed no significant association between *NGF* and *NTRK1* ($\rho = 0.18$, $p = 0.53$) or *NGF* and *BDNF* ($\rho = 0.17$, $p = 0.54$), suggesting that neurotrophin genes are not co-regulated at the transcript level. *NGF* expression also did not correlate with O'Leary–Sant Problem Index scores ($\rho = –0.21$, $p = 0.45$), implying that symptom burden is unlikely to be captured by *NGF* mRNA alone in an unstratified cohort.

In summary, while no group-wide transcriptomic changes support a universal neurogenic inflammation mechanism in BPS, the consistent elevation of *NGF* and related neurogenic markers in Y2336 indicates a distinct molecular subtype characterised by neurotrophin-driven signalling. This pattern aligns with the broader thesis findings of patient-specific transcriptional signatures and supports the potential value of neurogenic-targeted therapeutic strategies for select BPS subgroups.

**Table 3.4.24: Expression of key neurotrophin-related genes in BPS and non-BPS bladder tissue samples.**

Summary of mean TPM expression levels and Mann–Whitney U test results comparing BPS vs. non-BPS groups for genes relevant to neurotrophin signalling (Study 19). Genes analysed include *NGF* (central to neurogenic inflammation), *NTRK1* (its receptor), *BDNF* (chronic pain marker), and *GFRA1* (optional marker of neural sensitisation). Although no statistically significant differences were detected (all $p > 0.05$), trends suggest generally lower expression in BPS for *NGF*, *NTRK1*, and *BDNF*, while *GFRA1* showed a small, non-significant increase. These results, with small effect sizes, imply subtle differences in neurotrophin signalling rather than robust dysregulation at the transcript level. Further analyses integrating these data with clinical subtypes or symptom scores may clarify subgroup-specific roles in BPS pathophysiology.

| Gene | Function | Mean TPM (BPS) | Mean TPM (non-BPS) | Test Used | p-value | Direction of Change |
|---|---|---|---|---|---|---|
| ***NGF*** | Nerve Growth Factor | 0.02 | 0.03 | Mann–Whitney U | 0.75 | No significant difference |
| ***NTRK1*** | NGF receptor (*TrkA*) | 0.45 | 0.51 | Mann–Whitney U | 0.55 | No significant difference |
| ***BDNF*** | Brain-Derived Neurotrophic Factor | 0.05 | 0.07 | Mann–Whitney U | 0.58 | No significant difference |
| ***GFRA1*** | GDNF family receptor alpha-1 | 0.13 | 0.08 | Mann–Whitney U | 0.62 | No significant difference |

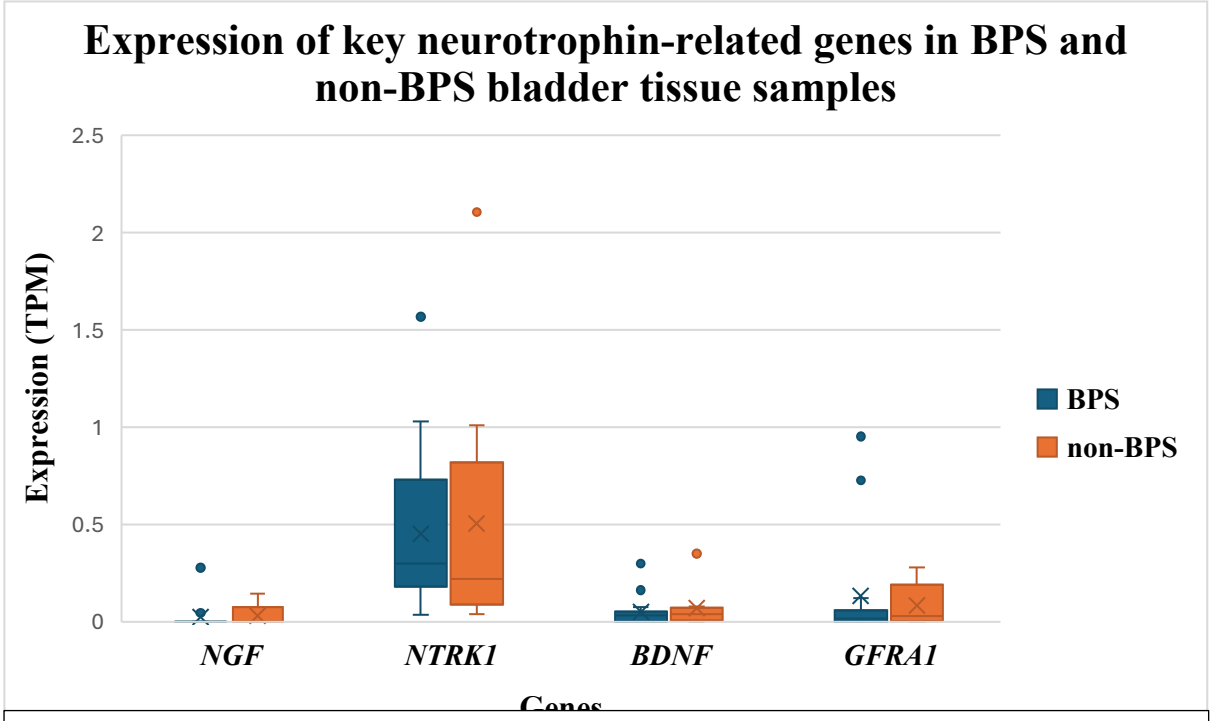


**Figure 3.4.58: Expression of key neurotrophin-related genes in BPS and non-BPS bladder tissue samples.**

Box-and-whisker plots showing TPM expression levels of *NGF*, *NTRK1*, *BDNF*, and *GFRA1* in BPS (blue) and non-BPS (orange) groups (Study 19). Each plot displays the median (horizontal line), mean (×), interquartile range (box), and outliers (individual points). No significant differences were observed between groups for any gene (all $p > 0.05$; Table 3.4.24). While *NGF*, *NTRK1*, and *BDNF* exhibited slightly lower expression in BPS, *GFRA1* showed a small, non-significant increase. These findings suggest no consistent transcriptomic upregulation of neurotrophin pathways in BPS overall, but outlier samples or downstream signalling may still contribute to patient heterogeneity.

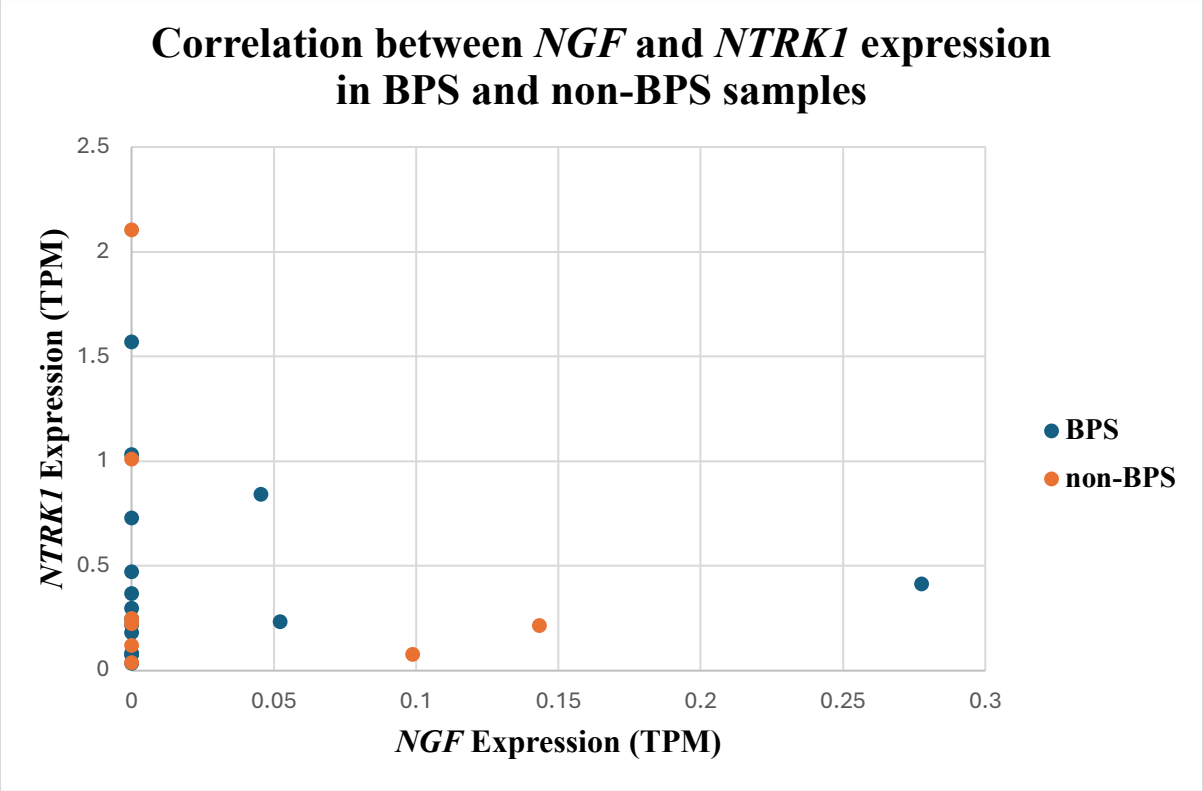


**Figure 3.4.59: Spearman correlation between *NGF* and *NTRK1* expression in BPS and non-BPS samples**.

Scatter plots with fitted trend lines illustrating the relationship between *NGF* and *NTRK1* expression in BPS (blue) and non-BPS (orange) samples. Spearman correlation analyses revealed a non-significant small positive relationship in BPS ($r_s = 0.18$, $p = 0.53$) and a non-significant medium negative relationship in non-BPS ($r_s = –0.34$, $p = 0.41$). These findings indicate no consistent co-regulation of *NGF* and its receptor gene *NTRK1* in either group, suggesting heterogeneous activation of NGF signalling across samples.

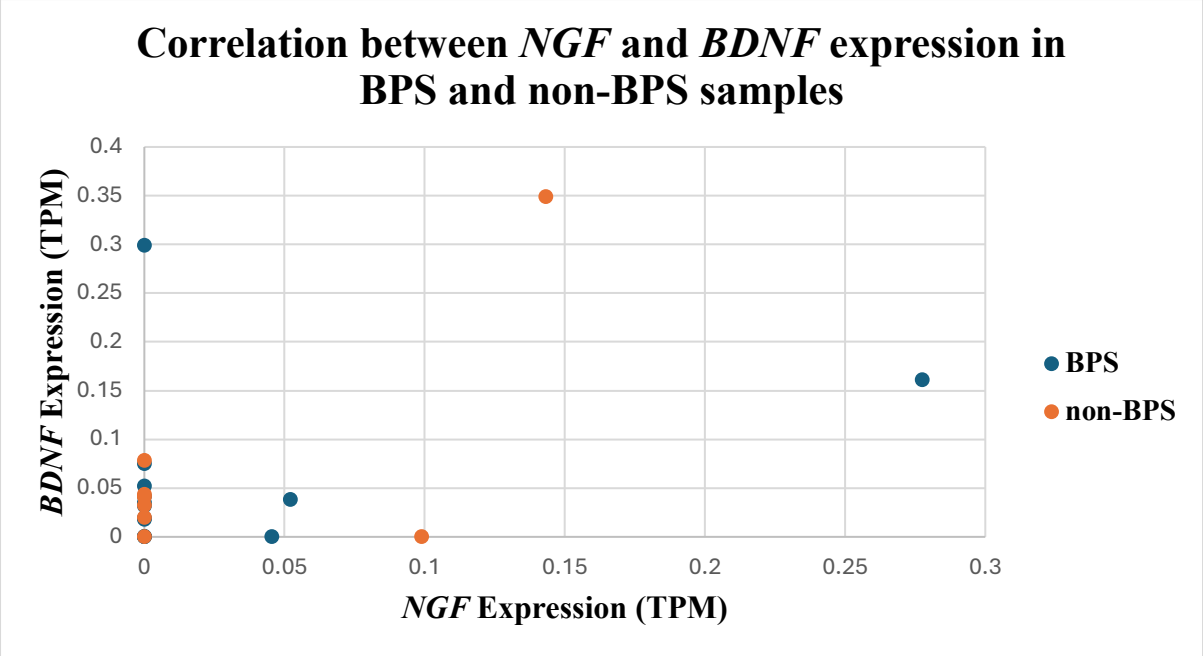


**Figure 3.4.60: Spearman correlation between *NGF* and *BDNF* expression in BPS and non-BPS samples.**

Scatter plots with fitted trend lines showing the relationship between *NGF* and *BDNF* expression in BPS (blue) and non-BPS (orange) samples. In BPS samples, a non-significant small positive correlation was observed ($r_s = 0.17$, $p = 0.54$), while a similarly weak positive relationship was seen in non-BPS samples ($r_s = 0.17$, $p = 0.70$). This suggests no strong co-expression of these neurotrophic factors in bladder tissue at the transcriptomic level.

**Study 20**

Ostardo et al. (2018) demonstrated that CYP-induced cystitis is driven by *NF-κB*–dependent inflammatory signalling, accompanied by oxidative stress and epithelial dysfunction. To explore whether a similar transcriptional pattern is detectable in human BPS, we analysed the expression of *TNF*, *IL1B*, *CCL2*, *NOS2*, *NFKB1*, *TJP1*, and *NGF* in P0 bladder urothelium.

Group-level comparisons revealed no significant differences for *TNF*, *IL1B*, *CCL2*, *NFKB1*, *TJP1*, or *NGF* (all $p > 0.05$; Table 3.4.25; Figure 3.4.61). However, *NOS2* expression was significantly higher in BPS than in non-BPS samples (0.33 vs. 0.13 TPM; $p = 0.03$), representing the only statistically significant gene-level difference across Studies 1–20. This finding highlights oxidative stress as a potential contributor to BPS pathophysiology in at least a subset of patients.

Individual sample analysis again reflected the recurrent heterogeneity observed throughout this chapter. Y2336—previously characterised as an inflammatory outlier in Studies 4, 6, 8, 13, 15, 16, and 19—showed pronounced co-expression of *CCL2* (54.51 TPM) and *NOS2* (4.37 TPM), suggesting convergence of chemotactic and oxidative pathways. Y2338 also demonstrated moderately elevated *CCL2* and *TNF*, consistent with its established immune-active profile.

Spearman correlations revealed a strong positive association between *NFKB1* and *IL1B* in BPS samples ($\rho = 0.73$, $p = 0.003$; Figure 3.4.65), consistent with canonical *NF-κB* regulation of pro-inflammatory cytokines and supporting the mechanistic model proposed by Ostardo et al. (2018). Other correlations involving *NFKB1*—including with *TNF* and *NOS2*—were non-significant, reflecting partial and variable pathway engagement across individuals.

Notably, Y2610 exhibited the highest *NFKB1* expression (153.29 TPM), alongside elevated *MAPK14* and *CDKN1A* in earlier studies, suggesting activation of stress-response pathways distinct from the immune-dominant profiles of Y2336 and Y2338. This reinforces the presence of multiple molecular phenotypes within BPS, including oxidative stress–linked, immune-driven, and neuroinflammatory subtypes.

In summary, Study 20 identifies *NOS2* upregulation as the first statistically significant transcript-level alteration across the thesis dataset, highlighting oxidative stress as a plausible pathogenic mechanism in BPS. When considered alongside prior evidence of immune

activation (Studies 4, 6, 15), apoptosis (Studies 8, 10), and neuroplasticity (Studies 13, 18, 19), these findings reinforce the central thesis argument: BPS is not a single molecular entity but a heterogeneous condition comprising biologically distinct subgroups, each potentially amenable to targeted therapeutic approaches.

**Table 3.4.25: Expression and differential analysis of NF-κB pathway–related genes and key inflammatory targets in BPS vs. non-BPS bladder tissue.**

This table summarizes the expression levels and Mann–Whitney U test results for *NGF*, *TJP1*, *TNF*, *IL1B*, *NOS2*, *CCL2*, and *NFKB1* in BPS vs. non-BPS bladder tissue. Mean TPM values reflect the average gene expression per group, while p-values indicate the significance of group differences. Direction of change highlights whether each gene is upregulated or downregulated in BPS relative to non-BPS samples. Notably, only *NOS2* showed a significant difference ($p = 0.03$), suggesting a potential role in BPS-related oxidative stress. All other genes exhibited non-significant differences, supporting the overall heterogeneity of gene expression profiles in BPS.

| Gene | Function | Mean TPM (BPS) | Mean TPM (non-BPS) | Statistical Test | p-value | Direction of Change |
|---|---|---|---|---|---|---|
| ***NGF*** | Neuroinflammatory pain mediator | 0.02 | 0.03 | Mann–Whitney U | 0.75 | No significant difference |
| ***TJP1*** | Tight junction protein (urothelial barrier) | 51.65 | 50.90 | Mann–Whitney U | 0.93 | No significant difference |
| ***TNF*** | Inflammatory cytokine | 2.38 | 2.91 | Mann–Whitney U | 0.36 | No significant difference |
| ***IL1B*** | Pro-inflammatory cytokine | 53.80 | 58.55 | Mann–Whitney U | 0.97 | No significant difference |

| | | | | | | |
|---|---|---|---|---|---|---|
| ***NOS2*** | Inducible nitric oxide synthase (oxidative stress) | 0.33 | 0.13 | Mann–Whitney U | 0.03 | ↑ in BPS (statistically significant) |
| ***CCL2*** | Chemokine (monocyte recruitment) | 4.37 | 15.73 | Mann–Whitney U | 0.23 | No significant difference |
| ***NFKB1*** | Transcription factor (inflammatory signalling) | 47.11 | 47.48 | Mann–Whitney U | 0.88 | No significant difference |

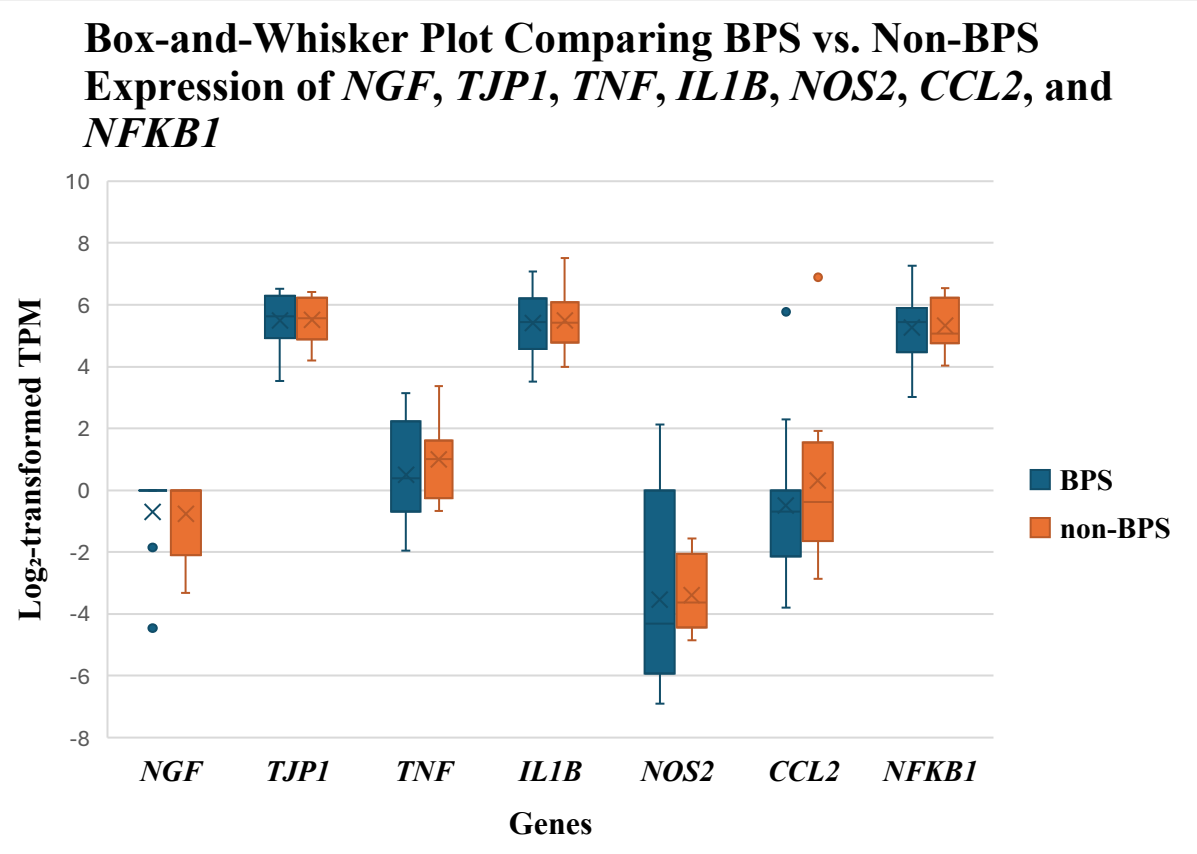


**Figure 3.4.61: Paired Box-and-Whisker Plot of *NGF*, *TJP1*, *TNF*, *IL1B*, *NOS2*, *CCL2*, and *NFKB1* Expression in BPS vs. Non-BPS Bladder Tissue.**

This figure illustrates the $\log_2$-transformed transcript per million (TPM) expression levels of *NGF*, *TJP1*, *TNF*, *IL1B*, *NOS2*, *CCL2*, and *NFKB1* in BPS (blue) and non-BPS (orange) bladder tissue. Each gene is presented as a paired box-and-whisker plot, with medians represented by horizontal lines, means indicated by an "×", and individual outliers displayed as points. This visualisation facilitates comparison of expression profiles between groups and highlights overall trends, such as the significant upregulation of *NOS2* in BPS and the largely comparable expression levels of the other genes, supporting the observed heterogeneity of inflammatory and barrier-related gene expression in BPS.

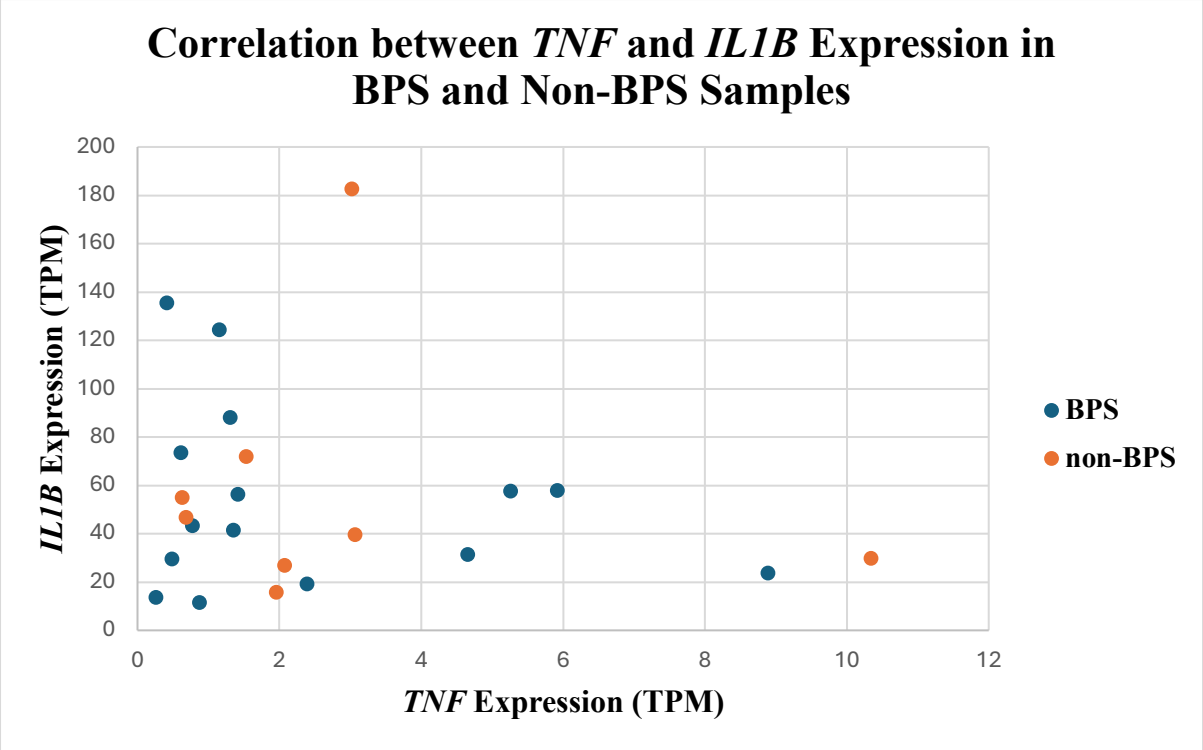


**Figure 3.4.62: Spearman Correlation analysis between *TNF* and *IL1B* Expression in BPS and Non-BPS Samples.**

This figure displays the Spearman rank correlation between *TNF* and *IL1B* expression in BPS and non-BPS bladder tissue samples. In BPS, the correlation is very small and negative ($r_s$ = -0.05, p = 0.66), while in non-BPS it is also small and negative ($r_s$ = -0.26, p = 0.59). These results suggest no significant co-expression between *TNF* and *IL1B* in either group.

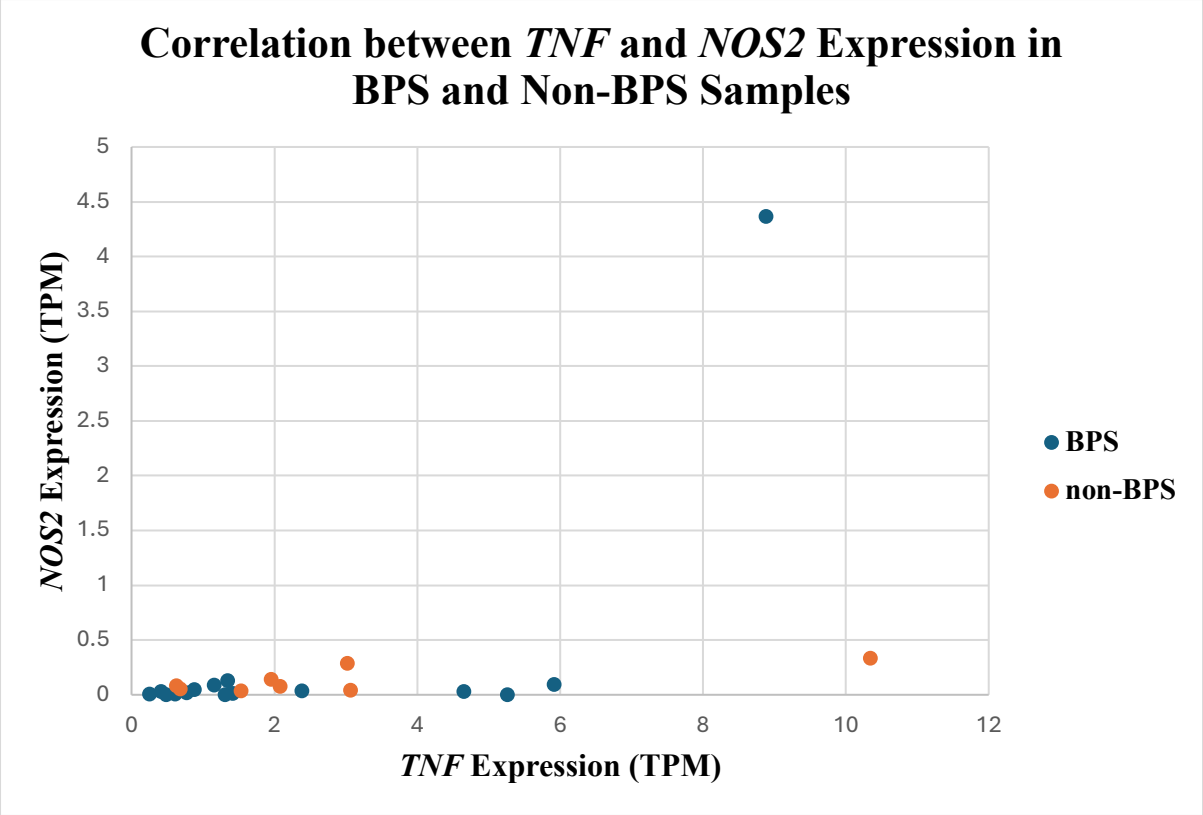


**Figure 3.4.63: Spearman Correlation analysis between *TNF* and *NOS2* Expression in BPS and Non-BPS Samples.**

This figure illustrates the Spearman rank correlation between *TNF* and *NOS2* expression. A medium positive (non-significant) correlation was observed in BPS ($r_s = 0.41$, $p = 0.13$) and non-BPS ($r_s = 0.38$, $p = 0.38$). These findings suggest a trend towards co-expression of *TNF* and *NOS2*, possibly implicating an oxidative stress–inflammatory link in a subset of patients.

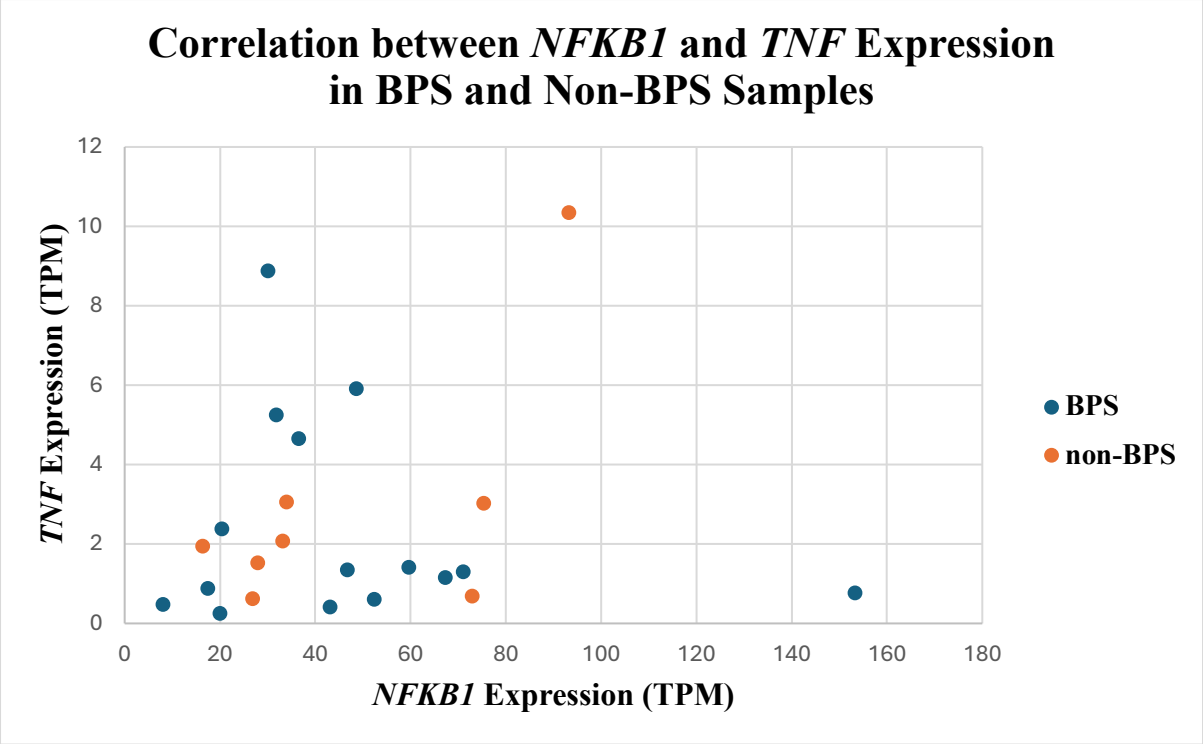


**Figure 3.4.64: Spearman Correlation analysis between *NFKB1* and *TNF* Expression in BPS and Non-BPS Samples**.

This figure shows the Spearman correlation between *NFKB1* and *TNF* expression levels. In BPS, the correlation is very small and positive ($r_s = 0.06$, $p = 0.78$), whereas in non-BPS, it is large and positive but not significant ($r_s = 0.62$, $p = 0.12$). These results suggest potential co-regulation in non-BPS but no significant trend overall.

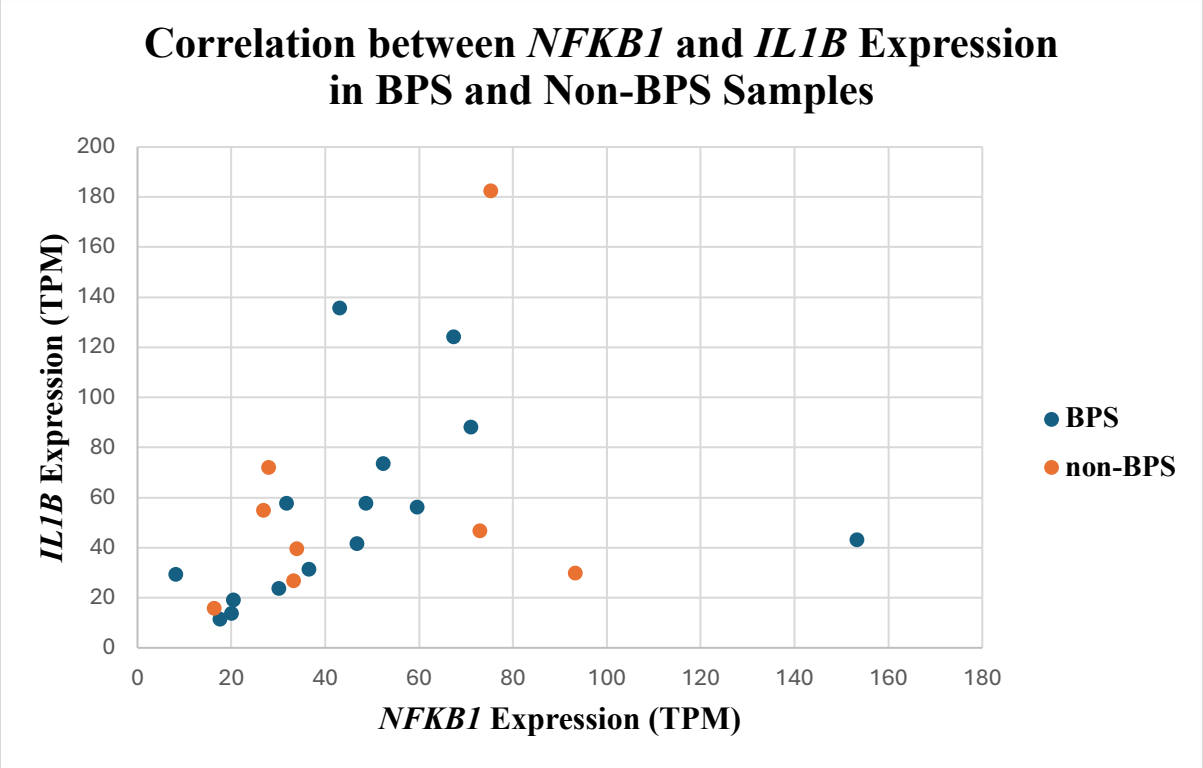


**Figure 3.4.65: Spearman Correlation analysis between *NFKB1* and *IL1B* Expression in BPS and Non-BPS Samples.**

This figure depicts the relationship between *NFKB1* and *IL1B* expression. A significant large positive correlation was detected in BPS ($r_s = 0.73$, $p = 0.003$), indicating potential coordinated regulation of these inflammatory genes. In non-BPS samples, the correlation was small and not significant ($r_s = 0.24$, $p = 0.64$).

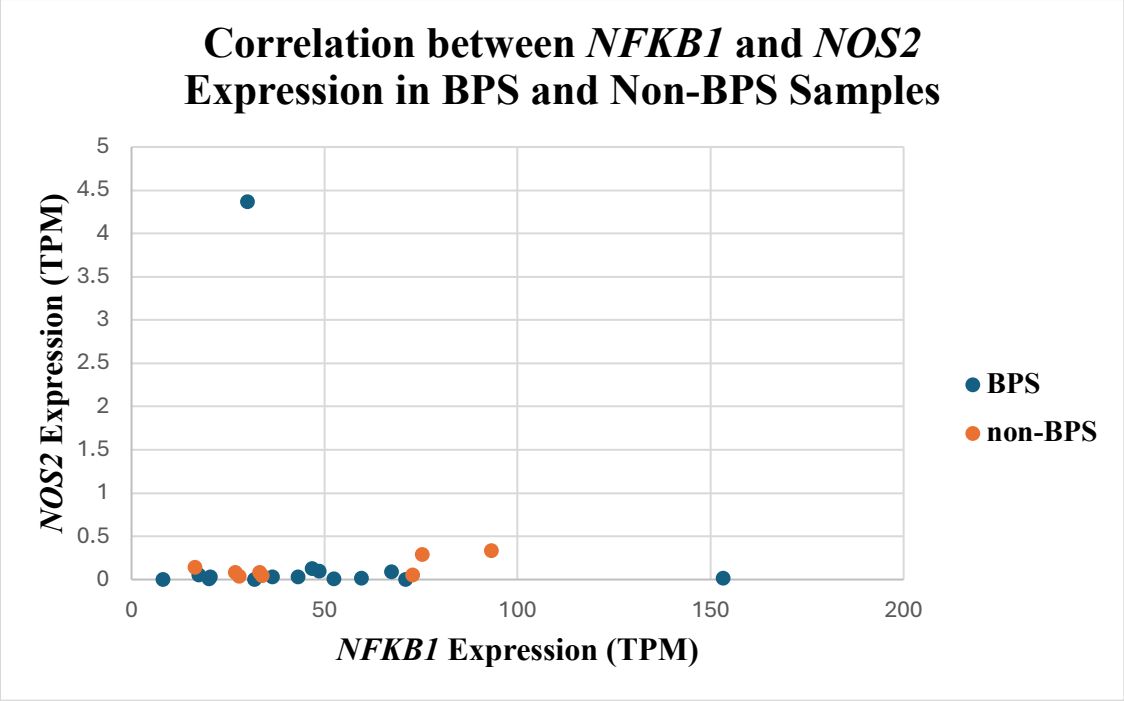


**Figure 3.4.66: Spearman Correlation analysis between *NFKB1* and *NOS2* Expression in BPS and Non-BPS Samples.**

This figure shows the relationship between *NFKB1* and *NOS2* expression. In BPS samples, a very small positive correlation ($r_s = 0.01$, $p = 0.97$) was observed, while a medium positive correlation ($r_s = 0.33$, $p = 0.46$) was detected in non-BPS samples. Both correlations are non-significant, suggesting no strong co-expression between these genes in either group.

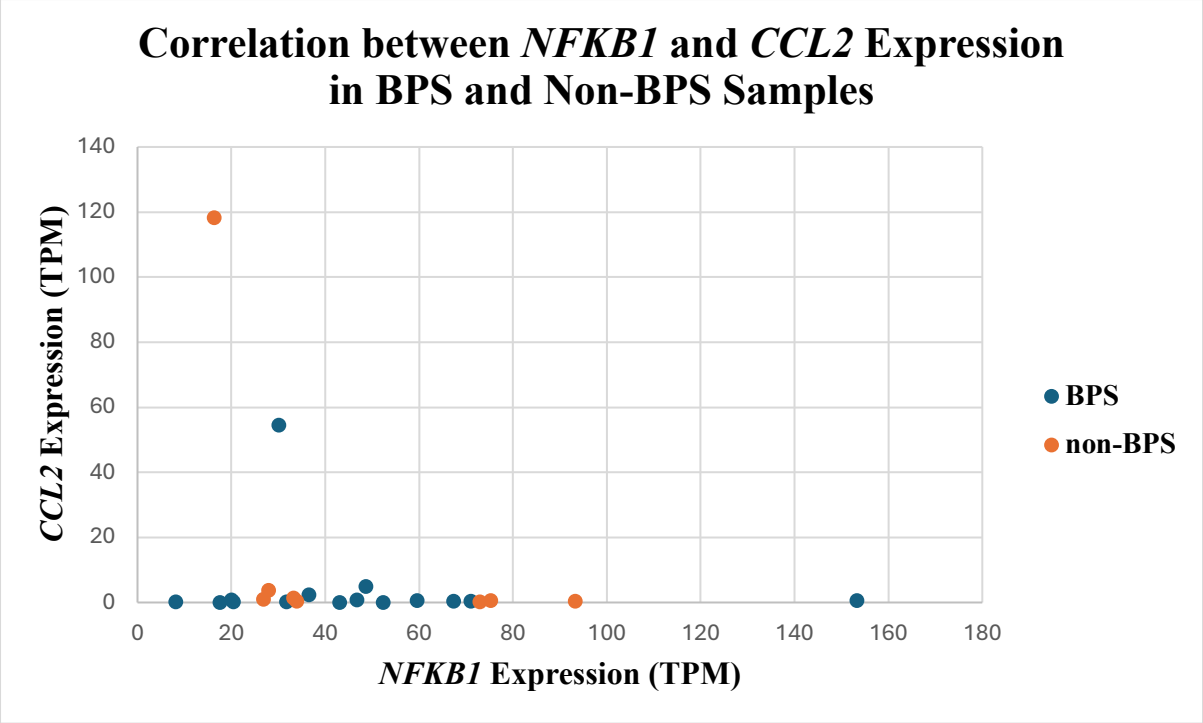


**Figure 3.4.67: Spearman Correlation analysis between *NFKB1* and *CCL2* Expression in BPS and Non-BPS Samples.**

This figure highlights the Spearman correlation between *NFKB1* and *CCL2* expression. A small positive correlation was observed in BPS ($r_s = 0.14$, $p = 0.62$). Interestingly, a significant large negative correlation was found in non-BPS ($r_s = -0.81$, $p = 0.03$), suggesting inverse regulation of *NFKB1* and *CCL2* in non-BPS bladder tissue.

## 3.5 Transcriptomic Insights into BPS Pathophysiology: A Synthesis of In-House Findings

Analysis of the in-house bladder transcriptomic dataset provided further evidence that BPS is molecularly heterogeneous, with most group-level comparisons showing modest or non-significant differences but several individuals displaying coherent, biologically meaningful transcriptional patterns. Rather than indicating an absence of pathology, these muted averaged signals reflect the condition's clinical variability and the limitations of aggregate analyses in a heterogeneous cohort. When examined at the individual level—and interpreted alongside symptoms, cystoscopic findings and barrier function assays—distinct molecular signatures emerged that parallel the mechanistic themes highlighted in Studies 1–20. The synthesis below integrates these patient-specific patterns across major pathophysiological domains, situating the in-house findings within the broader literature while identifying potential molecular subgroups within BPS.

Immune Dysregulation and Inflammatory Activation

Across the cohort, immune-associated transcripts—including *IL6*, *TNF*, *CXCL1*, *CCL2*, *IL1B*, and *IL18*—did not show significant group-level differences between BPS and non-BPS samples. Nonetheless, several analyses indicated coordinated inflammatory activity within a subset of BPS patients. Strong positive correlations such as *IL6–TNF* (Studies 15 and 16) and *NLRP3–IL1B* (Study 17) point to selective engagement of inflammatory pathways despite muted averaged effects.

Two individuals, Y2336 and Y2338, consistently demonstrated markedly higher expression of immune-related genes. Y2336 showed elevated *CCL2*, *IL6*, *TNF*, *PTGS2*, *NOS2*, and *STAT3*, while Y2338 exhibited increased *IL6*, *TNF*, *IL1B*, and *STAT1*. These molecular signals align with their clinical presentations—both reported suprapubic pain and urinary frequency, and cystoscopy confirmed glomerulations—supporting localised urothelial–immune activation in these patients.

Complementary findings in Studies 4 and 6 reinforced this pattern, with increased expression of adhesion and antigen-presentation genes (*ICAM1*, *VCAM1*, *HLA-DRB1*, *HLA-DRA*, *HLA-DPB1*) in the same samples. The strong correlation between *ICAM1* and *TNF* ($\rho = 0.66$, $p =$

0.01) suggests coordinated inflammatory and epithelial–immune interface signalling in these individuals.

By contrast, inflammasome-associated transcripts (*NLRP3*, *PYCARD*, *CASP1*) showed little variation across most samples, indicating that canonical inflammasome activation is unlikely to represent a dominant pathway in BPS, although it may contribute to the inflammatory phenotype of isolated cases such as Y2338.

Epithelial Barrier Dysfunction and Apoptosis

Markers of epithelial integrity (*CDH1*, *TJP1*) and apoptosis (*MAPK14*, *CASP3*, *BAX*) showed no significant group-level differences between BPS and non-BPS samples (Studies 9 and 10), diverging from protein-level reductions reported previously ( Liu et al., 2012; Lee, Jiang and Kuo, 2013). This discrepancy suggests that barrier impairment in BPS may arise from post-transcriptional regulation, protein turnover, or functional disruption not captured at the mRNA level.

Functional assessment via transepithelial resistance (TER) provided supporting evidence: several BPS samples, including Y2319 (404 Ω·cm²), Y2336 (20 Ω·cm²), Y2338 (302.7 Ω·cm²), and Y2371 (247.7 Ω·cm²), showed reduced TER despite largely unremarkable transcript profiles. These findings emphasise the added value of pairing transcriptomics with functional readouts when evaluating urothelial barrier integrity.

A strong *MAPK14–CASP3* correlation in BPS samples ($\rho = 0.85$, $p < 0.001$) indicates coordinated engagement of stress–apoptotic signalling, consistent with models proposing epithelial stress-induced apoptosis. The absence of a corresponding *MAPK14–TNF* association suggests that this response may occur independently of classical cytokine activation.

Sample-level patterns again revealed heterogeneity: Y2338 exhibited co-elevation of *MAPK14*, *TNF*, and *CASP3*, aligning with its broader immune–apoptotic profile, whereas Y2336 and Y2538 demonstrated isolated or partial pathway activation. Together, these distinctions reinforce the presence of mechanistically diverse epithelial phenotypes within BPS, with some individuals showing coordinated stress–apoptotic activity and others demonstrating more fragmented signalling.

## Neurogenic Inflammation and Sensory Pathways

Expression of neurogenic mediators—including *NGF*, *CNR1*, *ADCYAP1*, and *VIP*—was uniformly low across the cohort, with no significant differences between BPS and non-BPS groups (Studies 11, 13, 18, 19). Nonetheless, several individuals displayed coherent neurogenic patterns suggestive of subtype-specific involvement. Y2336 showed elevated *NGF*, *VIP*, and *ADCYAP1*, consistent with the neuropeptide-enriched profile identified in Studies 13 and 18 and aligning with this patient's higher symptom burden and inflammatory transcript profile. Y2610 exhibited the highest *CNR1* expression alongside the highest recorded pain score, despite minimal immune activation, indicating a possible neuroplasticity-dominant mechanism in this case.

Correlational analyses further emphasised this heterogeneity. In Study 19, *NGF* expression did not correlate with symptom severity, limiting its value as a general biomarker; however, its selective elevation in Y2336 reinforces the concept of patient-specific neurogenic contributions. Taken together, these findings indicate that while neurogenic pathways are not broadly dysregulated in BPS, they may play a meaningful role in defined subsets characterised by enhanced sensory signalling or neuroplastic adaptation.

## Oxidative Stress and NF-κB–Related Pathways

Among the few cohort-level findings to reach statistical significance, Study 20 identified increased *NOS2* expression in BPS, indicating engagement of oxidative stress pathways. A significant positive correlation between *NFKB1* and *IL1B* further supported participation of canonical NF-κB signalling, consistent with the mechanism proposed by Ostardo et al. (2018).

Y2336 again demonstrated a pronounced inflammatory–oxidative profile, with elevated *NOS2*, *CCL2*, and *TNF*, suggesting convergence of chemotactic and oxidative pathways in this individual. Whether these patterns reflect epithelial hyper-responsiveness or increased immune cell infiltration cannot be determined from bulk P0 tissue and would benefit from higher-resolution approaches such as single-cell or spatial transcriptomics.

## Epigenetic and Regulatory Signatures

Although direct miRNA measurements were not available, Studies 16 and 17 examined transcripts regulated by *miR-146a* and *miR-181a/b*, including *IRAK1*, *TRAF6*, *STAT1*, *STAT3*, and *PTPN22*. Elevated expression of several of these targets in Y2336 and Y2338 aligns with their broader inflammatory profiles and may reflect reduced miRNA-mediated repression or compensatory transcriptional upregulation under inflammatory stress. These patterns are consistent with the immune-enriched phenotype observed in these samples and point to potential epigenetic contributions to BPS heterogeneity.

## Summary of Outlier Samples and Preliminary Subtype Hypotheses

Across the BPS cohort, three samples—Y2336, Y2338 and Y2610—recurrently demonstrated coherent, pathway-level transcriptional patterns that may represent early signals of molecular subtypes. Although exploratory and based on small numbers, these profiles help contextualise the broader heterogeneity observed throughout Studies 1–20.

Immune-activated profile (Y2336, Y2338).
Both samples showed sustained elevation of inflammatory mediators (e.g., *IL6*, *TNF*, *CCL2*), increased expression of MHC class II and adhesion molecules, and higher levels of putative miRNA-regulated targets (*STAT1*, *STAT3*, *PTPN22*). Clinically, each patient reported suprapubic pain and urinary frequency with cystoscopic glomerulations, supporting the interpretation of a local immune-enriched phenotype.

Neurogenic–inflammatory overlap (Y2336).
Y2336 also exhibited increased *NGF*, *VIP* and *ADCYAP1*, suggesting a convergence of inflammatory and neurogenic signalling. This dual-pathway signature aligns with neurogenic inflammation models and may indicate heightened sensory pathway engagement superimposed on immune activation.

Neuroplasticity-dominant profile (Y2610).
Y2610 showed minimal inflammatory gene expression but the highest *CNR1* level within the

dataset, coinciding with the highest reported pain score. This combination suggests a sensory-dominant, rather than immune-driven, mechanism of symptom generation.

Together, these outlier profiles lend provisional support to a stratified model of BPS pathophysiology, incorporating immune-centric, neuro-inflammatory, and neuroplasticity-skewed patterns. However, the small number of such cases and the absence of robust clustering across the wider cohort underscore the tentative nature of these interpretations. Validation would require larger cohorts and higher-resolution approaches—such as single-cell, spatial, or proteomic profiling—to determine whether these signatures represent stable, clinically meaningful subtypes. For the present study, they highlight how patient-level transcriptomic variation may complement standard group-level analyses in elucidating BPS heterogeneity.

Beyond the Outliers: The “Quiet Majority” and the Limits of Averaged Analyses

Most BPS samples displayed low-to-moderate expression across all assessed pathways, forming no clear transcriptomic clusters and contributing to the absence of group-level significance in many analyses (e.g., Studies 8, 10, 15, 17). This “quiet majority” likely reflects a combination of milder disease activity, alternative pathogenic mechanisms not captured in urothelial transcriptomes, and sampling constraints inherent to primary (P0) epithelial tissue. The use of epithelial-only specimens may under-represent stromal, immune, or neuronal contributions, while clinical quiescence at the time of sampling may further dampen transcriptional signals.

Rather than contradicting immune- or neurogenic models of BPS, these muted transcriptional profiles indicate that such mechanisms are present but not pervasive, reinforcing the condition’s heterogeneity. Collectively, these findings underscore the limitations of averaged analyses in BPS and support the need for multi-omic, multi-compartment approaches—including stromal, immune, and neural profiling—to capture the full breadth of biological variation underlying chronic bladder pain.

# Chapter 4: Discussion

This study examined the molecular underpinnings of Bladder Pain Syndrome (BPS) through an integrated approach combining systematic review and transcriptomic profiling of human bladder tissue. The aims were to: (1) identify candidate biomarkers from existing literature; (2) evaluate their expression in a well-characterised clinical cohort; (3) explore the possibility of molecular subtypes; and (4) relate these signatures to symptoms, cystoscopic findings, and potential therapeutic implications.

The systematic review (Chapter 2) identified recurrent mechanistic themes—immune dysregulation (e.g., *IL6, TNF, CXCL1*), neurogenic inflammation (*NGF, VIP, CNR1*), epithelial barrier dysfunction (*CDH1, TJP1*), and oxidative stress (*NOS2*). Transcriptomic analyses in Chapter 3 broadly supported these pathways but also revealed substantial inter-individual variability. As observed in prior transcriptomic studies of IC/BPS (Ward et al., 2020), group-level differences were modest, whereas patient-level analyses highlighted distinct transcriptional outliers.

Sample Y2336 exemplified this pattern, demonstrating a multi-dimensional inflammatory signature characterised by elevated *IL6, TNF, NOS2, STAT3* and adhesion molecules (*ICAM1, VCAM1*). Y2338, although lacking Hunner lesions and diagnosed post-TVT surgery, showed a similar immune-skewed profile. Her symptoms—dyspareunia, urgency, glomerulations on cystoscopy, and moderate IC Symptom Index (10/20)—reinforce that molecular activity does not always track with symptom severity or cystoscopic appearance. This dissociation between clinical and molecular signals aligns with recent observations that BPS symptom scores alone insufficiently predict underlying biological mechanisms.

In contrast, Y2610 had the highest IC Symptom Index (20/20) but minimal inflammatory gene expression. Although Hunner lesions were visible at cystoscopy, *IL6*, *TNF*, and oxidative markers remained low. Instead, *CNR1*—encoding cannabinoid receptor 1—was strongly upregulated, suggesting a neuroplasticity-dominant phenotype. Given the superficial (P0) biopsy depth, it is plausible that deeper lesional inflammation was not captured. Hunner lesions typically involve suburothelial immune infiltrates and epithelial denudation (McIlraith et al., 2016), meaning that P0 biopsies may preferentially represent adjacent “field” tissue rather than the lesion itself (Li, Gheinani and Adam, 2019).

Together, these three transcriptional outliers—Y2336, Y2338 and Y2610—indicate the potential presence of biologically distinct subtypes within BPS. While exploratory and constrained by sample size, two provisional patterns emerged:

1. **Immune-Dominant Subtype (e.g., Y2336, Y2338):**
   Marked by elevated cytokines (*IL6, TNF, CCL2*), oxidative stress (*NOS2*), and increased expression of miRNA-regulated targets (*STAT3, PTPN22, IRAK1*), suggesting dysregulated inflammatory signalling. Such patients may plausibly benefit from immunomodulatory therapies.

2. **Neuroplasticity-Dominant Subtype (e.g., Y2610):**
   Characterised by high *CNR1* expression with minimal immune activation, raising the possibility of benefit from neuromodulatory or cannabinoid-based therapies.

However, many individuals did not exhibit clear pathway enrichment. This “quiet majority” showed muted or moderate transcript expression across domains, and IC Symptom and Problem Index scores varied widely, even among non-BPS comparators (Figures 4.1–4.2). Patients with microhaematuria or rUTI sometimes reported symptom levels comparable to classical BPS, further highlighting the difficulty of inferring biological mechanisms from symptoms alone.

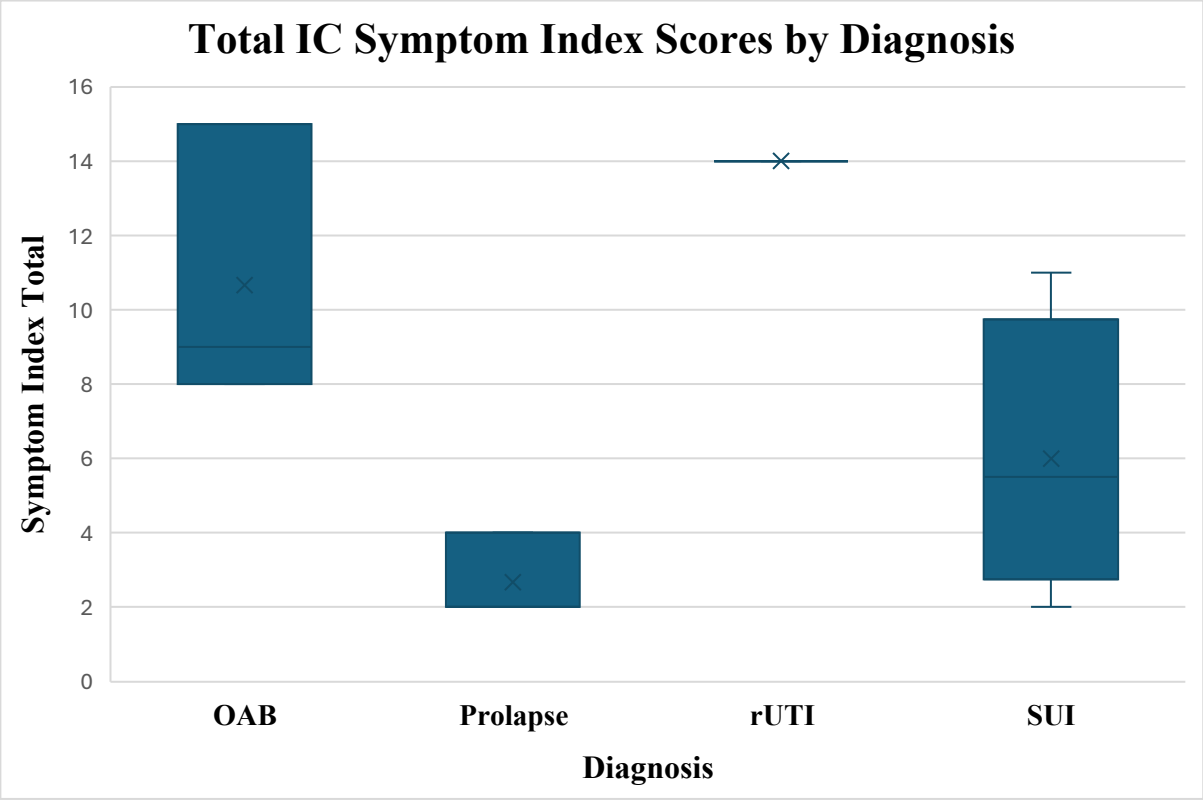


**Figure 4.1. Total IC Symptom Index Scores by Clinical Diagnosis**

Boxplot illustrating total IC Symptom Index scores across clinical diagnoses in the study cohort. Individual patient scores are overlaid to demonstrate within-group variability. While patients diagnosed with BPS/IC generally exhibited higher symptom burden, notable overlap was observed with other groups, including microhaematuria and rUTI. This distribution underscores the limited diagnostic specificity of symptom severity scores and highlights the need for molecular stratification alongside clinical assessment.

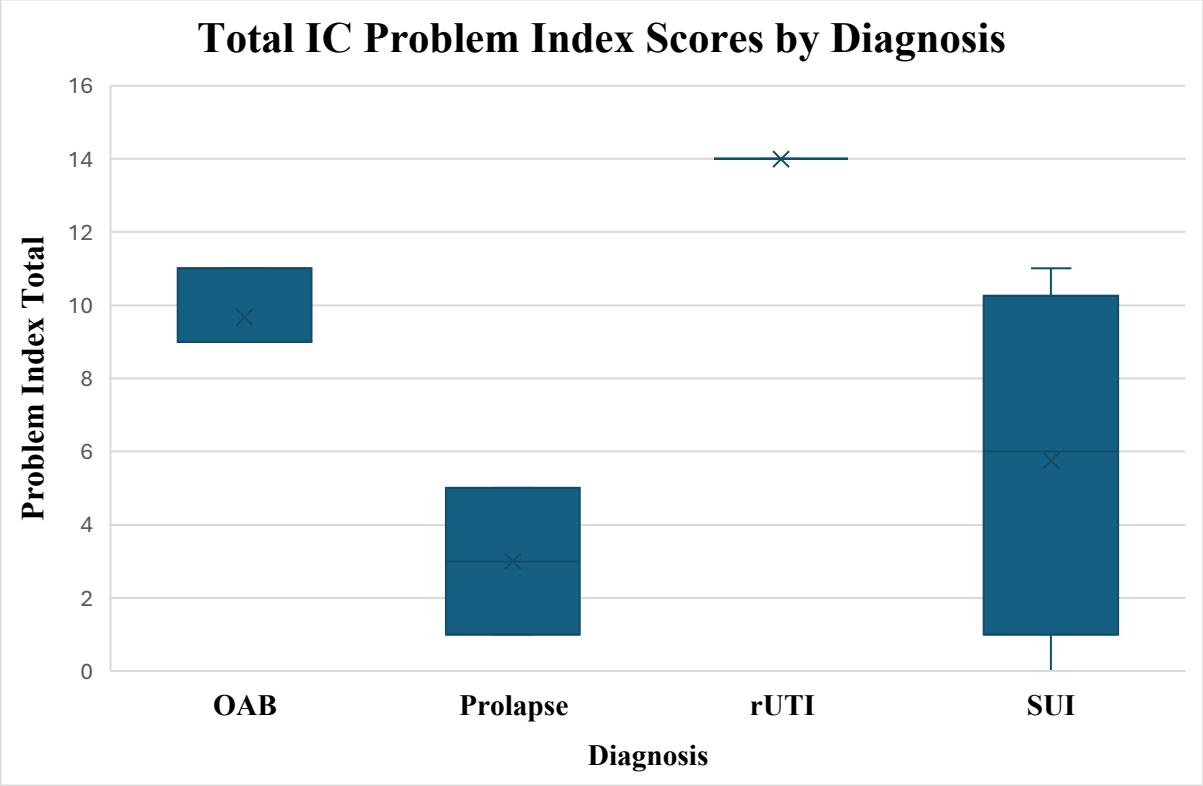


**Figure 4.2. Total IC Problem Index Scores by Clinical Diagnosis**

Boxplot showing IC Problem Index scores across the same diagnostic categories. Like the symptom index, substantial variability is observed within and between groups. Some non-IC diagnoses presented with problem scores comparable to or exceeding those of confirmed BPS patients. These findings reinforce the clinical heterogeneity of pelvic pain syndromes and support the integration of transcriptomic data to augment phenotype classification.

Molecular profiling therefore holds translational promise. Existing therapies for BPS often rely on sequential trial-and-error approaches, contributing to poor long-term outcomes (Clemens et al., 2022). Immune-activated patients (e.g., Y2336, Y2338) may be better suited to targeted anti-inflammatory agents such as COX-2 inhibitors, corticosteroids, or IL-1 antagonists (Wullt et al., 2021), consistent with murine evidence supporting COX-2 blockade in bladder inflammation (Hannan et al., 2014). Conversely, patients resembling Y2610 may benefit from intravesical botulinum toxin A or cannabinoid receptor agonists, both supported by preclinical data in neurogenic cystitis (Bjorling and Wang, 2018).

Finally, elevated *STAT3*, *PTPN22* and *IRAK1* in Y2336 and Y2338 align with patterns expected from reduced miR-146a and miR-181a/b activity. These miRNAs restrain NF-κB signalling via repression of IRAK1 and TRAF6 (Boldin et al., 2011); their dysregulation therefore suggests potential for miRNA-targeted therapeutic strategies.

## 4.1 Strengths of the Approach

This study's integrative design—bringing together systematic evidence, transcriptomic profiling, and detailed clinical metadata—represents a major strength. The use of primary human bladder biopsies is particularly valuable, as most prior work has relied on animal models (e.g., Saban et al., 2000; Braas et al., 2006; Peskar et al., 2023) or immortalised urothelial lines (Yang et al., 2012), both of which only partially recapitulate human disease biology. By contrast, the present cohort offers direct patient-level molecular insight, strengthening the translational relevance of the findings.

A second strength lies in the individualised analytical framework adopted throughout Chapter 3. Rather than relying solely on averaged comparisons—an approach known to obscure biologically meaningful variation in heterogeneous conditions—this study interrogated sample-specific profiles. This enabled the identification of coherent transcriptional outliers otherwise hidden in group-level analysis, consistent with emerging precision-medicine approaches in chronic inflammatory disease (Ward et al., 2020).

Finally, the integration of molecular data with clinical features—including symptom scores, cystoscopy findings, and functional assays—provided a richer interpretative context than either dataset alone. This mapping revealed clinically relevant disconnects (e.g., high

symptoms but low inflammation) and reinforced the need for molecular stratification within BPS. Despite the modest sample size, the combination of deep phenotyping and granular transcriptomic analysis produced a level of mechanistic insight uncommon in early-stage stratification research.

## 4.2 Limitations of the Study

This study has several limitations that should temper interpretation of the findings. First, the cohort was small and exclusively female, reducing statistical power and limiting generalisability—particularly to male patients in whom BPS may follow different inflammatory or neurogenic trajectories. Second, the use of superficial (P0) urothelial biopsies likely under-represented deeper inflammatory or stromal processes, including the characteristic subepithelial infiltrates of Hunner lesions, and may have obscured field effects beyond the sampled region. Third, the cross-sectional design precluded assessment of temporal stability or treatment responsiveness of the identified transcriptional patterns. Fourth, although the transcriptomic panel captured key mechanistic pathways, it did not include direct measurements of miRNA, protein, or cell-type–specific activity; nor did it incorporate single-cell or spatial resolution, limiting the ability to disentangle epithelial versus infiltrating immune contributions. These constraints collectively emphasise that the subtype signals identified here should be considered preliminary and hypothesis-generating.

## 4.3 Future Directions and Clinical Applications

Larger, multicentre studies should target approximately 60–80 BPS samples with matched controls and incorporate clear stratification by symptom burden, cystoscopic phenotype, and histopathology. Longitudinal sampling—ideally before and after therapeutic intervention—would clarify the stability of transcriptomic signatures and identify markers predictive of treatment response.

Future work should expand beyond bulk transcriptomics to include proteomics, epigenomics, and small RNA sequencing. Profiling miR-146a and miR-181a/b, for example, would help validate the inferred repression of *IRAK1/TRAF6* targets. Non-invasive biomarkers such as

urinary IL-6, NGF, or $PGE_2$ may provide clinically scalable correlates of tissue-based signatures. Integrating these molecular readouts with validated symptom indices and psychometric measures could support a more robust multimodal diagnostic framework.

From a translational standpoint, molecular stratification offers a potential route to more rational therapy selection. Immune-enriched profiles may warrant trials of targeted anti-inflammatory or antioxidant therapies, whereas neurogenic or neuroplasticity-skewed profiles may be better suited to neuromodulatory or cannabinoid-based interventions. Ultimately, transcriptomic classification could inform companion diagnostic development and personalised treatment algorithms. However, practical barriers—including tissue accessibility, regulatory considerations, and the need for subtype validation in larger cohorts—must be addressed before clinical implementation becomes feasible.

## Conclusion

This study provides evidence that Bladder Pain Syndrome (BPS) is a molecularly heterogeneous condition, characterised not by uniform pathway activation but by patient-specific transcriptional patterns across immune, epithelial, neurogenic, oxidative, and regulatory domains. Integrating findings from the systematic review with transcriptomic profiling of well-phenotyped clinical tissue revealed that group-level differences were modest, yet several individuals displayed coherent, biologically plausible signatures consistent with mechanisms proposed in the literature.

Although interpretations are necessarily tentative given the small cohort and reliance on superficial urothelial biopsies, the identification of immune-dominant and neuroplasticity-dominant profiles highlights the tractability of a stratified disease model. These molecular patterns aligned with symptom indices, cystoscopic findings, and barrier function assays, illustrating the value of integrating multi-level clinical metadata and underscoring that symptom severity does not uniformly reflect underlying molecular activity.

The findings refine existing models of BPS pathophysiology, suggest testable subtype hypotheses, and point towards translational avenues—including targeted immunomodulation, neuromodulation, and miRNA-focused therapies. They also emphasise the limitations of averaged analyses in a clinically diverse disorder and support the necessity of larger,

multimodal, and longitudinal studies to validate putative subtypes and assess their therapeutic relevance.

In sum, this work demonstrates that BPS, though complex, is amenable to mechanistic dissection when approached through integrated, patient-centred molecular science. The insights generated here offer a conceptual foundation for future precision diagnostic strategies and highlight the potential of transcriptomic profiling to move BPS research toward more personalised, biologically informed care.

# References

Birder, L. and Andersson, K.E., 2013. Urothelial signaling. *Physiological Reviews*, 93(2), pp.653–680. Available at: https://pubmed.ncbi.nlm.nih.gov/23589830/

Cervigni, M. and Natale, F., 2014. Gynecological disorders in bladder pain syndrome/interstitial cystitis patients. *International Journal of Urology*, 21(Suppl 1), pp.85–88. Available at: https://pubmed.ncbi.nlm.nih.gov/24807511/

Lee, C.L., Jiang, Y.H. and Kuo, H.C., 2013. Increased apoptosis and suburothelial inflammation in patients with ketamine-related cystitis: a comparison with non-ulcerative interstitial cystitis and controls. *BJU International*, 112(8), pp.1156–1162. Available at: https://pubmed.ncbi.nlm.nih.gov/23937072/

Roehrborn, C.G., 2005. Benign prostatic hyperplasia: an overview. *Reviews in Urology*, 7(Suppl 9), pp.S3–S14. Available at: https://pubmed.ncbi.nlm.nih.gov/16985902/

Flores-Mireles, A.L., Walker, J.N., Caparon, M. and Hultgren, S.J., 2015. Urinary tract infections: Epidemiology, mechanisms of infection and treatment options. *Nature Reviews Microbiology*, 13(5), pp.269–284. Available at: https://doi.org/10.1038/nrmicro3432

Foxman, B., 2010. The epidemiology of urinary tract infection. *Nature Reviews Urology*, 7(12), pp.653–660. Available at: https://pubmed.ncbi.nlm.nih.gov/21139641/

Mulvey MA, Lopez-Boado YS, Wilson CL, Roth R, Parks WC, Heuser J, Hultgren SJ. (1998). *Induction and evasion of host defenses by type 1-piliated uropathogenic Escherichia coli*. *Science*, 282(5393), 1494–1497. https://doi.org/10.1126/science.282.5393.1494

Hooton, T.M., Scholes, D., Hughes, J.P., Winter, C., Roberts, P.L., Stapleton, A.E., Stergachis, A. and Stamm, W.E., 1996. A prospective study of risk factors for symptomatic urinary tract infection in young women. *The New England Journal of Medicine*, 335(7), pp.468–474. Available at: https://pubmed.ncbi.nlm.nih.gov/8672152/

Beland, L., Martin, C. and Han, J.S., 2022. Lower urinary tract symptoms in young men—causes and management. *Current Urology Reports*, 23(2), pp.29–37. Available at: https://pubmed.ncbi.nlm.nih.gov/35132519/

Jhang, J.F., Birder, L.A. and Kuo, H.C., 2023. Pathophysiology, clinical presentation, and management of ketamine-induced cystitis. *Tzu Chi Medical Journal*, 35(3), pp.205–212. Available at: https://pubmed.ncbi.nlm.nih.gov/37545795/

Gajewski, J.B. and Drake, M.J., 2018. Neurological lower urinary tract dysfunction essential terminology. *Neurourology and Urodynamics*, 37(S6), pp.S25–S31. Available at: https://pubmed.ncbi.nlm.nih.gov/30614062/

Torelli, F., Terragni, E., Blanco, S., Di Bella, N., Grasso, M. and Bonaiuti, D., 2015. Lower urinary tract symptoms associated with neurological conditions: Observations on a clinical sample of outpatients neurorehabilitation service. *Archivio Italiano di Urologia e Andrologia*, 87(2), pp.154–157. Available at: https://pubmed.ncbi.nlm.nih.gov/26150035/

Haylen, B.T., de Ridder, D., Freeman, R.M., Swift, S.E., Berghmans, B., Lee, J., Monga, A., Petri, E., Rizk, D.E., Sand, P.K. and Schaer, G.N., 2010. An International Urogynecological Association (IUGA)/International Continence Society (ICS) joint report on the terminology for female pelvic floor dysfunction. *International Urogynecology Journal*, 21(1), pp.5–26. Available at: https://pubmed.ncbi.nlm.nih.gov/19937315/

NHS England, 2018. *Excellence in continence care: Practical guidance for commissioners and leaders*. [online] NHS England. Available at: https://www.england.nhs.uk/publication/excellence-in-continence-care/

Buckley, B.S. and Lapitan, M.C., 2009. Prevalence of urinary and faecal incontinence and nocturnal enuresis and attitudes to treatment and help-seeking amongst a community-based representative sample of adults in the United Kingdom. *International Journal of Clinical Practice*, 63(4), pp.568–573. https://doi.org/10.1111/j.1742-1241.2008.01974.x

Hakimi, Z., Houbiers, J., Pedersini, R. and Vietri, J., 2017. The burden of bladder pain in five European countries: A cross-sectional study. *Urology*, 99, pp.84–91. https://pubmed.ncbi.nlm.nih.gov/27616606/

Morales-Solchaga, G., Zubiaur-Libano, C., Peri-Cusí, L., Adot-Zurbano, J.M., Arlandis-Guzmán, S., Franco-de Castro, A., Castillejo, C., and Grupo IFU, 2019. Bladder pain syndrome: Prevalence and routine clinical practice in women attending functional urology and urodynamics units in Spain. *Actas Urol Esp (Engl Ed)*, 43(2), pp.62–70. Available at: https://pubmed.ncbi.nlm.nih.gov/30262204/

Clemens, J.Q., Meenan, R.T., Rosetti, M.C., Gao, S.Y. and Calhoun, E.A., 2005. Prevalence and incidence of interstitial cystitis in a managed care population. *The Journal of Urology*, 173(1), pp.98–102. https://pubmed.ncbi.nlm.nih.gov/15592041/

European Association of Urology (EAU), n.d. *Guidelines*. [online] Available at: https://uroweb.org/guidelines

Abrams, P., Cardozo, L. and Fall, M., 2002. The standardisation of terminology of lower urinary tract function: Report from the Standardisation Sub-committee of the International Continence Society. *Neurourology and Urodynamics*, 21(2), pp.167–178. Available at: https://pubmed.ncbi.nlm.nih.gov/11857671/

van de Merwe, J.P., Nordling, J., Bouchelouche, P., Cervigni, M., Daha, L.K., Elneil, S., Fall, M., Hohlbrugger, G., Irwin, P., Mortensen, S., van Ophoven, A., Peeker, R., Richter, B., van der Aa, F., Wyndaele, J.J. and ESSIC Working Group, 2008. Diagnostic criteria, classification, and nomenclature for painful bladder syndrome/interstitial cystitis: an ESSIC proposal. *European Urology*, 53(1), pp.60–67. Available at: https://pubmed.ncbi.nlm.nih.gov/17900797/

Homma, Y., Akiyama, Y., Tomoe, H., Furuta, A., Ueda, T., Maeda, D., Lin, A.T., Kuo, H.C., Lee, M.H., Oh, S.J., Kim, J.C. and Lee, K.S., 2020. Clinical guidelines for interstitial cystitis/bladder pain syndrome. *International Journal of Urology*, 27(7), pp.578–589. Available at: https://pubmed.ncbi.nlm.nih.gov/32291805/

Hanno, P. and Dmochowski, R., 2009. Status of international consensus on interstitial cystitis/bladder pain syndrome/painful bladder syndrome: 2008 snapshot. *Neurourology and Urodynamics*, 28(4), pp.274–286. doi: 10.1002/nau.20687. Available at: https://pubmed.ncbi.nlm.nih.gov/19260081/

Gillenwater, J.Y. and Wein, A.J. (1988) 'Summary of the National Institute of Arthritis, Diabetes, Digestive and Kidney Diseases Workshop on interstitial cystitis, National Institutes of Health, Bethesda, Maryland, August 28–29, 1987', *Journal of Urology*, 140(1), pp. 203–206. doi: 10.1016/S0022-5347(17)41529-1. Available at: https://pubmed.ncbi.nlm.nih.gov/3379688/

Parsons, C.L., 2002. Interstitial cystitis: epidemiology and clinical presentation. *Clinical Obstetrics and Gynecology*, 45(1), pp.242–249. Available at: https://pubmed.ncbi.nlm.nih.gov/11862076/

Meijlink, J.M. (2014) 'Interstitial cystitis and the painful bladder: a brief history of nomenclature, definitions and criteria', *International Journal of Urology*, 21(Suppl 1), pp. 4–12. doi: 10.1111/iju.12307. Available at: https://pubmed.ncbi.nlm.nih.gov/24807485/

Clemens, J.Q., Erickson, D.R., Varela, N.P. and Lai, H.H., 2022. Diagnosis and treatment of interstitial cystitis/bladder pain syndrome. *The Journal of Urology*, 208(1), pp.34–42. Available at: https://pubmed.ncbi.nlm.nih.gov/35536143/

Cox, A., Golda, N., Nadeau, G., Nickel, J.C., Carr, L., Corcos, J. and Teichman, J., 2016. CUA guideline: Diagnosis and treatment of interstitial cystitis/bladder pain syndrome. *Canadian Urological Association Journal*, 10(5–6), pp.E136–E155. Available at: https://pubmed.ncbi.nlm.nih.gov/27790294/

Jiang, Y.-H., Jhang, J.-F. and Hsu, Y.-H., 2022. Usefulness of urinary biomarkers for assessing bladder condition and histopathology in patients with interstitial cystitis/bladder pain syndrome. *International Journal of Molecular Sciences*, 23(19), p.12044. Available at: https://pubmed.ncbi.nlm.nih.gov/36233356/

Chermansky, C.J. and Guirguis, M.O. (2022) 'Pharmacologic management of interstitial cystitis/bladder pain syndrome', *Urologic Clinics of North America*, 49(2), pp. 273–282. doi: 10.1016/j.ucl.2022.01.003. Available at: https://pubmed.ncbi.nlm.nih.gov/35428433/

Padilla-Fernández, B., Hernández-Hernández, D. and Castro-Díaz, D.M., 2022. Current role of neuromodulation in bladder pain syndrome/interstitial cystitis. *Therapeutic Advances in Urology*, 14, p.17562872221135941. Available at: https://pubmed.ncbi.nlm.nih.gov/36438605/

Jhang, J.F., 2019. Using botulinum toxin A for treatment of interstitial cystitis/bladder pain syndrome—possible pathomechanisms and practical issues. *Toxins (Basel)*, 11(11), p.641. Available at: https://pubmed.ncbi.nlm.nih.gov/31689912/

Dayem, A.A., Song, K., Lee, S., Kim, A. and Cho, S.G., 2022. New therapeutic approach with extracellular vesicles from stem cells for interstitial cystitis/bladder pain syndrome. *BMB Reports*, 55(5), pp.205–212. Available at: https://pubmed.ncbi.nlm.nih.gov/35410640/

Augé, C., Basso, L., Blanpied, C., Vergnolle, N., Gamé, X., Chabot, S., Lluel, P. and Dietrich, G., 2021. Pain management in a model of interstitial cystitis/bladder pain syndrome by a vaccinal strategy. *Frontiers in Pain Research*, 2, p.642706. Available at: https://pubmed.ncbi.nlm.nih.gov/35295433/

Taubert, E., van der Aa, F. and Heesakkers, J., 2024. Bladder pain syndrome AKA interstitial cystitis – a condition with severe unmet medical need: an exploration of brimapitide as a potential treatment opportunity. *Current Opinion in Urology*, 34(2), pp.52–57. Available at: https://pubmed.ncbi.nlm.nih.gov/37975427/

Akiyama, Y. and Hanno, P., 2019. Phenotyping of interstitial cystitis/bladder pain syndrome. *International Journal of Urology*, 26(Suppl 1), pp.17–19. Available at: https://pubmed.ncbi.nlm.nih.gov/31144756/

Akshay, A., Besic, M., Kuhn, A., Burkhard, F.C., Bigger-Allen, A., Adam, R.M., Monastyrskaya, K. and Hashemi Gheinani, A., 2024. Machine learning-based classification of transcriptome signatures of non-ulcerative bladder pain syndrome. *International Journal of Molecular Sciences*, 25(3), p.1568. Available at: https://pubmed.ncbi.nlm.nih.gov/38338847/

HGNC (HUGO Gene Nomenclature Committee), n.d. *GENE NAMES*. [online] Available at: https://www.genenames.org

Zhao, J., Chen, S., Yang, C., Zhou, M. et al., 2022. Activation of CXCL13/CXCR5 axis aggravates experimental autoimmune cystitis and interstitial cystitis/bladder pain syndrome. *Biochemical Pharmacology*, 200, p.115047. Available at: https://pubmed.ncbi.nlm.nih.gov/35452631/

Zhang, W., Liu, X., Wang, J., Wang, X. and Zhang, Y. (2023) 'Immunogenic cell death associated molecular patterns and the dual role of IL17RA in interstitial cystitis/bladder pain syndrome', *Biomolecules*, 13(3), p. 421. Available at: https://pubmed.ncbi.nlm.nih.gov/36979355/

Ward, E.P., Bartolone, S.N., Chancellor, M.B., Peters, K.M. and Lamb, L.E. (2020) 'Proteomic analysis of bladder biopsies from interstitial cystitis/bladder pain syndrome patients with and without Hunner's lesions reveals differences in expression of inflammatory

and structural proteins', *BMC Urology*, 20(1), p. 180. Available at: https://pubmed.ncbi.nlm.nih.gov/33160333/

Christmas, T.J. and Bottazzo, G.F. (1992) 'Abnormal urothelial HLA-DR expression in interstitial cystitis', *Clinical and Experimental Immunology*, 87(3), pp. 450–454. Available at: https://pubmed.ncbi.nlm.nih.gov/1544229/

Liu, H.T., Jiang, Y.H. and Kuo, H.C. (2015) 'Alteration of urothelial inflammation, apoptosis, and junction protein in patients with various bladder conditions and storage bladder symptoms suggests common pathway involved in underlying pathophysiology', *Lower Urinary Tract Symptoms*, 7(2), pp. 102–107. Available at: https://pubmed.ncbi.nlm.nih.gov/26663690/

Green, M., Filippou, A., Sant, G. and Theoharides, T.C. (2004) 'Expression of intercellular adhesion molecules in the bladder of patients with interstitial cystitis', *Urology*, 63(4), pp. 688–693. Available at: https://pubmed.ncbi.nlm.nih.gov/15072882/

Yang, W., Kim, Y., Kim, T.K., Keay, S.K., Kim, K.P., Steen, H., Freeman, M.R., Hwang, D. and Kim, J. (2012) 'Integration analysis of quantitative proteomics and transcriptomics data identifies potential targets of frizzled-8 protein-related antiproliferative factor in vivo', *BJU International*, 110(11 Pt C), pp. E1138–E1146. Available at: https://pubmed.ncbi.nlm.nih.gov/22738385/

Shie, J.H., Liu, H.T. and Kuo, H.C. (2012) 'Increased cell apoptosis of urothelium mediated by inflammation in interstitial cystitis/painful bladder syndrome', *Urology*, 79(2), pp. 484.e7–484.e13. Available at: https://pubmed.ncbi.nlm.nih.gov/22310775/

Liu, H.T., Shie, J.H., Chen, S.H., Wang, Y.S. and Kuo, H.C. (2012) 'Differences in mast cell infiltration, E-cadherin, and zonula occludens-1 expression between patients with overactive bladder and interstitial cystitis/bladder pain syndrome', *Urology*, 80(1), pp. 225.e13–225.e18. Available at: https://pubmed.ncbi.nlm.nih.gov/22521193/

Lee, C.L., Jiang, Y.H. and Kuo, H.C. (2013) 'Increased apoptosis and suburothelial inflammation in patients with ketamine-related cystitis: a comparison with non-ulcerative interstitial cystitis and controls', *BJU International*, 112(8), pp. 1156–1162. Available at: https://pubmed.ncbi.nlm.nih.gov/23937072/

Mukerji, G., Yiangou, Y., Agarwal, S.K. and Anand, P. (2010) 'Increased cannabinoid receptor 1-immunoreactive nerve fibers in overactive and painful bladder disorders and their correlation with symptoms', *Urology*, 75(6), pp. 1514.e15–1514.e20. Available at: https://pubmed.ncbi.nlm.nih.gov/20346490/

Saban, R., Saban, M.R., Nguyen, N.B., Lu, B., Gerard, C., Gerard, N.P. and Hammond, T.G. (2000) 'Neurokinin-1 (NK-1) receptor is required in antigen-induced cystitis', *American Journal of Pathology*, 156(3), pp. 775–780. Available at: https://pubmed.ncbi.nlm.nih.gov/10702392/

Girard, B.M., Tompkins, J.D., Parsons, R.L., May, V. and Vizzard, M.A. (2012) 'Effects of CYP-induced cystitis on PACAP/VIP and receptor expression in micturition pathways and bladder function in mice with overexpression of NGF in urothelium', *Journal of Molecular Neuroscience*, 48(3), pp. 730–743. Available at: https://pubmed.ncbi.nlm.nih.gov/22700375/

Chopra, B., Barrick, S.R., Meyers, S., Beckel, J.M., Zeidel, M.L., Ford, A.P., de Groat, W.C. and Birder, L.A. (2005) 'Expression and function of bradykinin B1 and B2 receptors in

normal and inflamed rat urinary bladder urothelium', *The Journal of Physiology*, 562(3), pp. 859–871. Available at: https://pubmed.ncbi.nlm.nih.gov/15576455/

Peskar, D., Kuret, T., Lakota, K. and Erman, A. (2023) 'Molecular profiling of inflammatory processes in a mouse model of IC/BPS: From the complete transcriptome to major sex-related histological features of the urinary bladder', *International Journal of Molecular Sciences*, 24(6), p. 5758. Available at: https://pubmed.ncbi.nlm.nih.gov/36982831/

Kumar, V., Kiran, S., Shamran, H.A. and Singh, U.P. (2021) 'Differential expression of microRNAs correlates with the severity of experimental autoimmune cystitis', *Frontiers in Immunology*, 12, p. 716564. Available at: https://pubmed.ncbi.nlm.nih.gov/34335632/

Kiran, S., Rakib, A. and Singh, U.P. (2022) 'The NLRP3 inflammasome inhibitor dapansutrile attenuates cyclophosphamide-induced interstitial cystitis', *Frontiers in Immunology*, 13, p. 903834. Available at: https://pubmed.ncbi.nlm.nih.gov/35720309/

Braas, K.M., May, V., Zvara, P., Nausch, B., Kliment, J., Dunleavy, J.D., Nelson, M.T. and Vizzard, M.A. (2006) 'Role for pituitary adenylate cyclase activating polypeptide in cystitis-induced plasticity of micturition reflexes', *American Journal of Physiology-Regulatory, Integrative and Comparative Physiology*, 290(4), pp. R951–R962. Available at: https://pubmed.ncbi.nlm.nih.gov/16322346/

Liu, H.T. and Kuo, H.C. (2007) 'Intravesical botulinum toxin A injections plus hydrodistension can reduce nerve growth factor production and control bladder pain in interstitial cystitis', *Urology*, 70(3), pp. 463–468. Available at: https://pubmed.ncbi.nlm.nih.gov/17905097/

Ostardo, E., Impellizzeri, D., Cervigni, M., Porru, D., Sommariva, M., Cordaro, M., Siracusa, R., Fusco, R., Gugliandolo, E., Crupi, R., Schievano, C., Inferrera, A., Di Paola, R. and Cuzzocrea, S. (2018) 'Adelmidrol + sodium hyaluronate in IC/BPS or conditions associated to chronic urothelial inflammation. A translational study', *Pharmacological Research*, 134, pp. 16–30. Available at: https://pubmed.ncbi.nlm.nih.gov/29800607/

Yoshimura, N., Uno, T., Sasaki, M., Ohinata, A., Nawata, S. and Ueda, T. (2022) 'The O'Leary-Sant Interstitial Cystitis Symptom Index is a clinically useful indicator of treatment outcome in patients with interstitial cystitis/bladder pain syndrome with Hunner lesions: A post hoc analysis of the Japanese phase III trial of KRP-116D, 50% dimethyl sulfoxide solution', *International Journal of Urology*, 29(4), pp. 289–296. Available at: https://pubmed.ncbi.nlm.nih.gov/34929761/

Southgate, J., Masters, J.R.W. and Trejdosiewicz, L.K. (2002) 'Culture of human urothelium', in Freshney, R.I. and Freshney, M.G. (eds.) *Culture of Epithelial Cells*. 2nd edn. Hoboken, NJ: Wiley-Liss. Available at: https://doi.org/10.1002/0471221201.ch12

Varley, C., Hill, G., Pellegrin, S., Shaw, N.J., Selby, P.J., Trejdosiewicz, L.K. and Southgate, J. (2005) 'Autocrine regulation of human urothelial cell proliferation and migration during regenerative responses in vitro', *Experimental Cell Research*, 306(1), pp. 216–229. Available at: https://pubmed.ncbi.nlm.nih.gov/15878346/

Cross, W.R., Eardley, I., Leese, H.J. and Southgate, J. (2005) 'A biomimetic tissue from cultured normal human urothelial cells: analysis of physiological function', *American Journal of Physiology - Renal Physiology*, 289(2), pp. F459–F468. Available at: https://pubmed.ncbi.nlm.nih.gov/15784840/

Andrews, S. (2010) *FastQC: A Quality Control Tool for High Throughput Sequence Data*. Available at: https://www.bioinformatics.babraham.ac.uk/projects/fastqc/

Bray, N.L., Pimentel, H., Melsted, P. and Pachter, L. (2016) 'Near-optimal probabilistic RNA-seq quantification', *Nature Biotechnology*, 34(5), pp. 525–527. Available at: https://doi.org/10.1038/nbt.3519

Soneson, C., Love, M.I. and Robinson, M.D. (2015) 'Differential analyses for RNA-seq: transcript-level estimates improve gene-level inferences', *F1000Research*, 4, p.1521. Available at: https://doi.org/10.12688/f1000research.7563.2

R Core Team (2024) *R: A language and environment for statistical computing*. Vienna: R Foundation for Statistical Computing. Available at: https://www.r-project.org

StatsKingdom (n.d.) *Statistical calculators and tests for researchers*. Available at: https://www.statskingdom.com

Li, X., Gheinani, A.H. and Adam, R.M., 2019. A multi-omics approach to understanding the field effect in bladder cancer. *Translational Andrology and Urology*, 8(6), pp.775–778. doi:10.21037/tau.2019.07.11. Available at: https://pubmed.ncbi.nlm.nih.gov/32038978/

McIlraith, D., Mills, R., McCarthy, S., et al., 2016. Urothelial functional protein and sensory receptor differences in patients with Hunner lesion interstitial cystitis/bladder pain syndrome. *International Journal of Urology*, 26(Suppl 1), pp.35–40. Available at: https://pubmed.ncbi.nlm.nih.gov/27575016/

Hannan, T.J., Roberts, P.L., Riehl, T.E., van der Post, S., Binkley, J.M., Schwartz, D.J., Miyoshi, H., Mack, M., Schwendener, R.A., Hooton, T.M., Stappenbeck, T.S., Hansson, G.C., Stenson, W.F., Colonna, M., Stapleton, A.E. and Hultgren, S.J., 2014. Inhibition of cyclooxygenase-2 prevents chronic and recurrent cystitis. *EBioMedicine*, 1(1), pp.46–57. https://pubmed.ncbi.nlm.nih.gov/26125048/

Wullt, B., Butler, D.S.C., Ambite, I., Kinsolving, J., Krintel, C. and Svanborg, C., 2021. Immunomodulation—a molecular solution to treating patients with severe bladder pain syndrome? *European Urology Open Science*, 31, pp.49–58. https://pubmed.ncbi.nlm.nih.gov/34467240/

Bjorling, D.E. and Wang, Z.Y., 2018. Potential of endocannabinoids to control bladder pain. *Frontiers in Systems Neuroscience*, 12, p.17. https://pubmed.ncbi.nlm.nih.gov/29867382/

Boldin, M.P., Taganov, K.D., Rao, D.S., Yang, L., Zhao, J.L., Kalwani, M., Garcia-Flores, Y., Luong, M., Devrekanli, A., Xu, J., Sun, G., Tay, J., Linsley, P.S. and Baltimore, D., 2011. miR-146a is a significant brake on autoimmunity, myeloproliferation, and cancer in mice. *Journal of Experimental Medicine*, 208(6), pp.1189–1201. https://pubmed.ncbi.nlm.nih.gov/21555486/

# Appendices

**Table A1: Lower Urinary Tract Symptoms**

| Storage Symptoms | Voiding Symptoms | Post-micturition Symptoms |
|---|---|---|
| **Frequency:** needing to urinate more often than usual | **Hesitancy:** difficulty starting the flow of urine | **Dribbling:** involuntary leakage of urine after urination |
| **Urgency:** sudden, strong urge to urinate | **Weak stream:** reduced strength of the urine flow | **Incomplete emptying:** Feeling that the bladder has not fully emptied |
| **Nocturia:** waking up multiple times during the night to urinate | **Intermittency:** urine flow that stops and starts | |
| **Incontinence:** involuntary leakage of urine. Urinary incontinence (UI) is classified as urgency UI (UUI), stress urinary incontinence (SUI), mixed urinary incontinence (MUI), or other forms of urinary incontinence, such as overflow and continuous urinary incontinence | **Straining:** needing to push or strain to begin urination | |

| | | |
|---|---|---|
| | **Prolonged urination:** longer than usual time to empty the bladder | |

**Table A2: SPIDER Framework Used to Define Inclusion Criteria for the Systematic**

| SPIDER Component | Inclusion Criteria |
|---|---|
| **S**ample | • Patients or clinical samples diagnosed with Bladder Pain Syndrome (BPS)<br>• Animal models (in vivo) and cell-based models (in vitro) specific to BPS |
| **P**henomenon of **I**nterest | • Candidate molecules/markers (gene/transcript/protein) whose expression is associated with BPS |
| **D**esign | • Clinical and experimental studies, including cohort, case-control, and cross-sectional designs<br>• In vivo and in vitro studies reporting relevant molecular or biomarker data |
| **E**valuation | • Identification of candidate markers (genes, transcripts, proteins) associated with BPS<br>• Role of candidate markers in BPS pathogenesis<br>• Correlation with phenotypic diversity<br>• Potential diagnostic, prognostic, or therapeutic utility |
| **R**esearch Type | • Quantitative studies (e.g., molecular expression analysis)<br>• Qualitative studies (e.g., mechanistic insights)<br>• Mixed-methods studies with clinical relevance |

**Systematic Review Question using SPIDER:**

In clinical and experimental studies of Bladder Pain Syndrome (BPS) can differentially expressed molecules (gene/transcript/protein) provide unbiased markers for diagnosis, prognosis, and therapeutic targeting of disease subsets?

**Figure A1: PRISMA 2020 flow diagram outlining the study selection process for the systematic review**

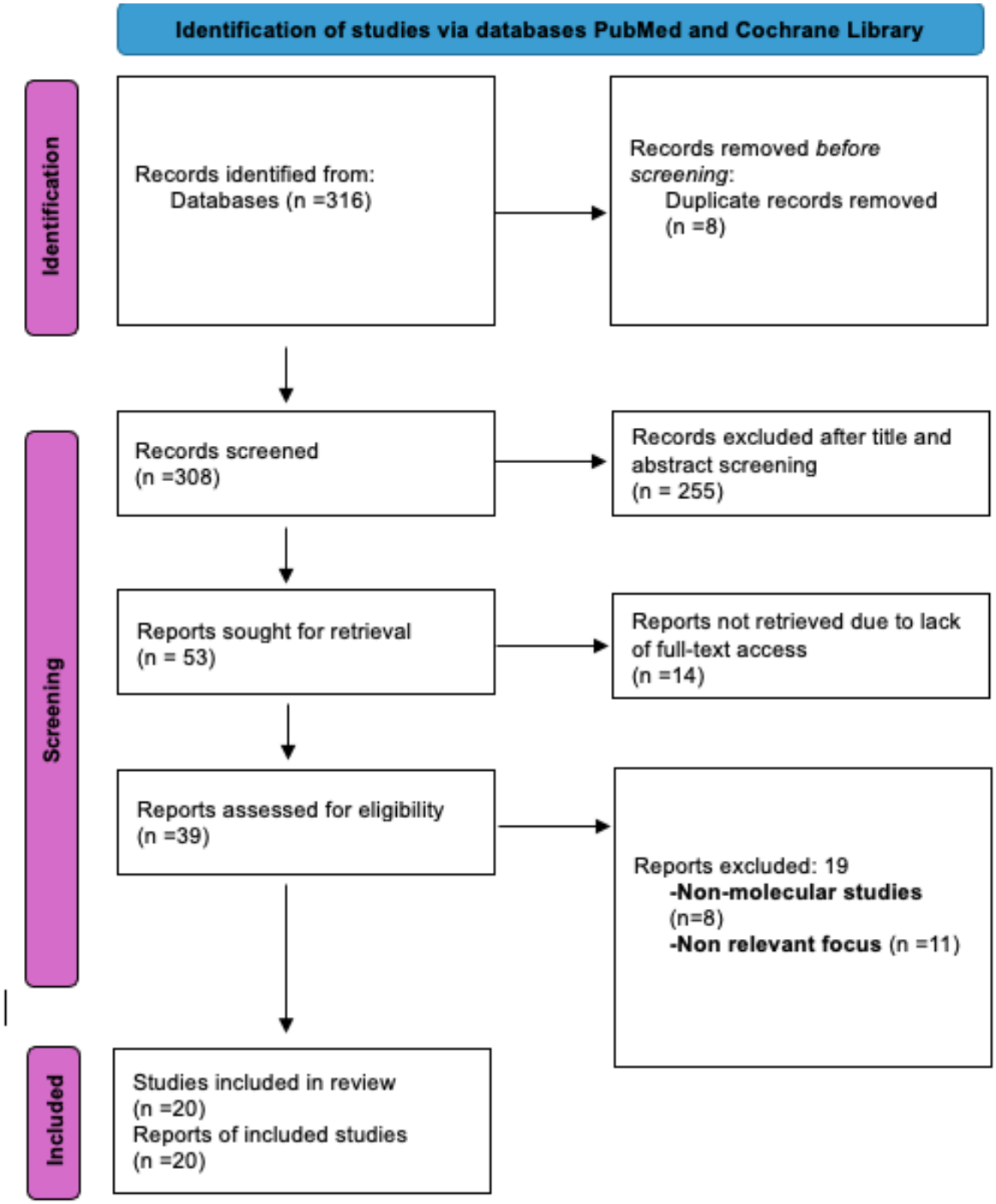

**Figure A2: O'Leary-Sant Interstitial Cystitis Symptom and Problem Index**

# O´Leary/Sant
# VOIDING AND PAIN INDICES

## INTERSTITIAL CYSTITIS SYMPTOM INDEX

**1.**
During the past month, how often have you felt the strong need to urinate wiht little or no warning?

0. _____ not at all
1. _____ less than l time in 5
2. _____ less than half the time
3. _____ about half the time
4. _____ more than half the time
5. _____ almonst always

**2.**
During the past month, have you had to urinate less than 2 hours after you finised urinating?

0. _____ not at all
1. _____ less than l time in 5
2. _____ less than half the time
3. _____ about half the time
4. _____ more than half the time
5. _____ almost always

**3.**
During the past month, how often did you most tupically get up at noght to urinate?

0. _____ never
1. _____ once
2. _____ 2 times
3. _____ 3 times
4. _____ 4 times
5. _____ 5 times
6. _____ 5 or more times

**4.**
During the past month, have you experienced pain or burning in your bladder?

0. _____ nat at all
1. _____ once
2. _____ a few times
3. _____ fairly often
4. _____ almost always
5. _____ usually

Add the numerical values of the checked entries;
**Total score _____.**

## INTERSTITIAL CYSTITIS PROBLEM INDEX

During the past month, how much has each of the following been a problem for you?

**1.** Frequent urination during the day?

0. _____ no problem
1. _____ very small problem
2. _____ small problem
3. _____ medium problem
4. _____ big problem

**2.** Getting up at nigth to urinate?

0. _____ no problem
1. _____ very small problem
2. _____ small problem
3. _____ medium problem
4. _____ big problem

**3.** Need to urinate with little warning?

0. _____ no problem
1. _____ very small problem
2. _____ small problem
3. _____ medium problem
4. _____ big problem

**4.** Burning, pain, discomfort, or pressure in your bladder?

0. _____ no problem
1. _____ very small problem
2. _____ small problem
3. _____ medium problem
4. _____ big problem

Add the numerical values of the check entries:
**Total score _____.**

# List of Abbreviations

| Abbreviation | Full Term |
|---|---|
| ABS | Adult Bovine Serum |
| ADCYAP1 | Adenylate Cyclase Activating Polypeptide 1 (PACAP) |
| APF | Antiproliferative Factor |
| AUA | American Urological Association |
| BDNF | Brain-Derived Neurotrophic Factor |
| BoNT-A | Botulinum Toxin A |
| BPS | Bladder Pain Syndrome |
| $Ca^{2+}$ | Calcium ion |
| CC | Cystitis Cystica |
| CDKN1A | Cyclin Dependent Kinase Inhibitor 1A |
| CIITA | Class II Transactivator |
| COX-2 | Cyclooxygenase-2 |
| CYP | Cyclophosphamide |
| CXCL | C-X-C Motif Chemokine Ligand |
| EGFR | Epidermal Growth Factor Receptor |
| ELISA | Enzyme-Linked Immunosorbent Assay |
| ER | Endoplasmic Reticulum |

| | |
|---|---|
| **FAAH** | **Fatty Acid Amide Hydrolase** |
| **GFRA1** | **GDNF Family Receptor Alpha 1** |
| **HIC** | **Hunner-type Interstitial Cystitis** |
| **IC** | **Interstitial Cystitis** |
| **ICAM1** | **Intercellular Adhesion Molecule 1** |
| **ICPI** | **Interstitial Cystitis Problem Index** |
| **ICSI** | **Interstitial Cystitis Symptom Index** |
| **IDO** | **Idiopathic Detrusor Overactivity** |
| **IFNG** | **Interferon-gamma** |
| **IL** | **Interleukin** |
| **IBS** | **Irritable Bowel Syndrome** |
| **JBU** | **Jack Birch Unit** |
| **KC** | **Ketamine Cystitis** |
| **MAPK** | **Mitogen-Activated Protein Kinase** |
| **MCP-1** | **Monocyte Chemoattractant Protein-1** |
| **MHC** | **Major Histocompatibility Complex** |
| **miRNA** | **MicroRNA** |
| **mRNA** | **Messenger Ribonucleic Acid** |
| **NF-κB** | **Nuclear Factor kappa-light-chain-enhancer of activated B cells** |
| **NHIC** | **Non-Hunner-type Interstitial Cystitis** |
| **NK-1 / NK-1R** | **Neurokinin-1 (Receptor)** |

| | |
|---|---|
| **NOS2** | **Nitric Oxide Synthase 2** |
| **NTP** | **Nerve Tissue Pathway (contextual)** |
| **NTRK1** | **Neurotrophic Receptor Tyrosine Kinase 1 (TrkA)** |
| **OAB** | **Overactive Bladder** |
| **PACAP** | **Pituitary Adenylate Cyclase-Activating Polypeptide** |
| **PBS** | **Painful Bladder Syndrome** |
| **PGE2** | **Prostaglandin E2** |
| **P0** | **Passage Zero (Primary Urothelial Culture)** |
| **POP** | **Pelvic Organ Prolapse** |
| **PRISMA** | **Preferred Reporting Items for Systematic Reviews and Meta-Analyses** |
| **PTGS2** | **Prostaglandin-Endoperoxide Synthase 2 (COX-2)** |
| **qPCR / qRT-PCR** | **Quantitative (Reverse Transcription) Polymerase Chain Reaction** |
| **QuOL** | **Quality of Life** |
| **RNA** | **Ribonucleic Acid** |
| **RISC** | **RNA-Induced Silencing Complex** |
| **rUTIs** | **Recurrent Urinary Tract Infections** |
| **SPIDER** | **Sample, Phenomenon of Interest, Design, Evaluation, Research Type** |
| **STAT** | **Signal Transducer and Activator of Transcription** |
| **SUI** | **Stress Urinary Incontinence** |

| | |
|---|---|
| **TACR1** | **Tachykinin Receptor 1 (NK-1 Receptor)** |
| **TER** | **Transepithelial Electrical Resistance** |
| **TNF** | **Tumour Necrosis Factor** |
| **TPM** | **Transcripts Per Million** |
| **TRPV1** | **Transient Receptor Potential Vanilloid 1** |
| **TVT** | **Transvaginal Tape** |
| **UTI** | **Urinary Tract Infection** |
| **VCAM1** | **Vascular Cell Adhesion Molecule 1** |
| **VEGFA** | **Vascular Endothelial Growth Factor A** |
| **VIP** | **Vasoactive Intestinal Peptide** |
| **VIPR1/2** | **Vasoactive Intestinal Peptide Receptors 1 and 2** |
| **ZO-1 / TJP1** | **Zonula Occludens-1 / Tight Junction Protein 1** |